Innovation, Sciences et Développement économique Canada
Office de la Propriété Intellectuelle du Canada

Innovation, Science and Economic Development Canada
Canadian Intellectual Property Office

CA 3096871 A1 2019/10/17

(21) 3 096 871

(12) DEMANDE DE BREVET CANADIEN
CANADIAN PATENT APPLICATION

(13) A1

(86) Date de dépôt PCT/PCT Filing Date: 2019/04/12
(87) Date publication PCT/PCT Publication Date: 2019/10/17
(85) Entrée phase nationale/National Entry: 2020/10/09
(86) N° demande PCT/PCT Application No.: US 2019/027201
(87) N° publication PCT/PCT Publication No.: 2019/200245
(30) Priorité/Priority: 2018/04/13 (US62/657,620)

(51) Cl.Int./Int.Cl. *C12N 9/12* (2006.01), *C12N 9/10* (2006.01), *G01N 33/50* (2006.01)

(71) Demandeur/Applicant:
THE REGENTS OF THE UNIVERSITY OF CALIFORNIA, US

(72) Inventeurs/Inventors:
COPPE, JEAN-PHILIPPE, US;
VAN 'T VEER, LAURA J., US

(74) Agent: SMART & BIGGAR LLP

(54) Titre : DETECTION DE SIGNATURES DE PHOSPHOKINASE
(54) Title: DETECTION OF PHOSPHOKINASE SIGNATURES

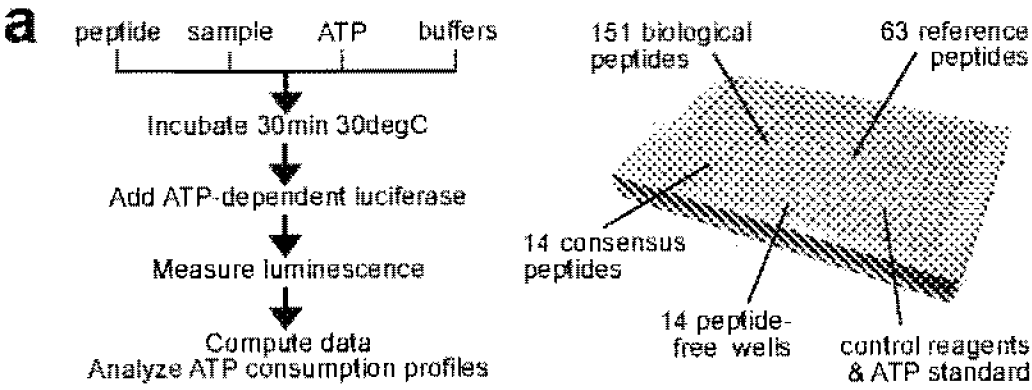

Fig. 1

(57) Abrégé/Abstract:
The disclosure provides methods and compositions for determining the kinase activity profile of a biological sample, e.g., that contains multiple kinases.

(12) INTERNATIONAL APPLICATION PUBLISHED UNDER THE PATENT COOPERATION TREATY (PCT)

(19) World Intellectual Property Organization
International Bureau

(43) International Publication Date
17 October 2019 (17.10.2019)

WIPO | PCT

(10) International Publication Number
WO 2019/200245 A1

(51) International Patent Classification:
C12N 9/12 (2006.01) *G01N 33/50* (2006.01)
C12N 9/10 (2006.01)

(21) International Application Number:
PCT/US2019/027201

(22) International Filing Date:
12 April 2019 (12.04.2019)

(25) Filing Language: English

(26) Publication Language: English

(30) Priority Data:
62/657,620 13 April 2018 (13.04.2018) US

(71) Applicant: **THE REGENTS OF THE UNIVERSITY OF CALIFORNIA** [US/US]; 1111 Franklin Street, 12th Floor, Oakland, California 94607-5200 (US).

(72) Inventors: **COPPE, Jean-Philippe**; c/o University of California, San Francisco, 2340 Sutter Street, S441, San Francisco, California 94115 (US). **VAN 'T VEER, Laura J.**; c/o University of California, San Francisco, 2340 Sutter Street, N415, San Francisco, California 94115 (US).

(74) Agent: **LOCKYER, Jean M.** et al.; Kilpatrick Townsend & Stockton LLP, Mailstop: IP Docketing - 22, 1100 Peachtree Street, Suite 2800, Atlanta, GA 30309 (US).

(81) Designated States *(unless otherwise indicated, for every kind of national protection available)*: AE, AG, AL, AM, AO, AT, AU, AZ, BA, BB, BG, BH, BN, BR, BW, BY, BZ, CA, CH, CL, CN, CO, CR, CU, CZ, DE, DJ, DK, DM, DO, DZ, EC, EE, EG, ES, FI, GB, GD, GE, GH, GM, GT, HN, HR, HU, ID, IL, IN, IR, IS, JO, JP, KE, KG, KH, KN, KP, KR, KW, KZ, LA, LC, LK, LR, LS, LU, LY, MA, MD, ME, MG, MK, MN, MW, MX, MY, MZ, NA, NG, NI, NO, NZ, OM, PA, PE, PG, PH, PL, PT, QA, RO, RS, RU, RW, SA, SC, SD, SE, SG, SK, SL, SM, ST, SV, SY, TH, TJ, TM, TN, TR, TT, TZ, UA, UG, US, UZ, VC, VN, ZA, ZM, ZW.

(84) Designated States *(unless otherwise indicated, for every kind of regional protection available)*: ARIPO (BW, GH, GM, KE, LR, LS, MW, MZ, NA, RW, SD, SL, ST, SZ, TZ, UG, ZM, ZW), Eurasian (AM, AZ, BY, KG, KZ, RU, TJ, TM), European (AL, AT, BE, BG, CH, CY, CZ, DE, DK, EE, ES, FI, FR, GB, GR, HR, HU, IE, IS, IT, LT, LU, LV, MC, MK, MT, NL, NO, PL, PT, RO, RS, SE, SI, SK, SM, TR), OAPI (BF, BJ, CF, CG, CI, CM, GA, GN, GQ, GW, KM, ML, MR, NE, SN, TD, TG).

Declarations under Rule 4.17:
— *as to the applicant's entitlement to claim the priority of the earlier application (Rule 4.17(iii))*

Published:
— *with international search report (Art. 21(3))*

(54) Title: DETECTION OF PHOSPHOKINASE SIGNATURES

(57) Abstract: The disclosure provides methods and compositions for determining the kinase activity profile of a biological sample, e.g., that contains multiple kinases.

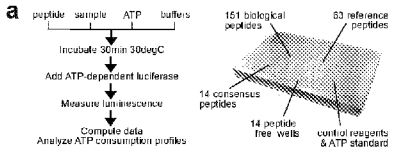

Fig. 1

WO 2019/200245 A1

DETECTION OF PHOSPHOKINASE SIGNATURES

CROSS-REFERENCE TO RELATED APPLICATIONS

[0001] This application claims priority benefit of U.S. provisional applicaton no. 62/657,620, filed April 13, 2018, which is incorporated by reference in its entirely for all purposes.

BACKGROUND OF THE INVENTION

[0002] In a functional sense, cancer is a proteomic disease that arises from selectively diverted signaling pathways[1,2]. Kinase phosphorylation cascades function as adaptive networks that are re-wired by oncogenic processes[3-7]. Half of all cancer-drugs that are FDA-approved or in clinical trials target hyperactive kinases, such as BCR-ABL, $BRAF^{V600E}$ or HER2[8,9]. While therapeutic decisions increasingly rely on the detection of mutated kinase genes or aberrantly expressed/phosphorylated proteins, few experimental platforms are practical enough to directly and comprehensively monitor the activity of kinase enzymes[10], and thus the key actionable dependencies of tumors remain often unclear[11,12]. A technology capable of identifying the phospho-catalytic signatures of kinases in biological samples could benefit the bio-medical field and improve therapeutic guidance.

[0003] Proteomic detection systems use the phosphorylatable regions of proteins to infer kinase activity. Antibody-based assays measure (phospho-)protein levels, which depend on availability and specificity of antibodies[1,13-15]. Mass spectrometry techniques[16-21], sometimes combined with kinase inhibitors[22-25], allow detection of raw amounts of (phospho-)proteins, but remain restricted due to cost, equipment and protocols. Alternatively, generic amino-acid sequences are used as individual biochemical probes to directly detect the phospho-catalytic activity of kinases in radioactive-labeling assays, microfluidic electrophoresis systems, ATP-consumption tests, hybrid peptide/phospho-antibody platforms, or SPR and FRET techniques[26-33]. Readouts from these approaches, however, rely on broad-spectrum consensus peptides originally designed for one-probe-to-many-kinases detection methods, well suited for pharmacological drug screens, but not intended to specifically identify or differentiate between kinases' activity in biological extracts.

BRIEF SUMMARY OF SOME ASPECTS FO THE DISCLOSURE

[0004] Provided herein is a new technological resource to distinguish and measure the phospho-catalytic activity of many kinases in parallel. This strategy relies on collections of peptide probes that are derived from the biological target sites of kinases[34,35], and are physically used as distinct combinatorial sets of sensors to monitor the activity of kinases in samples. The technology is modular by design: users can adapt probe libraries and assay conditions to their needs. Using a proof-of-concept 228-peptide library, computational methods to analyze phospho-catalytic signatures established from high throughput ATP-consumption measurements are provided in the examples section, which illustrate the present invention. Further, aspects of the invention relate to identification of kinase targets in specific types of cancer. For example, an analysis of $BRAF^{V600E}$ tumors for kinase activity is provided as an illustration. $BRAF^{V600E}$ colorectal cancers (CRC) and melanomas (MEL) remain clinical challenges, with poor prognosis and mostly palliative treatment options, that likely involve kinase-signaling pathways, which can hold the key to new therapeutic opportunities. In one aspect, this approach is used to identify new druggable kinase nodes that drive the unresponsiveness of CRC and MEL to anti-$BRAF^{V600E}$ therapy in cell models and patient tumors. Additional benefits of the present invention will also be apparent to one of skill in the art, *e.g.*, as discussed in the EXAMPLES section.

[0005] In some aspects, the disclosure is thus based, in part, on a high-throughput system to measure the activity of kinase enzymes using their biological peptide targets as phospho-sensors. In some embodiments, the disclosure provides a target peptide set to detect the activity of multiple kinase/kinase families, including, *e.g.*, ABL, AKT, CDK, EGFR, GSK3B, MAPK and SRC, using a multiplex assay, *e.g.*, an ATP-consumption screen, to identify the activity of kinases of interest to be evaluated, *e.g.*, kinase activities in cancer cells. Further, in some aspects, the disclosure provides methods and compositions for the analysis of drug sensitivity, *e.g.*, drug-sensitivity to BRAFV600E-targeted therapy in colorectal cancer; and identifies phosphocatalytic signatures of melanomas for designing and implementing therapies.

BRIEF DESCRIPTION OF THE FIGURES

[0006] Fig. 1. Libraries of biological peptides function as combinatorial sensors to identify, differentiate, and measure the phosphorylation activity of kinases.

(a) Schematic of the assay procedure.

(b) Unsupervised hierarchical clustering of phospho-catalytic activity signatures of 25 recombinant kinases established from 228 peptides. For each experimental run, the average value of ATP consumption across the 228 peptides was used for internal normalization. The kinase activity per-peptide was then calculated as the difference in ATP consumption between individual peptide-derived values and the overall internal mean. Next, peptide-specific activity values were averaged across independent repeats to establish the phospho-activity signature of each kinase for all peptide sensors. Finally, the 228-peptide-derived phospho-catalytic signatures of the 25 recombinant kinases were analyzed using unsupervised hierarchical clustering. Phospho-catalytic profiles are color-coded based on the relative level of activity measured in presence of each peptide, from blue for low-or-no activity, to white for intermediate-or-mean activity, to red for high phospho-catalytic activity. The red/gold/grey peptide color-key on the right side of the phospho-catalytic heatmap indicates the origin of peptides (biological, generic positive control, or random). The number of independent experimental repeats per kinase (*n*) is listed underneath the heatmap. The same concentration of recombinant kinases was used (see Supplemental Methods).

(c) Pearson-correlation heatmap highlighting the functional relationship between kinase enzymes established from their differential spectrum of 228-peptide-specific phospho-catalytic activities. Kinases are arranged by alphabetical order within their respective families.

(d) Profile of AUC values obtained for an increasing number of randomized sampling combinations of peptide sensors to predict the identity of HCK. AUC values (y-axis) reflect the performance of HT-KAM assay for predicting HCK's identity by comparing the 7x 228-peptide phospho-signatures of HCK versus the 113x 228-peptide phospho-signatures measured for all other 24 kinases, when relying on one or multiple peptide sensors (x-axis; random peptide sampling of a combination of up to 50 peptides out of 228). The AUC values corresponding to Diagonal Linear Discriminant Analysis (DLDA) classifiers that match HKC's specific all-biological peptide subset is shown as a red dot; HCK's all-generic positive control peptide subset as a gold dot; all-random peptides as a grey dot; exact AUC values and number of peptides for each combination are indicated.

(e) Distinct subsets of peptides can be identified as functional predictors of the differential activity signature of each kinase family. The number and origin of peptides composing the differential phospho-signature of kinases is shown in the bar graph. Peptides were classified as 'predicted' (dark shade) or not (i.e. 'other'; light shade), where 'predicted' defines a peptide sequence previously identified in the literature as a target of a given kinase. For a

biological peptide, it is an amino acid sequence that corresponds to a known phosphorylatable protein region[34], and for a generic positive control peptide it is an amino acid sequence that is commercially available. The AUC of each peptide set per kinase is listed underneath the graph.

5 (f) Phospho-catalytic profiles measured in presence of the biological peptide targets of AKT1, MAPK1/ERK2 or JAK2 kinase. The average activity per indicated biological peptide across '*n*' independent experiments is color-coded blue-to-white-to-red from low-to-medium-to-high kinase activity. Biological peptide probes are organized by decreasing phospho-catalytic activity per kinase. Each phospho-catalytic heatmap is shown side-by-side with a

10 grey-scale of significance (p-values for a pairwise t-test comparing the activity measured from '*n*' independent experimental runs for each biological peptide vs. the average activity measured with 5-random peptides). Average phospho-catalytic activities obtained from four distinct control peptide groups are shown for comparison at the bottom of each panel (random, Y/S/T-free, reference, or generic positive control).

15 (g) Box plots showing that the subsets of biological peptides specific to each kinase are associated with significantly higher levels of phosphorylation activities than activities measured from the pool of 5-random peptides. Box plot distribution of data displays minimum, first quartile, median, third quartile, and maximum. The difference in kinase activity experimentally measured with biological vs. reference peptides was highly

20 significant ($p<2E-100$; left vs. right set of box plots).

(h) Functional clustering of kinases based on the 151-biological peptides included in the assay. The analysis is based on all HT-KAM readouts, but only phospho-activity values derived from the 151 biological peptides were used for ranking analysis. Kinases belonging to distant genetic families are distinguishable. ABL and SRC kinases from non-receptor

25 tyrosine kinase families are identified as functionally related. Individual kinases of known distant biological/biochemical relationship with the rest of their genetic families can be singled out (e.g. $ABL1^{T315I}$; AKT2; MAPK14; SRMS).

(i) AUC forest-plots comparing the specificity/sensitivity of biological (red) vs. generic control positive (gold) vs. random (grey) peptide subsets. Biological peptides behave as good

30 functional sensors of kinases, and the identity of a kinase can be effectively predicted from the phospho-signature monitored with its subset of biological peptides.

(j) Enzymatic activity of ABL1 measured in presence of its 11-biological peptides, and either without treatment (left column; UNT) or treated with serial dilutions of ABL1-targeting

inhibitors imatinib and dasatinib (2 sets of 3 columns on the right; concentrations indicated at the top).

(k) Measurable effects of inhibitors on the activity of ABL1, ABL1^{T315I}, LYNA, AKT1 kinases using their biological peptides as reporters. Shifts in activity are represented as the average (colored dot) +/- StDev of the change in ATP consumption across all biological peptides in comparison to untreated control. While the activity of ABL1 was most reduced by these inhibitors, the anticipated specific effects of inhibitors was apparent by their relative low or lack of effect on ABL1^{T315I}, LYN A and AKT1 kinases (e.g. LYN A was affected by higher doses of Dasatinib). Staurosporine was used as a non-specific control of kinase activity inhibition.

[0007] Fig. 2. Mapping the phospho-catalytic signatures of cancer cells in their native or drug-treated/resistant states, identify their specific kinase dependencies and reveal their differential vulnerabilities to single and combinatorial kinase-targeting therapies.

(a) Identification of kinases known to participate in the response of BRAF^{V600}E CRC cells (WiDr) to BRAF^{V600E}-targeting therapy (VEM). Western blots for total and phospho- protein MEK1/2, ERK1/2 and EGFR are shown as controls on the left. Change in activity of these kinases after VEM treatment was measured using their respective subsets of biological peptides (shown as heatmaps and bar graphs). Briefly, for each experimental run, the average value of ATP consumption across the 228 peptides and 14 data-points from cell extract alone (i.e. established from 14 peptide-free control wells per 384-well plate) was used for internal normalization. Each sample's kinase activity per-peptide was then calculated as the difference in ATP consumption between individual peptide-derived read outs and the internal mean. Next, the peptide-specific activity values were averaged across independent repeats (3 independent biological replicates tested in 4 independent technical replicates). Finally, the difference in phosphorylation activity per peptide between VEM and UNT profiles was calculated across all 228 peptides. Results are represented as a series of kinase-focused heatmaps using their particular subset of biological peptides (top right panel). Each colored bar represents the differential activity in presence of a biological peptide of the indicated kinase, ranging from blue-to-white-to-red to respectively indicate lower-to-unchanged-to-higher activity after VEM treatment. The number of biological peptide sensors per kinase is indicated underneath the name of the kinase. A relative cumulative index of activity for each kinase was plotted as an indicator of the differential kinase signatures found in VEM-treated samples versus their control counterpart (bar plot on the bottom right; average of differential

activity values across all kinase-specific biological peptides, divided by the number of peptide sensors). Significance is measured in pairwise Student t-test comparisons between VEM and UNT across all runs (*/#: $p<0.05$; **/##: $p<0.01$), and either including all biological peptide sensors (*/**), or 75% of peptides that followed the main activity trend (#/##) to elude cross-reaction effects due to parallel feedback activation loops such as AKT or EGFR as illustrated from the biological peptide targets of ERK2 that paradoxically display higher activity (red bars at the top of the ERK2-heatmap) but relate to proteins directly involved in mechanism of therapeutic resistance, such as the EGFR-pathway[4,36] or TGFBR-pathway[47].

(b) Identification of new kinases that mediate intrinsic resistance to $BRAF^{V600E}$-targeted therapy in WiDr CRC cells.

(c) Validation of changes in activity of kinase enzymes using western blot. For example, increased phospho-S473 AKT1 relates to increased AKT1 activity, while increased phospho-S9 GSK3B foretells decreased GSK3B activity.

(d) Response of WiDr cells to combinatorial-targeted therapies. Survival graphs show cell growth sensitivity profiles to dual targeting of $BRAF^{V600E}$ + AKT1 or PDPK1 or PRKCA. Table insets provide characteristics of response to drug combinations: C.I. = combination index following Loewe Additivity model and measured as the average growth inhibition for VEM≤2uM and 2nd drug≤GI50 concentration (arbitrary threshold: synergy CI≤0.6; additivity 0.6<CI≤1.0); D.I. = drug interaction (two-way ANOVA p-val). Drug responses serve as a validation of kinase activity signatures found by HT-KAM screening, as well as a discovery of new vulnerabilities.

(e) Peptide phosphorylation activity signature of cancer cell lines. For each experimental run, the average value of ATP consumption in sample-containing wells measured across 228 peptides and 14 peptide-free controls, was used for internal normalization. The activity per-peptide was then calculated as the difference in ATP consumption between individual peptide-derived read outs and the internal mean. Next, phosphorylation activity values measured for each peptide were averaged from ≥3 independent replicates for each cell line. Finally, the phospho-catalytic activity signatures measured across the 228-peptide sensors were subjected to unsupervised hierarchical clustering. Phospho-catalytic activities are color-coded based on the relative level of activity measured in presence of each peptide for each cell line, from blue for low activity, to white for intermediate-or-mean activity, to red for high activity. The peptide class is indicated as a red/gold/grey color streak on the right side of the heatmap.

(f) Kinase activity signature of cancer cell lines. For each cell line, the activity of kinases was calculated as the average of the phosphorylation activities measured in presence of their respective biological peptide subsets. The profiles of 60 individual kinases or kinase families detected with ≥4 biological peptides are shown. Unsupervised hierarchical clustering was applied across both kinases and cell lines, and color-coded as a blue-to-black-to-yellow scale from low-to-medium-to-high activity. Profiles highlight the heterogeneity of kinases' activity across cancer cells. Control for ATP levels and protein concentrations across cells, and validation of phospho-signatures using complementary computational analysis, immuno-blotting, or drug treatment responses are available in **Figs. 18-22**.

(g) Comparison of kinase activity and drug sensitivity in two phenotypically distinct $BRAF^{V600E}$ cell lines: A375 (melanoma) vs. WiDr (colorectal), which are respectively considered to be inherently sensitive and resistant to BRAF-therapy. The activity of 10 different kinases was mean-centered between cell lines (y-axis) and compared to their GI50's (x-axis; drug concentration causing 50% inhibition of cell growth in 3-day assays) for 14 inhibitors. Color-coded drug names are indicated underneath each graph. Validation using a second, alternative drug was tested for four of the kinases. All drug concentrations are in uM, except dinaciclib and trametinib in nM.

(h) Graphical correlation of kinase activity with drug sensitivity. Kinase activity values (y-axis) correspond to activities shown in (c). The x-axis shows the sensitivity of A375 calculated as the Log_{10} of GI50(WiDr) / GI50(A375).

[0008] Fig. 3. Mapping the phospho-catalytic signatures of melanoma tumors reveals druggable kinases predictive of poor outcome and vemurafenib-unresponsiveness in $BRAF^{V600E}$ patients.

(a) Schematic of the procedure.

(b) Peptide phosphorylation signatures of patient tissues. Data analysis followed the same steps as for cancer cell extracts. HT-KAM data were clustered using Euclidean distance and ward linkage. Phospho-catalytic activity and peptide annotation are color-coded as indicated in the bottom right legend. Retrospective knowledge of survival outcome, recurrence and treatment-resistance are indicated above each map, along with their $BRAF^{V600E}$ mutational status. Within the deceased group, patients #4-5-9 were VEM-resistant (red squares), and patients #2-4-8 were ipilimumab-resistant (i.e. refractory to anti-CTLA4 immuno-therapy); **see Figs. 23-24** for details.

(c) Kinase activity signatures of tumor tissues. Analysis followed the same steps used to deconvolute the profiles of cell lines. For each tumor, the activity of kinases was calculated as the average of phosphorylation activities measured in presence of their respective biological peptide subsets (only kinases detected with ≥4 biological peptides are shown). Kinase activity profiles were mean-centered per tumor and then per kinase across samples. Semi-supervised hierarchical clustering was applied across kinases (tree on the left; Euclidean distance), while maintaining the order of patients established in (b). Kinases' catalytic activity is color-coded as a blue-to-black-to-yellow scale of relative low-to-high activity. Particular kinases are indicated by an arrow/letter on the right, and underline the balance between up/down-activation of proto-oncogenic kinases (RPS6KB, PIM, AKT) versus tumor suppressor kinase (GSK3B), either within each patient (top vs. bottom; e.g. VEM-resistant BRAFV600E mutated melanomas), or between patient groups (left vs. right; e.g. good vs. poor outcome).

(d) Table of kinases whose biological peptides are significantly represented among most differential peptides associated with survival outcome. The middle column shows significance based on enrichment analysis EASE – Fisher one-sided test using 34 out of 228 peptide sensors ($p<0.05$ as significance cut-off). The right column provides significance values (FDR-corrected Student t-test) using all (unselected) biological peptides per kinase subset, and comparing all experimental runs between surviving and deceased groups.

(e) Biological peptide-derived activity signatures of AKT, PIM, RPS6KB and GSK3B kinases averaged across tumors from VEM-resistant patients #4,5,9.

(f) Response of $BRAF^{V600E}$ melanoma cell lines to drugs that target vulnerabilities identified by HT-KAM assay. We chose to target AKT, PIM, RPS6KB and GSK3B kinases based on the kinase profiles of VEM-resistant patients shown in panels (c-e). The growth of A375 and Sk-Mel-28 cells was tested in presence of a range of concentrations of VEM (horizontal axis; concentrations indicated at the top) combined with a 2nd inhibitor (vertical axis; kinase target, drug name, range of concentrations indicated on the left) in 3-day survival assays. We elected to use Sk-Mel-28 cells because they are inherently highly resilient to BRAF-therapy. The relative scale of growth inhibition (GI) is color-coded (legend on the top left). GI heatmaps serve as visual indicators of whether the therapeutic index of BRAF-therapy alone can be improved when combined with a 2nd kinase-targeting drug.

(g) Streamlined side-by-side comparison of drugs' effects on cells' response to $BRAF^{V600E}$-targeting. Graphs show the percentage of growth inhibition (y-axis) resulting from combining VEM at various concentrations (x-axis) with a 2nd inhibitor at its GI50 concentration alone

(curves of VEM+2nd drug are color-coded; black lines represent the control VEM alone). The 2nd and 4th graph serve as control response profiles obtained from MTOR- and MEK-inhibitor treatment in A375 and Sk-Mel-28. Rectangles highlight the highest achievable response elicited by these various drug-combinations. Percent cell death at GI50 concentrations are provided underneath the graphs.

(h) Characteristics of drug combination effects. D.I. = drug interaction. C.I. = combination index following the Bliss Independence model and measured as the average of all experimental CI values (threshold: synergy CI<0; additivity CI=0; antagonism CI>0)[48].

(i) Primary tumor cells derived from a VEM-resistant melanoma PDX that displays high level of phospho-RPS6KB1 protein (used as readout of kinase activity), are sensitive to RPS6KB-targeting drug in 3-week colony formation assay.

[0009] Fig. 4. Source of peptide probes and arrangement of kinase assay plates.

(a) List of 228 peptides used in the assay. The table provides the connectivity details between kinases and peptide substrates (columns 3-5) for the 151 biological peptides, 14 generic positive control peptides, and 63 reference peptides included in the assay. Peptide ID's and categories are listed in the first two columns. The 25 kinases listed above the color-coded area (right side) are those tested in biochemical assay using purified recombinant kinases.

(b) Numerical-/color-coded connectivity used in table **(a)**. This defines the 'functional' relationship between each peptide lane and each tested recombinant kinase shown in table **(a)**. For instance, a peptide/kinase intersection coded 1-black corresponds to a biological peptide predicted from literature to be phosphorylated by the kinase indicated at the top of table. However, this same biological peptide is coded 2-yellow in adjacent columns, which indicates that other kinases are not predicted to phosphorylate this peptide/substrate target sites. Similarly, a peptide/kinase intersection coded 3-orange corresponds to a generic positive control peptide predicted from literature to be phosphorylated by the kinase indicated at the top of table. However, this same generic positive control peptide is coded 4-teal in adjacent columns, which indicates that other kinases are not predicted to phosphorylate this peptide/substrate target sites.

(c-d) Origin of peptide sensors. The functional relationship between kinases and peptides was previously established from computational curation resources built to mine public databases (see: website at http address cancer.ucsf.edu/phosphoatlas; US20120296880[1,2,15]). Panel **(c)** summarizes the curation process and molecular connectivity between kinases, substrate proteins, and phosphorylatable peptide target sequences. Panel **(d)** is a projection of the

coverage of biological peptide targets (left) and generic positive control peptides (right) per kinase across all human kinases/kinase families. Generic positive control peptides were curated from commonly available/advertised single-probe kinase assays or screens. The quantitative and qualitative coverage of peptides per kinase is represented as discs, which are dimensioned based on absolute number of peptide targets per kinase, and color-coded based on uniqueness of peptide targets per kinase.

(e) Biological peptide/kinase connectivity.

(f) Overall arrangement of individual 384-well plates. Besides the 228 peptides, each experimental plate includes: (i) 14 'peptide-free' wells (i.e. sample with buffers but without any peptide), (ii) internal duplicates for a series of peptides-containing wells and peptide-free wells, (iii) assay controls: ATP alone (ATP-loading control), kinase assay buffer alone, and ATP dilution standard.

[0010] Fig. 5. Activity signatures established for all recombinant kinases across all peptide sensors and all experiments.

(a) Repeatability of the assay across 120 different 384-well-plate assays. The graph shows a run-to-run comparison of activity profiles for individual kinases. The reproducibility of the assay was high, as measured by Pearson's correlation coefficient for replicate runs of 228-peptide-derived kinase activity profiles of 25 recombinant kinases, and based on >40,000 single ATP-consumption data points.

(b-e) Example of peptide-derived phospho-catalytic signatures for the JAK2 kinase. Four independent experimental runs are compared. ATP consumption profiles derived from luminescence readouts are shown in **(b)** and compared in **(c)**. Results transformed as internally normalized data by centering ATP consumption profiles against their overall 228-peptide-derived mean, are shown in **(d)** and compared in **(e)**. The stack bar graph in **(d)** visually shows that ATP consumption profiles follow similar trends across all different runs: most bars follow the same activity trend of "all-up/higher-than-the-mean", or "all-down/lower-than-the-mean", or "close-to-the-experimental-mean". This relates to the good correlation (>0.9) found between experiments as shown in table **(e)**, and in graph **(a)**.

(f-k) Cumulative bar plots for the other 24 recombinant kinases we tested. Each plot represents the stacked results of activities observed in experimental repeats and in presence of each individual peptide. In each graph, most bars follow the same "all medium" (around '0', i.e. mean kinase activity measured across all 228-peptides per experimental run), or "all-high" (above the mean), or "all-low" (below the mean) activity trends, which further

demonstrates run-to-run reproducibility and data consistency. Graph-to-graph comparisons (i.e. kinase-to-kinase) allow discerning kinases' specific catalytic signature.

(l) Cumulative bar plot resulting from merging all profiles of all 25 kinases/120 experiments together. Together, the comparison of panels **(d,f-l)** show that some peptides are associated with high kinase activity for a particular kinase, or a kinase family, or broadly across multiple kinases/kinase families. Some other peptides are associated with minimal kinase activity (see most negative stacked bars). Peptides from the pool of 63 reference peptides were broadly associated with low kinase activity. As also shown in main **Fig. 1b**, panels **(d,f-m)** show that differences in pattern and intensity of activity between members of a same kinase sub-family can be identified (e.g. ABL2 vs. ABL1; AKT2 versus AKT1/3; BRK, FRK or SRMS versus other SFK's; ERK2 vs. p38a). The differential activity of distinct kinase isoforms (LYN A versus LYN B) or 'wild type' versus oncogenic kinase (ABL1 versus mutated $ABL1^{T315I}$) can be found, which functionally corroborates what has been so far inferred from the differential interactomes (PPI) of distinct protein isoforms[16]. This shows that kinases affected by alternative-splicing events or 'minimal' genetic / oncogenic mutations can exhibit highly specific and distinctive phospho-catalytic functions (as if encoded by unrelated genes). Such results expand the anticipated complexity of cell signaling networks and their alternative cancer-state[1]. These data also illustrate the broad dynamic range (over 4 logs of magnitude) of measurable catalytic activities offered by the use of a large variety of peptides, and observable between different kinases. The differential distribution of 228-peptide-derived activities per kinase reveals that each kinase displays distinctive catalytic capabilities. These data show that the HT-KAM strategy is a robust discovery platform that detects and discerns the unique catalytic properties of different kinase enzymes.

[0011] Fig. 6. Dilution and time course assays. A subset of kinases and generic positive control peptide sensors commonly used in the field, were interrogated to assess the quality of the results generated with the HT-KAM assay platform.

(a) Activity of kinases measured at different concentrations and over time.

(b) Activity of kinases measured over time in presence of generic positive control peptides versus negative control (non-phosphorylatable) peptides. Significance is shown at the top of the box plot. Kinase-dead recombinant proteins or inactive kinase spliced isoforms (e.g. FYN C) were also used as negative controls to validate results from the assay (data not shown). Profiles in **(a-b)** match standards in the field, and show the quality of the assay was excellent.

[0012] Fig. 7. Comparison of dynamic range to data variation across peptides.

(a) Heatmaps of the top-20 peptides associated with the highest measurable activity per tested recombinant kinase. The first column of each kinase sub-panel indicates three peptide categories: (i) an orange square is for a kinase's generic positive control peptide (as advertised/commonly used); (ii) a yellow square is for any other generic positive control peptide out of the 14 generic positive control peptides included in the HT-KAM assay; (iii) a fuchsia square is for a biological peptide. The second column of each kinase sub-panel shows the peptide-phosphorylation activities for the top-20 peptides (red color scale). Activity profiles were normalized following the method applied in **Fig. 1b** and **Fig. 5**, i.e. raw luminescence data were transformed into ATP-consumption data, and then transformed in kinase activity profiles by mean-centering results across 228-peptide sensors per run and per kinase, before averaging profiles for each kinase and comparing significance of peptide phosphorylation profiles across experimental repeats. Activities are shown as a white-to-red scale (saturated red at +100nM above the mean ATP consumption measured across 228-peptide per kinase). In the third column of each kinase sub-panel, FDR-corrected t-test values per peptide probe are shown to assess the significance of activity profiles. The phosphorylation activities measured with each of the top-20 peptides were compared to the pool of 63-reference peptides included in HT-KAM assays across all experimental repeats for each kinase. FDR-corrected t-test values (BHp) are shown as a white-to-grey-to-black scale (white color cut-off at 0.05; saturated black at 1E-10).

These results indicate that, for many kinases, their best generic positive control peptides have a good, but not necessarily optimal, ability to report on their enzymatic activity. More specifically, the 'best' positive control peptide for 17 out of the 25 recombinant kinases did not correspond to one of their originally advertised generic positive control peptides (i.e. yellow surpasses orange for BLK, BRK, FRK, HCK, LCK, LYN A, SRC, YES1, ABL1, $ABL1^{T315I}$, EGFR, ErbB2, ErbB4, JAK2, CSK, AKT2, MAPK14). Furthermore, for 18 out of 25 kinases, biological peptides were better reporters than their best, originally advertised, generic positive control peptide (i.e. fuchsia surpasses orange for BLK, BRK, FGR, FRK, HCK, LCK, LYN A, SRMS, YES1, $ABL1^{T315I}$, EGFR, JAK2, CSK, AKT1, AKT2, AKT3, MAPK1/ERK2, MAPK14/p38a). In many instances, biological peptides can be considered as at least as good sensors of kinases' activity as currently available generic positive control peptides.

(b) Individual comparisons of FDR-corrected t-test across top activity reporting peptides per peptide category. This graph compares the significance (BH-p values) for the highest phosphorylation activities measured with the top peptide belonging to each of the three

categories: (i) best of the advertised/commonly used generic positive control peptide(s) for each kinase (orange dot); (ii) any other best generic positive control peptide (i.e. best of any of the 14 generic peptides other than the ones advertised for the indicated kinase; yellow triangle); (iii) best biological peptide (fuchsia lozenge). Along with data in panel **(a)**, kinase assays show that positive control peptides work well (as expected), but performance can be improved by using/including biological peptide sequences.

(c) Z-factor profiles. Comparing the dynamic range to data variation of 'positive' versus 'negative' controls is a standard method in the field to evaluate the performance of an enzymatic assay (i.e. Z-factor or Z'). We used this method to assess the quality of individual assays included in HT-KAM experimental sets, and to further assess how using different peptide probes impacts assay readout performance. Z' was evaluated by comparing ATP consumption values measured in presence of a peptide probe versus in absence of peptide (Z' = 1 – (3 * (StDev Pos + StDev Neg) / |Ave Pos - Ave Neg|)). Z' values from kinase activity profiles were calculated for the three kinds of peptide probes shown in panels **(a-b)**. Comparing the extent of the assay's dynamic range (~0.1 to ~250nM ATP consumption) to experimental variation (<1 to 20nM ATP standard deviation) using generic positive control peptides versus no-peptide negative controls (i.e. orange dots; measured across the 14 peptide-free wells), showed overall excellent performance of the HT-KAM assay at the level of individual peptide assays (average Z'=0.53). Yet, Z' could be significantly increased up to 0.59 when using "any" best peptide out of the 228 peptides included in the HT-KAM screen, and in particular when including biological peptide sensors (fuchsia lozenges). Along with results from activity and significance profiles shown in **(a-b)**, these data show that peptide sequences derived from biological substrate proteins are well suited to measure the phosphorylation activity of kinases.

[0013] Fig. 8. Profiles of Area Under the Curve (AUC) values obtained for an increasing number of randomized combinations of peptide sensors to predict the identity of an individual kinase or a kinase family.

(a-c) Progression profiles of AUCs for individual kinases and kinase families. In the analysis described below, the 'outcome' we wanted to predict was the identity of a kinase based on peptide activity profiles. For example, for AKT, the analysis outcome was "is this kinase in the AKT family: yes or no?" when using the activity profile from one or multiple peptides where peptide(s) were 'drawn' from any of the 228 peptides, and activities compared across all 25 recombinant kinases and all experimental repeats. To do so, Diagonal Linear

Discriminant Analysis (DLDA) class predictors were built for each kinase or kinase family using randomized combinations of an increasing number of peptides to discriminate one given kinase (or kinase family) from others. The performance of the DLDA classifier was defined as the AUC for predicting the identity of a kinase (or kinase family) from repeated iteration (i=1,000) of random peptide sampling. The confidence intervals of AUC's were computed using the DeLong method (from the pROC package of R). AUC values (y-axis) obtained for any number of combined peptides (x-axis) are shown as progression profiles of AUC's (box plots) for individual kinases (**a-b**) and kinase families (**c**). Plots show the effect of increasing n on AUC values, where n random peptides are drawn out of 228 peptides, and where *n* spans from 1 to a combination of 50 peptides (graphs in panels (**a,c**)) or from 1 to a combination of 100 peptides (graph in (**b**)). We analyzed individual kinases for which enough experimental repeats were executed (here we chose a stringent cut-off of ≥ 6 repeats; i.e. ABL1, AKT1, EGFR, MAPK1/ERK2, MAPK14/p38a, HCK, SRC; panels (a-b)), and for kinases grouped by subfamilies (with sufficient (≥6) repetitions per family; i.e. ABL, AKT, HER, MAPK, SFK; panel (c)). For each of the 50 boxplots per graph shown in (a,c), or for each of the 100 boxplots in the graph shown in (b), the line in the middle of each 'box' is the median of the data, the length of the box is 25% and 75% of the data, and the whisker is (25% - 1.5 x (InterQuartile Range)) (IQR) and (75% + 1.5x IQR). The outliers (points) are anything that falls outside of that range.

[0014] Results in (**a-c**) show that, for every kinase or kinase family, the sensitivity and specificity of a kinase-assay intended to measure their phospho-catalytic activity, is systematically improved when: (i) including an increasing number of combined peptide sensors; and/or (ii) when using particular subsets of peptides that perform significantly better than other combinations within a particular iterative number of peptides (i.e. higher AUC's within a given *n*-number of peptides). These results also show that some unique combinations of few peptides can behave as highly specific and sensitive reporters of a given kinase (i.e. these peptide subsets would be located toward the top left corner of each plot; note that the results of this method/analysis do not –however– define which peptide sets differentiate with the highest probability and highest specificity/sensitivity between different kinases, which is a question we resolve later in **Figs. 10, 11, 14, 15** and shows that biological peptide subsets happen to be exquisitely well-suited for). It can be noted from these data that, in the perspective of expanding the coverage of the HT-KAM platform to monitor more/other kinases, the computational analyses and modeled data in (**a-c**) already demonstrate that

including additional peptide probes would only increase the capability of the HT-KAM system to accurately predict the identity of more/different kinases out of their phospho-catalytic activity signatures. Together, these results demonstrate that our strategy of including a multiplicity of peptide sensors considerably improves the sensitivity and specificity of any kinase assay.

[0015] Fig. 9. Kinase phosphorylation activity measured in presence of individual generic positive control peptides. To further show that including a multiplicity of peptide sensors improves the performance of a kinase assay, we asked whether any individual generic positive control peptide could provide the specificity needed to accurately identify individual kinases.

(a) List of kinases whose activities are 'expected' to be measured with the positive control peptides included in the HT-KAM assay. The 14 generic peptides included in the 228-peptide library are commonly used as reporters of the phospho-catalytic activity of >63 individual kinases and >27 kinase families (e.g. ABL, AKT, ERK, HER, p38, SFK, TK, etc).

(b) Comparison of kinases' phosphorylation activity patterns across positive control peptides based on either what is anticipated from literature (top panel), or experimentally measured (bottom panel). In the top panel, the red-colored areas correspond to peptides expected to report on the activity of the indicated kinases, whereas the blue areas are not advertised as such. In the bottom panel, the blue-to-white-to-red heatmap corresponds to the experimental profile of recombinant kinases' activity levels measured in presence of these peptides. The bottom panel is an excerpt from the complete 228-peptide phospho-catalytic activity signature of kinases. In principle, the red areas from the top panel should match the 'redder' areas from the bottom panel, and, as critical, the blue areas from the top panel should match the 'bluer' areas from the bottom panel.

(c) Detailed comparison of kinases' activity level for each generic positive control peptide. The 14 individual graphs display the activity of all 25 recombinant kinases for each of the 14 peptides. In each graph, the red bars indicate catalytic activities expected to be the highest/most positive. Conversely, black bars are not anticipated to display high activity or any activity.

(d) Concordance between expected and experimental activities. The % concordance was evaluated based on whether experimental readouts belong or not to their expected activity groups (vertically: per kinase; horizontally: per peptide). The overall average concordance is ~52%. Cross-reactivity between kinases/peptides observed in **(b-d)** indicates that it would not

be possible to use any individual positive control peptide as a mean to specifically identify or differentiate a particular kinase from other kinases.

(e) Comparison of individual peptides' AUC to evaluate how specific and sensitive each of the 14 positive control peptides is to identify their respective kinases. AUCs were calculated from repeated iteration of single peptide sampling for kinases tested ≥6 times (i.e. HCK, SRC, ABL1, EGFR, AKT1, MAPK1/ERK2, MAPK14/p38a). This analysis compared all 228-peptide phospho-catalytic profiles across all 25 recombinant kinases and all experimental repeats (method described in **Fig. 8**). This method answers the question: "how good is an individual peptide at predicting the identity of a kinase?", and results can be interpreted as: "the higher a peptide's AUC is for a particular kinase, the more this peptide (and this particular level of phosphorylation for this peptide) is good at discriminating this kinase from all other kinases". The top section shows all calculated AUCs for all 14 positive control peptides across all interrogated kinases (color-coded scale of AUCs shown on the right; kinase name on top). A black side-bare next to AUC(s) designates positive control peptide(s) expected to report on the indicated kinase. To help compare the performance of individual positive control peptides' specificity and sensitivity, the bottom section displays the AUCs for 14 individual biological peptides with the highest AUCs for each kinase.

Results show that most individual positive control peptides do not provide the highest possible specificity and sensitivity for the kinases they are expected to report on. Furthermore, most individual positive control peptides are outperformed by individual biological peptides. These data provide new leads on how to improve single-peptide kinase assays using (biological) peptides found with the HT-KAM strategy. More critical to the concept underlying our study, these results underline why a multi-peptide approach is a valuable alternative to single peptide-based activity measurements when investigators want to specifically and differentially identify a given kinase from other kinases.

[0016] Fig. 10. Systematic identification of combinatorial peptide sets that best differentiate between kinase families. We implemented computational methods to define which unique set of peptides most significantly distinguishes a kinase from all other kinases. **(a-e)** Differential phospho-catalytic signatures of kinase families. The phospho-catalytic activity heatmaps of ABL **(a)**, AKT **(b)**, HER **(c)**, MAPK **(d)**, SFK **(e)** are established from the peptide subsets that best differentiate each kinase family from all other kinases. Peptide-IDs are listed on the right side of each heatmap. A scale of catalytic intensity is shown underneath (blue-to-white-to-red of mean-centered activities). The two color-coded columns

on the left of each heatmap show the type/origin of peptides, and the mean difference in activity: (i) peptide types or origin are shown in red shade (biological), yellow shade (generic positive control), grey (reference); (ii) the mean difference in activity is shown on the left, as an indicator of how significantly more (pink) or less (green) active a kinase family is in presence of the listed peptide that was included in their differential signature.

[0017] The first step of the computational method was to systematically compare each of the 228-peptide activity signatures from all kinases belonging to a given family with ≥ 6 experimental repeats (i.e. ABL, AKT, HER, MAPK, SFK), to the 228-peptide signatures of all other kinases belonging to all other families, and then select peptides associated with the most differential activities based on whether any of the 228 peptide-associated activity values passed or not a significance threshold of $p<0.05$ for both FDR-corrected t-test and Wilcoxon rank sum test. This implies that: (i) the selected, most differential peptides can be associated with either low, or high, or 'average' phospho-catalytic activities specific to a kinase family if it significantly contrasts with activities observed across all other kinases (following this principle, a peptide can be found as part of the differential signature of multiple kinase families owing activity levels and significances that are specific to the differential signature of its given kinase family versus all other kinases); (ii) the activities from the selected, most significantly differential peptides specific to a kinase family follow a trend that may vary from one individual kinase to another within that family (and between experimental read outs), and some individual kinases may also cluster away from the majority of other kinase family members (which underlines the functional precision of the combinatorial measurements provided by the HT-KAM assay toward the systematic identification of the specific functional attributes unique to a kinase family yet can distinguish sub-family members).

[0018] The second step of this analysis, was to extract all phospho-activity values that match the significantly differential peptides out of the 228-peptide-derived activity values for each individual family, and then apply unsupervised hierarchical clustering to group peptides and kinases based on their functional relationship (classification trees at the top and far left of each heatmap).

[0019] Each panel (**a-e**) also includes a graph on the top right that shows the Receiver Operating Characteristic (ROC) curve and AUC value calculated for the specific subset of most differential peptides for each kinase family. The method used to assess the performance of each peptide set (i.e. its sensitivity and specificity) was the same as the one used to predict

the performance of increasing numbers of random peptide sets described in **Fig. 8**. We used the 228-peptide / 25 kinases / 120 experiments dataset to build classifiers, and then predict and compare performance using the exact differential peptide set associated with each kinase.

[0020] As an example, panel **(b)** shows that a unique combination of 89 peptides out of 228 peptide sensors best differentiates AKT-family kinases from all other kinases/kinase families. This 89-peptide subset includes both significantly high, low and intermediate activity features of AKT that uniquely differentiate AKT from all other tested kinases. This unique set of 89 peptides is capable of detecting/identifying AKT with a high degree of sensitivity and specificity (i.e. AUC = 0.945). AKT's differential signature includes every type of peptides, whether biological, generic or reference, and whether phosphorylated or not by AKT. We complemented our analyses using Monte Carlo cross validation to further estimate how accurately our predictive model performed, which confirmed the validity of the differential peptide signature (data not shown).

[0021] Results in **(a-e)** show that differential peptide phosphorylation signatures can be assigned to every kinase families. This also demonstrates that using a multi-peptide activity-screening assay such as the HT-KAM strategy can find specific combinations of peptides that can serve as predictors of kinases' identity. As displayed in **(a-e)** and summarized in **Fig. 1e**, these results also indicate that the majority of peptides most capable of discerning kinases' unique phospho-catalytic activities are biological peptides.

[0022] **Fig. 11. Peptide sets that best differentiate individual kinases.** We applied the computational methods designed in **Fig. 10** to identify the subsets of peptides that most significantly distinguish an individual kinase from other kinases.
(a-e) Differential phospho-catalytic signatures of kinases. Differential signatures and AUCs were calculated for individual kinases with ≥ 6 experimental repeats: ABL1 **(a)**, AKT1 **(b)**, MAPK1/ERK1 **(c)**, MAPK14/p38a **(d)**, HCK **(e)**. We also identified the differential activity signatures of EGFR and SRC kinases, which respectively included 42 and 43 peptide features associated with AUC's of 0.840 and 0.893, and that successfully passed the significance threshold ($p<0.05$) for either FDR-corrected t-test or Wilcoxon rank sum test, but since they did not concurrently pass both criteria, we decided not to include their profiles here.
(f) Bar plot summarizing the number and origin of peptides composing each kinase-specific differential signature. Biological peptides constitute the majority of peptide sensors making the differential catalytic signatures of individual kinases.

[0023] Together, results from **Figs. 8-11** and **Fig. 1b-e** show that using an array of peptides to measure the activity of kinases is an effective approach to functionally distinguish and identify different kinases. Such multi-peptide sensor-based kinase identification system is superior to any single probe enzymatic assay, including assays relying on a generic positive control peptide or any individual peptide in general. The level of differentiability, sensitivity and specificity offered by our multi-peptide platform approach is such that all kinases/kinase families can be predictably identified based on their activity signatures. Even though some of the kinases we chose to examine can be considered as more difficult to distinguish since they are biologically closely related (e.g. SFKs or ABLs), our system was capable of identifying and differentiating them (a functional distinction that no individual peptide was able to predictably achieve). As well, the signatures of kinases of more distant biological functions/unrelated genetic families were more distinct from other kinases and systematically distinguishable (e.g. MAPKs or HERs). In fact, our computational analyses and experiential data demonstrate that if we were to test larger numbers of recombinant kinases belonging to more distant kinase families, their activities would be more divergent from other kinases, and thus easier to measure/identify. While these results imply that the HT-KAM strategy could be used as a discovery tool to identify peptide sensors most uniquely differential and predictive of the identity of a kinase/kinase family, these results also indicate that the biological peptides of kinases are an already available subsets of specific/sensitive/differential sensors that are well-suited to decipher between kinases and their respective levels of activity.

[0024] **Fig. 12. Phospho-catalytic signatures of kinases established from their respective biological peptides.** The computational analyses developed in **Figs. 10-11** and **Fig. 1e** show that biological peptides contribute most to the differential peptide signatures of kinases, so we asked whether kinases phosphorylate their respective biological peptide sequences.

(a-g) Activity profiles of recombinant kinases measured in presence of their respective biological peptides. Individual kinases are organized by kinase sub-families: AKTs **(a)**, MAPKs **(b)**, SFKs **(c)**, ABLs **(d)**, HERs **(e)**, and include JAK2 **(f)** and CSK **(g)**. The origin of peptides is indicated on the left of each panel. The phosphorylation activity per indicated biological peptide is averaged from 'n' independent experiments. Kinase activity is color-coded blue-to-white-to-red from low-to-medium-to-high activity (i.e. a white/dim color indicates measurable enzymatic activity within the spectrum of low-to-high activity). For each kinase heatmap, activities are organized by decreasing intensity from top/high to

bottom/low. The average catalytic activities obtained from three different peptide groups (random, Y/S/T-free, reference) are shown for comparison at the bottom of each panel. The t-test p-values comparing the activity profiles of each biological peptide to random or Y/S/T-free or reference peptide groups across all experimental runs for a given kinase (indicated by 'n' at the top of each kinase-specific panel), are represented as a grey scale.

(h) Box plots of kinases' activity measured in presence of either their biological peptide subset, or 5-random, or 16-Y/S/T-free, or 63-reference peptides. Each box plot distribution of data displays: minimum, first quartile, median, third quartile, and maximum. Each box plot includes all experimental values across all repeats. Normalization and analyses of profiles follow previously described steps. The number of biological peptides per kinase is indicated underneath each box plot in the top graph. The t-test p-values comparing the overall activity profiles established from biological peptide versus either of the three other peptide groups measured across all kinases, are indicated in brackets on the right side of the graphs (respectively $p<2E-100$, $p<2E-110$, $p<6E-121$).

(i) Table of significance comparing kinases' phosphorylation activity profile established from their biological peptide subsets versus either of the other 'control' peptide groups (i.e. random, or Y/S/T-free, or reference).

Results in **(a-i)** show that biological peptide probes established from substrate protein regions of kinases were overall associated with measurably and significantly higher levels of phosphorylation activities than 'control' peptides. More than 94% of all kinase activities measured in presence of their biological peptides were greater than activities measured in presence of the 5-random peptide set. Differences in kinase activity between biological and reference peptide sets were highly significant ($p<7E-11$ for AKT1, AKT3, MAPK1/ERK2, FYN A, HCK, LYN A, ABL1, and JAK2; $p<4E-2$ for AKT2, MAPK14/p38a, BLK, BRK, LCK, LYN B, SRC, HER2, HER4). Individual kinase activity values derived from their individual biological peptides were significantly different from the reference peptide set (27.2% with $p\leq0.01$ and 66.7% with $p\leq0.05$). Kinase activity levels were also significantly higher when measured in presence of their 'non-modified' biological peptides than with their mutated or pre-phosphorylated counterparts included in the assay (see **Fig. 13** for details). Finally, phosphorylation activities measured with biological peptides of nearly identical sequences were similar (e.g. MTOR T2446 and MTOR S2448; CDKN1A T145 and CDKN1A S146; RAF1 Y340 and RAF1 Y341; JAK2 Y1007 and JAK2 Y1008; GSK3B S9 and GSK3A S21), which further demonstrates the repeatability of the kinase activity measurements made with their biological peptides.

(j) Unsupervised hierarchical clustering of kinases' functional signatures using only biological peptides. The clustering of kinases (top) demonstrates that the 151 biological peptides included in the assay are excellent functional discriminators of kinases' catalytic signatures. Kinases belonging to a same sub-family most closely resemble each other, while most functionally distant kinases segregate away from each other.

Together, results in **(a-j)** demonstrate that biological peptides are effective combinatorial sensors to functionally differentiate kinases from each other, and to measure the enzymatic activity of their respective kinases. Kinases are significantly and specifically more capable of phosphorylating a vast majority of their predicted biological peptide targets than reference peptide sets.

[0025] Fig. 13. Comparing the activity of kinases measured in presence of their biological peptides versus modified peptide counterparts. To further assert the preference of kinases to phosphorylate their biological peptide targets, we compared how significantly different the levels of phosphorylation activity of kinases were when measured in presence of their biological targets versus in presence of the mutated or pre-phosphorylated biological peptide counterparts.

(a) Difference in the activity of kinases comparing pairs of non-modified versus modified biological peptide sequences. In the waterfall plot, each teal bar shows the difference in activity between a biological peptide and its mutated (Y / S / T → G) counterpart. Each violet bar shows the difference in activity between a biological peptide and its pre-phosphorylated (Y / S / T → pY / pS /pT) counterpart. Each peptide pair substrate's origin and target site along with its kinase is indicated underneath the graph. Results are derived from all experimental measures for all kinase. The significance of the difference in activity in presence of two different peptides was assessed in pairwise comparisons between experimental runs (grey scale of t-test values underneath the graph).

(b-c) Overall comparison of activity profiles of Tyrosine kinases or Serine/Threonine kinases measured in presence of their predicted Y/S/T-containing biological peptides versus any Y/S/T-free biological or reference peptide. The phosphorylation activities of both Tyrosine kinases and Serine/Threonine kinases are significantly higher in presence of their Y/S/T-containing biological peptides than any Y/S/T-free biological or reference peptides.

[0026] Along with results in **Fig. 12**, data in **(a-c)** indicate that the variety of biological peptides and control peptides included in our assay provides a practical framework to systematically validate and compare activity profiles within individual assays, or across

technical repeats, or between different samples. These analyses show that kinases significantly prefer to phosphorylate their 'un-modified' biological peptide targets.

[0027] Fig. 14. Using HT-KAM as a 'discovery platform' to identify best targets of kinases, finds that biological peptides are systematically included among the most significantly high activity profiles of kinases.

(**a**) Binary heatmap showing peptides associated with high (red) or low (blue) activity for each kinase. For this analysis, each kinase was tested independently of all others, and we used two separate computational approaches to compare levels of ATP consumption per individual peptide to the pool of 63-reference peptides.

[0028] In the first approach, the average 228-activity data points from all experimental repeats was used in a Kalmagorov-Smirnov (KS) test comparing each 165-non-reference peptides (i.e. 151 biological peptides, and 14 positive control peptides) to the 63-reference peptides (p values with or without BH correction controlling for false-discovery rate). In parallel, the mean and standard deviation (SD) of the 63-reference peptides was computed to then identify which peptides among the 165-non-reference peptides display activity signals >2 fold SD from the mean (>highest 2.5% of reference).

[0029] In the second approach, all experimental replicates (instead of averaging them as in the first method) were used in either a linear additive model with BH corrected p-values from each 165-non-reference peptide versus 63-reference peptide (BH.p.lam<0.05 threshold), or an ANOVA model with BH corrected replicate error.

[0030] The overlapping results of these two approaches and their statistical cut-offs identify the most significantly and stringently selected high –and low– activities per peptide per kinase. This highly conservative method finds that 110 biological peptides act as best probes/sensors of kinases' individual phospho-catalytic activities. Binomial high/low activity levels are represented as a heatmap in this panel (**a**; high in red, low in blue), along with the 25-tested recombinant kinases organized by subfamily (indicated at the top), and the identified 124 peptides organized based on unsupervised clustering (correlation tree on the left; peptides probe ID's/origin on the right).

(**b**) Analysis of activity profiles established in presence of inhibitors to validate results found in panel (**a**). Here, the underlying postulate is that, when the activity of a kinase is measured in presence of an inhibitor, any peptide associated with a significant decrease in activity may

be considered as a suitable probe to detect the activity of this kinase. Such data would also retrospectively validate (or not) the previously identified peptides from the method in (**a**). In the three graphs shown in (**b**), the model system uses ABL1 or LYN A kinases, and serial dilutions of imatinib or dasatinib.

[0031] For instance, quadrant **A** shows a strong correlation between levels of inhibition (captured by the Pearson correlation coefficient between imatinib concentration and ATP consumption for each peptide; y-axis), and the activity level per peptide in an untreated context (x-axis) (R^2 (Fisher(inhibition), activity) = -0.48; p = 2.75e-14). Importantly, the relationship between the activity levels of (all 228) peptides incubated with ABL1 in an untreated setting and their level of inhibition under increasing concentrations of imatinib, also showed that the peptides that report higher activity levels of ABL1 kinase (i.e. dots located toward the right end of the x-axis; indicating highest ATP consumption), exhibit greater inhibition of that activity in presence of increasing concentrations of imatinib (i.e. dots located toward the bottom end of the y-axis; indicating strongest negative correlation and thus strongest inhibition). These peptides (bottom right area) largely overlap with the peptides found with the previous method in (**a**) (indicated as red dots in quadrant **A**). For instance, biological peptides JUN Y170, CDK5 Y15, WASL Y256, or BTK Y223 are at the top of the list of peptides most significantly associated with high ABL1 activity, and they also show strong inhibition of activity in presence of imatinib (shown as red dots in (**b**)), which confirms that they are ABL1 substrates targetable by anti-ABL1 therapeutic drug. So, these data are a finding consistent with the initial validation purpose of the analysis. Importantly, this method also finds that the biological peptide targets of ABL1 are most systematically and significantly associated with the measurable response of ABL1 to ABL1-inhibitors (besides the 4 peptides previously mentioned, this method also finds JAK2 Y1007, MAP4K1 Y232, ABL1 Y226, TP73 Y99, CDKN1B/p27 Y88, MDM2 Y394, RAD51 Y54 as good reporters of ABL1's activity; shown in main **Fig. 1j**).

[0032] Similar results were obtained for dasatinib-treated ABL1 (quadrant **B**) and dasatinib-treated LYN A (quadrant **C**) using the same experimental validation approach and statistical analysis.

[0033] (**c-d**) Comparison of the most repeatable peptide-derived activities of ABL1 to the spectrum of activities established from the differential signature of ABL1. Following the x-axis of the graph shown in (**c**), the 22 peptides that behave as the most internally robust

sensors of ABL1 activity are represented as 14 green squares + 8 black triangles (data derived from the analysis used to generate panel (**a**)). Following the y-axis of this graph, the 40 peptides that best differentiate ABL1 activity signature from all other kinases' signatures are represented as 32 purple lozenges + 8 black triangles (data established in **Fig. 11a**). The dashed rectangles (i) and (ii) outlined in graph (**c**) match the dashed areas (i) and (ii) in panel (**d**), where peptides' IDs/origins are listed. The red-filled or red-highlighted-margin squares or lozenges or triangles or circles in (c) correspond to biological peptide targets of ABL1 as defined by PhosphoAtlas and included in the HT-KAM peptide library. Noticeably, all ABL1's biological peptide targets are located on the top right corner of the graph (i.e. reporting on high ABL1 activity). This analysis also finds that peptides associated with significantly low/minimal ABL1 activity correspond to biological targets of Ser/Thr-kinases (dashed rectangle (ii) in the lower left area in (**c**) and listed in panel (**d**) as biological peptides established from phospho-target sites: AKT1 T308, MAP2K1 T192, SOS1 S1193, BRCA1 S988, NFkB1 S907, SMAD2 T8, CREB1 S133, EGFR T678). These observations directly support why combinations of 'disparate' biological peptides are intrinsically good discriminators and identifiers of different kinases.

[0034] (**e-f**) Venn diagrams intersecting results from analysis in (**a**) (i.e. robustness of peptide-phosphorylation activities) and analysis in **Fig. 11** (i.e. most differential peptide activities). Results similar to ABL1 data (e) were found for other kinases, such as AKT1 (**f**), or SFK's, HER's, MAPK's (data not shown). In all cases, biological peptides act as robust sensors of the differential and individual phospho-catalytic activity signatures of kinases.

[0035] Based on the computational methods we developed and peptide library we designed to showcase our system, we find that biological peptides are systematically associated with most significantly and measurably high activity profiles of kinases.

[0036] **Fig. 15. Comparison of the specificity and sensitivity of kinases' signatures established with their biological peptide subsets, or their generic positive control peptide sets, or random peptide sequences.**

(**a-b**) ROC curves and AUC profiles of kinase families and individual kinases. The ROC curves and AUC values of each kinase measured with their specific subsets of either all-biological (red), or all-positive (gold), or all-random (grey) peptides are shown as lines and annotated within each graph. ROC curves and AUC values were established using the method explained in **Fig. 8**.

(**c**) Comparison of AUCs measured across kinases and measured from all-biological (red) vs. all-positive (gold) vs. all-random (grey) vs. differential (violet) peptide sets. Averages, standard deviations and p-val are calculated from AUC's values shown in (**a,b**) for biological (red), positive (gold) and random peptides (grey), and from AUC's values for the differential peptide subsets (violet) that were analyzed in **Figs. 10-11**.

[0037] Results from these plots show that the combinations of biological peptides are very good predictor of kinases' identity. Specifically, for kinase families ABL, AKT, HER, and MAPK, and for individual kinases AKT1, EGFR, MAPK1/ERK2, HCK, SRC, the AUC values obtained from their biological peptides are excellent (on average >0.94). It can be noted that the somewhat lower AUC observed for SFK's biological peptides (i.e. 0.859) was attributable to peculiar activity differences from individual SRC family members. Indeed, the AUC derived from the predicted biological peptides of SFK's was increased when the most dissimilar members of the SFK family and their related peptides were 'excluded' (AUC augments from 0.859 to >0.92, while singling out FGR and FRK kinases along with SRMS and BRK as majorly distinctive functional subclasses among SRC kinases, and in fact display little overlap among subsets of biological peptide target pools, hence the differential effect on specificity and sensitivity of SFK's catalytic signatures; analysis/data not shown). Following such principle, entire predictions on the functional distance between kinase enzymes (instead of kinase genes) could be made, and could reshape kinase classifications. This concept also relates to the good-yet-somewhat-lower AUC found for the MAPK family, since the two recombinant MAPK's (ERK2 vs. p38a) we studied are functionally/biologically quite distant from each other, and thus their enzymatic activities for their respective biological peptides are fairly dissimilar (which was already noticeable in earlier analyses/figures).

[0038] In addition, it can be noted from panel (**c**) that the specificity/sensitivity (AUC's) from biological peptide subsets performed almost to the same degree as the differential peptide sets computationally identified in **Figs. 10-11** (e.g. ABL AUC(biological peptide set; n=11) = 0.974 vs. ABL AUC(differential peptide set; n=34) = 0.911; AKT1 AUC(biological peptide set; n=20) = 0.986 vs. AKT1 AUC(differential peptide set; n=27) = 0.977; HER AUC(biological peptide set; n=22) = 0.967 vs. HER AUC(differential peptide set; n=76) = 0.948)). AUC's from positive control peptide subsets performed systematically and significantly less well.

[0039] These results demonstrate that biological peptide subsets are well-suited predictive sensors to specifically, sensitively, and differentially detect their respective kinases. These data underline the strict precision of the HT-KAM assay/data analysis system we developed, and its ability to accurately account for peculiar functional differences between kinases, including between individual kinases otherwise considered as genetically related.

[0040] Fig. 16. Measuring the effects of kinase inhibitors using biological peptides. Measuring the effects of inhibitors on kinases' activity is a good way to evaluate the performance of biological peptides as sensors of kinases. So, we tested whether biological peptides of kinases reported on the inhibited activity of their kinases in presence of drugs at multiple concentrations.

(a) Table of IC50 concentrations of imatinib, dasatinib, and staurosporine for ABL1, $ABL1^{T315I}$, LYN A and AKT1 kinases. IC50 values are indicative averages established from IC50 estimations measured in biochemical assays reported in the literature.

(b) Monitoring the effects of kinase inhibitors on the activity of ABL1, $ABL1^{T315I}$, LYN A and AKT1 kinases using their respective subsets of biological peptides as sensors of changes in activity. Experimental concentrations of imatinib and dasatinib correspond to 0.01x, 1x and 100x IC50 concentrations specific to ABL1 (i.e. 0.002uM, 0.2uM, 20uM, and 0.01nM, 1nM, 100nM, respectively). These concentrations are thus anticipated to affect the other recombinant kinases tested here ($ABL1^{T315I}$, LYN A and AKT1) with less or little-to-no effect on their levels of activity. This means that the relative differences in reported IC50 concentrations between ABL1 and LYN A for imatinib (0.2 versus 100uM) and dasatinib (1 versus 9nM) can be used to compare the measurable differences in effects of inhibitors. As well, AKT1 can be used as a 'negative control' for lack of response. Every experimental phospho-signature was initially measured across all-228 peptides, and either in presence or absence of inhibitor (i.e. each sample profile was normalized against the mean activity level measured across 228 peptides, and then averaged across all 3 independent replicates of each of the 8 different conditions for all 4 kinases). Only activities measured in presence of the predicted biological peptide targets of each kinase are shown (11 biological peptides for ABL1; 8 for LYN A; 20 for AKT1). The effect of increasing concentrations of inhibitors can be compared to control untreated (UNT) activity profiles (compare far left column to the two sets of three columns on the right). The sensitivity of ABL1, $ABL1^{T315I}$, LYN A and AKT1 kinases to imatinib and dasatinib can be assessed from changes in activity measured from their individual biological peptides. The averages of the kinase activity values measured

across their biological peptides in each experimental condition are provided at the bottom-end of the panel (blue-to-black-to-yellow scale of average ATP consumptions).
(c-e) Evaluation of the effects of inhibitors on kinase activity profiles using complementary analytical methods. In **(c)**, each 228-peptide-activity profile of each sample was first normalized against the baseline activity level measured from the 14 peptide-free well controls included in each experimental 384-well plate, and then each single peptide-derived activity level measured in presence of inhibitor was compared to the activity level found in untreated sample (i.e. all activities from all peptides in untreated sample become the baseline '0' value). Results of the average of the differential ATP consumption comparing inhibitor-treated versus untreated for each biological peptide are shown as color-coded kinase activity profiles in (c). (These data were used to plot Fig. 1k.) High concentration (10uM) of staurosporine is included as control of general shut down of kinases' activity.
In **(d)**, entire 228-peptide activity profiles of $ABL1^{T315I}$ comparing untreated versus imatinib- or dasatinib- treated samples were investigated for potential trends in inhibitory effects following the principles and statistical methods used in **Fig. 14b**. These data validate the overall lack of inhibition of $ABL1^{T315I}$ observed with imatinib using its biological peptides in **(b-c)**. A general dampening effect of dasatinib on $ABL1^{T315I}$ activity was observed (bottom graph in **(d)**; almost all 228 peptide probes display a negative R^2), which may relate to lower activity levels measured with some of the biological peptides shown in **(c)**.
In **(e)**, the analysis used ATP consumption levels measured in presence of peptides most robustly associated with high activity of ABL1 (derived from the analysis described in **Fig. 14a**, and including biological peptides). Results directly validate the gradually inhibited activity profiles found in panels **(b-c)**.

[0041] These data also enabled cross comparing the differential sensitivity of kinases to these different drugs. For instance, the mean correlation coefficient (meanR^2) relating ATP consumption and dasatinib concentration was -0.997 (SD=0.003), -0.766 (SD=0.21), -0.33 (SD=0.09) for ABL1, LYN A and $ABL1^{T315I}$ respectively (calculated using peptides associated with kinases' highest catalytic activity, including their biological peptides). So, dasatinib had the strongest inhibitory effects on ABL1, followed by LYN A, and had some limited but measurable effect on $ABL1^{T315I}$. As an additional validation of these data, a formal comparison of the t-test to the Fisher-transformed correlation coefficients established from the levels of drug inhibition measured either with the high-activity peptide group, or with the 63-reference peptide group (which is one of the principal peptide control groups

used to analyze HT-KAM readouts), showed that dasatinib inhibited significantly more the subsets of (biological) peptide targets of ABL1 and LYN A than the reference set (respective T-test (fisher): p=1.087e-07 and p=3.081e-06), but the effects of dasatinib did not differ significantly between these peptide groups for $ABL1^{T315I}$ (T-test (fisher) p=0.41; which is explained by the general dampening of activity profiles in (**d**)). Based on experimental conditions tested here, data indicate that the IC50 concentration of dasatinib for ABL1 may be relatively higher than the anticipated 1nM (but far lower than 100nM), while IC50(dasatinib) for LYN A is between 1 and 100nM (and probably close to the anticipated 9nM). Using the same series of comparisons and peptide sets, the imatinib drug could be identified as a strong inhibitor of ABL1 (mean(R^2)=-0.847; SD(R^2)=0.111), with no effect on $ABL1^{T315I}$ (mean(R^2)=0.66; SD(R^2)=0.025; which is the basis of the failure of imatinib therapy in leukemia), but with measurable, although limited, inhibitory effect on LYN A (mean(R^2)=-0.462; SD(R^2)=0.49). T-test to the Fisher-transformed correlation coefficients measuring levels of drug inhibition formally showed that imatinib inhibited significantly more the subsets of (biological) peptide targets of ABL1 and LYN A than the reference peptide set (p=0.00252 and p=2.054e-06, respectively). Conversely, the peptide sensor group appeared to be more activated by imatinib for $ABL1^{T315I}$ (p=0.027), which may relate to some of the observed increased activities monitored with biological peptides in (**c**). (Such phenomenon was also observed for imatinib- and dasatinib-treated AKT1 (bottom heatmaps in (**b-c**)), while AKT-targeting drug MK2206 treatment effectively decreased AKT1 activity (data not shown) in control assays using the same analytical methods presented in (**b-e**).) Based on the set of drug concentrations used in this experiment, the IC50(imatinib) for ABL1 may be higher than the anticipated 0.2uM (but far lower than 20uM), while IC50(imatinib) for LYN A may be lower than the anticipated 100uM (possibly close to 20uM).

[0042] Such kind of analyses also allowed comparing the effects of different drugs on a given kinase. In particular, these results showed that dasatinib is a more potent drug than Imatinib for ABL1, and this is also true for LYN A or $ABL1^{T315I}$. For example, the biological peptides of ABL1 revealed a stronger response to dasatinib than imatinib, which is corroborated by statistical analysis (dasatinib vs. imatinib: mean(R^2)= -0.997 vs. -0.847; T-test (fisher) p = 1.087e-07 vs. 0.00252). Moreover, representations in (**b,c,e**) indicate that the kinetics of response to drug treatment are not identical between different peptides, which suggests that the avidity for, and the phosphorylation of, particular peptide sensors may be differentially affected by an inhibitor.

[0043] These results indicate that drug-responses established from arrays of peptide probes provide the confidence and reliability that any single-peptide readout may not offer. These data also demonstrate that the HT-KAM can be used as a functional screen to assess the differential response of different kinases to inhibitors, which further illustrates the performance of the HT-KAM assay and its potential utility toward pharmacological screens. All these results directly show that biological peptides are excellent sensors to measure the activity of their cognate kinases.

[0044] **Fig. 17.** Measuring the effects of SFK-inhibitors using SFK's biological peptides as sensors of drug response.
(a) Activity of FYN A, HCK, LCK, and SRC kinases treated with PP2 (20nM) and SU6656 (250nM) inhibitors. Literature reports indicate that IC50 concentrations of PP2 and SU6656 are (5nM; 170nM) for FYN A; (5nM; not available) for HCK; (4 to 30nM; >5uM) for LCK; (35 to 100nM; 280nM) for SRC. Differences in drug sensitivity can be observed between kinases. Data overall corroborate previously reported ranges of sensitivities for these drugs.
(b) Activity of HCK treated with serial dilutions of SU6656 (1nM to 100uM). Of note, the sensitivity of HCK to SU6656 was more pronounced when measuring it with biological peptides than when monitoring it using HCK's generic control positive peptides (n=4; data not shown). In **(a-b)**, results were processed using the same analysis described in **Fig. 16c**. Together, these results show that the biological peptides of SRC kinases are adequate sensors to monitor the effects of SRC kinase-inhibitors.

[0045] **Fig. 18. Multi-peptide-based identification of kinases that mediate intrinsic resistance to BRAF^{V600E}-targeted therapy in colorectal cancer (CRC) cells.**
(a) Schematic of the experimental procedure.
(b) Previously identified mechanisms involved in resistance to BRAF^{V600E}-targeted therapy[3,17]. The anticipated reduction in MEK1/2 and ERK1/2 protein phosphorylation (blue shading), and increase in EGFR protein phosphorylation (red shading), served as validated knowledge to assess whether the HT-KAM platform can effectively detect MEK / ERK / EGFR kinases' activity in biological samples after vemurafenib (VEM) treatment.
(c) Baseline levels of protein and ATP concentrations comparing untreated (UNT) vs. VEM-treated WiDr cell extracts across all samples. VEM and UNT samples were comparable.
(d) Comparison of the activity levels of MAPKs, HERs, AKTs derived from kinases' biological peptide subsets (x-axis), versus those derived from peptides associated with kinases' most differential signature (y-axis; peptide sets previously computationally

identified in **Figs. 10-11**). The table on the right of the graph indicates the number of peptides per kinase. In the graph, the x- and y- axes represent a scale of the differential activity profile between VEM and UNT samples across all experimental repeats (total of 12 UNT and 12 VEM HT-KAM runs). Data plotted on the x-axis display the average of the activity differences across all experimental repeats and all biological peptides per kinase. Data plotted on the y-axis use kinase activity levels calculated as the difference between (i) the mean activity measured from the peptide subset that specifically differentiates the kinase in question from all other kinases, and that is associated with greater phosphorylation by the recombinant kinase in question, 'minus' (ii) the mean activity measured from the differential peptide subset specifically associated with lower phosphorylation by this kinase.

[0046] For example, after VEM treatment, the 'increase' in activity of AKT1 kinase (red mark) is +82 based on the 20 biological peptide targets of AKT1 (x-axis), and +46 based on the difference between the average activity measured from AKT1's 21 most differentially high-activity peptides 'minus' the average activity measured from AKT1's 6 most differentially low-activity peptides (y-axis).

[0047] The plot also incorporates activity profiles established from two different normalization methods. One normalization uses the average value of ATP consumption across 228 peptides + 14 peptide-free cell extracts (circles). The other normalization uses the average across 16 Y/S/T-free peptides (squares). Both normalizations lead to overall similar outputs of VEM-UNT differential activity profiles. Correlation between peptide subsets and for each normalization is indicated below the table, and the trend line of the linear regression between all data points is shown (overall correl. = 0.757).

[0048] **(e)** Comparison between changes in phospho-protein levels measured by western blot (top section), versus the changes in kinase activity measured with generic positive control peptides (middle section), versus the changes in kinase activity measured with their subsets of biological peptides (bottom section). Each blue-to-white-to-red color band represents the average of the difference in phospho-activities per peptide between VEM and UNT samples and across all experiments (i.e. UNT equals '0'; not shown). A gray side bar is drawn by the top-75% biological peptides that follow the main activity trend. Western blots serve as validation of kinases activity profiles.

[0049] **(f)** Formal comparison between changes in phospho-protein levels by western blot (x-axis), and the differences in levels of phosphorylation activity for individual kinases (y-

axis) based on either their generic positive control peptides (triangles), or biological peptide subsets (circles), or differential peptide subsets (squares). The identity of kinases is color-coded (markers' legend are shown in between the graph and the table). We used Image J to quantify intensities of bands identified by western blots. Phospho-protein amounts (x-axis) are plotted against the mean difference in kinase activity (y-axis; VEM 'minus' UNT) measured with 'n' peptides belonging to each category (indicated in the table on the right) across all experiments. In the case of GSK3B, we used the opposite value of the western blot quantification since higher phosphorylation of GSK3B is associated with a decrease in its activity.

[0050] Results show that kinase activity values established from either biological or differential peptide subsets correlate with protein levels: circles and squares are located either in the top right quadrant (i.e. high phospho-protein amount is associated with high kinase activity after VEM; which includes: EGFR, AKT1, PDPK1, SGK1, PRKCA, PKN1/2), or in the bottom left quadrant (i.e. low phospho-protein amount is associated with low kinase activity after VEM; which includes: MEK1, ERK2, p38a, GSK3B). Unlike kinase signatures established from biological or differential peptide subsets, positive control peptides did not correlate with kinases' activity (see triangles in the top left quadrant and the bottom right quadrant; e.g. positive control peptides did not identify ERK2 and EGFR kinase as respectively less and more active after VEM treatment). This is also visible in panel (**e**) (phosphorylation profiles of positive control peptides are shown below western blots).

[0051] Together, results in (**d-f**) show that the HT-KAM system can identify and differentiate individual kinases and kinase families from each other in cell extracts, which validates the utility of the HT-KAM platform. The different biological peptide subsets of different kinases can effectively be used to measure the activity of their related kinases in biological samples.

[0052] (**g**) Summary of the functional state of kinases found in WiDr $BRAF^{V600E}$ CRC cells treated with VEM using HT-KAM. Arrow linkers represent the functional connectivity between kinases, and colors indicate activity (e.g. VEM induces higher AKT activity, which leads to GSK3B phosphorylation, which reduces GSK3B activity).

[0053] **Fig. 19. Levels of phosphorylation activity measured with peptides derived from functionally related proteins or pathways.** We provide examples of phospho-

activities measured with individual biological peptides that we purposely selected and organized by protein of origin or by signaling pathway of interest.

(a) Peptide sensors related to EGFR-signaling (EGFR, PLCG1, GAB1, CBL, GRB10).

(b) Peptide sensors related to TGFBR-signaling (SMAD2 transcription factor).

(c) Peptide sensors related to transcription factors/regulators (CREB's, FOXO's, cFOS, STAT's, SP1, JUN's, NFkB1, cMYC).

(d) Peptide sensors related to kinase proteins: MTOR, JAK's.

(e) Peptide sensors related to phosphatase proteins: CDC25C, PTEN.

[0054] In all panels, the levels of phosphorylation activity measured with individual peptide sensors correspond to the differences in activity measured between VEM-treated and UNT-control samples. Significance per peptide (or peptide group) comparing all experimental read outs across samples and repeats is indicated (pairwise t-test p-val comparing UNT vs. VEM profiles).

[0055] Based on these observations, it is tempting to link levels of phosphorylation measured with biological peptides to the functional state of the signaling circuits these peptides originate from, and how they relate to mechanisms of VEM-resistance (e.g. EGFR, CDC25C[3], TGFBR[18], MTOR). Some of these biological peptides also happen to be those that are 'paradoxically' more phosphorylated within the peptide-phospho-signatures of kinases that otherwise exhibit low activity profiles after VEM treatment (e.g. ERK2's biological peptide subset includes peptides related to EGFR-reactivation circuit (GAB1 T476, GAB1 T312, GRB10 S150 peptides) and TGFBR-pathway (SMAD2 S250 peptide); see **Fig. 18e** first panel on the left). It would be interesting to investigate whether such peptides are early signs of re-activation of particular kinases (e.g. re-activation of MAPK signaling contributes to insensitivity to RAF inhibition[17,19]).

[0056] Inspection of the results for individual biological peptides demonstrate the robustness of the phospho-catalytic profiles established from cell extracts: (i) similar activity levels measured with biological peptides of similar sequences (e.g. peptides from MTOR, or JAK1, or CDKN1A, or CDC25C), (ii) systematically higher activity levels measured with biological peptides than with their mutated/pre-phosphorylated counterparts (e.g. EGFR, PLCG1, GAB1, GRB10, STAT1, GRIN2B, ABL1, MTOR; data not shown). The phosphorylation state of many biological peptides could also be corroborated by western blots, for example for EGFR (Y1068) (see **Fig. 18e** third panel), MTOR (S2448) **(d)**, and

others for which western blots are not shown (e.g. upregulation of phospho- EGFR (Y869), PLCG1 (Y1253), CBL (Y774), FOXO3 (S253), and downregulation of phospho- cMYC (T58), JUN (Y170), CDC25C (T48)).

[0057] Fig. 20. Response of BRAF^{V600E} CRC cells to targeted therapy combinations. To validate the kinase activity signatures of VEM-resistant WiDr cells found by HT-KAM screen, and as a mean to assess the role of these kinases (AKT1, PDPK1, PRKCA, SGK1) as mediators of the response to VEM and their potential value as druggable vulnerabilities in our model, we used 3-day cell viability assays to monitor the response of cells to drug combinations.

(a) Summary graph of WiDr cell growth response to VEM at 2uM (=GI50 concentration) or 0.25uM, and either used alone or in combination with other inhibitors. The bar graph is derived from complete cell growth response data curves (as shown in **Fig. 2d** or in the VEM+EVE graph shown underneath the main panel in **(a)**). All results were confirmed with PLX4702, a compound related to VEM (data not shown). Results show that lower than single-agent-GI50-doses resulted in effective combinatorial cell growth inhibition. These data validate that the significantly hyperactive kinases found by HT-KAM are biologically meaningful targetable vulnerabilities.

(b) Table summarizing the characteristics of WiDr cells' response to drug combinations. The significance of drug interaction (two-way ANOVA; p-val) and combination index (CI; following the Loewe Additivity model[6,7]; arbitrary threshold: synergy CI≤0.6; additivity 0.6<CI≤1.0; average for VEM≤2uM and 2nd drug≤IC50 concentrations) are listed.

(c) List of other drugs and additional BRAF^{V600E} cell lines intrinsically resistant to VEM that we tested to further validate kinase hits identified by HT-KAM profiling.

[0058] These results confirm that the kinases found by HT-KAM are involved in the response and resistance to VEM in BRAF^{V600E} CRC. Together with data in **Figs. 18-19** and **Fig. 2a-b**, these results show that a finite number of key functional dependencies can be identified as additional mechanisms participating in therapeutic resistance, which offers a selective choice of effective targets to explore. So, HT-KAM can be used as an exploratory/discovery platform to survey kinases and their activity levels, which is especially valuable in the case of diseases that cannot be defined by a single driver mutation or individual genetic dependencies such as BRAF^{V600E} CRC. As such, the HT-KAM system can help select drug candidates that target orthogonal modes of resistance with high likelihood of

restoring therapeutic sensitivity, thus providing a rational approach to design combination therapies.

[0059] Fig. 21. Ranges and levels of peptide phosphorylation measured across 20 cancer cell lines.

5 **(a)** Peptide phosphorylation activity signature of cancer cell lines. Protein extracts were generated for 20 cancer cell lines. Their phosphorylation activity was tested on the HT-KAM platform. For each experimental run, the average value of ATP consumption across the 228 peptides and 14 data-points from cell extract alone (i.e. established from 14 peptide-free control wells per 384-well plate) was used for internal normalization, and then the activity 10 per-peptide was calculated as the difference in ATP consumption between individual peptide-derived read outs and the internal mean. Next, phosphorylation activity values measured for each peptide were averaged across experimental repeats for each cell line. Finally, the phospho-catalytic activity signatures measured across the 228-peptide sensors were subjected to unsupervised hierarchical clustering. Phospho-catalytic activities are color-coded based on 15 the relative level of activity measured in presence of each peptide for each cell line, from blue for low activity, to white for intermediate-or-mean activity, to red for high activity. This analysis showed that each cancer cell displayed a unique phospho-catalytic fingerprint. On the right side of the main heatmap, the peptide class is indicated as a red/gold/grey color streak. At the bottom of the main heatmap, the phosphorylation activity profiles of cell 20 extracts without peptide (i.e. measured in the 14 peptide-free control wells) are shown.

[0060] **(b-d)** Examining the patterns of phosphorylation activity across cancer cells. The phospho-catalytic activity profile of cancer cell lines was examined for three technical variables: range of activity per peptide probe, level of phosphorylation intensity per peptide probe, and peptide class. The underlying reason is that, for an assay to best distinguish the 25 phosphorylation activities of different samples, it would be most appropriate to rely on phospho-sensing probes that capture the widest possible dynamic range of phosphorylation activities between cells, and/or provide the overall highest level of phosphorylation activity across cells. While asking this question, we also considered the possibility that the results of these two first variables may be different depending on the class of peptide used in the HT-30 KAM assay, that is: biological peptides, or positive control peptide probes, or reference peptides.

[0061] In **(b)**, results are sorted by peptide class, and then by highest to lowest range of phosphorylation activity per peptide.

[0062] In (**c**), the table lists the values calculated from (b) to compare the three-peptide classes.

[0063] In (**d**), results are sorted by highest to lowest average phosphorylation activity per peptide. Peptide classes are then grouped and counted in the lower graphs to provide a sense of which peptide class reports on the highest to lowest levels of phosphorylation activity.

[0064] Results in (**b-d**) show that biological peptides provide the broadest ranges and highest levels of measurable phosphorylation activities. Reference peptides provide the lowest activity measurements overall, while still providing a broad range of phospho-activities. Generic positive control peptides provide the lowest range of activities, and the measured phospho-activity levels remain lower than the overall mean activity per cell line across all cells. We conclude that, although virtually all peptides participate in defining the unique peptide-phosphorylation activity signature of every cancer cell line, the set of biological peptides are particularly well-suited catalytic activity sensors to measure and differentiate the unique functional phospho-fingerprint of cancer cells.

[0065] (**e**) ATP levels in peptide-free wells and protein concentrations per cell line. In the graph on the left, each bar represents the average +/- st dev of ATP concentration of cell extract alone measured across the 14 peptide-free control wells available for each experimental 384well/plate. All samples for each cell line were tested at least three times. The range of ATP-standard across all HT-KAM assays is shown on the far right of the graph (averages and standard deviations across all HT-KAM experiments are shown). These results show that ATP profiles of all samples fit within the limits of the range of ATP standard. ATP profiles were comparable between different cell lines or samples or experimental repeats. There is no evidence for any ATPase or phosphatase contamination. So, variations in phospho-catalytic activity measured in presence of peptides were both peptide-dependent and cell-specific (results shown across all figures). As such, phospho-catalytic activity profiles can be interpreted with confidence.

[0066] Fig. 22. The kinase activity signature of cancer cells identifies druggable vulnerabilities.

(**a**) Kinase activity signature of cancer cell lines. The activity of kinases was calculated as the average of the phosphorylation activities measured in presence of their respective subset of biological peptides. The kinase activity profile of each cell line was deconvoluted from the corresponding peptide phosphorylation profile shown in **Fig. 21a**, and for individual kinases

or kinase families with ≥3 biological peptides. Unsupervised hierarchical clustering was applied across cells and kinases. Each cancer cell line displayed a distinguishable kinase signature. Kinase activity is color-coded blue-to-black-to-yellow from low-to-medium-to-high activity.

5 **(b)** Pearson-correlation heatmap highlighting the functional relationship between cancer cells established from their kinase activity signature. Cells are arranged by tumor tissue of origin (MEL: melanoma; CRC: colorectal cancer; BC: breast cancer; LC: lung cancer; PC: prostate cancer).

(c-d) Comparing kinase activity and drug sensitivity of cancer cell lines. A good way to 10 evaluate the performance of HT-KAM-defined kinase signatures is to measure the effect of a kinase inhibitor on cell growth and then correlate it to kinase activity level. This would assess whether kinase signatures are predictive of drug sensitivity and indicative of cell-specific kinase dependencies. We tested the effects of 28 kinase-inhibiting drugs (list in **(c)**) in 3-day dose-response cell viability assays using a core set of cell lines (A375, AU565, H3122, 15 HCC70, HCT116, HT29, MCF7, MDA231, MDA436, SK-CO-1, SkMel2, T47D, WiDr; additional cell lines were tested on a case by case basis where it was deemed useful, such as PC9 to compare EGFR activity versus gefitinib sensitivity[20]). We intentionally chose to test more than one inhibitor per kinase for some of the kinases in order to validate results (the 28 drugs inhibit 17 different kinases/kinase families; see table in **(c)**). We also further 20 corroborated GI50 results from literature[21-23]. Kinase activity levels where extracted from signatures available in **(a)**. We then correlated cancer cells' GI50's with their kinase activity for each drug. Examples are shown in panel **(d)**. The table in **(c)** provides all correlations. The negative correlation between kinase activity and drug-GI50 across cells indicates that, overall, cell lines were more susceptible to inhibitors for which they displayed higher kinase 25 activity. These results directly verify that profiles measured by HT-KAM assays accurately predict differences in kinase activity.

(e) Correlation between kinase activity and drug sensitivity. Results from both the analysis in **(c-d)** and from **Fig. 2g** are included (total of 373 data points established from 37 inhibitors that target 22 kinases). For each kinase/drug pair, we compared the differential kinase 30 activities and drug-GI50s across tested cancer cell lines. These results show that the kinase signature of cancer cells can reveal their actionable vulnerabilities, and thus their kinase dependencies.

[0067] Along with **Figs. 18-21**, this demonstrates that the peptide phosphorylation signatures can be reasonably converted in kinase activity profiles with translational relevance. The HT-KAM platform is a practical solution to find active, druggable kinases in cell culture models.

[0068] **(f-g)** Controls for the comparison of A375 vs. WiDr cells. Protein concentration, baseline ATP levels, and protein expression/phosphorylation levels are provided for validation of Fig. 2g-h.

[0069] **Fig. 23. Melanoma specimens.**
(a) Table with details about treatments received by patients before and after the biopsy/excised biospecimen that was used for histo-pathology/diagnostic and retrospectively tested on the HT-KAM platform. Treatments (muphoran; dacarabazin; interferon (IFN; low/high dose); ipilimumab (anti-CTLA4); vemurafenib ($BRAF^{V600E}$ inhibitor); interleukin; irradiation) are color-/letter-coded. Numbers of treatment cycles are specified. Tumor stage, BRAF status, recurrence and survival are indicated. The flash-frozen tumor biospecimen of patient #1 was a superficial spreading melanoma (SSM) excised from the trunk; patient #2: SSM metastasis from the trunk; patient #3: subcutaneous metastasis from a recurrent cutaneous tumor from the leg; patient #4: nodular melanoma metastasis from the leg; patient #5: cutaneous metastasis from the cubital fossa; patient #6: cutaneous metastasis from the neck; patient #7: inguinal lymph node metastasis (axillary lymphadenectomy of positive sentinel); patient #8: cutaneous metastasis from a recurrent cutaneous tumor of the temporal area, patient #9: cutaneous metastasis from a recurrent cutaneous tumor located on the back.
(b) Baseline ATP levels measured across HT-KAM assays, and protein concentrations from tissue extracts. Levels are comparable between tumors and experiments.

[0070] **Fig. 24**. Analysis of the phospho-catalytic signatures of tumors.
(a) Peptide phosphorylation activity signature of melanoma specimens. Unsupervised clustering of 36 activity profiles measured across 228 peptides is shown (9 patient tumor tissues tested in 4 independent technical replicates).
(b-h) Principal component analysis (PCA). We investigated the potential association between 'variables of interest' and principal components (PCs) that define individual phospho-signatures (linear regression, overall fit of univariate model PC(i) for variable (j)). The table in **(b)** provides a summary of the results visually represented in graphs **(c-g)**.

In (**c**), results show that replicate runs from the same patient sample were significantly similar (9 patients are shown as 9 different colors, with 4 dots per patient for the 4 experimental replicates), with an association between patient ID and PC1 of p=1.44E-06. In (**d**), results show that days at which assays were run were not associated with the primary PCs of melanoma kinomes (3 different days of experimentation are shown as 3 different colors; p>0.05). So, the results of the PCA from the two technical variables in (c-d) demonstrate the excellent performance and high reproducibility of the HT-KAM system (i.e. experimental procedure, instrumentation, data analysis).

In (**e-f**), results show that survival status (**f**) and recurrence status (**g**) were highly associated with the PCs of the kinome signatures (respectively PC1:p= 5.14E-06 and PC2:p=0.028; and PC1:p=2.31E-07). So, the results of the PCA from the two clinical variables in (**f-g**) reveal the strong predictive and prognostic value of the phospho-catalytic signature of tumors.

In (**g**), results show that PCs of melanoma phospho-signatures do not associate with BRAF mutational status. This demonstrates that, even if a $BRAF^{V600E}$ mutation is a dominant oncogenic driver, HT-KAM effectively discerns different types of $BRAF^{V600E}$ tumors depending on other critical variables that the phospho-signatures of tumors reflect. HT-KAM differentiates fatal $BRAF^{V600E}$-postive conditions (patients #4,5,8,9) from non-fatal $BRAF^{V600E}$-postive conditions (patients #3,7). And similarly, HT-KAM distinguishes fatal non-$BRAF^{V600E}$ conditions (patient #2) from non-fatal non-$BRAF^{V600E}$ conditions (patients #1,6).

In (**h**), we overlaid PC results from (**e-g**) and annotated patients groups for outcome and therapeutic resistance. This shows that the PCs from VEM treated-but-resistant patients (#4,5,9) cluster together, indicating that tumor phospho-signatures reflect patients' unresponsiveness to BRAF-targeted therapy. The strong association between BRAF-therapy resistant lethal melanoma tumors and the PCs of their phospho-signatures fully validates the results generated from the clustering analysis available in **Fig. 3b**.

[0071] The results of the PCA shown in (**b-g**) were established from phospho-signatures normalized to the 228-peptides + 14 peptide-free readouts, and were closely recapitulated when signatures were normalized using the 63-reference peptides, or the 14 peptide-free tissue extract alone readouts, or 16-Y/S/T-free peptides, or when using raw ATP-consumption data (data not shown). Collectively, this formal investigation of the PCs of tumor phospho-signatures demonstrates the robustness of the HT-KAM system, and the reliability of its output to map the phospho-catalytic signatures of tumor tissues.

[0072] Fig. 25. Identifying the predictive peptide signature of patients with poor survival outcome, including BRAF^{V600E}-mutated patients resistant to BRAF-therapy. Since survival is a significant clinical variable identified from patients' phospho-signatures (clustering analysis in **Fig. 3b**, and PCA in **Fig. 24**), we asked whether we could find peptides that would qualify as best predictors of patients' survival outcome. To do so, we applied two methods.

(a-c) Method #1: analysis of peptide phosphorylation signatures using dual significance threshold selection. In **(a)**, the waterfall plot shows the differential activity profile across all 228-peptides comparing patients #1,3,6,7 (alive) versus patients #2,4,5,8,9 (dead). Significance values (t-test and Wilcoxon rank sum test; FDR-adjusted or not) are provided underneath the graph. Peptide phosphorylation signatures were normalized to the 228-peptides + 14 peptide-free readouts. In **(b)**, peptide phosphorylation activities were selected when concurrently passing FDR-adjusted t-test $p<0.05$ and Wilcoxon rank sum test $p<0.05$. This rigorous dual selection threshold identified 34 peptides as the most significantly differentially phosphorylated peptides associated with poor survival. In **(c)**, peptide phosphorylation activities shown in **(b)** are detailed across all patient signatures. Two thirds of the peptides are biological peptides (listed and color-coded on the right side of the heatmap), most of which are associated with higher phosphorylation activity in tumors from patients with poor survival outcome. We further validated these data using alternative normalization schemes (data not shown), and by applying this same computational analysis to identify peptides qualifying as best predictors of recurrence (identifying an overlapping set of 27 peptides; data not shown).

(d-e) Method #2: analysis of peptide phosphorylation signatures using top-25%-activity threshold selection. The top 25% peptides displaying phospho-activities that were most variable between all patients and all experimental repeats were selected. Panel **(d)** shows the unsupervised hierarchical clustering of these 57 most differential signals (same normalization as in **a-c**). In **(e)**, the waterfall plot shows the differential activity per peptide across these 57 peptides and between patient groups (differential survival outcome as black bars; differential recurrence outcome in violet; differential BRAF status in blue; data sorted by highest to lowest differential activities comparing survival outcome).

[0073] Results in **(a-e)** show that the most significant and consistently high signals associated with fatal outcome were measured with biological peptides such as SMAD2 S465 and S245 and S250, KHDRBS1/SAM68 Y440 and Y435, MTOR T2446 and S2448,

CDKN1A/p21 T145 and S146, BRCA1 S988 and T509, ABL1 Y226 (corresponding to Y245 in another ABL1 isoform), FCGR2B Y292, or CHEK1 S280. Likewise, peptide sensors associated with consistently low activity in fatal outcome were biological peptides NOTCH2 S2070, JUN Y170, TERT Y707, GAB1 Y627, and reference peptides from modified biological peptides PA_128, PA_134, or PA_230. Interestingly, the phospho-signatures of poor survival outcome included peptide sensors related to kinases such as SFK's, MTOR, or TGFBR-signaling, some of which were found to confer acquired resistance to BRAF or MEK inhibitors in cell culture models of melanoma[24-28]. Phospho-catalytic activities measured with peptides of related sequences behaved similarly and were useful internal controls validating assay repeatability (e.g. MTOR T2446 and S2448; CDKN1A T145 and S146; CDK5 Y15 and generic positive control PA_240 which is originally derived from CDK1 Y15 and is mostly conserved between these two CDK's). So, the peptides included in the HT-KAM platform are robust sensors that can be used to generate clinically valuable signatures to diagnose cancer specimens.

[0074] Fig. 26. Identifying the kinase signature of patient tumors. Determining the activity of kinases in tumors could reveal tractable candidates for therapeutic interventions. So, we explored the potential clinical utility of the kinase activity signatures of melanomas. **(a)** Waterfall plot showing the differential activity of kinases between patient groups. For each tumor, the activity of kinases with ≥4 biological peptides was calculated as the average of the phosphorylation activities measured in presence of their respective biological peptide subsets across all experimental repeats. Next, we calculated the mean activity per kinase for each patient group, and then plotted the differential activity between groups of interests, i.e. survival / black bars, recurrence / violet, BRAF status / blue. Significance was calculated using all experimental repeats between patient groups (shown underneath the graph).
(b) Differential kinase activity signature of tumors. Kinase activity profiles were mean-centered per tumor tissue and then mean-centered across patient tumors. Semi-supervised hierarchical clustering was applied across the 60 individual kinases or kinase families. As a validation of the results in **(a-b)**, the differential activities of some of the kinases we found in patient tumors are corroborated by gene over-expression screen for RAF-inhibitor resistance in melanoma cell lines 25 (e.g. upregulated kinase activity of PRKC(E), RAF(1), MAP3K8/COT1, PAK(1)).
(c) Comparison of the activity of ABL1, AKT1, ERK2, HCK and p38a deconvoluted from kinases' biological peptide subsets (x-axis), versus activity levels converted from kinases'

differential peptide signature (y-axis; method explained in **Figs. 11, 18d**). Results show good concordance across kinases and tumor groups (e.g. the correlation between kinases' activity related to survival (circles) was 0.847).

(d) Validation of differential kinase signatures using enrichment analysis. We applied an enrichment analysis (EASE – Fisher one-sided test; $p<0.05$) to identify kinases whose biological peptides were most represented among the 34 peptides most significantly associated with survival outcome (identified in **Fig. 25b-c**). Results are shown in the table, and formally identify AKT's, PIM's, and RPS6KB's as most significantly related to the melanoma survival outcome phospho-signatures.

(e) Differential biological peptide-activity profiles comparing different patient groups. We chose to show AKT, PIM, RPS6KB, and GSK3B kinase families because analyses in (a-b,d) showed their changes were most significant and most profound (increase or decrease). Significance per peptide across patients groups (grey scale) are shown. The bottom graph compares the kinase profiles of $BRAF^{V600E}$ tumors from patients retrospectively known to survive (#3,7) versus patients who died (#4,5,8,9; which includes all patients who did not respond to BRAF-therapy). This means that the intrinsic vulnerabilities of these tumors were not inhibited, and that alternative treatment options would have been available at the time of biopsy based on kinase signatures revealed by HT-KAM.

[0075] Together, these results demonstrate that differences in the activity of kinases can be measured within a tumor biospecimen (i.e. for each patient), and between different tumors (i.e. across patients and their individual malignancies). As well, significant changes in levels of kinase activity can be identified between different groups of patients (e.g. survival outcome). So, the HT-KAM assay successfully maps the oncogenic kinase signatures of tumor tissues, and reveals the significantly hyperactive kinases that are most predictive of poor outcome. Accordingly, HT-KAM identifies druggable kinase vulnerabilities most tractable to treat patients with highest likelihood of recurrence and poorest survival outcome, including patients who are unresponsive to BRAF-therapy. Specifically, our results indicate that AKT1, PIM1 and RPS6KB1 kinases are most conserved and overly active in poor outcome melanoma.

[0076] **Fig. 27. Analysis of gene expression data as an indirect mean to corroborate phospho-catalytic signatures**. Even though gene expression is a relatively distant factor influencing the oncogenic activity of kinase enzymes and phospho-signaling circuits[29,30], we asked whether melanoma patients with poorer outcome available in the TCGA resource[14]

displayed changes in mRNA levels that match kinases we found by HT-KAM. We confirmed that patients who express high levels of AKT1 or PIM1 displayed significantly worse overall survival or disease-free survival, as shown in (**a-b**) and (**c-e**). Kaplan-Meier curves and logrank t-test p-values are provided in (**a,c**). Not shown here, we also found from the TCGA data set: (i) co-occurrence of AKT1 and RPS6KB1 mRNA alteration in poor outcome melanoma (log odds ratio of +2.66; $p<0.001$); (ii) up-regulation of CDKN1A mRNA expression in worse progression-free survival which is interesting since CDKN1A-derived peptide sensors are among top predictors of poor outcome (see **Fig. 25c**).

[0077] Fig. 28. Response of BRAF^{V600E} melanoma cell lines to drug combinations. (**a**) Summary of possible cell responses to the combination of two drugs. The heatmap on the left represents the experimental effects of combining increasing concentrations of drug A+B as changes in cancer cell growth. The middle graph is a conceptual representation of how differences in effects of drugs alone or combined can be interpreted as either synergistic, additive, or antagonistic (derived from [10]). The heatmap on the right represents the calculated combination index from all experimental cell growth data points. We decided to analyze experimental profiles using the Bliss Independence model to calculate combination indices (CI) and avoid inaccuracies from dose-effect curve estimations (CI = log2 (Eab/(Ea*Eb); synergy CI<0; additivity CI=0; antagonism CI>0) 10-12.

(**b**) Maps of cell growth responses (left) and combination indices (right). We tested the dependency of BRAF^{V600E} melanoma cell lines for kinases found as differentially active by HT-KAM in patient tumors (**Fig. 26a,b**). We included everolimus or trametinib (bottom two rows) as experimental 'positive' controls and for side-by-side comparison of the effects of other kinase-targeting drugs we tested. Arrows located above and on the left of each cell growth heatmaps serve as indicators of GI50 concentrations for each drug alone. The GI50s of A375 maintained in 5% or 0.25% FBS media for drug alone were: VEM (0.15uM; 0.02uM); MK2206 (10uM; 2.5uM); AZD1208 (12.5uM; 12.5uM); LY2584702 (50uM; >200uM); PF-4708671 (32uM; 16uM); 1-Azakenpaullone (20uM; 2.5uM); BI-D1870 (12.5uM; >50uM); everolimus (5uM; 10uM); trametinib (5nM; 2.5nM). The GI50s of Sk-Mel-28 maintained in 5% or 0.25% FBS media for drug alone were: VEM (0.63uM; 0.31uM); MK2206 (2.5uM; 5uM); AZD1208 (25uM; 25uM); LY2584702 (100uM; 100uM); PF-4708671 (32uM; 16uM); 1-Azakenpaullone (20uM; 10uM); BI-D1870 (25uM; 12.5uM); everolimus (10uM; 10uM); trametinib (10nM; 10nM).

[0078] Results of growth responses (left) and combination indices (right) show that strong growth inhibitory effects were found when combining VEM with inhibitors of RPS6KB (LY2584702 or PF-4708671) or PIM kinases (AZD1208). Overall, synergistic effects of these drugs were superior to, or at least as good as, those of drugs targeting MTOR (everolimus) or MEK (trametinib) that are currently used in the clinic, but whose effects in patients remain variable and often transient.

[0079] Our results also show that other kinases whose catalytic activities were originally identified by HT-KAM as less highly or less significantly upregulated than RPS6KB, PIM or AKT kinases in $BRAF^{V600E}$ melanoma tumors were indeed less effective therapeutic targets. This is exemplified by RPS6KA inhibition (additive effects only of the BI-D1870 drug; see heatmaps), or PKC inhibition (limited additivity effects of Go6983 or Sotrastaurin; data not shown).

[0080] Furthermore, we found that inhibiting the GSK3B kinase, which is a tumor suppressor kinase we identified as systematically less catalytically active in melanoma tumors of poor outcome patients, resulted in antagonizing the effects of VEM treatment, which means that melanoma cells became more resistant to $BRAF^{V600E}$-targeting drug when it was combined with the GSK3B inhibitor 1-Azakenpaullone, as visually noticeable from the patterns of cell growth and CI in heatmaps. This also strongly suggests that some of the 'good' effects of VEM rely in part on 'proper' kinase activity of the GSK3B tumor suppressor.

[0081] **(c-e)** Evaluating the effects of drug combinations on melanoma cell death. We used Fluorescence-Activated Cell Sorting (FACS) and measured cell death in melanoma cells treated at GI50 concentration of drug alone in 5% and 0.25% FBS culture conditions. Panel **(c)** shows examples of flow cytometry profiles obtained for Sk-Mel-28. Graphs in **(d-e)** show percentages of apoptosis for Sk-Mel-28 and A375 are graphically (averages of cell death measured in 5% or 0.25% FBS conditions). Numbers above grey bars in **(d-e)** indicate gain or loss in apoptosis when combining VEM with a 2nd kinase-targeting drug.

[0082] Increase in apoptosis was systematically found when combining VEM with inhibitors of RPS6KB or PIM, and these effects were overall more potent than when combined with MTOR or MEK targeting drugs. Decrease in apoptosis was found when combining VEM with GSK3B inhibitor (i.e. GSK3B inhibition rescues $BRAF^{V600E}$ melanoma cells from cell death upon VEM treatment). Highest level of apoptotic cell death was induced

by RPS6KB-targeting combined with VEM in Sk-Mel-28, thus achieving a critical endpoint in the perspective of eradicating tumor cells.

[0083] Altogether, these results demonstrate that the top kinase hits identified in patient tumors as predictive of their therapeutic failure (see **Fig. 3c-e** and **Fig. 26**) correspond to central kinase dependencies in $BRAF^{V600E}$ melanoma cells. We conclude that inhibitors of RPS6KB, PIM or AKT are strong therapeutic candidates to restore therapeutic sensitivity. The HT-KAM platform successfully identifies new exploitable vulnerabilities of melanoma tumors based on the kinome profiling of patient tumor tissues.

[0084] **Fig. 29. A375 expressing a constitutively active AKT1 oncogenic kinase remain sensitive to RPS6KB- or PIM-targeting.** We exogenously expressed myrAKT1 (i.e. a constitutively active oncogenic AKT1) in A375 cells. We then tested the sensitivity of A375 myrAKT1 cells to drug combinations.
(a) Control for myrAKT1 expression. myrAKT1-expressing A375 cells were significantly less sensitive to VEM than their control counterpart (p=2.77E-06; 65% increase in GI50).
(b-c) Cell response of A375 myrAKT1 cells to drug treatments (same experimental settings and analysis as in **Fig. 28**). Cell growth is shown in **(b)**, cell death is shown in **(c)**.
(d) Ranking treatment effects by comparing CI values between melanoma cell lines. Data from both **Figs. 28-29** are included.

[0085] Results indicated that $BRAF^{V600E}$ melanoma cells that acquired the expression of the AKT oncogene remained sensitive to combinations of VEM with inhibitors of RPS6KB or PIM kinases. As well, mimicking the loss of tumor suppressive activity by inhibiting GSK3B in myrAKT1-expressing cells to recapitulate the coordinated inactivation of GSK3B kinase and hyper-activation of AKT1 found in tissues from $BRAF^{V600E}$ melanoma patients with poorest outcome, led to strong resistance to VEM treatment. The growth response of myrAKT1-expressing A375 cells treated with combinations of VEM + MTOR or MEK targeting drugs was comparable to wild type A375 cells. These results support the notion that these multiple oncogenic phospho-signaling hubs can function independently of each other's. These kinases are suitable alternative targets to restore response in melanoma cells.

[0086] **Fig. 30. Restoring therapeutic sensitivity by targeting the RPS6KB kinase in melanoma tumor cells from patients that acquired resistance to $BRAF^{V600E}$-therapy.**

(**a-b**) Phospho-RPS6KB profiles of two patient-derived xenografts (PDXs) tumor tissues (**a**) and related cell lines (**b**). PDXs were previously[4,5] established from patients refractory to $BRAF^{V600E}$-therapy. A limited number of primary cell lines were derived from these PDX's. (**c**) Sensitivity of primary melanoma cell lines to RPS6KB-inhibitor PF-4708671 in 3-week colony formation assays.

[0087] The PDX tumor M032R6.X1 displayed high levels of RPS6KB1 in tumor tissue, and the PDX-derived cell line M032R6.X1.CL maintained high levels of RPS6KB1, and the cell line M032R6.X1.CL was sensitive to RPS6KB1 targeting. This corresponds to data shown in **Fig. 3i**.

[0088] Conversely, the PDX tumor M061R.X1 did not display high levels of RPS6KB1 in tumor tissue, and the PDX-derived cell line M061R.X1.CL also did not display high levels of RPS6KB1, and the cell line M061R.X1.CL was not sensitive to RPS6KB1 targeting. This can be considered as a control for results in **Fig. 3i**.

[0089] The results indicate that targeting RPS6KB can be a successful therapeutic intervention in $BRAF^{V600E}$ melanoma tumors/tumor cells where RPS6KB1 is elevated. Such vulnerability may be valuable to restore therapeutic sensitivity in patients who do not respond to, or relapse from, current therapies.

DETAILED DESCRIPTION OF THE INVENTION

[0090] The disclosure is based, in part, on the discovery of an effective, sensitive assay for determining a phospho-kinase activity profile of cells, *e.g.*, tumor cells, or other biological samples in which it is desirable to evaluate kinase activity. The method comprises using a panel of sensor peptides that comprise biologiocal substrate regions for different kinases. Evaluation of all of the members of the panel provide an indication of the kinase pathways that are active in the sample. In one embodiment, provided herein is a 228-peptide panel developed to detect the activity of over 60 kinases/kinase families, including ABL, AKT, CDK, EGFR, GSK3B, MAPK, or SRC. Such a panel provides a method of defining new mechanisms of resistance to targeted therapy, *e.g.*, $BRAF^{V600E}$-targeted therapy in colorectal cancer, can identify new druggable targets, *e.g.*, RPS6KB1 and PIM1 as new druggable vulnerabilities predictive of poor outcome in $BRAFV^{600E}$ melanomas patient; and otherwise provides for comprehensive evaluation of kinase activity in cancer and in other complex or previously uncharacterized samples of interest to identify kinase type.

[0091] Accordingly, provided herein are panels of sensor peptides that can be used in combination to assay for the activities of multiple kinases at the same time to identify the kinase activity and/or determine the kinase signature of a biological sample of interest, *e.g.*, a cancer sample obtained from a patient. The invention further comprises methods of assigning a kinase activity identified in a biological sample, *e.g.*, a cancer sample, to a kinase family and/or of identifying the kinase activity as belonging to a particular kinase. Such information can be used, for example, to further characterize the kinases/kinase activities from biological samples of interest. In some embodiments, *e.g.*, evaluation of kinase activity in cancer or other disease states, analysis of a combinatorial peptide panel in accordance with the invention can be used to develop therapeutic strategies or for further development of drug candidates.

[0092] A "sensor" peptide in the context of this invention refers to any peptide that is contained in a kinase peptide activity panel as described herein which is used to assess kinase activity. These include biological sensor peptides and sensor peptides that have mutations relative to the naturally occurring sequences that influence kinase activity. As used herein, the terms "kinase activity" and "phosphorylation activity" are used interchangeably to refer to the ability of a phosphokinase to phosphorylate a sensor peptide.

[0093] The term "peptide" is used herein to refer to a polymer of amino acid residues. The term appies to amino acid polymers in which one or more amino acid residue is an artificial chemical mimetic of a corresponding naturally occurring amino acid, as well as to naturally occurring amino acid polymers and non-naturally occurring amino acid polymers. Thus, a peptide for used in a panel of peptides to assess kinase activity as described herein can comprise naturally occurring and/or synthetic amino acids, including analogs and amino acid mimetics that function in a manner similar to the naturally occurring amino acids. "Naturally occurring" amino acids are those encoded by the genetic code, as well as those amino acids that are later modified, *e.g.*, hydroxyproline, γ-carboxyglutamate, and O-phosphoserine. " Synthetic amino acids" or "amino acid analogs" refers to compounds that have the same basic chemical structure as a naturally occurring amino acid, *i.e.*, an α carbon that is bound to a hydrogen, a carboxyl group, an amino group, and an R group, *e.g.*, homoserine, norleucine, methionine sulfoxide, methionine methyl sulfonium. Such analogs have modified R groups (*e.g.*, norleucine) or modified polypeptide backbones, but retain the same basic chemical structure as a naturally occurring amino acid. Amino acid mimetics refers to chemical compounds that have a structure that is different from the general chemical structure of an

amino acid, but that functions in a manner similar to a naturally occurring amino acid. Amino acid is also meant to include -amino acids having L or D configuration at the α-carbon.

[0094] Amino acids may be referred to herein by either their commonly known three letter symbols or by the one-letter symbols recommended by the IUPAC-IUB Biochemical Nomenclature Commission.

Biological Sensor Peptides

[0095] In the context of this disclosure, a "biological sensor peptide" refers to a peptide that comprises a substrate region that is derived from a naturally occurring substrate region. Thus, a biological sensor peptide as used herein refers to a peptide a known substrate region phosphorylated by a kinase belonging to a kinase family. Such substrate regions can be identified, *e.g.*, from the PhosphoAtlas or PhosphoSitePlus databases (see, *e.g.*, *Olow et al.*, "An Atlas of the Human Kinome Reveals the Mutational Landscape Underlying Dysregulated Phosphorylation Cascade in Cancer" *Cancer Res.* 76(7):1733-45, April 1, 2016; Epub 2016 Feb 26; and Hornbeck *et al.*, "PhosphositePLus, 2014: Mutations, PTMs and recalibrations. *Nucl. Acids Res.* 43:D512-D520, 2015).

[0096] Biological sensor peptide can vary in length, *e.g.*, from 7 to 25 amino acids in length, or from 9 to 21 amino acids in length. In some embodiments, a peptide may be up to 50 amino acids in length, or even up to 100 amino acids in length and at least 6 amino acids in length. In some embodiments, a biological peptide is 9, 10, 11, or 12 amino acids in length. In some embodiments, a biological sensor peptide is 11 amino acids in length. In some embodiments, biological peptides can comprise additional amino acids at the C-terminal and/or N-terminal ends of the peptide. For example, an 11-mer may comprise 9 amino acids from the naturally occurring substrate region sequence and 2 amino aicds, *e.g.*, GC at the C-terminus or CG at the N-terminus. In other embodiments, the biological peptide does not contain a GC or CG tag at the end terminus.

[0097] Although the sequence of a biological sensor peptide is typically identical to the corresponding region of the native substrate phosphorylation site, in some embodiments, the biological sensor peptide may contain one or more amino acid residues at the end of the peptide, relative to the native sequence, that does not influence kinase activity, as explained in the preceding paragraph. In further embodiments, a biological sensor peptide may contain an amino acid change relative to the sequence of a naturally occurring substrate region that

does not influence activity of the kinase that phosphorylate that region. In some embodiments, a biological peptide may have a conservative substitution that does not influence kinase activity. In some embodiments, a biological sensor peptide may include modified amino acids. For example, modifying a peptide to have a pre-phosphorylated peptide on one Y residue may make it easier for a kinase to phosphorylate a 'free' Y nearby within that peptide sequence. This is also applicable to other post-translational modifications that may be biologically relevant and thus, a peptide that mimics such a state may imrove the sensitivity/specificity/differentiability of detection for one or more kinases.

[0098] The number of biological sensor peptides employed in the panel per kinase is variable, but the panel comprises a pluarility of biological sensor peptides for the majority of the kinases to be represented in the panel. For example, in some embodiments, a panel of comprises, 8, 9, 10, 11, 12, 13, 14, or 15 biological sensor peptide per kinase, but may range from 3 to 50 biological sensor peptides per kinase. In some embodiments, a panel of kinases may employ at least 4 biological sensor peptides per kinase. In some embodiments, the number of biological sensor peptides per kinase that is included in a panel is 5, 6, 7, 8, 9, 10, 11, 12, 13, 14, 16, 16, 17, 18, 19, or 20. In some embodiments, the number of biological sensor peptides per family ranges from 4 to 20 or more.

[0099] In some embodiments, a panel of sensor peptide comprises at least 15 biological sensor peptides per the majority of kinase families to be represented in the panel. In some embodiments, at least 10 biological sensor peptide, or at least 15 biological sensor peptides are included per kinase family represented in the panel. In some embodiments, nor more than 50 peptides is included per kinase family.

Control sensor peptides

[0100] Various control sensor peptides are included in a peptide panel of the present invention for experimental controls and statistical analysis, as detailed in the Examples section and accompanying figures and figure descriptions. The controls, also referred to herein as reference peptides, include generic positive controls, and mutated peptides, in which a naturally occurring substrate region is mutated such that a known kinase that phosphorylates the substrate in nature is exhibits modified activity towards the mutant peptide, *e.g.*, is inactive against the mutated peptide. Mutated control sensor peptides provide increased confidence in the assay and improves analysis/interpretation and visualization of data from the screening assay. For example, a mutated reference peptide may contain an

amino acid substitution at a phosphorylatable tyrosine, serine, or threonine, *e.g.*, a tyrosine, serine, or threonine, may be substituted with a glycine or othe residue that is not longer able to be phosphorylated. In some embodiments, a control peptide may have a phosphorylatable site that is pre-phosphorylated to render it insensitive to kinases that may be present in a given sample. Control peptides may also include peptides that have random peptide sequences. Finally, know generic peptides that can serve as positive controls are available, including commercially available. Such peptides may also be included in the panel as further controls.

Sensor peptide panels

[0101] A 'sensor peptide panel" or "kinase activity panel" as used herein refers to an assemblage of peptides that collectively provides phosphorylation activity data (for a sample of interest being evaluated to characterize the kinases in the sample) for multiple kinases at the same time and thus is sufficient to assign kinase activy in the sample to a kinase family, or one or more specific kinases; or can be used to characterize kinases in a biological sample of interest. In a kinase activity assay panel of the present invention, it is the combination of different kinase-specific sets of peptides that provides the read out of activity for multiple kinases at once.

[0102] Further, even though many kinases may have few identified target sites or even substrate protein targets, a kinase activity panel assessment as described herein can be used to identify peptides that best match a kinase and thus provide greater insight into the kinase function.

[0103] In some embodiments, a kinase activity panel of the present invention comprises a multiplicity of sensor peptides to determine kinase activity for at least two, at least three, at least four, or at least five, or more kinases families. In some embodiments, a kinase activity panel of the present invention comprises a multiplicity of sensor peptides to determine kinase activity for at least ten, at least fifteen, at least twenty, at least twenty five, or more kinase families. In some embodiments, a kinase activity panel of the present invention comprises a mutliplicity of sensor peptides to determine kinase activity for at least two, at least three, at least four, or at least five, or more specific kinases. In some embodiments, a kinase activity panel of the present invention comprises a multiplicity of sensor peptides to determine kinase activity for at least ten, at least fifteen, at least twenty, at least twenty five, or more specific kinases. Accordingly, a panel may comprise any number of peptides. Indeed, a panel and

assay of the present invention is modular by design in that users can adapt panels and assay conditions to their needs. Indeed, in some embodiments, a set of peptide sensors may be employed to study particular kinases under specific condtions, e.g., pH, ion, etc.; however, the panel still employs multiple peptides to capture kinase activity for multiple kinases.

[0104] In some embodiments, a kinase activity panel of the present invention can comprise a multiplicity of sensor peptides to determine kinase activity for multiple kinases, *e.g.*, at least five, at least ten, at least fifteen, at least twenty, at least thirty, at least forty, at least fifty, or more, kinases selected from the group consisting of ABL1, ABL1(H396P), ABL1(Q252H), ABL1(T315I), BCR-ABL (fusion gene, Philadelphia translocation), ABL2, BLK, BRK (PTK6), FGR, FRK, FYN, HCK, LCK, LYNA, LYNB, SRC, SRMS, YES1, CSK, BTK, BTK(E41K), FER (TYK3), FES, ITK, LTK (TYK1), SYK, TEC, TEK (TIE2), TXK, TYRO3, ZAP70, JAK1, JAK2, JAK3, TYK2, PTK2 (FAK, FAK1), PTK2B (FAK2, PYK2), ALK, AXL, AXL(R499C), CSF1R, DDR1 (NTRK4, RTK6, PTK3), DDR2 (NTRKR3, TYRO10), EGFR, ERBB2, ERBB3 (in its dimeric state with another HER fam. member), ERBB4, FGFR1, FGFR2, FGFR2(N549H), FGFR3, FGFR4, FLT1 (VEGFR1), FLT3, FLT3(D835Y), FLT4 (VEGFR3), KDR (VEGFR2), IGF1R, INSRR (IRR), INSR, ROS1, KIT (SCFR), MET, PDGFRA, PDGFRB, RET, ROR1 (ROR1 (NTRKR1), ROR2 (NTRKR2)), ROR2 (NTRKR2), EPHA1, EPHA2, EPHA3, EPHA4, EPHA5, EPHA8, EPHB1, EPHB2, EPHB3, EPHB4, RON (MST1R), NTRK1 (TRKA), NTRK2 (TRKB), NTRK3 (TRKC), MERTK (MER), WEE1 (WEE1A), WEE2 (WEE1B), MUSK, ACVR1 (ACVR1A, ALK2), ACVR1B (ALK4), TGFBR1 (ALK5), TGFBR2, BMPR1B (ALK6), AKT1, AKT1(E17K), AKT2, AKT2(E17K), AKT3, AKT3(E17K), AKT3(G171R), ARAF, BRAF, RAF1 (cRAF), ATM, ATR, AURKA, AURKB, AURKC, CHEK1, CHEK2, PRKDC (DNA-PKcs, DNAPK), PLK1, PLK3, BRSK1, BRSK2, BUB1, C11orf7, CAMK1, CAMK1beta, CAMK1delta, CAMK1gamma, CAMK2, CAMK2A, CAMK2B, CAMK2D, CAMK2G, CAMK4, CAMKK1, CDC42BPA (MRCK alpha), CDC42BPB (MRCK beta), CDK1 (CDC2), CDK2, CDK3, CDK4, CDK5, CDK6, CDK7, CDK8, CDK9, CDK11, CHUK (IKK alpha), IKBKB (IKK beta), IKBKE (IKK-E), CLK1, CLK2, CSNK1A1 (CK1A), CSNK1D (CK1D), CSNK2A1 (CK2A1), CSNK2A2 (CK2A2), CSNK2B (CK2B), DAPK3 (ZIPK), DMPK (DM1) , DYRK1A, DYRK2, IRAK1, IRAK4, EIF2AK1, EIF2AK2, EIF2AK3 (PEK), EIF2AK4, GRK3 (ADRBK2), GRK5, GSK3A, GSK3B, HIPK2, ILK (p59integrin-linked kinase RAF-like kinase), STK3 (MST2, KRS1), STK4 (MST1, KRS2), STK10 (LOK), STK11 (LKB), MTOR (FRAP1), KSR1, KSR1(A635F), KSR1(L639F),

KSR2, KSR2(R676S), MAPK1 (ERK2), MAPK3 (ERK1), MAPK7 (ERK5/6), MAPK8 (JNK1), MAPK9 (JNK2), MAPK10 (JNK3), MAPK11 (p38b), MAPK12 (p38g), MAPK13 (p38d), MAPK14 (p38a), MAP2K1 (MEK1, MKK1, MAPKK1), MAP2K2 (MEK2, MKK2, MAPKK2), MAP2K4 (MEK4, MKK4, MAPKK4, JNKK1), MAP2K7 (MEK7, MKK7, MAPKK7, JNKK2), MAP3K1 (MEKK1, MAPKKK1), MAP3K7 (MEKK7, TAK1), MAP3K8 (COT), MAP3K14 (NIK), MAP3K17 (TAOK2, PSK1), MAP4K2, MAP4K4 (MEKKK4), MAP4K5, MAP4K6 (MINK), MAPKAPK2 (MK2), MAPKAPK3 (MK3), MAPKAPK5 (MK5), MARK1, MARK2 (EMK1), MARK3 (CTAK1), PKMYT1 (MYT1), NDR1 (STK38), NDR2 (STK38L), NEK1, NEK2, NEK6, NEK7, NLK, NME1 (NM23, NDPK-A), NME2 (NM23B, NDPK-B), NME1-NME2, NUAK1, PAK1, PAK2 (p21 (RAC1) activated kinase 2), PAK3, PAK4, PAK7, PDK1 (pyruvate dehydrogenase kinase 1, GeneID: 5163), PDPK1 (3-phosphoinositide dependent protein kinase 1, GeneID: 5170), PHKG1, PIM1, PIM2, PIM3, PKN1 (PRK1), PKN2 (PRK2), PRKAA1 (AMPKa1), PRKAA2 (AMPKa2), PRKACA (PKA C-alpha, PKACA = protein kinase cAMP-activated (PKA) catalytic subunit alpha), PRKACB (PKA C-beta, PKACB = protein kinase cAMP-activated (PKA) catalytic subunit beta), PRKACG (PKA C-gamma, PKACG = protein kinase cAMP-activated (PKA) catalytic subunit gamma), PRKCA (PKC alpha, PKCA), PRKCB (PKC beta, PKCB), PRKCD (PKC delta, PKCD), PRKCE (PKC epsilon, PKCE), PRKCG (PKC gamma, PKCG), PRKCH (PKC eta, PKCL), PRKCI (PKC iota, PKCI), PRKCM (PKC mu, PKCM), PRKCN (PKC nu), PRKCQ (PKC theta), PRKCZ (PKC zeta), PRKD1 (PKD1, PKD), PRKD2 (PKD2), PRKD3 (PKD3), PRKG1 (PKG 1, subunits I-alpha & I-beta, PRKGR1, PRKG1 = protein kinase, cGMP-dependent (PKG), type I), PRKG2 (PKG 2, PRKGR2, PRKG2 = protein kinase, cGMP-dependent (PKG), type II), PRKRIR (THAP12, DAP4, P52rIPK), ROCK1, ROCK2, RPS6KA1 (RSK1, p90RSK), RPS6KA2 (RSK3, p90RSK2, S6K-alpha-2), RPS6KA3 (RSK2, p90RSK2, S6K-alpha-3), RPS6KA4 (MSK2, S6K-alpha-4), RPS6KA5 (MSK1), RPS6KA6 (RSK4, p90RSK6, S6K-alpha-6), RPS6KB1 (S6K1, p70S6K, S6K-beta-1), RPS6KB2 (S6K2, p70S6Kb, S6K-beta-2), SGK1 (SGK), SGK2, SGK3 (SGKL), SMG1, TAF1, TBK1 (NAK, T2K), TP53RK (PRPK), TSSK1, TSSK2, TSSK4, VRK1, ABL fam. (=ABL1, ABL1(H396P), ABL1(Q252H), ABL1(T315I), BCR-ABL, ABL2), SRC fam. (BRK (PTK6), FGR, FRK, FYN, HCK, LCK, LYNA, LYNB, SRC, SRMS, YES1), JAK fam. (JAK1, JAK2, JAK3, TYK2), PTK2/FAK fam. (PTK2/FAK1, PTK2B/FAK2), EGFR fam. (EGFR, ERBB2, ERBB3, ERBB4), FGFR fam. (FGFR1, FGFR2, FGFR2(N549H), FGFR3, FGFR4), FLT/VEGFR fam. (FLT1 (VEGFR1), FLT3, FLT3(D835Y), FLT4 (VEGFR3), KDR (VEGFR2)), IGFR/INSR fam. (IGF1R,

INSRR (IRR), INSR), PDGFR fam. (PDGFRA, PDGFRB), ROR fam. (PDGFRA, PDGFRB), EPHA/B fam. (EPHA1, EPHA2, EPHA3, EPHA4, EPHA5, EPHA8, EPHB1, EPHB2, EPHB3, EPHB4), ALK fam. (ACVR1, ACVR1B, TGFBR1, TGFBR2, BMPR1B), AKT fam. (AKT1, AKT1(E17K), AKT2, AKT2(E17K), AKT3, AKT3(E17K), AKT3(G171R)), RAF fam. (ARAF, BRAF, RAF1 (cRAF)), AURK fam. (AURKA, AURKB, AURKC), CHEK fam. (CHEK1, CHEK2), PLK fam. (PLK1, PLK3), BRSK fam. (BRSK1, BRSK2), CAMK fam. (CAMK1, CAMK1beta, CAMK1delta, CAMK1gamma, CAMK2, CAMK2A, CAMK2B, CAMK2D, CAMK2G, CAMK4), CDK fam. (CDK1 (CDC2), CDK2, CDK3, CDK4, CDK5, CDK6, CDK7, CDK8, CDK9, CDK11), IKK fam. (CHUK (IKK alpha), IKBKB (IKK beta), IKBKE (IKK-E)), CLK fam. (CLK1, CLK2), CK fam. (CSNK1A1 (CK1A), CSNK1D (CK1D), CSNK2A1 (CK2A1), CSNK2A2 (CK2A2), CSNK2B (CK2B)), IRAK fam. (IRAK1, IRAK4), EIF2AK fam. (EIF2AK1, EIF2AK2, EIF2AK3 (PEK), EIF2AK4), GRK fam. (GRK3 (ADRBK2), GRK5), GSK3 fam. (GSK3A, GSK3B), ERK fam. (MAPK1 (ERK2), MAPK3 (ERK1)), JNK fam. (MAPK8 (JNK1), MAPK9 (JNK2), MAPK10 (JNK3)), p38 fam. (MAPK11 (p38b), MAPK12 (p38g), MAPK13 (p38d), MAPK14 (p38a)), MEK fam. (MAP2K1 (MEK1, MKK1, MAPKK1), MAP2K2 (MEK2, MKK2, MAPKK2)), MAP3K fam. (MAP3K1 (MEKK1, MAPKKK1), MAP3K7 (MEKK7, TAK1), MAP3K8 (COT), MAP3K14 (NIK), MAP3K17 (TAOK2, PSK1)), MAPKAPK fam. (MAPKAPK2 (MK2), MAPKAPK3 (MK3), MAPKAPK5 (MK5)), MARK fam. (MARK1, MARK2 (EMK1), MARK3 (CTAK1)), NEK fam. (NEK1, NEK2, NEK6, NEK7), NME fam. (NME1 (NM23, NDPK-A), NME2 (NM23B, NDPK-B), NME1-NME2), PAK fam. (PAK1, PAK2 (p21 (RAC1) activated kinase 2), PAK3, PAK4, PAK7), PIM fam. (PIM1, PIM2, PIM3), PKN fam. (PKN1 (PRK1), PKN2 (PRK2)), AMPKa fam. (PRKAA1 (AMPKa1), PRKAA2 (AMPKa2)), PKA fam. (PRKACA (PKA C-alpha), PRKACB (PKA C-beta), PRKACG (PKA C-gamma)), PKC fam. (PRKCA (PKC alpha, PKCA), PRKCB (PKC beta, PKCB), PRKCD (PKC delta, PKCD), PRKCE (PKC epsilon, PKCE), PRKCG (PKC gamma, PKCG), PRKCH (PKC eta, PKCL), PRKCI (PKC iota, PKCI), PRKCM (PKC mu, PKCM), PRKCN (PKC nu), PRKCQ (PKC theta), PRKCZ (PKC zeta)), PKD fam. (PRKD1 (PKD1, PKD), PRKD2 (PKD2), PRKD3 (PKD3)), PKG fam. (PRKG1 (PKG 1, subunits I-alpha & I-beta, PRKGR1, PRKG1 = protein kinase, cGMP-dependent (PKG), type I), PRKG2 (PKG 2, PRKGR2, PRKG2 = protein kinase, cGMP-dependent (PKG), type II)), ROCK fam. (ROCK,1 ROCK2), RPS6KA fam. (RPS6KA1 (RSK1, p90RSK), RPS6KA2 (RSK3, p90RSK2, S6K-alpha-2), RPS6KA3 (RSK2, p90RSK2, S6K-alpha-3), RPS6KA4 (MSK2, S6K-alpha-4), RPS6KA5 (MSK1), RPS6KA6

(RSK4, p90RSK6, S6K-alpha-6)), RPS6KB fam. (RPS6KB1 (S6K1, p70S6K, S6K-beta-1), RPS6KB2 (S6K2, p70S6Kb, S6K-beta-2)), SGK fam. (SGK1 (SGK), SGK2, SGK3 (SGKL)), and TSSK fam. (TSSK1, TSSK2, TSSK4).

[0105] In some embodiments, a kinase activity panel to identify a kinase signature that represents a kinase family or a specific kinase comprises biological sensor peptides that correspond to phosphorylated substrate regions from naturally occurring peptides that are phosphorylated by members of various kinase families, *e.g.*, ABL, AKT, ERK, HER, p38, SFK, and TK kinase families. A kinase activity panel can, however, include a plurality of sensor peptides for any kinase of interest, including pseudo kinases and orphan kinases.

[0106] In some embodiments, a kinase activity panel in accordance with the invention comprises biological peptides that are phosphorylated by kinases enzymes that can include kinases evaluated in cancer cells and tumor cells, or other disease conditions, including BLK, BRK (PTK6), FGR, FRK, FYN, HCK, LCK, LYN, SRC, SRMS, YES1, ABL1, ABL2, EGFR, ErbB2, ErbB4, JAK2, CSK, AKT1, AKT2, AKT3, MAPK1 (ERK2), and/or MAPK14 (p38a) kinases. In some embodiments, a panel may comprises biological peptides that are phosphorylated by kinases found in cancer and tumor cells and may include biological sensor peptide fro one or more of PIMs, RPS6KBs, PAKs, PDPK1, GSK3B, PKCs, PKDs, PKAs and the like. In some embodiments, the panel comprises at least 3, or at least 4, biological peptides for each kinase; or at least 4 peptides for each of the kinase families. In some embodiments, the panel comprises 5, 6, 7, 8, 9, 10, 11, or 12 peptides for each kinase family represented in the panel. In some embodiments, the panel comprises 5, 6, 7, 8, 9, 10, 11, or 12 peptides for each kinase represented in the panel.

[0107] In some embodiments, a kinase panel in accordance with the invention comprises at least 75, at least 80, at least 90, at least 100, at least, 110 at least 120, at least 125, at least 130, at least, or at least 140, or at least 150, or 151 of the biological peptides comprise a sequence as shown in Table 1 of a peptide having a peptide ID as shown in Fig. 4. In some embodiments, the kinase activity panel further comprises at least 10, at least 15, at least 20, at least 25, or 27 mutated peptides having a mutation in the substrate region as shown in Fig. 4. In some embodiments, the mutated peptides have the sequence as shown in Table 1 for the peptide ID shown in Fig. 4. In some embodiments, the panel further comprises pre-phosphorylated reference peptides as mutated peptides.

[0108] In some embodiments, a kinase activity panel in accordance with the invention comprises 228 peptides as described in Fig. 4. The sequences of the peptides are provided in Table 1 for each peptide under the peptide probe ID number shown in Fig. 4. The panel comprises 151 biological peptides, 14 generic positive control peptides and 63 reference peptides, i.e., mutated peptides. The 14 generic positive control peptides are communly uses as industry standards. The 63 reference peptides include 27 mutated peptide sequences, 31 pre-phosphorylated peptides and 5 peptides having random sequences. The phosphoresidue target is shown in Fig. 4, as is the origin of the peptide probe (i.e., the name of the biological substrate protein). The kinase enzyme associated with the biological peptides are also provided.

Activity

[0109] Kinase activity can be evaluated using any number of assays, including, *e.g.*, measuring ATP consumption; measuring consumption of any factor related to catalytic activity of an enzyme (e.g. GTP for GTPases instead of ATP for ATP-dependent kinases), measuring post-translational modification of any substrate molecule (e.g. the physical detection of the catalytic addition of a phosphorylation group onto a peptide; and the like). In some embodiments, ATP consumption is conveniently measured using an ATP consumption assay. An illustrative assay is detailed in the Examples under the **Kinase activity assay** section.

[0110] Activity pattern against various peptides in an assay panel can be assessed to determine kinase signature patterns as described herein. Activity can thus be used to assign the kinase activity of a sample undergoing evaluation to one or more kinase families. In some embodiments, kinase activity is assigned to one or more members of a kinase family. Assigning the activity of the kinase can be performed by comparing the activity to control patterns of activity of known kinases. The range of kinases activity of the test sample can vary from a high level of activity to little activity compared to the various control kinases.

[0111] In some embodiments, activity is evaluated as follows. Although this illustration of activity assessment uses ATP consumption to define activity, one of skill understands that similar analyses can be performed using endpoints other than ATP consumption to assess Activity. In an illustrative assay, ATP consumption is measured across a matrix comprising the kinase sensor peptides, *e.g.*, the matrix may be wells or other containers that will hold the kinase assay contents. Again, although this is illustrated using a "well" as a container, other

container may be used. Each well contains reagents/buffers, including the sensor peptide, ATP, and sample. In some embodiments, a kinase inhibitor may be included as a reagent component. A subset of control wells are also employed in which no peptide is present to assess basedline ATP consumption in the sample. ATP consumption measured across all experimental wells provides an activity signature of a sample. A first activity analysis is performed to determine ATP consumption per peptide. This provides an 'agnostic' view of the results. All ATP consumptions for a sample represent a 'fingerprint'. These fingerprints can be compared between samples to determine how different samples are. One example is to use such fingerprints to compare cancer cell lines or tumor tissues (or even recombinant kinases). The results can then be interpreted to assess ATP consumption per kinase.

[0112] In the kinase activity screening panel, as explained above, some of the peptides are typically biological sensor peptides, i.e., they have naturally occurring amino acid sequences that are phosphorylated by a kinase enzyme. In some embodiments, a variant of such a peptide may be employed where the peptide may a minor change *e.g.*, a conservative substitution, that does not influence kinase activity. Kinase activity obtained using the biological sensor peptides can then be used to deconvolute the agnostic peptide phosphorylation signatures to measure the activity of their respective kinases.

[0113] In some embodiments, some kinases may have only one biological sensor peptide associated with them in the assay. Some kinases may have two, some three, etc. More peptides per kinase typically provide for higher sensitivity, specificity and differentiability to identify kinases and their activity levels (i.e. ATP consumption measured and averaged across peptides that are biologically related to each kinase). In typical embodiments, a threshold of at least four biological peptides per kinase is employed to measure the activity of a given kinase, although alternative values, such as three biological peptides per kinase, may also be used.

[0114] For a given kinase, all ATP consumption per biological peptide of this kinase is included to measure the average ATP consumption (i.e. activity) for this kinase. Thus, all activities (ATP consumptions) per peptide can be useful to measure a kinase activity. Activity levels between knases within a sample can then be compared, as can activity levels between samples. Normalization is performed by creating a scale and using a threshold value. This is illustrated in the descriptions of Figs. 1 and 2. Determination of signature patterns and use of a panel to characterizes a kinase in a sample to be evaluated can be

determined as described in the Figures; and in the descripton of Figures, *e.g.*, Figs. 5, 7, 9, 12, 16, 18, 21, 24, and 26. For example, a sample obtained from a melanoma patient may be evaluated for phosphorylation signatures using a 228-petide phosphorylation panel as described herein, see, *e.g.*, 4a and Table 1. Phosphorylation activity can be analyzed using unsupervised heriarchical clustering, principal component analysis, and dual significance threshold selections. Such an analysis can identify not only phosphosignatures that are indicative or particular kinases, or kinases families, but hyperactivity can be identified; and such associates can be associated with outcome.

[0115] In some embodiments, identification of overly active AKT1, PIM1, and RPS6Kb1 kinases as overly active in a melanoma sample is indicative of a poor prognosis (see, *e.g.*, Fig. 23). In some embodiments, targeting RPS6KB or PIM1 in a patient having a $BRAF^{V600E}$ melanoma in which RPS6KB1or PIM1 is elevated can provde an improved outcome compared to therapies that rarget other kinases.

Samples

[0116] A "sample" as used herein comprises cells or is derived from cells, *e.g.*, comprises cellular extracts, to be evaluated that can be obtained from any biological source, such as tissues, extracts, or cell cultures, including cells (e.g. tumor cells), cell lines, cell lysates. The sample can be obtained from animals, preferably mammals, most preferably humans. Samples can be from a single individual or in some embodiments, can be pooled prior to analysis. Samples may from any source may be evaluate dusing a panel of sensor peptides that provide the ability to simultaneous evaluated activities of different activities. Thus, a sample can be obtained from any prokaryote or eukaryote, including plants, yeast, bacteria, cyanobacteria, or any other biological sour ce of interest.

[0117] Samples for analysis employing sensor peptides in accordance with the disclosure can be from any source for which it is desired to determine a kinase activity profile. In some embodiments, the sample is a mammalian sample, *e.g.*, from primates (such as humans and non-human primates, *e.g.*, apes, monkeys) or from other mammals, *e.g.*, a bovine, ovine, porcine, equine, canine, feline, caprine, a murine, or other mammal.

[0118] In some embodiments, the sample is obtained from a patient that has a disease for which it is interest to assess kinase actvitiy, where the sample comprises cells from a tissue that is affected by the disease. A “disease" refers to any disorder, disease, condition, syndrome or combination of manifestations or symptoms recognized or diagnosed as a

disorder that may be correlated by a kinase activity profile. Illustrative disease include, but are not limited to, cancer, cardiovascular diseases including heart failure, hypertension and atherosclerosis, respiratory diseases, renal diseases, gastrointestinal diseases including inflammatory bowel diseases such as Crohn's disease and ulcerative colitis, hepatic, gallbladder and bile duct diseases, including hepatitis and cirrhosis, hematologic diseases, metabolic diseases, endocrine and reproductive diseases, including diabetes, bone and bone mineral metabolism diseases, immune system diseases including autoimmune diseases such as rheumatoid arthritis, lupus erythematosus, and other autoimmune diseases, musculoskeletal and connective tissue diseases, including including arthritis, achondroplasia infectious diseases and neurological diseases such as Alzheimer's disease, Huntington's disease and Parkinson's disease.

Cancer

[0119] In some embodiments, a sample evaluated in accordance with the disclosure is a cancer. Cancer for which kinase activity profiles can be obtained include breast cancer, melanoma, colorectal cancer, lung cancer, ovarian cancer, uterine cancer, cervical cancer, prostate cancer, pancreatic cancer, bladder cancer, head and neck cancers, liver cancer, kidney cancer, brain cancer, including glioma and astrocytomas, thyroid cancer, laryngeal cancer, nasopharyngeal cancer, and oropharyngeal cancer; stomach cancer, and testicular cancer.

[0120] In some embodiments, the cancer is a hematological cancer, such as a lymphoma or leukemia, or multiple myeloma. Examples of leukemias include acute lymphoblastic leukemia, acute myeloid leukemia, chronic myeloid leukemia, hairy cell leukemia, acute nonlymphocytic leukemia, chronic lymphocytic leukemia, acute granulocytic leukemia, chronic granulocytic leukemia, and acute promyelocytic leukemia, among others. Examples of lymphomas include cutaneous T-cell lymphoma, Hodgkin's lymphoma, an non-Hodgkin's lymphoma.

[0121] In some embodiments, a sample comprising cancer cells is obtained from a patient who has been treated with a therapeutic agent, such as a chemotherapeutic agent, *e.g.*, a protein kinase inhibitor.

[0122] In some embodiments, the analysis of kinase activity in cancer cells can be used to select a therapeutic agent that targets a kinase identified as being overactive in cancer cells.

[0123] The following examples are intended to illustrate, but not limit, the claimed invention. Thus, a panel of the invention may comprise a multiplicity of sensor peptides to detect activity for any kinases of interest and the reaction conditions and reagents for assessing activity can be modified as appropriate for evaluation of the kinase activity of interest.

EXAMPLES

Example 1. Peptide multiplex platform as a robust sensor of kinases' activity

[0124] Directly measuring the activity of kinases is the most proximal assessment of their functional status. This example describes the development of a high throughput kinase activity-mapping (HT-KAM) assay, whereby a compendium of biological peptide targets of kinase enzymes serves as combinatorial sensors of phospho-catalytic activity.

Description of experimental results

Peptide sensing platform to monitor phospho-signatures

[0125] We sought to develop a high-throughput kinase activity-mapping (HT-KAM) assay, whereby a compendium of peptides serves as combinatorial sensors of the phospho-catalytic activity of kinase enzymes. To demonstrate our strategy, we synthesized a 228-peptide library (**Fig. 4**) that includes 151 biological 11-mer peptides corresponding to substrate protein regions variously phosphorylated by kinases involved in oncogenic processes[34]. The library also includes 14 generic 'positive control' peptides commonly used as industry standards, and 63 reference peptides comprising 27 mutated, 31 pre-phosphorylated, and 5 random peptide sequences. A liquid dispensing instrument was programmed to aliquot peptide, sample, ATP, and buffer solutions in 384-well plates (**Fig. 1a**; **Additional Methods** section). Each well contains one peptide, and each plate simultaneously assesses the phospho-signature of one sample.

[0126] The description section below concentrates on the biological relevance and technical advance offered by our strategy. Analyses demonstrating repeatability, specificity and validation for recombinant kinases (**Fig. 1; Figs. 5-17**), cell extracts (**Fig. 2; Figs. 18-21**) and tissue extracts (**Fig. 3; Figs. 23-26**) are briefly explained in this section, and more fully described in the **Additional Methods** section.

Multi-peptide-derived phospho-catalytic signatures distinguish individual kinases and their enzymatic subfamilies

[0127] The phospho-catalytic activity profile of 25 recombinant kinases was measured in presence of all 228-peptides (**Fig. 1b; Figs. 5-7**). Inspection of kinases' activity across all peptides revealed that each kinase displayed a unique phosphorylation fingerprint (**Fig. 1b**). Particular family members were functionally distinguishable from genetically related kinases (e.g. BRK or SRMS vs. other SFK's; MAPK14 vs. MAPK1), and the activities of kinase isoforms or oncogenic variant were discernable (LYN A vs. LYN B; ABL1 vs. $ABL1^{T315I}$). Nevertheless, the principal factor clustering kinases was their family of origin (**Fig. 1b**, horizontal clustering; **Fig. 1c**, Pearson correlation grid).

[0128] We then examined how including a multiplicity of peptide sensors impacted the sensitivity and specificity of the assay for predicting the identity of an individual kinase. We computed Area Under the Curve (AUC) from repeated iteration of random peptide sampling. Sensitivity and specificity systematically improved when including an increasing number of peptides, while any single peptide performed poorly overall (example in **Fig. 1d**; **Figs. 8-9**). For any given number of peptides, specific subsets performed significantly better than others. For instance, for HCK, the AUC derived from the specific combination of its 8 biological peptide targets was higher than most other 8-peptide combinations (**Fig. 1d**).

[0129] Next, we asked whether our system could find peptide sets that best differentiate a kinase from others. We compared all phospho-catalytic profiles of kinases using a dual significance threshold ($p<0.05$ for FDR-corrected t-test and Wilcoxon rank sum test). This revealed that a unique differential phospho-signature could be systematically assigned to every kinase (**Fig. 1e; Figs. 10-11**). Optimal signatures included every type of peptide (biological, generic, reference) associated with both significantly high and significantly low phosphorylation activities. So, using a large spectrum of phospho-catalytic activity sensors is a highly sensitive reporting system to differentially identify a specific kinase/kinase family.

Biological peptides are effective combinatorial activity sensors of their kinase enzymes

[0130] We then asked whether kinases preferentially phosphorylated their respective biological peptides. We found that kinases were significantly more capable of phosphorylating the great majority of their biological peptide targets than control pools of 63-reference, or 5-random, or 16-Y/S/T-free peptides (example of AKT1, MAPK1, JAK2 in **Fig. 1f**; box plots in **Fig. 1g**; complete dataset in **Figs. 12-13**). Unsupervised clustering of kinases' activity using only biological peptides showed that biological peptides distinguished individual kinases, yet grouped them by functional relationships and kinase families (**Fig.**

1h). Biological peptides contributed most to kinases' differential phospho-signature (**Fig. 1e,h**; **Figs. 10-11**) and highest measurable activity (**Fig. 14**). Computational analysis revealed that the phospho-catalytic signatures of kinases derived from their biological peptides outperformed generic peptides and provided excellent specificity and sensitivity (average AUC>0.9; **Fig. 1d,i; Fig15**).

[0131] To further evaluate the performance of biological peptides as sensors of kinases, we measured the effect of kinase inhibitors. The activity profiles of ABL1, ABL1^{T315I}, LYN A and AKT1 treated with dasatinib, imatinib and staurosporine showed that biological peptides effectively revealed the distinct drug-sensitivities of kinases (**Fig. 1j-k; Figs. 14b, 16**). Statistical analyses determined that biological peptide sets systematically and significantly correlated with kinases' activity inhibition (**Figs. 14b, 16**). Similar results were found when measuring the effects of SFK-inhibitor PP2 and SU6656 on FYN A, HCK, LCK, and SRC (**Fig. 17**). Altogether, these results show that the identity and activity of kinases can be measured using their respective biological peptides.

Identifying druggable kinases that mediate intrinsic resistance to BRAF^{V600E}- targeted therapy

[0132] Providing a functional assay that identifies hyperactive, druggable kinases in cell culture models would be valuable to investigators. In the case of BRAF^{V600E} CRC, finding targeted therapies has been a biomedical challenge. RNA-interference screens performed in WiDr BRAF^{V600E} CRC cells originally found that parallel feedback activation of EGFR caused intrinsic resistance to vemurafenib (VEM)[4,36], but the limited response of patients treated with BRAF+EGFR combination therapy[37] underlines how crosstalk between signaling pathways often confounds genetic screen–drug response relationships. We applied our assay to explore whether other kinases drive such unresponsiveness to BRAF-therapy.

[0133] We used WiDr cells as a model system. WiDr treated with VEM displayed reduced MEK1 and ERK2 kinase activity, and increased EGFR activity (**Fig. 2a; Fig. 18**). This matched the reduction in phospho-MEK1/2 and ERK1/2 proteins, and increase in phospho-EGFR, which confirmed that the HT-KAM assay could functionally replicate what is anticipated from literature. We then concentrated on finding novel targets. Examination of kinase signatures revealed that AKT1 was overly active, while its downstream tumor suppressor kinase GSK3B was inactivated (**Fig. 2b**, left). Furthermore, the activity of PDPK1 and its downstream effector kinases SGK1, PRKCA, PKNs were increased (**Fig. 2b**, right). These changes in kinase activity were significant (**Fig. 2b; Figs. 18-19**) and confirmed by

immuno-detection (**Fig. 2c**). Such specific changes are cancer-promoting processes implicated in cell cycle, survival and metabolism, which suggests that drug resistance can be functionally defined by our assay as the coordinated re-programing of multiple signaling pathways.

5 **[0134]** To assess the role of these kinases as mediators of resistance to VEM, we tested the response of WiDr to drug combinations in cell survival assays. Besides AKT1, strong synergy was observed when $BRAF^{V600E}$-targeting was paired with inhibitors for PDPK1 and PRKCA (**Fig. 2d**). Results were confirmed using other $BRAF^{V600E}$ CRC cell lines and inhibitors (**Fig. 20**). This demonstrates that our strategy can serve as a discovery platform to 10 predict differences in kinase activity and provide a rational design for new combination therapies.

The phospho-catalytic signatures of cancer cells reveal their specific kinase dependencies

[0135] Next, we asked whether our approach could be used to survey the activity of kinases across different cancer cell lines. **Fig. 2e-f** and **Figs. 21-22a,b** show that cancer cell lines 15 could be systematically distinguished based on either their 228-peptide phosphorylation profiles, or their kinase activity signatures. We then evaluated whether the differential kinase activities of different cells could foretell their drug sensitivity (**Fig. 22c-e**), and specifically asked whether HT-KAM could identify kinases that functionally distinguish $BRAF^{V600E}$ CRC from $BRAF^{V600E}$ MEL cells (WiDr vs. A375; **Fig. 2g-h**). Graphs in **Fig. 2g** compare kinase 20 activity (y-axis) to GI50 concentration for individual drugs (x-axis). Data for the 10 kinases and 14 inhibitors we tested, are compiled in **Fig. 2h**. Results showed that the higher the activity of a kinase, the more a cell line was susceptible to respond to a matching drug. For instance, CDKs and MEKs were significantly more catalytically active in A375 than in WiDr, and A375 cells responded to much lower concentrations of the related drugs dinaciclib 25 and trametinib than WiDr did. So, $BRAF^{V600E}$ cells of different tumor origins inherently relied on distinct kinase dependencies that were predictive of their drug sensitivities. Altogether, results in **Fig. 2f-h** and **Fig. 22** indicate that our platform provides a pragmatic solution to find active, druggable kinases in cell culture models.

Mapping the phospho-catalytic signatures of patients' melanomas

30 **[0136]** Identifying which kinases are overly active in patients' tumors would be of high clinical value. Malignant melanoma is a disease ultimately refractory to most current forms of therapy, including BRAF/MEK/ERK inhibitors used to treat metastatic $BRAF^{V600E}$ tumors[38-

[41]. We thus evaluated the potential utility of our assay to map the phospho-catalytic signatures of patients' melanomas.

[0137] Nine surgically excised, fresh-frozen tumors from melanoma patients (**Fig. 3a; Fig. 23**) were tested in four independent HT-KAM technical replicates. The 228-peptide phosphorylation signatures were analyzed using unsupervised hierarchical clustering (**Fig. 3b**), principal component analysis (**Fig. 24**), and dual significance threshold selection (**Fig. 25**). We found that the phospho-fingerprints of tumors were highly robust signatures that strongly associated with outcome (**Fig. 3b**, black squares; **Figs. 24, 25**). The group of signatures that retrospectively predicted poor outcome included $BRAF^{V600E}$ tumors that did not respond to VEM treatment (**Fig. 3b**, red squares; **Figs. 24, 25b-e**).

[0138] Next, we asked whether peptide phosphorylation profiles could reveal the hyperactive kinases of poor outcome tumors. **Fig. 3c** and **Fig. 26a-c** show that kinase activity signatures established from biological peptides and compared across tumors, were associated with outcome. Enrichment analysis using the most significantly and differentially phosphorylated biological peptides in poor outcome patients, determined that PIM, RPS6KB and AKT kinases were most active (**Fig. 3d; Figs. 26d-e, 27**), and highest in VEM-resistant melanomas (**Fig. 3c**, arrows; **Fig. 3e**). GSK3B was significantly downregulated in these tumors (**Fig. 3c,e**). These hyperactive kinases suggest new vulnerabilities that may be exploitable in the clinic.

<u>Translating kinase hits into new therapeutic opportunities for BRAFV600E melanoma treatment</u>

[0139] Based on these patient tumor kinase activity profiles, we assessed the growth response of A375 and Sk-Mel-28 cells to kinase-targeting drug combinations. **Fig. 3f-h** and **Fig. 28** show that inhibitors of PIM, RPS6KB or AKT significantly potentiated the anti-cancer effects of BRAF inhibition, and outperformed MTOR- or MEK-inhibitors whose effects in patients are variable and transient. Cells exogenously expressing constitutively active AKT1 remained sensitive to RPS6KB- or PIM-targeting (**Fig. 29**), suggesting that these signaling hubs can function independently and represent suitable alternative targets to alleviate therapeutic resistance. GSK3B inhibition antagonized VEM effects, thus mimicking a loss of tumor suppressive function by promoting resistance to BRAF-therapy. These results support observations we made in patient tumors (**Fig. 3c-e**), where unresponsiveness to

$BRAF^{V600E}$-therapy was accompanied with the coordinated inactivation of GSK3B and activation of PIM, RPS6KB and AKT kinases.

[0140] Finally, we used tumor cells isolated from a patient-derived xenograft (PDX) established from a $BRAF^{V600E}$ melanoma patient refractory to VEM 42, and that maintained high levels of phospho-RPS6KB1 (**Fig. 3i; Fig. 30**). Colony formation showed these tumor cells were particularly sensitive to RPS6KB inhibition (**Fig. 3i**). So, the activation of RPS6KB is a confirmed vulnerability that can be targeted to restore therapeutic sensitivity in BRAF therapy-resistant melanomas.

Discussion of experimental results described above

[0141] A key to successful therapy is the identification of critical aberrant signaling networks whose inhibition would result in system failure of diseased cells. This example demonstrates the use of an innovative proteomic approach to identify specific kinase vulnerabilities that lie within the proto-oncogenic phospho-circuits of cancer cells and tumor tissues.

[0142] We developed a system that relies on collections of peptides to directly monitor the phospho-catalytic signatures of biological samples. Our strategy provides access to a vast, untapped resource of meaningful measurements, whether readouts are interpreted irrespective of which enzymes phosphorylate which probes, or analyzed to convert global phospho-signatures into functional profiles of kinase activities.

[0143] In-depth computational analyses and systematic drug targeting of kinases established the advantages of our system to gain biological insights into phospho-signaling circuits. The combination of single phospho-activities measured across peptide sensors collectively distinguished the activity of different kinases within or between samples of simple or complex composition (purified kinases, cells, tissues). Particular subsets of peptides –especially kinases' biological targets– provided superior sensitivity, specificity and discernibility over any single probe-derived measurement. The identity and activity of kinases across a broad range of kinase families could be simultaneously assessed from their subset of biological peptides in various cancer cells and tumor tissues.

[0144] Based on our analyses, the differential spectrum of low-to-high phospho-catalytic activities measured across peptides predicts that expanding the peptide library beyond the current 228 peptides will enable mapping many more kinases with even finer accuracy. It will

also be possible to build 'fit-for-purpose kits' relying on narrow sets of best-predictor peptides customized to monitor the activity of particular kinases for research or diagnostic purposes. The HT-KAM strategy is a versatile platform adaptable to users' needs (e.g. interchangeable peptide library, or assay conditions), and practical to both laboratory research and clinical settings.

[0145] Mechanisms of drug resistance are the cornerstone of therapeutic failure. We established that peptide phospho-signatures of cancer cells could be deconvoluted to identify hyperactive, druggable kinases. We showed that the intrinsic and adaptive kinase dependencies of different $BRAF^{V600E}$ cancers were distinctive and predictive of their drug-sensitivity to single or combinatorial targeted therapies. The newly revealed kinase vulnerabilities of VEM-resistance in $BRAF^{V600E}$ CRC cells included signaling pathways orchestrated by PDPK1, PRKCA, SGK1 and GSK3B. In melanoma, PIM1 and RPS6KB1 were identified as new druggable vulnerabilities predictive of poor outcome in $BRAF^{V600E}$ patients. Some of these susceptibilities are new therapeutic alternatives that could be tested in the clinic. Since kinase circuits are likely cell/patient specific, it will be important to profile the kinome signatures of individual patients' tumors to personalize medical treatments.

[0146] Our approach effectively identified kinase targets beyond those previously found by synthetic lethality genetic dropout screens in same model systems. While shRNA approaches focus more on individual genetic dependencies, our assay allows capturing the functional fingerprint of kinases in their native state, without requiring exogenous interventions that may alter the dynamics of signaling circuits. Furthermore, large scale gene expression or mutation analyses would not identify the kinase targets we found because no evident genetic alteration are reported for these genes in cell lines or patient tumors (e.g. RPS6KB1 or PIM1 in MEL; PRKCA or PDPK1 in CRC)[18,34,42,43]. As well, the results of considerable genomic study efforts suggest that, for many cancers including CRC, therapeutic resistance is likely not driven by individual genetic dependencies or caused by some dominant driver mutations. Therefore, functional proteomic platforms designed to detect the activity of kinases –and eventually the functionality of the whole kinome– such as HT-KAM, are needed to start elaborating higher-order functional maps of signaling networks that can directly pinpoint actionable vulnerabilities of tumors.

[0147] How to choose and pair limitless combinations of drugs is a pressing need for pharmaceutical industries and physicians who grapple with treatment resistance in patients[44-

[46]. Our platform provides a new rational design to help prioritize drug combinations and maximize likelihood of success. Furthermore, the phospho-peptide signatures uncovered in our study represent a new parameter that has the potential to be configured into diagnostic tests. For instance, $BRAF^{V600E}$ melanoma patients who retrospectively displayed phospho-signatures indicative of aggressive disease, may have benefited from targeting BRAF + RPS6KB1 or PIM1, instead of standard therapies on which patients almost inevitably relapse.

[0148] The fact that our assay identifies multiple kinases as a cause of drug-resistance defies the usual scenario of trying to map a highly specific feedback loop that ends up describing a 'unique' pathway that mediates 'all' of the observed resistance. Instead, our results argue that resistance can result from a combination of pathways that are upregulated, working in concert, and interdependent on each other, such that it requires their coordinated signaling activities to drive the resistance. As such, a finite number of key cooperative dependencies can be identified, thus offering a highly selective choice of relevant targets to explore. Such herd-like mode of resistance can only be discovered by the kind of mass-scale functional proteomic approach we developed.

[0149] The combinatorial peptide sensing system described herein is thus a new, effective way to capture the functionality of kinases in cells and tissues. This modular strategy addresses a central issue in the bio-medical field, and could play an integral role in improving research productivity and guiding therapeutic decisions. Mapping the phospho-catalytic signatures of diseases innovates the molecular exploration of signaling networks, and supports the discovery of new actionable dependencies for precision medicine.

<u>References Cited By Number in Above Experimental Results and Discussion, Figure Descriptions For Figs. 1-3, Background of the Invention section, and First Paragraph of Brief Summary of Aspects of the Disclosure Section</u>:

1. Petricoin, E.F., Zoon, K.C., Kohn, E.C., Barrett, J.C. & Liotta, L.A. Clinical proteomics: translating benchside promise into bedside reality. Nature reviews. Drug discovery 1, 683-695 (2002).

2. Blume-Jensen, P. & Hunter, T. Oncogenic kinase signalling. Nature 411, 355-365 (2001).

3. Poulikakos, P.I., Zhang, C., Bollag, G., Shokat, K.M. & Rosen, N. RAF inhibitors transactivate RAF dimers and ERK signalling in cells with wild-type BRAF. Nature 464, 427-430 (2010).

4. Prahallad, A., et al. Unresponsiveness of colon cancer to BRAF(V600E) inhibition through feedback activation of EGFR. Nature 483, 100-103 (2012).

5. Duncan, J.S., et al. Dynamic reprogramming of the kinome in response to targeted MEK inhibition in triple-negative breast cancer. Cell 149, 307-321 (2012).

6. Sos, M.L., et al. Oncogene mimicry as a mechanism of primary resistance to BRAF inhibitors. Cell reports 8, 1037-1048 (2014).

7. Johannessen, C.M., et al. COT drives resistance to RAF inhibition through MAP kinase pathway reactivation. Nature 468, 968-972 (2010).

8. Janne, P.A., Gray, N. & Settleman, J. Factors underlying sensitivity of cancers to small-molecule kinase inhibitors. Nature reviews. Drug discovery 8, 709-723 (2009).

9. Fleuren, E.D., Zhang, L., Wu, J. & Daly, R.J. The kinome 'at large' in cancer. Nature reviews. Cancer 16, 83-98 (2016).

10. Johnson, S.A. & Hunter, T. Kinomics: methods for deciphering the kinome. Nature methods 2, 17-25 (2005).

11. Krogan, N.J., Lippman, S., Agard, D.A., Ashworth, A. & Ideker, T. The Cancer Cell Map Initiative: Defining the Hallmark Networks of Cancer. Molecular cell 58, 690-698 (2015).

12. Hoadley, K.A., et al. Multiplatform analysis of 12 cancer types reveals molecular classification within and across tissues of origin. Cell 158, 929-944 (2014).

13. Akbani, R., et al. A pan-cancer proteomic perspective on The Cancer Genome Atlas. Nature communications 5, 3887 (2014).

14. Chandarlapaty, S., et al. AKT inhibition relieves feedback suppression of receptor tyrosine kinase expression and activity. Cancer cell 19, 58-71 (2011).

15. Coppe, J.P., et al. Senescence-associated secretory phenotypes reveal cell-nonautonomous functions of oncogenic RAS and the p53 tumor suppressor. PLoS Biol 6, 2853-2868 (2008).

16. Huttlin, E.L., et al. The BioPlex Network: A Systematic Exploration of the Human Interactome. Cell 162, 425-440 (2015).

17. Rikova, K., et al. Global survey of phosphotyrosine signaling identifies oncogenic kinases in lung cancer. Cell 131, 1190-1203 (2007).

18. Zhang, B., et al. Proteogenomic characterization of human colon and rectal cancer. Nature 513, 382-387 (2014).

19. Uhlen, M., et al. Proteomics. Tissue-based map of the human proteome. Science 347, 1260419 (2015).

20. Drake, J.M., et al. Phosphoproteome Integration Reveals Patient-Specific Networks in Prostate Cancer. Cell 166, 1041-1054 (2016).

21. Sharma, K., et al. Ultradeep human phosphoproteome reveals a distinct regulatory nature of Tyr and Ser/Thr-based signaling. Cell reports 8, 1583-1594 (2014).

22. Bantscheff, M., et al. Quantitative chemical proteomics reveals mechanisms of action of clinical ABL kinase inhibitors. Nature biotechnology 25, 1035-1044 (2007).

23. Daub, H., et al. Kinase-selective enrichment enables quantitative phosphoproteomics of the kinome across the cell cycle. Molecular cell 31, 438-448 (2008).

24. Kubota, K., et al. Sensitive multiplexed analysis of kinase activities and activity-based kinase identification. Nature biotechnology 27, 933-940 (2009).

25. Nomura, D.K., Dix, M.M. & Cravatt, B.F. Activity-based protein profiling for biochemical pathway discovery in cancer. Nature reviews. Cancer 10, 630-638 (2010).

26. Ren, W., Damayanti, N.P., Wang, X. & Irudayaraj, J.M. Kinase phosphorylation monitoring with i-motif DNA cross-linked SERS probes. Chem Commun (Camb) 52, 410-413 (2016).

27. Anastassiadis, T., Deacon, S.W., Devarajan, K., Ma, H. & Peterson, J.R. Comprehensive assay of kinase catalytic activity reveals features of kinase inhibitor selectivity. Nature biotechnology 29, 1039-1045 (2011).

28. Houseman, B.T., Huh, J.H., Kron, S.J. & Mrksich, M. Peptide chips for the quantitative evaluation of protein kinase activity. Nature biotechnology 20, 270-274 (2002).

29. Karaman, M.W., et al. A quantitative analysis of kinase inhibitor selectivity. Nature biotechnology 26, 127-132 (2008).

30. Fang, C., et al. Integrated microfluidic and imaging platform for a kinase activity radioassay to analyze minute patient cancer samples. Cancer research 70, 8299-8308 (2010).

31. Li, X., et al. The reverse in-gel kinase assay to profile physiological kinase substrates. Nature methods 4, 957-962 (2007).

32. Wu, J., Barbero, R., Vajjhala, S. & O'Connor, S.D. Real-time analysis of enzyme kinetics via micro parallel liquid chromatography. Assay Drug Dev Technol 4, 653-660 (2006).

33. Sanz, A., et al. Analysis of Jak2 catalytic function by peptide microarrays: the role of the JH2 domain and V617F mutation. PloS one 6, e18522 (2011).

34. Olow, A., et al. An Atlas of the Human Kinome Reveals the Mutational Landscape Underlying Dysregulated Phosphorylation Cascades in Cancer. Cancer research (2016).

35. Hornbeck, P.V., et al. PhosphoSitePlus, 2014: mutations, PTMs and recalibrations. Nucleic acids research 43, D512-520 (2015).

36. Corcoran, R.B., et al. EGFR-mediated re-activation of MAPK signaling contributes to insensitivity of BRAF mutant colorectal cancers to RAF inhibition with vemurafenib. Cancer discovery 2, 227-235 (2012).

37. van Geel, R.M., Beijnen, J.H., Bernards, R. & Schellens, J.H. Treatment Individualization in Colorectal Cancer. Curr Colorectal Cancer Rep 11, 335-344 (2015).

38. Flaherty, K.T., et al. Combined BRAF and MEK inhibition in melanoma with BRAF V600 mutations. The New England journal of medicine 367, 1694-1703 (2012).

39. Larkin, J., et al. Combined vemurafenib and cobimetinib in BRAF-mutated melanoma. The New England journal of medicine 371, 1867-1876 (2014).

40. Van Allen, E.M., et al. The genetic landscape of clinical resistance to RAF inhibition in metastatic melanoma. Cancer discovery 4, 94-109 (2014).

41. Wagle, N., et al. MAP kinase pathway alterations in BRAF-mutant melanoma patients with acquired resistance to combined RAF/MEK inhibition. Cancer discovery 4, 61-68 (2014).

42. Kemper, K., et al. BRAF(V600E) Kinase Domain Duplication Identified in Therapy-Refractory Melanoma Patient-Derived Xenografts. Cell reports 16, 263-277 (2016).

43. Cancer Genome Atlas, N. Genomic Classification of Cutaneous Melanoma. Cell 161, 1681-1696 (2015).

44. Bernards, R. A missing link in genotype-directed cancer therapy. Cell 151, 465-468 (2012).

45. Cohen, R.L. & Settleman, J. From cancer genomics to precision oncology--tissue's still an issue. Cell 157, 1509-1514 (2014).

46. Holohan, C., Van Schaeybroeck, S., Longley, D.B. & Johnston, P.G. Cancer drug resistance: an evolving paradigm. Nature reviews. Cancer 13, 714-726 (2013).

47. Brunen, D., et al. TGF-beta: an emerging player in drug resistance. Cell Cycle 12, 2960-2968 (2013).

48. Foucquier, J. & Guedj, M. Analysis of drug combinations: current methodological landscape. Pharmacol Res Perspect 3, e00149 (2015).

Additional Methods—Results are summarized in the Desriptions of the Figures

[0150] Kinase activity assay. The phospho-catalytic signature of samples was established from simultaneously occurring ATP-consumption tests measured in presence of peptides that are experimentally isolated from each other in multi-well plates. Assays were run in 384 well-plates (solid white flat bottom plates; Corning, cat.# 3570), where each experimental well contained one kind of peptide. The final 8 uL reaction mixtures per well contained the following final concentrations of reagents: (i) kinase assay buffer (KaB1x prepared daily and diluted in ddH_2O from a 10x stock solution of 25mM Tris-HCl (pH7.5), 10mM $MgCl_2$, 0.1mM Na3VO4, 5mM β-glycerophosphate, 2mM dithiothreitol (DTT); or purchased from Cell Signaling cat.# 9802), (ii) 250 nM ATP (prepared from a 10mM stock solution of adenosine-5'-triphosphate in ddH2O, and diluted daily with KaB1x; Cell Signaling cat.# 9804), (iii) 200 ug/mL 11-mer peptide (lyophilized stocks originally prepared as 1mg/mL in KaB1x, 5% DMSO), and (iv) samples typically made of either 5ng/uL recombinant kinase enzyme protein or 10 ug/mL protein extract from cell or tissue lysates (see below for protocol) that were kept on ice and diluted in KaB1x <30min before experimental testing.

Controls with no-ATP, or no-peptide, or no-sample as well as ATP standards, were run side-by-side within each 384-well plate.

[0151] High-throughput liquid dispensing of all reagents was achieved using the Biomek® FX Laboratory Automation Workstation from Beckman Coulter (hosted by the Center for Advanced Technologies, UCSF), and was programmed to specifically address the dispensing requirements of the assay (timing, sequence, tip-touch location/height/depth, etc). Accurate dispensing was thoroughly and regularly validated. All reagents were kept on ice and plates on cold blocks (VWR/BioCision; COOLRACK XT PCR96 cat.# 89239-498; COOLSINK XT 96F cat.# 89239-504) until enzymatic reactions were started. For all intermediary steps over the course of the assay (i.e. buffer and sample preparation, dispensing, etc), we used micro-centrifuge tubes (Costar; cat.# 3621) and clear 96-well PCR-plates (VWR; cat.# 83007-374).

[0152] Once the dispensing of reaction mixtures was completed, 384-well reaction plates were typically incubated for 30min at 30degC. After enzymatic reactions were completed, the final detection step used Kinase-Glo revealing reagent (Promega; cat.# V3772; dispensed using Biomek automated workstation), which stops the activity of kinase enzymes and produces a luminescent signal directly correlated with the amount of remaining ATP in samples over a broad range of ATP concentrations (repeatability and accuracy of the ATP-dependent luminescence assay measurements were tested and validated over 5 logs of ATP concentration; R^2>0.99). Luminescence data are inversely correlated with the amount of kinase activity. Luminescence was measured using the Synergy 2 Multi-Mode Microplate Reader from BioTek, and occasionally the Molecular Devices Analyst AD Microplate Reader from McKinley Scientific.

[0153] **Peptide sensors.** 11-mer amino acid sequences were made-to-order and mass synthesized by GenScript at >95% purity. The 228-peptide library included 151 biological peptides, 14 generic positive control peptides, and 63 reference peptides that include 27 mutated (Tyrosine (Y) / Serine (S) / Threonine (T) → Glycine (G)) and 31 pre-phosphorylated (Y / S / T → pY / pS / pT) peptides, and 5 random peptide sequences (**Fig. 4** provides peptide sequence details and connectivity between peptides and kinases). Biological peptides correspond to phosphorylatable amino acid regions of substrate protein identified from literature and curated in resources such as PhosphoAtlas[1] (**Fig. 4c-d**) or PhosphoSitePlus[2]. Each generic positive control peptide corresponds to a kinase activity

reporting probe commonly used in single-peptide assays, as available/advertised from literature. Some of the generic positive control peptides were purchased from SignalChem (e.g. Abltide, cat.# A02-58; Poly (4:1 Glu, Tyr) peptide, cat# P61-58).

[0154] Recombinant kinases. The following purified, recombinant kinase enzymes were purchased from SignalChem: ABL1/c-ABL (cat.# A03-18H), ABL1^{T315I} (cat.# A03-12DG), ABL2/ARG (cat.# A04-11H), AKT1/PKB/RAC (cat.# A16-10G), AKT2 (cat.# A17-10G), AKT3 (cat.# A18-10G), BLK (cat.# B02-10G), BRK/PTK6 (cat.# P94-10G), CSK (cat# C63-10G), EGFR/HER1 (cat# E10-11G), ErbB2/HER2/NEU (cat# E27-11G), ErbB4/HER4 (cat.# E29-11G), ERK2/MAPK1/p42 (cat.# M28-10G), FGR (cat.# F10-10G), FRK (cat.# F14-11G), FYN isoforms A (cat.# F15-10G), FYN isoform C (inactive; cat.# F15-14G-20), HCK (cat.# H02-11G), JAK2 (cat.# J02-11H), LCK (cat.# L03-10G), LYN isoform A (cat.# L13-18G), LYN isoform B (cat.# L13-10G), p38a/MAPK14 (cat.# M39-10BG), SRC/c-SRC (cat.# S19-18G), SRM/SRMS (cat.# S20-11G), YES/YES1 (cat.# Y01-10G). The same concentration of every kinase was used in all experiments (**Fig. 1**, **Figs. 5-17**).

[0155] Kinase inhibitors. The following 46 inhibitors were used in biochemical assays or cell culture. Inhibitors purchased from Selleck Chemicals are: AT13148 (cat.# S7563), AZD1208 (cat.# S7104), AZD7762 (cat.# S1532), BAY-61-3606 (cat.# S7006), BI-D1870 (cat.# S2843), bosutinib / SKI-606 (cat.# S1014), CI-1040 / PD184352 (cat.# S1020), CHIR-99021 (cat.# S1263), dasatinib (cat.# S1021), dinaciclib / SCH-727965 (cat.# S2768), everolimus / RAD001 (cat.# S1120), fedratinib / SAR302503 (cat.# S2736), gefitinib / ZD-1839 (cat.# S1025), Go6983 (cat.# S2911), GSK2334470 (cat.# S7087), H89 (cat.# S1582), imatinib (cat.# S1026), IPA-3 (cat.# S7093), JNK Inhibitor VIII (cat.# S4901), LFM-A13 (cat.# S7734), LY2584702 (cat.# S7704), MK2206 (cat.# S1078), nilotinib / AMN-107 (cat.# S1033), NPK76-ii-72-1 (cat.# S), OSU-03012 (cat.# S1106), pelitinib / EKB-569 (cat.# S1392), PLX-4720 (cat.# S1152), PF-4708671 (cat.# S2163), ponatinib / AP24534 (cat.# S1490), RO-3306 (cat.# S7747), ruxolitinib / INCB018424 (cat.# S1378), saracatinib / AZD0530 (cat.# S1006), selumetinib / AZD6244 (cat.# S1008), sotrastaurin (cat.# S2791), TAK-715 (cat.# S2928), trametinib / GSK1120212 (cat.# S2673), vemurafenib / PLX4032 (cat.# S1267), VX-702 (cat.# S6005), 1-Azakenpaullone (cat.# S7193). Inhibitors obtained from other companies are AS601245 (Cayman; cat.# 17542), bryostatin 1 (Sigma-Aldrich; cat.# B7431), PP2 (Invitrogen; cat.# PHZ1223), PP3 (Tocris; cat.# 2794), SL 0101-1 (Tocris; cat.# 2250), staurosporine (Sigma-Aldrich; cat.# S4400), SU6656 (EMD-CalBiochem; cat# 572635). Conditions of use are indicated in the text.

[0156] **Cell culture.** The 23 cancer cell lines used in this study were purchased from ATCC or provided by the laboratories of Drs. R. Bernards, S. Ortiz-Urda, M. Bissell, or F. McCormick (colorectal: WiDr, HT29, SK-CO-1, HCT-116, RKO-1; melanoma: A375, Sk-Mel-28, Mel888, MM485, Sk-Mel-2; lung: H1755, H3122, PC9; breast: AU565, HCC70, MCF7, MDA-MB-231, MDA-MB-436, T47D, HMT-3522 S1, HMT-3522 T4; prostate: PC3; thyroid: 8505C). Cells were cultured following ATCC's instructions or as previously described [3]. Information regarding primary melanoma cell lines derived from therapy-resistant $BRAF^{V600E}$-melanoma patient-derived xenografts (PDXs) are previously described [4,5].

[0157] To assess the growth/survival response of cell lines to single or combinatorial drug treatments in **Figs. 2-3** and **Figs. 20, 22, 28, 29**, we used CellTiter-Glo cell viability assay (Promega; cat# G7571). Cell culture and luminescence readouts were performed in 96- and 384-well plates after 3-day treatments. Drug treatment conditions are described in the text. The effects of drug combinations on cell growth were assessed by calculating drug interaction (D.I.; two-way ANOVA using Prism or Sigma Plot software) and combination index (C.I.; following either the Loewe Additivity [6-9] or Bliss Independence models [10-12]). IC50 and GI50 correspond to the concentration of a given drug that causes 50% inhibition of kinase activity (IC50) or cell growth (GI50). We systematically tested the effects of drugs in both regular and low serum culture conditions (i.e. 5% and 0.25% FBS media). To quantitate cell death in **Fig. 3** and **Figs. 28-29**, FACS analysis of nuclear degradation was performed as previously described [13]. Colony formation assay in **Fig. 3** and **Fig. 30** were performed as previously described [5].

[0158] To test the responses of WiDr cells treated with VEM in **Fig. 2** and **Figs. 18-20**, cells were plated in medium containing 10% FBS 24h prior to being washed with serum-free medium, and cultured for 24h in medium containing 0.1% serum [3]. After low serum incubation, cells were treated with drugs for 30min and stimulated by 10% FBS. After 8h, 85% confluent cells were washed in PBS, then lyzed, and supernatants stored at -80degC. In cases where experiments happened at the Netherlands Cancer Institute, samples were shipped on dry-ice to the University of California at San Francisco.

[0159] Preparing protein lysates from cell lines for kinase assay. To measure the phospho-catalytic activity of cancer cell lines (Fig. 2 and Figs.18, 19, 21, 22), cultured cells were lyzed for 5min in ice-cold cell lysis buffer. Freshly prepared lysis buffer (1mL per 5.10^6 cells)

contained non-denaturing Cell Lysis Buffer 1x (diluted in ddH2O from 10x stock of 20mM Tris-HCl (pH7.5), 150mM NaCl, 1mM Na2EDTA, 1mM EGTA, 1% Triton, 2.5mM sodium pyrophosphate, 1mM b-glycerophosphate, 1mM Na3VO4, 1ug/mL leupeptin; or purchased from Cell Signaling, cat.# 9803), complemented with 1x Halt Protease & Phosphatase (ThermoScientific cat.# 1861281, which contains inhibitors of Ser/Thr-phosphatases and Tyr-phosphatases). Scraped off lysates were then spun down at 14,000rpm for 15min, and supernatants stored at -80degC. Protein and ATP concentrations were quantified. Since every HT-KAM assay plate includes 14 wells with sample alone (i.e. without peptide; see (Fig. 4f), internal controls for ATP levels were systematically available for all assays/samples (see Figs. 18, 21, 22).

[0160] Immuno-detection and antibodies. Cell lysates were resolved by SDS gel electrophoresis (gels from BioRad), followed by immuno-blotting as previously described [3,5] and following manufacturer's instructions. The following primary antibodies and phospho-antibodies were used. Antibodies to detect ATK1/2/3 (cat.# 4691), AKT1/2 pS473 (cat.# 4060), AKT1/2 pT308 (cat.# 2965), EGFR (cat.# 4267 and 3771), EGFR pY1068 (cat.# 3777 and 2234), ERK1/2 (i.e. MAPK1/ERK2/p44 and MAPK3/ERK1/p42; cat.# 4695), ERK1/2 pT202/Y204 (cat.# 4370), GSK3B (cat.# 9315), GSK3B pS9 (cat.# 9323), MAPK14/p38a (cat.# 8690), MAPK14/p38a pT180/pY182 (cat.# 9215), MEK1/2 (i.e. MAP2K1 and MAP2K2; cat.# 4694), MEK1/2 pS217/221 (cat.# 9121), MTOR (cat.# 2972), MTOR pS2448 (cat.# 2971), PIM1 (cat.# 3247), PDPK1/PDK1 (cat.# 3062), PDPK1/PDK1 pS241 (cat.# 3438), PKN1/PRK1 pT774 and PKN2/PRK2 pT816 (cat.# 2611), PRKCA/PKCa (cat.# 2056), PRKCA/PKCa pT514 (cat.# 9379), RPS6KA1/p90RSK1 (cat.# 8408), RPS6KA1/p90RSK1 pT353 (cat.# 8753), RPS6KB1/p70S6K1 (cat.# 2708), RPS6KB1 pT389 (cat.# 9234), RPS6KB1/p70S6K1 pT421/pS424 (cat.# 9204), SGK1 (cat.# 3272), SGK1 pS78 (cat.# 5599), were from Cell Signaling. Antibodies to detect ERK1 (C-16), ERK2 (C-14), ERK1/2 pT202/pY204 (E-4), HSP90 (cat.# sc-7947) were from SantaCruz. A mixture of ERK1 and ERK2 antibodies was used for detection of total ERK [3]. Dilutions followed manufacturers' instructions.

[0161] Tumor specimens from melanoma patients. Clinical details regarding patients are available in **Fig. 23a**. Patient samples were collected at The Rudolfstiftung Hospital, Vienna Austria, and the University of California San Francisco, California USA, under the IRB# 13-204-VK and 12-09483, respectively. Tumor tissue not needed for diagnostic purposes were collected intraoperatively, macroscopically dissected and flash frozen. A small piece of tumor

tissue was O.C.T.-embedded, sectioned, H&E stained and analyzed to ensure >80% tumor cell content in tumor tissue samples.

[0162] Preparing protein lysates from tumor tissues for kinase assay. Flash frozen melanoma tissue specimens were pulverized using BioSpec 59012MS. Protein extracts from powdered samples were prepared following the lysis protocol used for cultured cells, i.e. lyzed for 5min in ice-cold non-denaturing CLB1x diluted in ddH2O from 10x stock of 20mM Tris-HCl (pH7.5), 150mM NaCl, 1mM Na2EDTA, 1mM EGTA, 1% Triton, 2.5mM sodium pyrophosphate, 1mM b-glycerophosphate, 1mM Na3VO4, 1ug/mL leupeptin, complemented with 1x Halt Protease & Phosphatase (containing Ser/Thr- and Tyr- phosphatases inhibitors), then spun down at 14,000rpm for 15min, and supernatants collected. All samples were stored at -80degC. Internal controls for ATP levels in peptide-free wells were systematically measured (see Fig. 23b). The total amount of tumor tissue sample necessary to profile the activity of kinases across 384well/plates, ranged from 20ug to 30ug (which is less than the typical 100ug collected per core biopsy).

[0163] **TCGA data analysis.** mRNA data from melanoma specimens available from the TCGA resource [14] were analyzed to identify samples with altered gene expression in comparison to reference samples using a z-score cut off of +/-2. The z-score is defined as (expression in tumor sample - mean expression in reference sample) / (standard deviation of expression in reference sample), where the reference population is either all tumors that are diploid for the gene in question, or, when available, normal adjacent tissue. Other statistical analysis details are described in **Fig. 27**.

[0164] **Analysis of phosphorylation activity profiles.** The computational methods, technical notes, and statistical tools developed to analyze the peptide phosphorylation activity profiles and kinase activity signatures are explained in the main text and supplemental information.

References Cited by Number in **"Additional Methods"** Section and Descriptions of Figures.

1. Olow, A., et al. An Atlas of the Human Kinome Reveals the Mutational Landscape Underlying Dysregulated Phosphorylation Cascades in Cancer. Cancer research (2016).

2. Hornbeck, P.V., et al. PhosphoSitePlus, 2014: mutations, PTMs and recalibrations. Nucleic acids research 43, D512-520 (2015).

3. Prahallad, A., et al. Unresponsiveness of colon cancer to BRAF(V600E) inhibition through feedback activation of EGFR. Nature 483, 100-103 (2012).

4. Kemper, K., et al. Intra- and inter-tumor heterogeneity in a vemurafenib-resistant melanoma patient and derived xenografts. EMBO Mol Med 7, 1104-1118 (2015).

5. Kemper, K., et al. BRAF(V600E) Kinase Domain Duplication Identified in Therapy-Refractory Melanoma Patient-Derived Xenografts. Cell reports 16, 263-277 (2016).

6. Breitinger, H.-G. Drug Synergy – Mechanisms and Methods of Analysis, (InTech, 2012).

7. Chou, T.C. Drug combination studies and their synergy quantification using the Chou-Talalay method. Cancer research 70, 440-446 (2010).

8. Chou, T.C. & Talalay, P. Quantitative analysis of dose-effect relationships: the combined effects of multiple drugs or enzyme inhibitors. Adv Enzyme Regul 22, 27-55 (1984).

9. Berenbaum, M.C. Synergy, additivism and antagonism in immunosuppression. A critical review. Clin Exp Immunol 28, 1-18 (1977).

10. Foucquier, J. & Guedj, M. Analysis of drug combinations: current methodological landscape. Pharmacol Res Perspect 3, e00149 (2015).

11. Berenbaum, M.C. What is synergy? Pharmacol Rev 41, 93-141 (1989).

12. Bliss, W.L. Early Man in Western and Northwestern Canada. Science 89, 365-366 (1939).

13. Moasser, M.M., Srethapakdi, M., Sachar, K.S., Kraker, A.J. & Rosen, N. Inhibition of Src Kinases by a Selective Tyrosine Kinase Inhibitor Causes Mitotic Arrest. Cancer Res 59, 6145-6152 (1999).

14. Cancer Genome Atlas, N. Genomic Classification of Cutaneous Melanoma. Cell 161, 1681-1696 (2015).

15. Chen, Z. & Coppé, J.-P. Method and system for building and using a centralized and harmonized relational database (US2012/0296880). (United States, 2012).

16. Yang, X., et al. Widespread Expansion of Protein Interaction Capabilities by Alternative Splicing. Cell 164, 805-817 (2016).

17. Corcoran, R.B., et al. EGFR-mediated re-activation of MAPK signaling contributes to insensitivity of BRAF mutant colorectal cancers to RAF inhibition with vemurafenib. Cancer discovery 2, 227-235 (2012).

18. Brunen, D., et al. TGF-beta: an emerging player in drug resistance. Cell Cycle 12, 2960-2968 (2013).

19. Ahronian, L.G., et al. Clinical Acquired Resistance to RAF Inhibitor Combinations in BRAF-Mutant Colorectal Cancer through MAPK Pathway Alterations. Cancer discovery 5, 358-367 (2015).

20. Arao, T., et al. Small in-frame deletion in the epidermal growth factor receptor as a target for ZD6474. Cancer research 64, 9101-9104 (2004).

21. Garnett, M.J., et al. Systematic identification of genomic markers of drug sensitivity in cancer cells. Nature 483, 570-575 (2012).

22. Yang, W., et al. Genomics of Drug Sensitivity in Cancer (GDSC): a resource for therapeutic biomarker discovery in cancer cells. Nucleic acids research 41, D955-961 (2013).

23. Daemen, A., et al. Modeling precision treatment of breast cancer. Genome biology 14, R110 (2013).

24. Nazarian, R.M., Prieto, V.G., Elder, D.E. & Duncan, L.M. Melanoma biomarker expression in melanocytic tumor progression: a tissue microarray study. J Cutan Pathol 37 Suppl 1, 41-47 (2010).

25. Johannessen, C.M., et al. COT drives resistance to RAF inhibition through MAP kinase pathway reactivation. Nature 468, 968-972 (2010).

26. Girotti, M.R., et al. Paradox-breaking RAF inhibitors that also target SRC are effective in drug-resistant BRAF mutant melanoma. Cancer cell 27, 85-96 (2015).

27. Girotti, M.R., et al. Inhibiting EGF receptor or SRC family kinase signaling overcomes BRAF inhibitor resistance in melanoma. Cancer discovery 3, 158-167 (2013).

28. Sun, C., et al. Reversible and adaptive resistance to BRAF(V600E) inhibition in melanoma. Nature 508, 118-122 (2014).

29. Petricoin, E.F., Zoon, K.C., Kohn, E.C., Barrett, J.C. & Liotta, L.A. Clinical proteomics: translating benchside promise into bedside reality. Nature reviews. Drug discovery 1, 683-695 (2002).

30. Bernards, R. A missing link in genotype-directed cancer therapy. Cell 151, 465-468 (2012).

[0165] It is understood that the examples and embodiments described herein are for illustrative purposes only and that various modifications or changes in light thereof will be suggested to persons skilled in the art and are to be included within the spirit and purview of this application and scope of the appended claims. All publications, patents, accession numbers, and patent applications cited herein are hereby incorporated by reference for the purposes in the context of which they are cited.

Table 1

Peptide ID (total of 615 peptides included in the assay, with 575 unique peptides + 20 peptides in duplicate/triplicate)	Lane / Column location in 384 well plates	well description	Peptide Group (A=biological, B=consensus, C=mutated biological, D=mutated consensus, E=random	color-coded per peptide class (i.e. BIO=grpA vs. CON+=grpB vs. REF=grps CDE)	type of peptide probe	13-mer PEPTIDE probe (11-mer sequ. with terminal GC) (NOTES: (1) in bright red is the middle target site (with sometime additional site next to it), (2) in dark red are additional nearby sites within that sequence, (3) in lowercase letters are nsV, (4) in bold black are mutated amino acids in negative control peptides)	SUBSTRATE PROTEIN (NOTES: (1) /	are between 'different' substrate proteins with same peptide target sequence,	PHOSPHO-RESIDUE target (NOTES: (1) ; are between 'alternative sites' of the same protein substrate, (2) / / are between 'different' substrate proteins with same sequence but different location within the protein sequence, (3) , are between 'next to each other' sites within the same protein substrate sequence), (4) (#) are sites nearby each other within the same protein substrate sequence,	KINASE PROTEIN (NOTES: (1) ; are in between kinases that target the same substrate/target site/peptide (2)	are between 'different' kinase proteins with the different/alternative substrate/peptide target sequences mentioned in the next columns
PA_001	1G01	Key_L1_001 - sample + KaB + ATP + pept. PA_001	A		BIO	ENTITYSLLMHGC	FCGR2B	Y292	BLK; LYNA; LYNB;
PA_002	1I01	Key_L1_002 - sample + KaB + ATP + pept. PA_002	A		BIO	ODKNYLTLPPGC	FCGR2A	Y304	BLK; FYN; LYNA; LYNB; SYK
PA_003	1K01	Key_L1_003 - sample + KaB + ATP + pept. PA_003	A		BIO	PVKGAYREHPYGC	KHDRBS1 (SAM68)	Y435	BRK (PTK6)
PA_004	1M01	Key_L1_004 - sample + KaB + ATP + pept. PA_004	A		BIO	IKEDVYLSHDHGC	BRK (PTK6)	Y342	BRK (PTK6)
PA_005	1O01	Key_L1_005 - sample + KaB + ATP + pept. PA_005	A		BIO	IKDDEYNPCQGGC	FGR	Y412	FGR
PA_006	1A03	Key_L1_006 - sample + KaB + ATP + pept. PA_006	A		BIO	STEPQYQPGENGC	SRC	Y530	FGR; CSK
PA_007	1C03	Key_L1_007 - sample + KaB + ATP + pept. PA_007	A		BIO	PDNEAYEMPSEGC	SNCA	Y125	FGR; FYN; LYNA; LYNB; PTK2B (FAK2, PYK2); SYK
PA_008	1EE03	Key_L1_008 - sample + KaB + ATP + pept. PA_008	A		BIO	KVEQLSPEEEEGC	FOS	S133	FRK
PA_009	1G03	Key_L1_009 - sample + KaB + ATP + pept. PA_009	A		BIO	LPEVATPESEEGC	FOS	T232	FRK
PA_010	1I03	Key_L1_010 - sample + KaB + ATP + pept. PA_010	A		BIO	DDCSMYEDISRGC	CD79A	Y199	FYN
PA_011	1K03	Key_L1_011 - sample + KaB + ATP + pept. PA_011	A		BIO	VNLINYQDDAEGC	CTNNB1	Y142	FYN; BRK (PTK6); EGFR; FGFR2; FGFR3; NTRK1
PA_012	1M03	Key_L1_012 - sample + KaB + ATP + pept. PA_012	A		BIO	IEDNEYTARQGGC	FYN / SRC / YES1	Y420 / Y419 / Y426	FYN | SRC | YES1
PA_013	1O03	Key_L1_013 - sample + KaB + ATP + pept. PA_013	A		BIO	SDQVLYGQLLGGC	CSF3R	Y752	HCK
PA_014	1A05	Key_L1_014 - sample + KaB + ATP + pept. PA_014	A		BIO	KEPSNYDFVYDGC	ELMO1	Y720	HCK
PA_015	1C05	Key_L1_015 - sample + KaB + ATP + pept. PA_015	A		BIO	IEDNEYTAREGGC	HCK / LCK / LYNA; LYNB	Y411 / Y394 / Y397	HCK | LCK | LYNA; LYNB
PA_016	1EE05	Key_L1_016 - sample + KaB + ATP + pept. PA_016	A		BIO	GLHGSYVLRVEGC	DOK1	Y174	LCK
PA_017	1G05	Key_L1_017 - sample + KaB + ATP + pept. PA_017	A		BIO	DNSGTYGKIWEGC	PRKCD	Y334	LCK; SRC
PA_018	1I05	Key_L1_018 - sample + KaB + ATP + pept. PA_018	A		BIO	GADDSYATARSGC	ZAP70	Y492	LCK
PA_019	1K05	Key_L1_019 - sample + KaB + ATP + pept. PA_019	A		BIO	SLPEFYYRPPRGC	CDKN1B (p27; KIP1)	Y88	ABL1; LYNA; LYNB; SRC; YES1
PA_020	1M05	Key_L1_020 - sample + KaB + ATP + pept. PA_020	A		BIO	FDAHIYEGRVIGC	PRKCD	Y64	LYNA; LYNB;
PA_021	1A12	Key_L1_021 - sample + KaB + ATP + pept. PA_021	A		BIO	NIKPTVYGVSPNGC	ABL1	Y226	SRC; ABL1
PA_022	1A07	Key_L1_022 - sample + KaB + ATP + pept. PA_022	A		BIO	LEDNDYGRAVDGC	AKT1	Y326	SRC; BRK (PTK6)
PA_023	1C07	Key_L1_023 - sample + KaB + ATP + pept. PA_023	A		BIO	PEQDEYDIPRHGC	BCAR1	Y234	SRC
PA_024	1EE07	Key_L1_024 - sample + KaB + ATP + pept. PA_024	A		BIO	PQQPTYVQALFGC	GRB2	Y160	SRC; ALK
PA_025	1C12	Key_L1_025 - sample + KaB + ATP + pept. PA_025	A		BIO	CTIDVYMIMVKGC	EGFR	Y944	SRC
PA_026	1I07	Key_L1_026 - sample + KaB + ATP + pept. PA_026	A		BIO	LPEGYYEEAVPGC	AFAP1	Y94	SRC
PA_027	1K07	Key_L1_027 - sample + KaB + ATP + pept. PA_027	A		BIO	PPPELYFVKVDGC	TERT	Y707	SRC
PA_028	1M07	Key_L1_028 - sample + KaB + ATP + pept. PA_028	A		BIO	RDSSYYWEIEAGC	RAF1 (cRAF)	Y341	SRC; JAK2
PA_029	1EE12	Key_L1_029 - sample + KaB + ATP + pept. PA_029	A		BIO	GSAAPYLKTKFGC	STAT3	Y705	SRC; HCK; BRK (PTK6); FGFR3; FGFR4; JAK1; JAK2; ALK; FER; RET
PA_030	1A09	Key_L1_030 - sample + KaB + ATP + pept. PA_030	A		BIO	VVPYRYLQRRKGC	CD46	Y354	SRC; YES1
PA_031	1C09	Key_L1_031 - sample + KaB + ATP + pept. PA_031	A		BIO	QESEDYSQPSTGC	MDM2	Y394	ABL1
PA_032	1EE09	Key_L1_032 - sample + KaB + ATP + pept. PA_032	A		BIO	KVVALYDYMPMGC	BTK	Y223	ABL1; LYNA; LYNB; BTK; ITK; TEC
PA_033	1G09	Key_L1_033 - sample + KaB + ATP + pept. PA_033	A		BIO	IGEGTYGTVFKGC	CDK5	Y15	ABL1; FYN; EPHA4

Table 1

PA_035	1K09	Key_L1_034 - sample + KaB + ATP + pept. PA_035	E		CON - _ random	AAAAA(pY)AAAAAGC	_	_	_
PA_036	1G12	Key_L1_035 - sample + KaB + ATP + pept. PA_036	E		CON - _ random	GGGGGYGGGGGGC	_	_	_
PA_037	1I12	Key_L1_036 - sample + KaB + ATP + pept. PA_037	E		CON - _ random	GGGGG(pY)GGGGGGC	_	_	_
PA_039	1C11	Key_L1_037 - sample + KaB + ATP + pept. PA_039	C		CON - _ mutated BIO	IEDNEGTARQGGC	FYN / SRC / YES1 _ CON (-) _ Y to G	Y420 / Y419 / Y426 _ Y to G	FYN | SRC | YES1
PA_040	1EE11	Key_L1_038 - sample + KaB + ATP + pept. PA_040	C		CON - _ mutated BIO	IEDNE(pY)TARQGGC	FYN / SRC / YES1 _ CON (-) _ Y to pY	Y420 / Y419 / Y426 _ Y to pY	FYN | SRC | YES1
PA_041	1G11	Key_L1_039 - sample + KaB + ATP + pept. PA_041	C		CON - _ mutated BIO	STEPQGQPGENGC	SRC _ CON (-) _ Y to G	Y530 _ Y to G	FGR; CSK
PA_042	1I11	Key_L1_040 - sample + KaB + ATP + pept. PA_042	C		CON - _ mutated BIO	STEPQ(pY)QPGENGC	SRC _ CON (-) _ Y to pY	Y530 _ Y to pY	FGR; CSK
PA_043	1K11	Key_L1_041 - sample + KaB + ATP + pept. PA_043	C		CON - _ mutated BIO	GSAAPGLKTKFGC	STAT3 _ CON (-) _ Y to G	Y705 _ Y to G	SRC; HCK; FGFR3; FGFR4; JAK1; JAK2
PA_044	1M11	Key_L1_042 - sample + KaB + ATP + pept. PA_044	C		CON - _ mutated BIO	GSAAP(pY)LKTKFGC	STAT3 _ CON (-) _ Y to pY	Y705 _ Y to pY	SRC; HCK; FGFR3; FGFR4; JAK1; JAK2
PA_045	1O11	Key_L1_043 - sample + KaB + ATP + pept. PA_045	C		CON - _ mutated BIO	NKPTVGGVSPNGC	ABL1 _ CON (-) _ Y to G	Y226 _ Y to G	SRC; ABL1
PA_046	1A13	Key_L1_044 - sample + KaB + ATP + pept. PA_046	C		CON - _ mutated BIO	NKPTV(pY)GVSPNGC	ABL1 _ CON (-) _ Y to pY	Y226 _ Y to pY	SRC; ABL1
PA_049	1K12	Key_L1_045 - sample + KaB + ATP + pept. PA_049	B		CON +	IYGEFKKKAAC	consensus _ CON+	_	all TKs (>90 Tyrosine Kinases)
PA_051	1K13	Key_L1_046 - sample + KaB + ATP + pept. PA_051	D		CON - _ mutated CON+	ITGEFKKKAAC	consensus _ CON- _ Y to T	_	all TKs (>90 Tyrosine Kinases)
PA_066	1A02	Key_L1_047 - sample + KaB + ATP + pept. PA_066	A		BIO	KGAYREHPYGRGC	KHDRBS1 (SAM68)	Y440	BRK (PTK6)
PA_067	1C02	Key_L1_048 - sample + KaB + ATP + pept. PA_067	A		BIO	KAGNLYDISEDGC	GRIN2B	Y1252	FYN
PA_068	1EE02	Key_L1_049 - sample + KaB + ATP + pept. PA_068	A		BIO	QEKMVYSLVSVGC	ITPR1	Y353	FYN
PA_069	1G02	Key_L1_050 - sample + KaB + ATP + pept. PA_069	A		BIO	SFESRYQQPFEGC	PLCG1	Y1253	HCK
PA_070	1I02	Key_L1_051 - sample + KaB + ATP + pept. PA_070	A		BIO	IPSVPYAPFAAGC	RAPGEF1	Y504	HCK; SRC; ABL1
PA_071	1K02	Key_L1_052 - sample + KaB + ATP + pept. PA_071	A		BIO	VLDDQYTSSTGGC	ITK	Y512	LCK
PA_072	1M02	Key_L1_053 - sample + KaB + ATP + pept. PA_072	A		BIO	EPYNLYSSLKEGC	PIK3R1	Y688	LCK
PA_073	1O02	Key_L1_054 - sample + KaB + ATP + pept. PA_073	A		BIO	NLIREYVKQTWGC	SYK	Y131	LYNA; LYNB; SYK
PA_074	1A04	Key_L1_055 - sample + KaB + ATP + pept. PA_074	A		BIO	ANNPLYKEATSGC	ITGB3	Y773	SRC
PA_075	1C04	Key_L1_056 - sample + KaB + ATP + pept. PA_075	A		BIO	SEDPDYYQYNGC	GTF2I	Y248	SRC; BTK; JAK2
PA_076	1C15	Key_L1_057 - sample + KaB + ATP + pept. PA_076	A		BIO _ Rep (lib1-4)_i1	SLESLYSACSMGC	GRB10	Y67	SRC; FYN; TEC
PA_076	1EE04	Key_L1_058 - sample + KaB + ATP + pept. PA_076	A		BIO	SLESLYSACSMGC	GRB10	Y67	SRC; FYN; TEC
PA_076	2C15	Key_L2_001 - sample + KaB + ATP + pept. PA_076	A		BIO _ Rep (lib1-4)_s1	SLESLYSACSMGC	GRB10	Y67	SRC; FYN; TEC
PA_077	1G04	Key_L1_059 - sample + KaB + ATP + pept. PA_077	C		CON - _ mutated BIO	KAGNLGDISEDGC	GRIN2B _ CON (-) _ Y to G	Y1252 _ Y to G	FYN
PA_078	1I04	Key_L1_060 - sample + KaB + ATP + pept. PA_078	C		CON - _ mutated BIO	EPYNLGSSLKEGC	PIK3R1 _ CON (-) _ Y to G	Y688 _ Y to G	LCK
PA_079	1K04	Key_L1_061 - sample + KaB + ATP + pept. PA_079	C		CON - _ mutated BIO	SLESLGSACSMGC	GRB10 _ CON (-) _ Y to G	Y67 _ Y to G	SRC; FYN; TEC
PA_080	1M04	Key_L1_062 - sample + KaB + ATP + pept. PA_080	C		CON - _ mutated BIO	NLIREGVKQTWGC	SYK _ CON (-) _ Y to G	Y131 _ Y to G	LYNA; LYNB; SYK
PA_081	1O04	Key_L1_063 - sample + KaB + ATP + pept. PA_081	C		CON - _ mutated BIO	KAGNL(pY)DISEDGC	GRIN2B _ CON (-) _ Y to pY	Y1252 _ Y to pY	FYN
PA_082	1A06	Key_L1_064 - sample + KaB + ATP + pept. PA_082	C		CON - _ mutated BIO	EPYNL(pY)SSLKEGC	PIK3R1 _ CON (-) _ Y to pY	Y688 _ Y to pY	LCK
PA_083	1C05	Key_L1_065 - sample + KaB + ATP + pept. PA_083	C		CON - _ mutated BIO	SLESL(pY)SACSMGC	GRB10 _ CON (-) _ Y to pY	Y67 _ Y to pY	SRC; FYN; TEC
PA_084	1EE06	Key_L1_066 - sample + KaB + ATP + pept. PA_084	C		CON - _ mutated BIO	NLIRE(pY)VKQTWGC	SYK _ CON (-) _ Y to pY	Y131 _ Y to pY	LYNA; LYNB; SYK
PA_085	1G05	Key_L1_067 - sample + KaB + ATP + pept. PA_085	A		BIO	MTKSGYQPPRLGC	MAP4K1	Y232	ABL1
PA_086	1I06	Key_L1_068 - sample + KaB + ATP + pept. PA_086	A		BIO	PQDKEYYKVKEGC	JAK2	Y1007	ABL1; JAK2
PA_087	1K06	Key_L1_069 - sample + KaB + ATP + pept. PA_087	A		BIO	SEPPVYANLSNGC	JUN	Y170	ABL1
PA_088	1M06	Key_L1_070 - sample + KaB + ATP + pept. PA_088	A		BIO	VEAVAYAPKKEGC	RAD51	Y54	ABL1

Table 1

PA_089	1O05	Key_L1_071 - sample + KaB + ATP + pept. PA_089	A	BIO	PTHSPYAQPSSGC	TP73	Y99	ABL1
PA_090	1A06	Key_L1_072 - sample + KaB + ATP + pept. PA_090	A	BIO	TSKVIYDFIEKGC	WASL	Y256	ABL1; PTK2 (FAK, FAK1)
PA_091	1C06	Key_L1_073 - sample + KaB + ATP + pept. PA_091	C	CON - _ mutated BIO	VEAVAGAPKKEGC	RAD51 _ CON (-) _ Y to G	Y54 _ Y to G	ABL1
PA_092	1EE06	Key_L1_074 - sample + KaB + ATP + pept. PA_092	C	CON - _ mutated BIO	VEAVA(pY)APKKEGC	RAD51 _ CON (-) _ Y to pY	Y54 _ Y to pY	ABL1
PA_093	1G06	Key_L1_075 - sample + KaB + ATP + pept. PA_093	B	CON +	EGIYGVLGC	consensus _ CON+	--	FYN; HCK; LCK; LYNA; LYNB; SRC
PA_094	1I06	Key_L1_076 - sample + KaB + ATP + pept. PA_094	B	CON +	KYVVGYTGEGIKEVKGC	consensus _ CON+	--	BLK; BRK (PTK6); FGR, FRK; FYN; HCK; LCK; LYNA; LYNB; SRC; SRMS; YES1
PA_095	1K06	Key_L1_077 - sample + KaB + ATP + pept. PA_095	B	CON +	EAIYAAPGC	consensus _ CON+	--	ABL1; ABL1(H396P); ABL1(Q252H); ABL1(T315I); ABL2; BTK; FLT3; FLT3(D835Y); KIT (SCFR); MET; RET
PA_096	1M06	Key_L1_078 - sample + KaB + ATP + pept. PA_096	B	CON +	EAIYAAPFAKKKGC	consensus _ CON+	--	ABL1; ABL2
PA_097	1K15	Key_L1_079 - sample + KaB + ATP + pept. PA_097	B	CON + _ Rep (lib1-4)_i2	EFPIYDFLPAKKKGC	--	--	LYNB; SRMS; EPHA1; EPHA2; EPHA3; EPHA4; EPHA5; EPHA8; EPHB1; EPHB2; EPHB3; EPHB4; FGFR3; MERTK (MER); NTRK2 (TRKB); NTRK3 (TRKC); FES; ITK; PTK2B (FAK2, PYK2); TXK; TYRO3
PA_097	1O06	Key_L1_080 - sample + KaB + ATP + pept. PA_097	B	CON +	EFPIYDFLPAKKKGC	consensus _ CON+	--	LYNB; SRMS; EPHA1; EPHA2; EPHA3; EPHA4; EPHA5; EPHA8; EPHB1; EPHB2; EPHB3; EPHB4; FGFR3; MERTK (MER); NTRK2 (TRKB); NTRK3 (TRKC); FES; ITK; PTK2B (FAK2, PYK2); TXK; TYRO3
PA_097	2K15	Key_L2_002 - sample + KaB + ATP + pept. PA_097	B	CON + _ Rep (lib1-4)_e2	EFPIYDFLPAKKKGC	--	--	LYNB; SRMS; EPHA1; EPHA2; EPHA3; EPHA4; EPHA5; EPHA8; EPHB1; EPHB2; EPHB3; EPHB4; FGFR3; MERTK (MER); NTRK2 (TRKB); NTRK3 (TRKC); FES; ITK; PTK2B (FAK2, PYK2); TXK; TYRO3
PA_098	1A10	Key_L1_081 - sample + KaB + ATP + pept. PA_098	E	CON - _ random	EEEEYEEEEYEEEEYEEEEGC	--	--	--
PA_098	1G17	Key_L1_082 - sample + KaB + ATP + pept. PA_098	E	CON - _ random _ Rep (lib1-4)_i3	EEEEYEEEEYEEEEYEEEEGC	--	--	--
PA_098	2G17	Key_L2_003 - sample + KaB + ATP + pept. PA_098	E	CON - _ random _ Rep (lib1-4)_e3	EEEEYEEEEYEEEEYEEEEGC	--	--	--
PA_099	1C10	Key_L1_083 - sample + KaB + ATP + pept. PA_099	B	CON +	EPLYWSFPAGC	consensus _ CON+	--	EGFR, FGFR2; FGFR2(N549H); FGFR3; FGFR4; PDGFRA; KDR (VEGFR2); FER (TYK3); SYK
PA_100	1EE10	Key_L1_084 - sample + KaB + ATP + pept. PA_100	D	CON - _ mutated CON+	EGIGGVLGC	consensus _ CON- _ Y to G	--	FYN; HCK; LCK; LYNA; LYNB; SRC
PA_101	1G10	Key_L1_085 - sample + KaB + ATP + pept. PA_101	D	CON - _ mutated CON+	EAIGAAPGC	consensus _ CON- _ Y to G	--	ABL1; ABL1(H396P); ABL1(Q252H); ABL1(T315I); ABL2; BTK; FLT3; FLT3(D835Y); KIT (SCFR); MET; RET
PA_102	1I10	Key_L1_086 - sample + KaB + ATP + pept. PA_102	D	CON - _ mutated CON+	EPLGWSFPAGC	consensus _ CON- _ Y to G	--	EGFR, FGFR2; FGFR2(N549H); FGFR3; FGFR4; PDGFRA; KDR (VEGFR2); FER (TYK3); SYK
PA_103	1K10	Key_L1_087 - sample + KaB + ATP + pept. PA_103	D	CON - _ mutated CON+	EGI(pY)GVLGC	consensus _ CON- _ Y to pY	--	FYN; HCK; LCK; LYNA; LYNB; SRC
PA_104	1M10	Key_L1_088 - sample + KaB + ATP + pept. PA_104	D	CON - _ mutated CON+	EAI(pY)AAPGC	consensus _ CON- _ Y to pY	--	ABL1; ABL1(H396P); ABL1(Q252H); ABL1(T315I); ABL2; BTK; FLT3; FLT3(D835Y); KIT (SCFR); MET; RET
PA_105	1O10	Key_L1_089 - sample + KaB + ATP + pept. PA_105	D	CON - _ mutated CON+	EPL(pY)WSFPAGC	consensus _ CON- _ Y to pY	--	EGFR; FGFR2; FGFR2(N549H); FGFR3; FGFR4; PDGFRA; KDR (VEGFR2); FER (TYK3); SYK
PA_106	1A16	Key_L1_090 - sample + KaB + ATP + pept. PA_106	A	BIO	TAEPDYGALYEGC	PLCG1	Y771	EGFR; ERBB3 (in its dimeric state with another HER fam. member); ERBB4; HCK; LYNA; LYNB; SYK; ABL1
PA_106	1A19	Key_L1_091 - sample + KaB + ATP + pept. PA_106	A	BIO _ Rep (lib1-4)_i4	TAEPDYGALYEGC	PLCG1	Y771	EGFR; ERBB3 (in its dimeric state with another HER fam. member); ERBB4; HCK; LYNA; LYNB; SYK; ABL1
PA_106	2A19	Key_L2_004 - sample + KaB + ATP + pept. PA_106	A	BIO _ Rep (lib1-4)_e4	TAEPDYGALYEGC	PLCG1	Y771	EGFR; ERBB3 (in its dimeric state with another HER fam. member); ERBB4; HCK; LYNA; LYNB; SYK; ABL1
PA_107	1C15	Key_L1_092 - sample + KaB + ATP + pept. PA_107	A	BIO	DGKEIYNTIRRGC	RASA1 (GAP)	Y460	EGFR; ERBB3 (in its dimeric state with another HER fam. member); ERBB4; LCK
PA_108	1EE15	Key_L1_093 - sample + KaB + ATP + pept. PA_108	A	BIO	IDSCTYEAMYNGC	CBL	Y731	EGFR; FYN; HCK
PA_109	1G15	Key_L1_094 - sample + KaB + ATP + pept. PA_109	A	BIO	PKGTGYIKTELGC	STAT1	Y701	EGFR; LCK; FGFR3; FGFR4; JAK1; JAK2; KIT (SCFR); TYK2
PA_110	1I15	Key_L1_095 - sample + KaB + ATP + pept. PA_110	A	BIO	DKQVEYLDLDLGC	GAB1	Y627	EGFR; MET; INSR
PA_111	1K15	Key_L1_096 - sample + KaB + ATP + pept. PA_111	A	BIO	IQEANYVPMTPGC	GAB1	Y472	EGFR; MET; INSR

Table 1

PA_112	1M16	Key_L1_097 - sample + KaB + ATP + pept. PA_112	A	BIO	TDRSPYEKVSAGC	MUC1	Y1229	EGFR; ZAP70
PA_113	1O16	Key_L1_098 - sample + KaB + ATP + pept. PA_113	A	BIO	AEGSAYEEVPTGC	PLCG1	Y472	EGFR
PA_114	1A18	Key_L1_099 - sample + KaB + ATP + pept. PA_114	A	BIO	CPQAHYNMYPQGC	STAT5B	Y740	EGFR
PA_115	1C18	Key_L1_100 - sample + KaB + ATP + pept. PA_115	A	BIO	NEDDGYDVPKPGC	CBL	Y744	EGFR; SYK
PA_116	1EE18	Key_L1_101 - sample + KaB + ATP + pept. PA_116	A	BIO	DVETTYADFIAGC	PKIA	Y8	EGFR
PA_117	1G18	Key_L1_102 - sample + KaB + ATP + pept. PA_117	A	BIO	VDAEEYLVPQQGC	ERBB2	Y1023	ERBB2
PA_118	1I18	Key_L1_103 - sample + KaB + ATP + pept. PA_118	A	BIO	RRSLGYAYVNFGC	PABPC1	Y54	ERBB3 (in its dimeric state with another HER fam. member)
PA_119	1K18	Key_L1_104 - sample + KaB + ATP + pept. PA_119	A	BIO	TCAELYEKLPQGC	TEK (TIE2)	Y1048	ERBB4
PA_120	1M16	Key_L1_105 - sample + KaB + ATP + pept. PA_120	A	BIO	AENPEYLGLDVGC	ERBB2	Y1248	EGFR; ERBB2
PA_121	1O18	Key_L1_106 - sample + KaB + ATP + pept. PA_121	A	BIO	AENAEYLRVAPGC	EGFR	Y1197	EGFR; ERBB4
PA_122	1A20	Key_L1_107 - sample + KaB + ATP + pept. PA_122	A	BIO	KAVDGYVKPQIGC	STAT5A / STAT5B	Y694 / Y699	ERBB4; JAK2; JAK3; BTK; SYK; LCK; SRC | EGFR; JAK2; BRK (PTK6); HCK; SRC
PA_123	1C20	Key_L1_108 - sample + KaB + ATP + pept. PA_123	A	BIO	TVPNDYMTSPAGC	ABI1	Y213	ERBB3 (in its dimeric state with another HER fam. member); ERBB4
PA_124	1EE20	Key_L1_109 - sample + KaB + ATP + pept. PA_124	A	BIO	GWMEDYDYVHLGC	BCAR1	Y664	ERBB3 (in its dimeric state with another HER fam. member); ERBB4; PTK2 (FAK,FAK1); BRK (PTK6)
PA_125	1G20	Key_L1_110 - sample + KaB + ATP + pept. PA_125	A	BIO	IGEGAYGKVFKGC	CDK6	Y24	ERBB3 (in its dimeric state with another HER fam. member); ERBB4
PA_126	1I20	Key_L1_111 - sample + KaB + ATP + pept. PA_126	A	BIO	EDELPYDDCVFGC	NFKBIA (IKBA)	Y305	ERBB3 (in its dimeric state with another HER fam. member); ERBB4
PA_127	1K20	Key_L1_112 - sample + KaB + ATP + pept. PA_127	A	BIO	RADENYYKAQYGC	SYK	Y525	ERBB3 (in its dimeric state with another HER fam. member); ERBB4; SYK
PA_128	1M20	Key_L1_113 - sample + KaB + ATP + pept. PA_128	C	CON - _ mutated BIO	PKGTGGIKTELGC	STAT1 _ CON (-) _ Y to G	Y701 _ Y to G	EGFR; LCK; FGFR3; FGFR4; JAK1; JAK2; KIT (SCFR); TYK2
PA_129	1O20	Key_L1_114 - sample + KaB + ATP + pept. PA_129	C	CON - _ mutated BIO	DKQVEGLDLDLGC	GAB1 _ CON (-) _ Y to G	Y627 _ Y to G	EGFR; MET; INSR
PA_130	1B14	Key_L1_115 - sample + KaB + ATP + pept. PA_130	C	CON - _ mutated BIO	AEGSAGEEVPTGC	PLCG1 _ CON (-) _ Y to G	Y472 _ Y to G	EGFR
PA_131	1D14	Key_L1_116 - sample + KaB + ATP + pept. PA_131	C	CON - _ mutated BIO	VDAEEGLVPQQGC	ERBB2 _ CON (-) _ Y to G	Y1023 _ Y to G	ERBB2
PA_132	1F14	Key_L1_117 - sample + KaB + ATP + pept. PA_132	C	CON - _ mutated BIO	RRSLGGAYVNFGC	PABPC1 _ CON (-) _ Y to G	Y54 _ Y to G	ERBB3 (in its dimeric state with another HER fam. member)
PA_133	1H14	Key_L1_118 - sample + KaB + ATP + pept. PA_133	C	CON - _ mutated BIO	TCAELGEKLPQGC	TEK (TIE2) _ CON (-) _ Y to G	Y1048 _ Y to G	ERBB4
PA_134	1J14	Key_L1_119 - sample + KaB + ATP + pept. PA_134	C	CON - _ mutated BIO	GWMEDGDYVHLGC	BCAR1 _ CON (-) _ Y to G	Y664 _ Y to G	ERBB3 (in its dimeric state with another HER fam. member); ERBB4; PTK2 (FAK,FAK1)
PA_135	1L14	Key_L1_120 - sample + KaB + ATP + pept. PA_135	C	CON - _ mutated BIO	EDELPGDDCVFGC	NFKBIA (IKBA) _ CON (-) _ Y to G	Y305 _ Y to G	ERBB3 (in its dimeric state with another HER fam. member); ERBB4
PA_136	1N14	Key_L1_121 - sample + KaB + ATP + pept. PA_136	C	CON - _ mutated BIO	PKGTG(pY)IKTELGC	STAT1 _ CON (-) _ Y to pY	Y701 _ Y to pY	EGFR; LCK; FGFR3; FGFR4; JAK1; JAK2; KIT (SCFR); TYK2
PA_137	1P14	Key_L1_122 - sample + KaB + ATP + pept. PA_137	C	CON - _ mutated BIO	DKQVE(pY)LDLDLGC	GAB1 _ CON (-) _ Y to pY	Y627 _ Y to pY	EGFR; MET; INSR
PA_138	1B16	Key_L1_123 - sample + KaB + ATP + pept. PA_138	C	CON - _ mutated BIO	AEGSA(pY)EEVPTGC	PLCG1 _ CON (-) _ Y to pY	Y472 _ Y to pY	EGFR
PA_138	1G14	Key_L1_124 - sample + KaB + ATP + pept. PA_138	C	CON - _ mutated BIO – Rep (lib1-4)_i5	AEGSA(pY)EEVPTGC	PLCG1 _ CON (-) _ Y to pY	Y472 _ Y to pY	EGFR
PA_138	2G14	Key_L2_005 - sample + KaB + ATP + pept. PA_138	C	CON - _ mutated BIO – Rep (lib1-4)_e5	AEGSA(pY)EEVPTGC	PLCG1 _ CON (-) _ Y to pY	Y472 _ Y to pY	EGFR
PA_139	1D16	Key_L1_125 - sample + KaB + ATP + pept. PA_139	C	CON - _ mutated BIO	VDAEE(pY)LVPQQGC	ERBB2 _ CON (-) _ Y to pY	Y1023 _ Y to pY	ERBB2
PA_140	1F16	Key_L1_126 - sample + KaB + ATP + pept. PA_140	C	CON - _ mutated BIO	RRSLG(pY)AYVNFGC	PABPC1 _ CON (-) _ Y to pY	Y54 _ Y to pY	ERBB3 (in its dimeric state with another HER fam. member)
PA_141	1H16	Key_L1_127 - sample + KaB + ATP + pept. PA_141	C	CON - _ mutated BIO	TCAEL(pY)EKLPQGC	TEK (TIE2) _ CON (-) _ Y to pY	Y1048 _ Y to pY	ERBB4
PA_142	1J16	Key_L1_128 - sample + KaB + ATP + pept. PA_142	C	CON - _ mutated BIO	GWMED(pY)DYVHLGC	BCAR1 _ CON (-) _ Y to pY	Y664 _ Y to pY	ERBB3 (in its dimeric state with another HER fam. member); ERBB4; PTK2 (FAK, FAK1)
PA_143	1L16	Key_L1_129 - sample + KaB + ATP + pept. PA_143	C	CON - _ mutated BIO	EDELP(pY)DDCVFGC	NFKBIA (IKBA) _ CON (-) _ Y to pY	Y305 _ Y to pY	ERBB3 (in its dimeric state with another HER fam. member); ERBB4
PA_144	1B01	Key_L1_130 - sample + KaB + ATP + pept. PA_144	A	BIO	SFLQRYSSDPTGC	EGFR	Y1069	EGFR; JAK2
PA_145	1D01	Key_L1_131 - sample + KaB + ATP + pept. PA_145	A	BIO	IVRKRTLRRLGC	EGFR	T678	PRKCA (PKC alpha, PKCA); PRKCD (PKC delta, PKCD); PRKD1 (PKD1, PKD); PKN1 (PRK1)
PA_146	1F01	Key_L1_132 - sample + KaB + ATP + pept. PA_146	A	BIO	AEEKEYHAEGGGC	EGFR	Y869	SRC; EGFR

Table 1

PA_147	1H01	Key_L1_133 - sample + KaB + ATP + pept. PA_147	A	BIO	CGGSPSVRCS$MS	SMAD2	S465	ACVR1B (ALK4); TGFBR1 (ALK5); BMPR1B (ALK6)
PA_148	1J01	Key_L1_134 - sample + KaB + ATP + pept. PA_148	A	BIO	SPAELSPTTLSGC	SMAD2	S250	MAPK1 (ERK2); MAPK3 (ERK1)
PA_149	1L01	Key_L1_135 - sample + KaB + ATP + pept. PA_149	A	BIO	SMDTGSPAELSGC	SMAD2	S245	MAPK1 (ERK2); MAPK3 (ERK1)
PA_150	1N01	Key_L1_136 - sample + KaB + ATP + pept. PA_150	A	BIO	NYIPETPPPGYGC	SMAD2	T220	MAPK1 (ERK2); MAPK3 (ERK1)
PA_151	1P01	Key_L1_137 - sample + KaB + ATP + pept. PA_151	A	BIO	SILPFTPPVVKGC	SMAD2	T8	MAPK3 (ERK1)
PA_152	1B03	Key_L1_138 - sample + KaB + ATP + pept. PA_152	A	BIO	RQRSTSTPNVHGC	RAF1 (cRAF)	S259	AKT1; PRKACA (PKA C-alpha); RAF1 (cRAF)
PA_153	1D03	Key_L1_139 - sample + KaB + ATP + pept. PA_153	A	BIO	QRDSSYYWEIEGC	RAF1 (cRAF)	Y340	JAK2
PA_154	1F03	Key_L1_140 - sample + KaB + ATP + pept. PA_154	A	BIO	HSESASPSALSGC	RAF1 (cRAF)	S289	MAPK1 (ERK2); MAPK3 (ERK1)
PA_155	1H03	Key_L1_141 - sample + KaB + ATP + pept. PA_155	A	BIO	SALSSSPNNLSGC	RAF1 (cRAF)	S296	MAPK1 (ERK2)
PA_156	1J03	Key_L1_142 - sample + KaB + ATP + pept. PA_156	A	BIO	RGQRDSSYYWEGC	RAF1 (cRAF)	S338	PAK1; PAK2; PAK3; PAK7; MAP2K1 (MEK1, MKK1, MAPKK1); RAF1 (cRAF)
PA_157	1L03	Key_L1_143 - sample + KaB + ATP + pept. PA_157	A	BIO	RDRSSSAPNVHGC	BRAF	S365	AKT1; AKT3; SGK1 (SGK)
PA_158	1N03	Key_L1_144 - sample + KaB + ATP + pept. PA_158	A	BIO	GQLIDSMANSFGC	MAP2K1 (MEK1) / MAP2K2 (MEK2)	S218 / S222	ARAF; BRAF; RAF1 (cRAF); MAP3K1 (MEKK1, MAPKKK1); MAP3K8 (COT) | BRAF; MAP3K8 (COT)
PA_159	1P03	Key_L1_145 - sample + KaB + ATP + pept. PA_159	A	BIO	DSMANSFVGTRGC	MAP2K1 (MEK1) / MAP2K2 (MEK2)	S222 / S226	ARAF; BRAF; RAF1 (cRAF); MAP3K1 (MEKK1, MAPKKK1); MAP3K8 (COT); PDPK1 | BRAF; MAP3K8 (COT); PDPK1
PA_160	1B05	Key_L1_146 - sample + KaB + ATP + pept. PA_160	A	BIO	GDAAETPPRPRGC	MAP2K1 (MEK1)	T286	CDK1 (CDC2); CDK5; RAF1 (cRAF)
PA_161	1D05	Key_L1_147 - sample + KaB + ATP + pept. PA_161	A	BIO	PPRPRTPGRPLGC	MAP2K1 (MEK1)	T292	CDK1 (CDC2); MAPK1 (ERK2); RAF1 (cRAF)
PA_162	1F05	Key_L1_148 - sample + KaB + ATP + pept. PA_162	A	BIO	PGRPLSSYGMDGC	MAP2K1 (MEK1)	S298	PAK1
PA_163	1H05	Key_L1_149 - sample + KaB + ATP + pept. PA_163	A	BIO	GFLTEYVATRWGC	MAPK1 (ERK2) / MAPK3 (ERK1)	Y187 (+T185) / Y204 (+T202)	MAP2K1 (MEK1, MKK1, MAPKK1); MAP2K2 (MEK2, MKK2, MAPKK2); MAPK1 (ERK2); MAPK3 (ERK1); RET; JAK2
PA_164	1J05	Key_L1_150 - sample + KaB + ATP + pept. PA_164	A	BIO	HTGFLTEYVATGC	MAPK1 (ERK2) / MAPK3 (ERK1)	T185 (+Y187) / T202 (+Y204)	MAP2K2 (MEK2, MKK2, MAPKK2); MAPK3 (ERK1) | MAPK1 (ERK2)
PA_165	1L05	Key_L1_151 - sample + KaB + ATP + pept. PA_165	A	BIO	RYTNLSYIGEGGC	MAPK1 (ERK2)	S29	RAF1 (cRAF)
PA_166	1N05	Key_L1_152 - sample + KaB + ATP + pept. PA_166	A	BIO	HFPQFSYSASGGC	AKT1 / AKT2 / AKT3	S473 / S474 / S472	IKBKE (IKK-E); ILK; LRRK2; MAPKAPK2 (MK2); MTOR (FRAP1); PDK1; PDPK1; PRKDC (DNA-PKcs, DNAPK); PRKCA (PKC alpha, PKCA); PRKCB (PKC beta, PKCB); PRKCD (PKC delta, PKCD); PRKD1 (PKD1, PKD); PIKFYVE (PIP5K3); TBK1 (NAK, T2K) | PDPK1 | PRKCD (PKC delta, PKCD); PRKCZ (PKC zeta)
PA_167	1P05	Key_L1_153 - sample + KaB + ATP + pept. PA_167	A	BIO	GATMKTFCGTPGC	AKT1 / AKT2 / AKT3	T308 / T309 / T305	CAMKK1; IKBKE (IKK-E); PDK1; PDPK1; PRKCA (PKC alpha, PKCA); PRKCB (PKC beta, PKCB); PRKCZ (PKC zeta); PRKD1 (PKD1, PKD); TBK1 (NAK, T2K) | PDPK1 | PDPK1; PRKCZ (PKC zeta)
PA_168	1B07	Key_L1_154 - sample + KaB + ATP + pept. PA_168	A	BIO	GTDPEYLAPEVGC	AKT1	Y315	SRC; RET
PA_169	1D07	Key_L1_155 - sample + KaB + ATP + pept. PA_169	A	BIO	PDVPRTPVGKFGC	CDC25C	T48	CDK1 (CDC2)
PA_170	1F07	Key_L1_156 - sample + KaB + ATP + pept. PA_170	A	BIO	LYRSPSMPENLGC	CDC25C	S216	BRSK1; BRSK2; C11orf7; CHEK1; CHEK2; MAPK14 (p38a); MAPK3 (CTAK1); PKN1 (PRK1); PLK3
PA_171	1H07	Key_L1_157 - sample + KaB + ATP + pept. PA_171	A	BIO	SGLYRSPSMPEGC	CDC25C	S214	CDK1 (CDC2)
PA_172	1J07	Key_L1_158 - sample + KaB + ATP + pept. PA_172	A	BIO	GSGTATPSALIGC	SP1	T739	MAPK1 (ERK2); MAPK3 (ERK1); MAPK8 (JNK1); CDK1 (CDC2)
PA_173	1L07	Key_L1_159 - sample + KaB + ATP + pept. PA_173	A	BIO	PIIRTPTVGPGC	SP1	T453	MAPK1 (ERK2); MAPK3 (ERK1)
PA_174	1N07	Key_L1_160 - sample + KaB + ATP + pept. PA_174	A	BIO	SQRRRSLEPAEGC	SRC	S17	PRKACA (PKA C-alpha)
PA_175	1P04	Key_L1_161 - sample + KaB + ATP + pept. PA_175	A	BIO _ Rep (lib1-4)_i8	ETDKEYYTVKDGC	JAK1	Y1034	JAK3; JAK1
PA_175	1P07	Key_L1_162 - sample + KaB + ATP + pept. PA_175	A	BIO	ETDKEYYTVKDGC	JAK1	Y1034	JAK3; JAK1
PA_175	2F04	Key_L2_006 - sample + KaB + ATP + pept. PA_175	A	BIO _ Rep (lib1-4)_e5	ETDKEYYTVKDGC	JAK1	Y1034	JAK3; JAK1
PA_176	1B09	Key_L1_163 - sample + KaB + ATP + pept. PA_176	A	BIO	TDKEYYTVKDDGC	JAK1	Y1035	JAK3; JAK1

Table 1

PA_177	1D09	Key_L1_164 - sample + KaB + ATP + pept. PA_177	A	BIO	LSYLQSPITTSGC	DUSP1	S359	MAPK1 (ERK2), MAPK3 (ERK1)
PA_178	1F09	Key_L1_165 - sample + KaB + ATP + pept. PA_178	A	BIO	QDKEYYKVKEPGC	JAK2	Y1008	JAK2
PA_179	1H09	Key_L1_166 - sample + KaB + ATP + pept. PA_179	A	BIO	VLRPEYPRPVDGC	CASP9	T125	MAP2K1 (MEK1, MKK1, MAPKK1); MAP2K2 (MEK2, MKK2, MAPKK2); MAPK1 (ERK2); MAPK3 (ERK1)
PA_180	1J09	Key_L1_167 - sample + KaB + ATP + pept. PA_180	A	BIO	GVITTPYPPGGC	JUN / JUNB	T91 / T102	MAPK8 (JNK1); MAPK9 (JNK2); MAPK14 (p38a) | MAPK8 (JNK1)
PA_181	1L09	Key_L1_168 - sample + KaB + ATP + pept. PA_181	A	BIO	IDLPMSPRTLDGC	STAT3	S727	MAPK1 (ERK2), MAPK3 (ERK1); MAPK8 (JNK1); MAPK9 (JNK2); CDK5; DAPK3 (ZIPK); DYRK2; IRAK1; NEK6; NLK; PRKCD (PKC delta, PKCD); PRKCE (PKC epsilon, PKCE); RPS6KA3 (RSK2, p90RSK2, S6K-alpha-3); RPS6KA5 (MSK1)
PA_182	1N09	Key_L1_169 - sample + KaB + ATP + pept. PA_182	A	BIO	RPRTTSFAESCGC	GSK3B	S9	AKT1; AKT3; AURKA; PRKACA (PKA C-alpha); MAP4K5; PRKCA (PKC alpha, PKCA); PRKCB (PKC beta, PKCB); PRKCD (PKC delta, PKCD); PRKCG (PKC gamma, PKCG); PRKCH (PKC eta, PKCL); RPS6KA1 (RSK1, p90RSK); RPS6KA3 (RSK2, p90RSK2, S6K-alpha-3); RPS6KB1 (S6K1, p70S6K, S6K-beta-1); RPS6KB2 (S6K2, p70S6Kb, S6K-beta-2); SGK1 (SGK); SGK3 (SGKL)
PA_183	1P09	Key_L1_170 - sample + KaB + ATP + pept. PA_183	A	BIO	RARTSSFAEPGGC	GSK3A	S21	AKT1; IKBKE (IKK-E), PRKACA (PKA C-alpha); PRKCA (PKC alpha, PKCA); PRKCB (PKC beta, PKCB); PRKCD (PKC delta, PKCD); PRKCG (PKC gamma, PKCG); PRKCH (PKC eta, PKCL); PRKD3 (PKD3); RPS6KA3 (RSK2, p90RSK2, S6K-alpha-3); SGK1 (SGK); SGK3 (SGKL)
PA_184	1B11	Key_L1_171 - sample + KaB + ATP + pept. PA_184	B	CON +	KRPRAASFAEGC	consensus _ CON+	--	AKT1, AKT2; AKT3; PAK4, PAK7; SGK1 (SGK); SGK2
PA_185	1D11	Key_L1_172 - sample + KaB + ATP + pept. PA_185	B	CON +	RPRAATFPSGC	consensus _ CON+	--	AKT1, AKT2; AKT3; SGK1 (SGK)
PA_186	1F11	Key_L1_173 - sample + KaB + ATP + pept. PA_186	B	CON +	PRTSSFAEGC	consensus _ CON+	--	AKT1, AKT1(E17K); AKT2, AKT2(E17K); AKT3; AKT3(E17K); AKT3(G171R); PDK1; PLK3; RPS6KA3 (RSK2); RPS6KA4 (MSK2); RPS6KA5 (MSK1); RPS6KB1 (S6K1); SGK1 (SGK); SGK2; SGK3 (SGKL)
PA_187	1H11	Key_L1_174 - sample + KaB + ATP + pept. PA_187	B	CON +	IPTSPITTTYFGC	consensus _ CON+	--	MAPK1 (ERK2); MAPK3 (ERK1), MAPK11 (p38b); MAPK12 (p38g); MAPK13 (p38d); MAPK14 (p38a); CDK6; IRAK4
PA_188	1J11	Key_L1_175 - sample + KaB + ATP + pept. PA_188	A	BIO	ADQTPTPTRFLGC	ATF2 (CREB2)	T71	MAPK8 (JNK1); MAPK9 (JNK2); MAPK14 (p38a); VRK1
PA_189	1L11	Key_L1_176 - sample + KaB + ATP + pept. PA_189	A	BIO	RSRHSSYPAGTGC	BAD	S75	AKT1, AKT3; PAK1; PAK2, PAK4, PAK7; PIM1; PIM2; PIM3, PKN2 (PRK2); RPS6KA1 (RSK1, p90RSK), RPS6KA2 (RSK3, p90RSK2, S6K-alpha-2), RPS6KA3 (RSK2, p90RSK2, S6K-alpha-3), PRKACA (PKA C-alpha), PRKCE (PKC epsilon, PKCE), PRKCI (PKC iota, PKCI), PRKCQ (PKC theta); PRKD1 (PKD1, PKD), ARAF, BRAF; RAF1 (cRAF)
PA_190	1N11	Key_L1_177 - sample + KaB + ATP + pept. PA_190	A	BIO	RGRSRSAPPNLGC	BAD	S99	AKT1; AKT3; PAK1; PIM1; PIM2, PIM3; PRKACA (PKA C-alpha); PRKCE (PKC epsilon, PKCE), PRKCI (PKC iota, PKCI), PRKCQ (PKC theta); PRKD1 (PKD1, PKD); RPS6KA3 (RSK2, p90RSK2, S6K-alpha-3); ARAF; BRAF; RAF1 (cRAF)
PA_191	1P11	Key_L1_178 - sample + KaB + ATP + pept. PA_191	A	BIO	RKRRPTSGLHPGC	BRCA1	T509	AKT1
PA_192	1B13	Key_L1_179 - sample + KaB + ATP + pept. PA_192	A	BIO	LFPIKSFVKTKGC	BRCA1	S988	CHEK2
PA_193	1D13	Key_L1_180 - sample + KaB + ATP + pept. PA_193	A	BIO	KRRQTSMTDFYGC	CDKN1A (p21, WAF1, CIP1)	S146	AKT1; PIM1; PIM2; PRKCA (PKC alpha, PKCA); NUAK1; LATS2
PA_194	1F06	Key_L1_181 - sample + KaB + ATP + pept. PA_194	A	BIO _ Rep (lib1-4)_i7	RKRRQTSMTDFGC	CDKN1A (p21, WAF1, CIP1)	T145	AKT1; DAPK3 (ZIPK), PIM1
PA_194	1F13	Key_L1_182 - sample + KaB + ATP + pept. PA_194	A	BIO	RKRRQTSMTDFGC	CDKN1A (p21, WAF1, CIP1)	T145	AKT1; DAPK3 (ZIPK); PIM1
PA_194	2F06	Key_L2_007 - sample + KaB + ATP + pept. PA_194	A	BIO _ Rep (lib1-4)_e7	RKRRQTSMTDFGC	CDKN1A (p21, WAF1, CIP1)	T145	AKT1, DAPK3 (ZIPK); PIM1
PA_195	1H13	Key_L1_183 - sample + KaB + ATP + pept. PA_195	A	BIO	RPRVTSGGVSEGC	CHEK1	S280	AKT1

Table 1

PA_196	1J13	Key_L1_184 - sample + KaB + ATP + pept. PA_196	A	BIO	LSRRPSYRKILGC	CREB1 / CREM	S133 / S136		AKT1; ATM; CAMK1; CAMK2D; CAMK2G; CAMK4; CDK1 (CDC2); MAP3K8 (COT); MAPKAPK2 (MK2); PRKACA (PKA C-alpha); PRKCA (PKC alpha, PKCA); PRKCE (PKC epsilon, PKCE); PRKD1 (PKD1, PKD); PRKG1 (PKG 1); RPS6KA1 (RSK1); RPS6KA2 (RSK3); RPS6KA3 (RSK2); RPS6KA4 (MSK2); RPS6KA5 (MSK1); SGK1 (SGK); TSSK4 | CAMK2D; CAMK2G; CDK1 (CDC2); PRKACA (PKA C-alpha); PRKCA (PKC alpha, PKCA)
PA_197	1L13	Key_L1_185 - sample + KaB + ATP + pept. PA_197	A	BIO	MECRNSPVTKTGC	EIF4EBP1 (4EBP1)	S65		AKT1, MAPK1 (ERK2); MAPK14 (p38a); MTOR (FRAP1); RPS6KA5 (MSK1); DYRK2
PA_198	1N13	Key_L1_186 - sample + KaB + ATP + pept. PA_198	A	BIO	GDYSTTPGGTLGC	EIF4EBP1 (4EBP1)	T37		AKT1; MAPK1 (ERK2); MAPK14 (p38a); MTOR (FRAP1); GSK3B
PA_199	1P13	Key_L1_187 - sample + KaB + ATP + pept. PA_199	A	BIO	RRRAVSMDNSNGC	FOXO3	S253		AKT1; MAPKAPK5; PIM1; SGK1 (SGK)
PA_200	1B15	Key_L1_188 - sample + KaB + ATP + pept. PA_200	A	BIO	RPRSCTWPLQRGC	FOXO3 / FOXO1	T32 / T24		AKT1, AKT2; SGK1 (SGK); PIM1 | AKT1; AKT2; SGK1 (SGK)
PA_201	1D15	Key_L1_189 - sample + KaB + ATP + pept. PA_201	A	BIO	RTRTDSYSAGQGC	MTOR (FRAP1)	S2446		AKT1; AKT3; RPS6KB1 (S6K1); RPS6KB2 (S6K2)
PA_202	1F06	Key_L1_190 - sample + KaB + ATP + pept. PA_202	A	BIO _ Rep (ib1-4)_i6	RSRTRTDSYSAGC	MTOR (FRAP1)	T2446		AKT1, AKT3; RPS6KB1 (S6K1)
PA_202	1F15	Key_L1_191 - sample + KaB + ATP + pept. PA_202	A	BIO	RSRTRTDSYSAGC	MTOR (FRAP1)	T2446		AKT1; AKT3; RPS6KB1 (S6K1)
PA_202	2F06	Key_L2_008 - sample + KaB + ATP + pept. PA_202	A	BIO _ Rep (ib1-4)_e8	RSRTRTDSYSAGC	MTOR (FRAP1)	T2446		AKT1; AKT3; RPS6KB1 (S6K1)
PA_203	1H15	Key_L1_192 - sample + KaB + ATP + pept. PA_203	A	BIO	YDIPPTPGNTYGC	GAB1	T312		MAPK1 (ERK2); MAPK3 (ERK1)
PA_204	1J15	Key_L1_193 - sample + KaB + ATP + pept. PA_204	A	BIO	NYVPMTPGTFDGC	GAB1	T476		MAPK1 (ERK2); MAPK3 (ERK1)
PA_205	1L15	Key_L1_194 - sample + KaB + ATP + pept. PA_205	A	BIO	RERKGSAPSHSGC	GAB2	S159		AKT1
PA_206	1N15	Key_L1_195 - sample + KaB + ATP + pept. PA_206	A	BIO	DFQPSSPSPHRGC	GAB2	S623		MAPK1 (ERK2); MAPK3 (ERK1)
PA_207	1P15	Key_L1_196 - sample + KaB + ATP + pept. PA_207	A	BIO	TPGPGSPPVLTGC	GRB10	S150		MAPK1 (ERK2); MAPK3 (ERK1), MTOR (FRAP1)
PA_208	1B17	Key_L1_197 - sample + KaB + ATP + pept. PA_208	A	BIO	ILGSQSPLHPSGC	GRB10	S476		MAPK1 (ERK2); MAPK3 (ERK1); MTOR (FRAP1)
PA_209	1D17	Key_L1_198 - sample + KaB + ATP + pept. PA_209	A	BIO	SNPPASPLQDNGC	LCK	S59		MAPK1 (ERK2); MAPK3 (ERK1)
PA_210	1F17	Key_L1_199 - sample + KaB + ATP + pept. PA_210	A	BIO	GSLPSTPPPAEGC	MCL1	T163		MAPK1 (ERK2); MAPK8 (JNK1); GSK3A; GSK3B
PA_211	1H17	Key_L1_200 - sample + KaB + ATP + pept. PA_211	A	BIO	RRRAISETEENGC	MDM2	S166		AKT1; CSNK1D (CK1D); DAPK3 (ZIPK); MAPKAPK2; PIM1; SGK1 (SGK)
PA_212	1J10	Key_L1_201 - sample + KaB + ATP + pept. PA_212	A	BIO _ Rep (ib1-4)_i9	FELLPTPPLSPGC	MYC	T58		GSK3B; CSNK2A1 (CK2A1); CSNK2A2 (CK2A2)
PA_212	1J17	Key_L1_202 - sample + KaB + ATP + pept. PA_212	A	BIO	FELLPTPPLSPGC	MYC	T58		GSK3B; CSNK2A1 (CK2A1); CSNK2A2 (CK2A2)
PA_212	2J10	Key_L2_009 - sample + KaB + ATP + pept. PA_212	A	BIO _ Rep (ib1-4)_e9	FELLPTPPLSPGC	MYC	T58		GSK3B; CSNK2A1 (CK2A1); CSNK2A2 (CK2A2)
PA_213	1J12	Key_L1_203 - sample + KaB + ATP + pept. PA_213	A	BIO _ Rep (ib1-4)_i10	HSLPLSPASTRGC	NFKB1	S907		GSK3B
PA_213	1L17	Key_L1_204 - sample + KaB + ATP + pept. PA_213	A	BIO	HSLPLSPASTRGC	NFKB1	S907		GSK3B
PA_213	2J12	Key_L2_010 - sample + KaB + ATP + pept. PA_213	A	BIO _ Rep (ib1-4)_e10	HSLPLSPASTRGC	NFKB1	S907		GSK3B
PA_214	1N17	Key_L1_205 - sample + KaB + ATP + pept. PA_214	A	BIO	YNVTPSPPGTVGC	NOTCH2	S2070		GSK3B
PA_215	1P17	Key_L1_206 - sample + KaB + ATP + pept. PA_215	A	BIO	EPLPVYPTRDVGC	PAK1	T212		MAPK1 (ERK2); CDK5
PA_216	1B19	Key_L1_207 - sample + KaB + ATP + pept. PA_216	A	BIO	PLCPLSPLEAGGC	PPARA	S12		MAPK1 (ERK2); MAPK3 (ERK1)
PA_217	1D19	Key_L1_208 - sample + KaB + ATP + pept. PA_217	A	BIO	AGDLESPLSEEGC	PPARA	S21		MAPK1 (ERK2), MAPK3 (ERK1)
PA_218	1F19	Key_L1_209 - sample + KaB + ATP + pept. PA_218	A	BIO	KVEPASPPYYSGC	PPARG	S112		MAPK1 (ERK2); MAPK8 (JNK1); CDK9
PA_219	1H19	Key_L1_210 - sample + KaB + ATP + pept. PA_219	A	BIO	DHYRYSDTTDSGC	PTEN	S380, T382, T383		AKT1, CSNK2A1 (CK2A1), PLK1; PRKCZ (PKC zeta); ROCK1; STK11 (LKB)
PA_220	1J19	Key_L1_211 - sample + KaB + ATP + pept. PA_220	A	BIO	GVPMQTPCFTLGC	RPS6KA4 (MSK2)	T568		MAP2K1 (MEK1, MKK1, MAPKK1); MAPK14 (p38a)
PA_221	1L19	Key_L1_212 - sample + KaB + ATP + pept. PA_221	A	BIO	LEPVYSPPGSPGC	RPS6KA4 (MSK2)	S343		MAP2K1 (MEK1, MKK1, MAPKK1); MAPK14 (p38a)
PA_222	1N19	Key_L1_213 - sample + KaB + ATP + pept. PA_222	A	BIO	PHGPRSASVSSGC	SOS1	S1132		MAPK1 (ERK2)
PA_223	1P19	Key_L1_214 - sample + KaB + ATP + pept. PA_223	A	BIO	TSKAYSPRYSIGC	SOS1	S1193		MAPK1 (ERK2)

Table 1

PA_224	1B16	Key_L1_215 - sample + KaB + ATP + pept. PA_224	A	BIO	VEPPLSQETFSGC	TP53	S15		MAPK1 (ERK2); MAPK3 (ERK1); MAPK14 (p38a); ATM; ATR; CHEK1; CHEK2; PRKDC (DNA-PKcs, DNAPK); CDK5; DYRK1A; NUAK1; PRKAA1 (AMPKa1); SMG1; STK11 (LKB); TP53RK (PRPK)
PA_225	1D16	Key_L1_216 - sample + KaB + ATP + pept. PA_225	A	BIO	IEQWFTEDPGPGC	TP53	T55		MAPK1 (ERK2); GRK5; TAF1
PA_226	1F16	Key_L1_217 - sample + KaB + ATP + pept. PA_226	A	BIO	CGLMFKTEGPDSD	TP53	S392		MAPK14 (p38a), CDK2, CDK7; CDK9; CSNK2A1 (CK2A1); EIF2AK2, NUAK1; STK11 (LKB)
PA_227	1H16	Key_L1_218 - sample + KaB + ATP + pept. PA_227	C	CON - _ mutated BIO	AEEKE(pY)HAEGGGC	EGFR _ CON (-) _ Y to pY	Y869 _ Y to pY		SRC; EGFR
PA_228	1J16	Key_L1_219 - sample + KaB + ATP + pept. PA_228	C	CON - _ mutated BIO	AEEKEGHAEGGGC	EGFR _ CON (-) _ Y to G	Y869 _ Y to G		SRC; EGFR
PA_229	1L16	Key_L1_220 - sample + KaB + ATP + pept. PA_229	C	CON - _ mutated BIO	GFL(pT)E(pY)VATRWGC	MAPK1 (ERK2) / MAPK3 (ERK1) _ CON (-) _ T/Y to pT/pY	Y187 (+T185) / Y204 (+T202) _ T/Y to pT/pY		MAP2K1 (MEK1, MKK1, MAPKK1); MAP2K2 (MEK2, MKK2, MAPKK2); MAPK1 (ERK2); MAPK3 (ERK1); RET; JAK2
PA_230	1N16	Key_L1_221 - sample + KaB + ATP + pept. PA_230	C	CON - _ mutated BIO	GFLGEGVATRWGC	MAPK1 (ERK2) / MAPK3 (ERK1) _ CON (-) _ T/Y to G/G	Y187 (+T185) / Y204 (+T202) _ T/Y to G/G		MAP2K1 (MEK1, MKK1, MAPKK1); MAP2K2 (MEK2, MKK2, MAPKK2); MAPK1 (ERK2); MAPK3 (ERK1); RET; JAK2
PA_231	1P16	Key_L1_222 - sample + KaB + ATP + pept. PA_231	C	CON - _ mutated BIO	HTGFL(pT)E(pY)VATGC	MAPK1 (ERK2) / MAPK3 (ERK1) _ CON (-) _ T to pT	T185 (+Y187) / T202 (+Y204) _ T to pT		MAP2K2 (MEK2, MKK2, MAPKK2); MAPK3 (ERK1) | MAPK1 (ERK2)
PA_232	1B20	Key_L1_223 - sample + KaB + ATP + pept. PA_232	C	CON - _ mutated BIO	RPRTT(pS)FAESCGC	GSK3B _ CON (-) _ S to pS	S9 _ S to pS		AKT1; AKT3; AURKA; PRKACA (PKA C-alpha); MAP4K5; PRKCA (PKC alpha, PKCA); PRKCB (PKC beta, PKCB); PRKCD (PKC delta, PKCD); PRKCG (PKC gamma, PKCG); PRKCH (PKC eta, PKCL); RPS6KA1 (RSK1, p90RSK); RPS6KA3 (RSK2, p90RSK2, S6K-alpha-3); RPS6KB1 (S6K1, p70S6K, S6K-beta-1); RPS6KB2 (S6K2, p70S6Kb, S6K-beta-2); SGK1 (SGK); SGK3 (SGKL)
PA_233	1D20	Key_L1_224 - sample + KaB + ATP + pept. PA_233	C	CON - _ mutated BIO	RGR(pS)R(pS)APPNLGC	BAD _ CON (-) _ S/S to pS/pS	S99 _ S/S to pS/pS		AKT1; AKT3; PAK1; PIM1; PIM2; PIM3; PRKACA (PKA C-alpha); PRKCE (PKC epsilon, PKCE); PRKCI (PKC iota, PKCI); PRKCQ (PKC theta); PRKD1 (PKD1, PKD); RPS6KA3 (RSK2, p90RSK2, S6K-alpha-3); ARAF; BRAF; RAF1 (cRAF)
PA_234	1F20	Key_L1_225 - sample + KaB + ATP + pept. PA_234	C	CON - _ mutated BIO	RSRTR(pT)D(pS)YSAGC	MTOR (FRAP1) _ CON (-) _ T/S to pT/pS	T2446 _ T/S to pT/pS		AKT1; AKT3; RPS6KB1 (S6K1)
PA_235	1H20	Key_L1_226 - sample + KaB + ATP + pept. PA_235	C	CON - _ mutated BIO	SNPPA(pS)PLQDNGC	LCK _ CON (-) _ S to pS	S59 _ S to pS		MAPK1 (ERK2); MAPK3 (ERK1)
PA_236	1J20	Key_L1_227 - sample + KaB + ATP + pept. PA_236	C	CON - _ mutated BIO	SNPPAGPLQDNGC	LCK _ CON (-) _ S to G	S59 _ S to G		MAPK1 (ERK2); MAPK3 (ERK1)
PA_237	1L20	Key_L1_228 - sample + KaB + ATP + pept. PA_237	C	CON - _ mutated BIO	RRRAI(pS)E(pT)EENGC	MDM2 _ CON (-) _ S/T to pS/pT	S166 _ S/T to pS/pT		AKT1; CSNK1D (CK1D); DAPK3 (ZIPK); MAPKAPK2; PIM1; SGK1 (SGK)
PA_238	1N20	Key_L1_229 - sample + KaB + ATP + pept. PA_238	C	CON - _ mutated BIO	RRRAIGEGEENGC	MDM2 _ CON (-) _ S/T to G/G	S166 _ S/T to G/G		AKT1, CSNK1D (CK1D); DAPK3 (ZIPK); MAPKAPK2; PIM1; SGK1 (SGK)
PA_239	1P20	Key_L1_230 - sample + KaB + ATP + pept. PA_239	C	CON - _ mutated BIO	EPLPV(pT)P(pT)RDVGC	PAK1_ CON (-) _ T/T to pT/pT	T212 _ T/T to pT/pT		MAPK1 (ERK2); CDK5
PA_240	1G07	Key_L1_231 - sample + KaB + ATP + pept. PA_240	B	CON +	KVEKIGEGTYGVVYK-amide	consensus _ CON+	--		ABL1; BCR-ABL; ABL2, AXL, AXL(R499C); FLT3, FLT3(D835Y); LTK (TYK1)
PA_241	1M09	Key_L1_232 - sample + KaB + ATP + pept. PA_241	B	CON +	(EEEEY)*--45	consensus _ CON+	--		all TKs (>90 Tyrosine Kinases, but more commonly used for: ALK; BTK; BTK(E41K); EPHA1; EPHB1, PTK2 (FAK, FAK1); PTK2B (FAK2, PYK2), FES; FGFR1; FGFR1(V561M); FGFR2 ; FGFR3; FGFR4; FLT1 (VEGFR1); FLT4 (VEGFR3); JAK1; JAK2; JAK3; KDR (VEGFR2), KIT (SCFR); MET; NRTK1; NTRK2 (TRKB); PDGFRA; PDGFRB, SYK; TIE2 (TEK); TYK2; ZAP70)
PA_242	1M12	Key_L1_233 - sample + KaB + ATP + pept. PA_242	B	CON +	EAIIAAPFAKKK	consensus _ CON+	--		BLK; BRK (PTK6); FGR; FRK; FYN; HCK; LCK; LYNA; LYNB; SRC; SRMS; YES1
PA_245	1A01	Key_L1_234 - sample + KaB + ATP + pept. PA_245	A	BIO	ELRRMSDEFVDGC	BAD	S118		AKT1; PIM1; PIM2, PIM3, PRKACA (PKA C-alpha); RPS6KA1 (RSK1, p90RSK), RPS6KA2 (RSK3, p90RSK2, S6K-alpha-2)
PA_246	1C01	Key_L1_235 - sample + KaB + ATP + pept. PA_246	B	CON +	KKVSRSGLYRSPSMPENLGC	consensus _ CON+	--		BRSK1, BRSK2; CHEK1; CHEK2; MARK1; MARK2 (EMK1); MARK3 (CTAK1); TSSK1; TSSK2
PA_247	1EE01	Key_L1_236 - sample + KaB + ATP + pept. PA_247	A	BIO	PPPQLSPFLQPGC	ESR1	S118		CDK7; MAPK1 (ERK2); RPS6KA1 (RSK1, p90RSK)
PA_248	1C07	Key_L1_237 - sample + KaB + ATP + pept. PA_248	A	BIO	CGGKKATQASQEY	H2AFX	S140 (C-term end)		ATM
PA_249	1C09	Key_L1_238 - sample + KaB + ATP + pept. PA_249	A	BIO	NDDDVYRSLEEGC	VAV2	Y142		EGFR
PA_250	1A11	Key_L1_239 - sample + KaB + ATP + pept. PA_250	A	BIO	ISEGTTLKDLIGC	TGFBR1	T176		CLK1; TGFBR2

Table 1

PA_251	1M13	Key_L1_240 - sample + KaB + ATP + pept. PA_251	C		CON - _ mutated BIO	PVPPLAPARRAGC	MYC _ CON (-) _ S/T to A/V	S62	MAPK8 (JNK1)
PA_252	1O13	Key_L1_241 - sample + KaB + ATP + pept. PA_252	A		BIO	ELDQGSLCTSFGC	IKBKB (IKK beta)	S177	CHUK (IKK alpha); MAP3K7 (MEKK7, TAK1); MAP3K14 (NIK); PRKCQ (PKC theta); PRKCZ (PKC zeta)
PA_253	1A15	Key_L1_242 - sample + KaB + ATP + pept. PA_253	A		BIO	DEDDSYLEPDSGC	SH3BP2	Y183	SYK
PA_254	1G15	Key_L1_243 - sample + KaB + ATP + pept. PA_254	A		BIO	VDPDMSWSSSLGC	BRCA2	S193	PLK1
PA_255	1I15	Key_L1_244 - sample + KaB + ATP + pept. PA_255	A		BIO	CGTPKKPGLRRRQT	CDKN1B (p27, KIP1)	T198 (C-term end)	PKN2 (PRK2)
PA_256	1O15	Key_L1_245 - sample + KaB + ATP + pept. PA_256	A		BIO	NKRRRSVTPPEGC	CDC25B	S353	AURKA
PA_257	1A17	Key_L1_246 - sample + KaB + ATP + pept. PA_257	C		CON - _ mutated BIO	LEVVAVQELFAGC	CHEK2 _ CON (-) _ S/T/Y to A/V/F	T68	ATM; CHEK2; PLK1; PLK3
PA_258	1C17	Key_L1_247 - sample + KaB + ATP + pept. PA_258	A		BIO	FETQRYPRKSNGC	RB1	T356	CDK4
PA_259	1K17	Key_L1_248 - sample + KaB + ATP + pept. PA_259	A		BIO	EFTSRYPKDSPGC	RPS6KA1 (RSK1)	T359	MAPK1 (ERK2)
PA_260	1M17	Key_L1_249 - sample + KaB + ATP + pept. PA_260	A		BIO	MEDSMDMDMSPGC	NPM1	S4 (N-term end)	PLK1
PA_261	1EE19	Key_L1_250 - sample + KaB + ATP + pept. PA_261	A		BIO	ISSVPTPSPLGGC	CSNK2A1 (CK2A1)	T360	CDK1 (CDC2)
PA_262	1G19	Key_L1_251 - sample + KaB + ATP + pept. PA_262	A		BIO	KEDPIYDEPEGGC	DOK1	Y362	INSR
PA_263	1I19	Key_L1_252 - sample + KaB + ATP + pept. PA_263	B		CON +	CKRREILSRRPSYRK	consensus _ CON+	--	AKT1; AKT2; AKT3; AURKA; CAMK1beta; CAMK1delta; CAMK1gamma; CAMK2; CAMK4; IKBKB (IKK beta); IRAK4; KSR1; KSR1(A633F); KSR1(L639F); KSR2; KSR2(R676S); PAK2; PRKACA (PKA C-alpha); PRKACB (PKA C-beta); PRKACG (PKA C-gamma); PRKCA (PKC alpha, PKCA); PRKCB (PKC beta, PKCB); PRKCD (PKC delta, PKCD); PRKCI (PKC iota, PKCI); PRKCM (PKC mu, PKCM); PRKCN (PKC nu); PRKCZ (PKC zeta); PRKD2 (PKD2); RPS6KA5 (MSK1)
PA_264	1M19	Key_L1_253 - sample + KaB + ATP + pept. PA_264	A		BIO	AHRKGSSSNEPGC	FOS	S362	PRKACA (PKA C-alpha); RPS6KA1 (RSK1, p90RSK)
PA_265	1O19	Key_L1_254 - sample + KaB + ATP + pept. PA_265	A		BIO	SFAPSYPLTGRGC	RBL1	T369	CDK4
PA_266	1C14	Key_L1_255 - sample + KaB + ATP + pept. PA_266	E		CON - _ random	NEVERLANDGC	--	--	--
PA_266	1I17	Key_L1_256 - sample + KaB + ATP + pept. PA_266	E		CON - _ random _ Rep (lib5-8)_e3	NEVERLANDGC	--	--	--
PA_266	2I17	Key_L2_011 - sample + KaB + ATP + pept. PA_266	E		CON - _ random _ Rep (lib5-8)_i3	NEVERLANDGC	--	--	--
PA_267	1EE14	Key_L1_257 - sample + KaB + ATP + pept. PA_267	A		BIO	DINSLYDVSRMGC	PLCG2	Y753	FYN; HCK; LCK; LYNA; LYNB
PA_268	1K14	Key_L1_258 - sample + KaB + ATP + pept. PA_268	A		BIO	CGSSDSLSSPTLLAL	FOS	S374	MAPK1 (ERK2); MAPK9 (JNK2)
PA_269	1M14	Key_L1_259 - sample + KaB + ATP + pept. PA_269	A		BIO	KEVSKYSDIQRGC	PDGFRA	Y754	PDGFRA
PA_270	1O14	Key_L1_260 - sample + KaB + ATP + pept. PA_270	A		BIO	CGKEATSYFTNITYRG	ITGB3	T779 (C-term)	AKT1; PDK1; PDPK1
PA_271	1B02	Key_L1_261 - sample + KaB + ATP + pept. PA_271	B		CON +	IPTTPITTTYFFFKKGC	consensus _ CON+	--	MAPK1 (ERK2); MAPK9 (JNK2); MAPK10 (JNK3); MAPK11 (p38b); MAPK12 (p38g); MAPK13 (p38d); MAPK14 (p38a)
PA_272	1D02	Key_L1_262 - sample + KaB + ATP + pept. PA_272	A		BIO	RPPTLSPIPHIGC	RB1	S780	CDK4
PA_273	1F02	Key_L1_263 - sample + KaB + ATP + pept. PA_273	A		BIO	ESIDDYVNVPEGC	LAT	Y200	ZAP70
PA_274	1H02	Key_L1_264 - sample + KaB + ATP + pept. PA_274	A		BIO	LTTGVYVKMPPGC	CTLA4	Y201	FYN; JAK2; LCK; TXK
PA_275	1L02	Key_L1_265 - sample + KaB + ATP + pept. PA_275	A		BIO	SMDAGSPNLSPGC	SMAD3	S204	CDK2; CDK4; MAPK1 (ERK2)
PA_276	1N02	Key_L1_266 - sample + KaB + ATP + pept. PA_276	A		BIO	KLMEFSEHCAIGC	TGFBR2	S213	CLK1; TGFBR2
PA_277	1M15	Key_L1_267 - sample + KaB + ATP + pept. PA_277	B		CON + _ Rep (lib5-8)_e2	ADEYLIPQQGC	--	--	EGFR
PA_277	1P02	Key_L1_268 - sample + KaB + ATP + pept. PA_277	B		CON +	ADEYLIPQQGC	consensus _ CON+	--	EGFR
PA_277	2M15	Key_L2_012 - sample + KaB + ATP + pept. PA_277	B		CON + _ Rep (lib5-8)_i2	ADEYLIPQQGC	--	--	EGFR
PA_278	1B04	Key_L1_269 - sample + KaB + ATP + pept. PA_278	A		BIO	TSLAQYDSNSKGC	BMX	Y216	BTK; ITK; TEC

Table 1

PA_279	1J04	Key_L1_270 - sample + KaB + ATP + pept. PA_279	A	BIO	MSGRGKQGGKAGC	HIST3H2A	S2 (N-term end)	RPS6KA5 (MSK1)
PA_281	1N04	Key_L1_271 - sample + KaB + ATP + pept. PA_281	A	BIO	PEPGPYAQPSVGC	CRK	Y221	ABL1; ABL2; EGFR; IGF1R
PA_282	1P04	Key_L1_272 - sample + KaB + ATP + pept. PA_282	A	BIO	EKKAYSFCGTVGC	RPS6KA1 (RSK1)	S221	PDPK1
PA_283	1B06	Key_L1_273 - sample + KaB + ATP + pept. PA_283	A	BIO	VSPDVSDNEPDGC	PTEN	S370	CSNK2A1 (CK2A1); CSNK2A2 (CK2A2)
PA_284	1D06	Key_L1_274 - sample + KaB + ATP + pept. PA_284	D	CON - _ mutated CON+	RRADDGDDDDGC	consensus _ CON- _ S/T to A/V	_	CSNK2A1 (CK2A1); CSNK2A2 (CK2A2)
PA_285	1J06	Key_L1_275 - sample + KaB + ATP + pept. PA_285	A	BIO	QTPVDSPDDTAGC	RPS6KB2 (S6K2)	S370	MTOR (FRAP1), PDPK1
PA_286	1N06	Key_L1_276 - sample + KaB + ATP + pept. PA_286	A	BIO	DTDSSYCIPTAGC	GAB1	Y373	EGFR; INSR; MET
PA_287	1P06	Key_L1_277 - sample + KaB + ATP + pept. PA_287	A	BIO	DDEDCYGNYDNGC	PDPK1	Y373	SRC
PA_288	1B08	Key_L1_278 - sample + KaB + ATP + pept. PA_288	A	BIO	ENCLLSPLAGEGC	NR3C1	S226	MAPK1 (ERK2); MAPK8 (JNK1)
PA_289	1D08	Key_L1_279 - sample + KaB + ATP + pept. PA_289	A	BIO	SLLACYLKSRQGC	IL15RA	Y227	SYK
PA_290	1J08	Key_L1_280 - sample + KaB + ATP + pept. PA_290	A	BIO	RRRGGSASRSLGC	TERT	S228	AKT1
PA_291	1N08	Key_L1_281 - sample + KaB + ATP + pept. PA_291	A	BIO	VLGEESPLGKPGC	IKBKG (IKKG, NEMO)	S31	IKBKB (IKK beta)
PA_292	1P08	Key_L1_282 - sample + KaB + ATP + pept. PA_292	A	BIO	DDRHDSGLDSMGC	NFKBIA (IKBA)	S32	CSNK2A1 (CK2A1); EIF2AK2; IKBKB (IKK beta); RPS6KA1 (RSK1, p90RSK)
PA_293	1B10	Key_L1_283 - sample + KaB + ATP + pept. PA_293	A	BIO	SQGSSSQSQGIGC	CHEK2	S33	ATM; ATR
PA_294	1F10	Key_L1_284 - sample + KaB + ATP + pept. PA_294	A	BIO	ENNVLSPLPSQGC	TP53	S33	ATM; CDK5; CDK9; GSK3B; PRKDC (DNA-PKcs, DNAPK)
PA_295	1H10	Key_L1_285 - sample + KaB + ATP + pept. PA_295	A	BIO	DSGLDSMKDEEGC	NFKBIA (IKBA)	S36	CSNK2A1 (CK2A1); IKBKB (IKK beta); IKBKE (IKK-E); TBK1 (NAK, T2K)
PA_296	1N10	Key_L1_286 - sample + KaB + ATP + pept. PA_296	B	CON +	KRRRLASLRAGC	consensus _ CON+	_	CDC42BPA (MRCK alpha); CDC42BPB (MRCK beta); CHUK (IKK alpha); IKBKB (IKK beta); CLK2; PAK2; PIM1; PIM2; PIM3; PRKG1 (PKG1); PRKG2 (PKG2); ROCK1; ROCK2; RPS6KA1 (RSK1, p90RSK); RPS6KA2 (RSK3, p90RSK2, S6K-alpha-2); RPS6KA3 (RSK2, p90RSK2, S6K-alpha-3); RPS6KA4 (MSK2, S6K-alpha-4); RPS6KA5 (MSK1); RPS6KA6 (RSK4, p90RSK6, S6K-alpha-6); RPS6KB1 (S6K1, p70S6K, S6K-beta-1)
PA_297	1P10	Key_L1_287 - sample + KaB + ATP + pept. PA_297	A	BIO	LSPLPSQAMDDGC	TP53	S37	ATM; ATR, CHEK1; PRKDC (DNA-PKcs, DNAPK)
PA_298	1B12	Key_L1_288 - sample + KaB + ATP + pept. PA_298	A	BIO	PEFPLSPPKKKGC	STMN1	S38	CDK1 (CDC2)
PA_299	1D12	Key_L1_289 - sample + KaB + ATP + pept. PA_299	C	CON - _ mutated BIO	AEGLPVPVKMVGC	RB1 _ CON (-) _ S/T to A/V	T821	CDK2
PA_301	1N12	Key_L1_290 - sample + KaB + ATP + pept. PA_301	A	BIO	AGPAPSPMRAAGC	CDC20	S41	BUB1
PA_302	1P12	Key_L1_291 - sample + KaB + ATP + pept. PA_302	A	BIO	TQRQNSAPARMGC	CDC25A	S178	CHEK1; CHEK2
PA_303	1P16	Key_L1_292 - sample + KaB + ATP + pept. PA_303	A	BIO	SNIPETPPPGYGC	SMAD3	T179	CDK2, CDK4, MAPK1 (ERK2)
PA_304	2A01	Key_L2_013 - sample + KaB + ATP + pept. PA_304	A	BIO	MKDEEYEQMVKGC	NFKBIA (IKBA)	Y42	LCK; SRC
PA_305	2C01	Key_L2_014 - sample + KaB + ATP + pept. PA_305	A	BIO	KFLRASEEHLKGC	NME2	S44	NME1-NME2; NME2 (NM23B, NDPK-B)
PA_306	2EE01	Key_L2_015 - sample + KaB + ATP + pept. PA_306	A	BIO	SITATSPASMVGC	IRS1	S312	IKBKB (IKK beta); MAPK8 (JNK1)
PA_307	2G01	Key_L2_016 - sample + KaB + ATP + pept. PA_307	A	BIO	RSRTNSNASTVGC	FOXO3	S315	SGK1 (SGK)
PA_308	1EE15	Key_L1_293 - sample + KaB + ATP + pept. PA_308	B	CON + _ Rep (lib5-8)_e1	LGFTYVAPGC	_	_	CHUK (IKK alpha); IKBKB (IKK beta); IRAK1; IRAK4; MAP3K8 (COT); MAP3K17 (TAOK2, PSK1); MAP4K2; MAP4K4 (HGK); MAP4K6 (MINK); STK3 (MST2, KRS1); STK4 (MST1, KRS2); MTOR (FRAP1); NEK1; NEK2; NEK8; NEK7; EIF2AK3 (PEK); PLK1
PA_308	2EE15	Key_L2_017 - sample + KaB + ATP + pept. PA_308	B	CON + _ Rep (lib5-8)_i1	LGFTYVAPGC	_	_	CHUK (IKK alpha); IKBKB (IKK beta); IRAK1; IRAK4; MAP3K8 (COT); MAP3K17 (TAOK2, PSK1); MAP4K2; MAP4K4 (HGK); MAP4K6 (MINK); STK3 (MST2, KRS1); STK4 (MST1, KRS2); MTOR (FRAP1); NEK1; NEK2; NEK8; NEK7; EIF2AK3 (PEK); PLK1

Table 1

PA_308	2I01	Key_L2_018 - sample + KaB + ATP + pept. PA_308	B	CON +	LGFTYVAPGC	consensus _ CON+	--		CHUK (IKK alpha); IKBKB (IKK beta); IRAK1; IRAK4; MAP3K8 (COT); MAP3K17 (TAOK2, PSK1); MAP4K2; MAP4K4 (HGK); MAP4K6 (MINK); STK3 (MST2, KRS1); STK4 (MST1, KRS2); MTOR (FRAP1); NEK1; NEK2; NEK8; NEK7; EIF2AK3 (PEK); PLK1
PA_309	2K01	Key_L2_019 - sample + KaB + ATP + pept. PA_309	A	BIO	NNTSSSPQPKKGC	TP53	S315		CDK2; CDK5; CDK9
PA_310	2M01	Key_L2_020 - sample + KaB + ATP + pept. PA_310	A	BIO	VKYSSSQPEPRGC	CHEK1	S317		ATM; ATR
PA_311	2O01	Key_L2_021 - sample + KaB + ATP + pept. PA_311	A	BIO	VYESPYSDPEEGC	ZAP70	Y319		LCK; ZAP70
PA_312	2A03	Key_L2_022 - sample + KaB + ATP + pept. PA_312	A	BIO	SDTTTTFCGTPGC	SGK3	T320		PDPK1
PA_313	2C03	Key_L2_023 - sample + KaB + ATP + pept. PA_313	A	BIO	SEDDVSDEEGQGC	GTF2A1	S321		CSNK2A1 (CK2A1); CSNK2A2 (CK2A2); TAF1
PA_314	2EE03	Key_L2_024 - sample + KaB + ATP + pept. PA_314	B	CON +	APRTPGGRRGC	consensus _ CON+	--		MAPK1 (ERK2); MAPK3 (ERK1)
PA_315	2G03	Key_L2_025 - sample + KaB + ATP + pept. PA_315	A	BIO	SVYTRSTGEQEGC	CCR5	T342		GRK3 (ADRBK2)
PA_316	2I03	Key_L2_026 - sample + KaB + ATP + pept. PA_316	A	BIO	DDLMLSPDDIEGC	TP53	S46		ATM; HIPK2
PA_317	2K03	Key_L2_027 - sample + KaB + ATP + pept. PA_317	A	BIO	GNIDDSLIGGNGC	TPT1	S46		PLK1
PA_318	2M03	Key_L2_028 - sample + KaB + ATP + pept. PA_318	A	BIO	GRNIIHGSDSVGC	NME2	S120 (*mistake: sequence shifted*)		NME1-NME2; NME2 (NM23B; NDPK-B)
PA_319	2O03	Key_L2_029 - sample + KaB + ATP + pept. PA_319	A	BIO	SPSQSSMVARTGC	IRAK1	S376		IRAK1; IRAK4
PA_320	2A05	Key_L2_030 - sample + KaB + ATP + pept. PA_320	A	BIO	PEETQYQDQPMEEGC	HSP90AA1	T7		PRKDC (DNA-PKcs, DNAPK)
PA_321	2C05	Key_L2_031 - sample + KaB + ATP + pept. PA_321	A	BIO	SSDDDYDDVDIGC	MAP4K1	Y381		FGFR1; FGFR2; LYNA; LYNB; SYK
PA_322	2EE05	Key_L2_032 - sample + KaB + ATP + pept. PA_322	A	BIO	GSPNLSPNPMSGC	SMAD3	S208		CDK2, CDK4, MAPK1 (ERK2); MAPK14 (p38a)
PA_323	1I14	Key_L1_294 - sample + KaB + ATP + pept. PA_323	C	CON - _ mutated BIO _ Rep (lib5-8)_e5	DAMANAFVGVRGC	MAP2K1 (MEK1) _ CON (-) _ S/T to A/V	S222		ARAF; BRAF; RAF1 (cRAF)
PA_323	2G05	Key_L2_033 - sample + KaB + ATP + pept. PA_323	C	CON - _ mutated BIO	DAMANAFVGVRGC	MAP2K1 (MEK1) _ CON (-) _ S/T to A/V	S222		ARAF; BRAF; RAF1 (cRAF)
PA_323	2I14	Key_L2_034 - sample + KaB + ATP + pept. PA_323	C	CON - _ mutated BIO _ Rep (lib5-8)_j5	DAMANAFVGVRGC	MAP2K1 (MEK1) _ CON (-) _ S/T to A/V	S222		ARAF; BRAF; RAF1 (cRAF)
PA_324	2I05	Key_L2_035 - sample + KaB + ATP + pept. PA_324	A	BIO	DSLPSSPSSATPHGC	EEF2K	S396, S398		MAPK8 (JNK1); MAPK9 (JNK2); MAPK11 (p38b); MAPK12 (p38g); MAPK13 (p38d); MAPK14 (p38a); PRKAA1 (AMPKa1); PRKAA2 (AMPKa2)
PA_325	2K05	Key_L2_036 - sample + KaB + ATP + pept. PA_325	A	BIO	EEFSDSEEEGEGC	HDAC1 / HDAC2	S423 / S424		CSNK2A1 (CK2A1); CSNK2A2 (CK2A2)
PA_326	1L12	Key_L1_295 - sample + KaB + ATP + pept. PA_326	A	BIO _ Rep (lib5-8)_e10	GTLFSTTPGGTRGC	EIF4EBP1 (4EBP1)	T45, T46		AKT1, MAPK1 (ERK2); MAPK14 (p38a); MTOR (FRAP1); RPS6KA5 (MSK1)
PA_326	2L12	Key_L2_037 - sample + KaB + ATP + pept. PA_326	A	BIO _ Rep (lib5-8)_j10	GTLFSTTPGGTRGC	EIF4EBP1 (4EBP1)	T45, T46		AKT1; MAPK1 (ERK2); MAPK14 (p38a); MTOR (FRAP1); RPS6KA5 (MSK1)
PA_326	2M05	Key_L2_038 - sample + KaB + ATP + pept. PA_326	A	BIO	GTLFSTTPGGTRGC	EIF4EBP1 (4EBP1)	T45, T46		AKT1; MAPK1 (ERK2); MAPK14 (p38a); MTOR (FRAP1); RPS6KA5 (MSK1)
PA_327	2A07	Key_L2_039 - sample + KaB + ATP + pept. PA_327	A	BIO	MEDSTYYKASKGKGC	PTK2 (FAK1)	Y576, Y577		INSR; RET; SRC
PA_328	2C07	Key_L2_040 - sample + KaB + ATP + pept. PA_328	A	BIO	FWSTLSPIAPRGC	ELK1	S383		MAPK1 (ERK2), MAPK9 (JNK2); MAPK14 (p38a); MAP3K17 (TACK2, PSK1)
PA_329	2EE07	Key_L2_041 - sample + KaB + ATP + pept. PA_329	B	CON +	EPPLSQEAFADLWKKGC	consensus _ CON+	--		PRKDC (DNA-PKcs, DNAPK)
PA_330	2G07	Key_L2_042 - sample + KaB + ATP + pept. PA_330	A	BIO	SDTTDSDPENEGC	PTEN	S385		AKT1; STK11 (LKB)
PA_331	2I07	Key_L2_043 - sample + KaB + ATP + pept. PA_331	A	BIO	CGLNQPSTPTHAA	MAP2K1 (MEK1)	T386 (C-term)		RAF1 (cRAF)
PA_332	2K07	Key_L2_044 - sample + KaB + ATP + pept. PA_332	A	BIO	QTVRGTLAYLPGC	IRAK1	T387		IRAK1; IRAK4
PA_333	2M07	Key_L2_045 - sample + KaB + ATP + pept. PA_333	A	BIO	GLYRSGCDRTGC	RACGAP1	S387		AURKB
PA_334	2O07	Key_L2_046 - sample + KaB + ATP + pept. PA_334	A	BIO	AFLGFTYVAPSGC	RPS6KB2 (S6K2)	T388		MTOR (FRAP1); PDPK1
PA_335	2A09	Key_L2_047 - sample + KaB + ATP + pept. PA_335	A	BIO	TIEDSYTKICSGC	RRA5	Y68		EPHB2
PA_336	1C19	Key_L1_296 - sample + KaB + ATP + pept. PA_336	A	BIO _ Rep (lib5-8)_e4	LETVSTQELYSGC	CHEK2	T68		ATM; CHEK2; PLK1; PLK3
PA_336	2C09	Key_L2_048 - sample + KaB + ATP + pept. PA_336	A	BIO	LETVSTQELYSGC	CHEK2	T68		ATM, CHEK2, PLK1, PLK3
PA_336	2C19	Key_L2_049 - sample + KaB + ATP + pept. PA_336	A	BIO _ Rep (lib5-8)_j4	LETVSTQELYSGC	CHEK2	T68		ATM; CHEK2, PLK1; PLK3

Table 1

PA_337	2EE09	Key_L2_050 - sample + KaB + ATP + pept. PA_337	D	CON - _ mutated CON+	KKVGRGGLGRGPGMPENLGC	consensus _ CON- _ S/T to A/V	_	BRSK1; BRSK2, CHEK1; CHEK2; MARK1; MARK2 (EMK1), MARK3 (CTAK1); TSSK1; TSSK2
PA_338	2G08	Key_L2_051 - sample + KaB + ATP + pept. PA_338	A	BIO	LAPPASPGPFAGC	BCL2L11	S69	MAPK8 (JNK1); MAPK9 (JNK2); MAPK10 (JNK3)
PA_339	2I09	Key_L2_052 - sample + KaB + ATP + pept. PA_339	A	BIO	QGISFSQPTCPGC	CHEK1	S345	ATR
PA_340	2K09	Key_L2_053 - sample + KaB + ATP + pept. PA_340	A	BIO	SPVTKTPPRDLGC	EIF4EBP1 (4EBP1)	T70	MAPK1 (ERK2), MTOR (FRAP1)
PA_341	2M09	Key_L2_054 - sample + KaB + ATP + pept. PA_341	A	BIO	RSGLCSPSYVAGC	MYC	S71	MAPK8 (JNK1)
PA_342	2O09	Key_L2_055 - sample + KaB + ATP + pept. PA_342	E	CON - _ random	DREAMLEENAGC	_	_	_
PA_343	2A11	Key_L2_056 - sample + KaB + ATP + pept. PA_343	A	BIO	RLRPLSYPQTDGC	RAC1	S71	AKT1
PA_344	2C11	Key_L2_057 - sample + KaB + ATP + pept. PA_344	A	BIO	LATRLSRRRVSGC	CNKSR1	S392	NME1-NME2; NME1 (NM23, NDPK-A)
PA_345	2EE11	Key_L2_058 - sample + KaB + ATP + pept. PA_345	A	BIO	QTPVDSPDDSTGC	RPS6KB1 (S6K1)	S394	CDK1 (CDC2), MTOR (FRAP1)
PA_346	2G11	Key_L2_059 - sample + KaB + ATP + pept. PA_346	D	CON - _ mutated CON+	AVPPAPALARHAAPHQAEDEEEGC	consensus _ CON- _ S/T to A/V	_	GSK3A; GSK3B
PA_347	2I11	Key_L2_060 - sample + KaB + ATP + pept. PA_347	A	BIO	PSGLLTPPQSGGC	CCNE1	T395	GSK3B
PA_348	2K11	Key_L2_061 - sample + KaB + ATP + pept. PA_348	A	BIO	SETDDYAEIDGC	PTK2 (FAK1)	Y397	FGFR1; FGFR2; PTK2 (FAK; FAK1)
PA_349	2M11	Key_L2_062 - sample + KaB + ATP + pept. PA_349	A	BIO	VKEEGYELPYNGC	DOK1	Y398	INSR; RET
PA_350	2O11	Key_L2_063 - sample + KaB + ATP + pept. PA_350	A	BIO	HVEDLYVEGLPGC	GTF2I	Y398	BTK
PA_351	2A13	Key_L2_064 - sample + KaB + ATP + pept. PA_351	A	BIO	LTPPQSGKKQSGC	CCNE1	T399	CDK2
PA_352	2C13	Key_L2_065 - sample + KaB + ATP + pept. PA_352	B	CON +	KKKSPGEYVNIEFGGC	consensus _ CON+	--	ALK; FGFR1; FLT1 (VEGFR1); IGF1R; JAK2; MET; RET; ROS1
PA_353	2EE13	Key_L2_066 - sample + KaB + ATP + pept. PA_353	A	BIO	TSFMMTPYVVTGC	MAPK8 (JNK1) / MAPK9 (JNK2) / MAPK10 (JNK3)	T183 (Y185) / T183 (Y185) / T221 (Y223)	MAPK8 (JNK1); MAPK9 (JNK2); MAP2K4 (MEK4, MKK4, MAPKK4, JNKK1); MAP2K7 (MEK7, MKK7, MAPKK7, JNKK2)
PA_354	2K13	Key_L2_067 - sample + KaB + ATP + pept. PA_354	A	BIO	EFISLSPPHEAGC	E2F1	S403	CDK7
PA_355	2M13	Key_L2_068 - sample + KaB + ATP + pept. PA_355	A	BIO_nsSNP	KSPVVSGDTSPRHLSNGC	MAPT (TAU) _ R723W variant (ALZ/FTD)	S717, T720, S721	GSK3B; CDK5
PA_356	2O13	Key_L2_069 - sample + KaB + ATP + pept. PA_356	A	BIO	DEEDTYTMPSTGC	PTK2 (FAK1)	Y407	PTK2B (FAK2, PYK2); SRC
PA_357	2A15	Key_L2_070 - sample + KaB + ATP + pept. PA_357	A	BIO	VFLGFTYVAPSGC	RPS6KB1 (S6K1)	T412	PDPK1
PA_358	2G15	Key_L2_071 - sample + KaB + ATP + pept. PA_358	A	BIO	CGEAFLGFSYAPPTDS	SGK1	S422	NEK6; PDPK1
PA_359	2I15	Key_L2_072 - sample + KaB + ATP + pept. PA_359	A	BIO	CGGSPSIRCSSVS	SMAD3	S422	MAP3K7 (MEKK7, TAK1)
PA_360	2O15	Key_L2_073 - sample + KaB + ATP + pept. PA_360	A	BIO	PNPGFYVEANPGC	PLCG1	Y783	EGFR; HCK; LYNA; LYNB; RET; SRC; SYK
PA_361	2A17	Key_L2_074 - sample + KaB + ATP + pept. PA_361	B	CON +	RRADDSDDDDGC	consensus _ CON+	--	CSNK2A1 (CK2A1); CSNK2A2 (CK2A2)
PA_362	2C17	Key_L2_075 - sample + KaB + ATP + pept. PA_362	A	BIO	CGLAQAPPVYLDVLG	NTRK1 (TRKA)	Y791 (C-term end)	ERBB3 (in its dimeric state with another HER fam. member); ERBB4; NTRK1 (TRKA)
PA_363	2K17	Key_L2_076 - sample + KaB + ATP + pept. PA_363	A	BIO	YKFPSSPLRIPGC	RB1	S795	CDK4
PA_364	2M17	Key_L2_077 - sample + KaB + ATP + pept. PA_364	A	BIO	RIRGKSYVQCQGC	TERT	S824	AKT1
PA_365	2EE19	Key_L2_078 - sample + KaB + ATP + pept. PA_365	A	BIO	TPTKMTPRSRIGC	RB1	T826	CDK4
PA_366	2G19	Key_L2_079 - sample + KaB + ATP + pept. PA_366	A	BIO	YNRAVSLDSPVGC	NCOA3	S857	CHUK (IKK alpha); IKBKB (IKK beta)
PA_367	2I19	Key_L2_080 - sample + KaB + ATP + pept. PA_367	A	BIO	MRDSNYISKGSGC	PDGFRB	Y857	PDGFRB
PA_368	2M19	Key_L2_081 - sample + KaB + ATP + pept. PA_368	D	CON - _ mutated CON+	LGF**GG**VAPGC	consensus _ CON- _ S/T to A/V	--	CHUK (IKK alpha); IKBKB (IKK beta); IRAK1; IRAK4; MAP3K8 (COT); MAP3K17 (TAOK2, PSK1); MAP4K2; MAP4K4 (HGK); MAP4K6 (MINK); STK3 (MST2, KRS1); STK4 (MST1, KRS2); MTOR (FRAP1); NEK1; NEK2; NEK6; NEK7; EIF2AK3 (PEK); PLK1
PA_369	2O19	Key_L2_082 - sample + KaB + ATP + pept. PA_369	A	BIO	DPRRRSLPAGDGC	ARHGEF2	S886	PAK1
PA_370	2A02	Key_L2_083 - sample + KaB + ATP + pept. PA_370	A	BIO	VERFETVGMEAGC	IL6ST	T890	PRKCD (PKC delta, PKCD)
PA_371	2C02	Key_L2_084 - sample + KaB + ATP + pept. PA_371	A	BIO	KSPGEYVNIEFGC	IRS1	Y896	FGFR1; FGFR2, IGF1R

Table 1

PA_372	1H05	Key_L1_297 - sample + KaB + ATP + pept. PA_372	A		BIO _ Rep (lib5-8)_e7	LRDSDSVCDSGGC	NFKB1	S923	CHUK (IKK alpha); IKBKB (IKK beta)
PA_372	2EE02	Key_L2_085 - sample + KaB + ATP + pept. PA_372	A		BIO	LRDSDSVCDSGGC	NFKB1	S923	CHUK (IKK alpha); IKBKB (IKK beta)
PA_372	2H06	Key_L2_086 - sample + KaB + ATP + pept. PA_372	A		BIO _ Rep (lib5-8)_i7	LRDSDSVCDSGGC	NFKB1	S923	CHUK (IKK alpha); IKBKB (IKK beta)
PA_373	2G02	Key_L2_087 - sample + KaB + ATP + pept. PA_373	A		BIO	DSEENYVPMNPGC	GAB1	Y589	EGFR; INSR; MET
PA_374	2I02	Key_L2_088 - sample + KaB + ATP + pept. PA_374	A		BIO	RARSTSLNERPGC	TSC2	S939	AKT1
PA_375	2K02	Key_L2_089 - sample + KaB + ATP + pept. PA_375	A		BIO	EGDNDYIIPLPGC	PDGFRB	Y1021	FGFR1; FGFR2; PDGFRB
PA_376	2M02	Key_L2_090 - sample + KaB + ATP + pept. PA_376	A		BIO	LDNPDYQQDFFGC	EGFR	Y1172	EGFR
PA_377	2O02	Key_L2_091 - sample + KaB + ATP + pept. PA_377	B		CON +	CGRSRSRSRSRSRSRSR	consensus _ CON+	--	EIF2AK1; EIF2AK2; EIF2AK3 (PEK); EIF2AK4
PA_378	2A04	Key_L2_092 - sample + KaB + ATP + pept. PA_378	A		BIO	SEEELYSSCRQGC	PLCG2	Y1197	BTK; ERBB3 (in its dimeric state with another HER fam. member); ERBB4
PA_379	2C04	Key_L2_093 - sample + KaB + ATP + pept. PA_379	A		BIO	SDDVRYVNAFKGC	FLT1 (VEGFR1)	Y1213	FLT1 (VEGFR1)
PA_380	2EE04	Key_L2_094 - sample + KaB + ATP + pept. PA_380	A		BIO	EPQSDPSVEPPLGC	TP53	S9	ATM; CSNK1A1 (CK1a)
PA_381	2G04	Key_L2_095 - sample + KaB + ATP + pept. PA_381	A		BIO	QTARKSTGGKAGC	HIST3H3	S11	RPS6KA3 (RSK2, p90RSK2, S6K-alpha-3); RPS6KA5 (MSK1)
PA_382	2I04	Key_L2_096 - sample + KaB + ATP + pept. PA_382	A		BIO	SSQRVSSYRRTGC	DES	S12	AURKB
PA_383	2K04	Key_L2_097 - sample + KaB + ATP + pept. PA_383	A		BIO	PLSQETFSDLWGC	TP53	T18	ATR; CSNK1D (CK1d); CSNK2A1 (CK2A1); CSNK2B (CK2B); PRKDC (DNA-PKcs, DNAPK); VRK1
PA_384	2M04	Key_L2_098 - sample + KaB + ATP + pept. PA_384	A		BIO	ADTTQYVPMLEGC	PDGFRA	Y742	FGFR1; FGFR2
PA_385	2O04	Key_L2_099 - sample + KaB + ATP + pept. PA_385	A		BIO	SSTDRSPYEKVGC	MUC1	S1227	GSK3B
PA_386	2A06	Key_L2_100 - sample + KaB + ATP + pept. PA_386	D		CON - _ mutated CON+	CGGGGPAVPKKAKKL	consensus _ CON- _ S/T to A/V	_	CDK1 (CDC2); CDK2; CDK3; CDK5; PRKACA (PKA C-alpha); PRKACB (PKA C-beta); PRKACG (PKA C-gamma)
PA_387	2C06	Key_L2_101 - sample + KaB + ATP + pept. PA_387	A		BIO	DFDEKYDDEDFGC	TOP2A	T1343	CSNK2A1 (CK2A1)
PA_388	1H08	Key_L1_298 - sample + KaB + ATP + pept. PA_388	A		BIO _ Rep (lib5-8)_e8	DESGLSSQSDILTGC	BRCA1	S1387	ATM; ATR
PA_388	2EE06	Key_L2_102 - sample + KaB + ATP + pept. PA_388	A		BIO	DESGLSSQSDILTGC	BRCA1	S1387	ATM; ATR
PA_388	2H08	Key_L2_103 - sample + KaB + ATP + pept. PA_388	A		BIO _ Rep (lib5-8)_i8	DESGLSSQSDILTGC	BRCA1	S1387	ATM; ATR
PA_389	2G08	Key_L2_104 - sample + KaB + ATP + pept. PA_389	D		CON - _ mutated CON+	EFPIGDFLPAKKKGC	consensus _ CON- _ S/T to A/V	--	LYNB; SRMS; EPHA1; EPHA2; EPHA3; EPHA4; EPHA5; EPHA8; EPHB1; EPHB2; EPHB3; EPHB4; FGFR3; MERTK (MER); NTRK2 (TRKB); NTRK3 (TRKC); FES; ITK; PTK2B (FAK2, PYK2); TXK; TYRO3
PA_390	2I08	Key_L2_105 - sample + KaB + ATP + pept. PA_390	A		BIO	MKAFSPVRSVRKGC	ID2	S5	CDK2
PA_391	2K08	Key_L2_106 - sample + KaB + ATP + pept. PA_391	A		BIO	NRNYPSQEELIGC	BRCA1	S1524	ATM
PA_392	2M08	Key_L2_107 - sample + KaB + ATP + pept. PA_392	A		BIO	PSPPGTVLTSAGC	NOTCH2	T2074	GSK3B
PA_393	2O08	Key_L2_108 - sample + KaB + ATP + pept. PA_393	A		BIO	PESIHSFIGDGGC	MTOR (FRAP1)	S2481	MTOR (FRAP1)
PA_394	2A08	Key_L2_109 - sample + KaB + ATP + pept. PA_394	A		BIO	GSLCTSFVGTLGC	CHUK (IKK alpha) / IKBKB (IKK beta)	S180 / S181	CHUK (IKK alpha); MAP3K7 (MEKK7, TAK1); MAP3K14 (NIK), PRKCQ (PKC theta); PRKCZ (PKC zeta)
PA_395	2C08	Key_L2_110 - sample + KaB + ATP + pept. PA_395	A		BIO	FMMTPYVVTRYGC	MAPK8 (JNK1) / MAPK9 (JNK2) / MAPK10 (JNK3)	Y185 (T183) / Y185 (T183) / Y223 (T221)	MAP2K4 (MEK4, MKK4, MAPKK4, JNKK1); MAP2K7 (MEK7, MKK7, MAPKK7, JNKK2); RET
PA_396	2EE08	Key_L2_111 - sample + KaB + ATP + pept. PA_396	B		CON +	CKKRNRRLSVA	consensus _ CON+	--	NDR1 (STK38); NDR2 (STK38L); SGK1 (SGK); SGK2; SGK3 (SGKL)
PA_397	2G08	Key_L2_112 - sample + KaB + ATP + pept. PA_397	A		BIO	DDIIYQDFTVGC	STK11 (LKB)	T363	ATM
PA_398	2I08	Key_L2_113 - sample + KaB + ATP + pept. PA_398	A		BIO	CGALSYLQSPITTSPS	DUSP1	S364	MAPK3 (ERK1)
PA_399	2K08	Key_L2_114 - sample + KaB + ATP + pept. PA_399	A		BIO	LSRMGSLRAPVGC	E2F1	S364	CHEK2
PA_400	2M08	Key_L2_115 - sample + KaB + ATP + pept. PA_400	A		BIO	DYMPMSPKSVSGC	IRS1	S636	MAPK1 (ERK2), MAPK8 (JNK1)
PA_401	2O08	Key_L2_116 - sample + KaB + ATP + pept. PA_401	A		BIO	EPQRRSARLSAGC	HMGN2	S25	PRKACA (PKA C-alpha); PRKCA (PKC alpha, PKCA); RPS6KA3 (RSK2, p90RSK2, S6K-alpha-3)

Table 1

PA_402	2A10	Key_L2_117 - sample + KaB + ATP + pept. PA_402	A	BIO	FTNQGYFFFHLGC	IL2RB	Y364	JAK1
PA_403	2C10	Key_L2_118 - sample + KaB + ATP + pept. PA_403	A	BIO	QVRTLSGSRPPGC	EEF2K	S366	PRKAA1 (AMPKa1); PRKAA2 (AMPKa2), PRKACA (PKA C-alpha); RPS6KA1 (RSK1, p90RSK), RPS6KB1 (S6K1, p70S6K, S6K-beta-1)
PA_404	2EE10	Key_L2_119 - sample + KaB + ATP + pept. PA_404	A	BIO	PIPQPYTPVSSFGC	PAX6	T303, T304	HIPK2
PA_405	2G10	Key_L2_120 - sample + KaB + ATP + pept. PA_405	A	BIO	APERASSVYTRSGC	CCR5	S336, S337	GRK3 (ADRBK2)
PA_406	2I10	Key_L2_121 - sample + KaB + ATP + pept. PA_406	A	BIO	NSGFESYGSSSYGGC	RPA2	S8	PRKDC (DNA-PKcs, DNAPK)
PA_407	2K10	Key_L2_122 - sample + KaB + ATP + pept. PA_407	B	CON +	CKKSRGDYMTMQIG	consensus _ CON+	--	AXL, DDR1 (NTRK4, RTK6, PTK3); DDR2 (NTRKR3, TYRO10), DMPK (DM1), FGFR1; IGF1R; INSR, INSRR (IRR); JAK2, RON (MST1R); STK3 (MST2, KRS1); STK4 (MST1, KRS2); STK10 (LOK), TYK2
PA_408	2M10	Key_L2_123 - sample + KaB + ATP + pept. PA_408	A	BIO	RGRLPSKPKSPGC	NR4A2 / NR4A3	S347 / S376	RPS6KA1 (RSK1, p90RSK)
PA_409	2O10	Key_L2_124 - sample + KaB + ATP + pept. PA_409	A	BIO	IESSNYMAPYDGC	PDGFRB	Y771	PDGFRB
PA_410	2A12	Key_L2_125 - sample + KaB + ATP + pept. PA_410	A	BIO	PPDHQYYNDFPGGC	SHC1 (p66Shc / p52Shc / p46Shc)	Y349, Y350	FLT3; SRC; SYK; ZAP70
PA_411	2C12	Key_L2_126 - sample + KaB + ATP + pept. PA_411	A	BIO	KSKIGSTENLKGC	MAPT (TAU)	S579	CAMK2A; GSK3B; MARK1; PHKG1; PRKACA (PKA C-alpha); PRKCD (PKC delta, PKCD)
PA_412	2EE12	Key_L2_127 - sample + KaB + ATP + pept. PA_412	A	BIO	IEDEDYYKASVTGC	PTK2B (FAK2)	Y579, Y580	PTK2B (FAK2, PYK2)
PA_413	2G12	Key_L2_128 - sample + KaB + ATP + pept. PA_413	C	CON - _ mutated BIO	KRRQVAMVDFFGC	CDKN1A (p21, WAF1, CIP1) _ CON (-) _ S/T/Y to A/V/F	S146	AKT1; PIM1; PIM2, PRKCA (PKC alpha, PKCA), NUAK1; LATS2
PA_414	2I12	Key_L2_129 - sample + KaB + ATP + pept. PA_414	A	BIO	DPVARTSPLQTPGC	BCL2	T69, S70	MAPK8 (JNK1)
PA_415	2K12	Key_L2_130 - sample + KaB + ATP + pept. PA_415	C	CON - _ mutated BIO	KSPVVAGDVAPRHLANGC	MAPT (TAU) _ CON (-) _ S/T to A/V	S717, T720, S721	GSK3B; CDK5
PA_416	2M12	Key_L2_131 - sample + KaB + ATP + pept. PA_416	A	BIO	KSPVVSGDTSPRHLSNGC	MAPT (TAU)	S717, T720, S721	GSK3B, CDK5
PA_417	2C14	Key_L2_132 - sample + KaB + ATP + pept. PA_417	A	BIO	QSKRSTMVGTPGC	PAK1	T423	PDPK1
PA_418	2EE14	Key_L2_133 - sample + KaB + ATP + pept. PA_418	A	BIO	CGSSKIRRLSACKQQ	STK11 (LKB)	S428 (C-term)	PRKACA (PKA C-alpha); RPS6KA3 (RSK2, p90RSK2, S6K-alpha-3); RPS6KA5 (MSK1), RPS6KB1 (S6K1, p70S6K, S6K-beta-1)
PA_419	2K14	Key_L2_134 - sample + KaB + ATP + pept. PA_419	A	BIO	RERKSSSSSEDGC	BRAF	S429	AKT1
PA_420	2M14	Key_L2_135 - sample + KaB + ATP + pept. PA_420	A	BIO	MWNSGFESYGSSGC	RPA2	S4 (N-term)	PRKDC (DNA-PKcs, DNAPK)
PA_421	2O14	Key_L2_136 - sample + KaB + ATP + pept. PA_421	E	CON - _ random	KINA(pS)EMAPPINGC	-	--	--
PA_422	3A16	Key_L2_137 - sample + KaB + ATP + pept. PA_422	A	BIO	RKSYYSKDPSRGC	MYT1	S429	PLK1
PA_423	2C16	Key_L2_138 - sample + KaB + ATP + pept. PA_423	A	BIO	EPKIRSPRRFIGC	RPS6KB1 (S6K1)	S434	CDK1 (CDC2)
PA_424	2EE16	Key_L2_139 - sample + KaB + ATP + pept. PA_424	A	BIO	VLNAFSQAPSTGC	SRF	S435	PRKDC (DNA-PKcs, DNAPK)
PA_425	2G16	Key_L2_140 - sample + KaB + ATP + pept. PA_425	D	CON - _ mutated CON+	LRRAALGGC	consensus _ CON- _ S/T to A/V		AURKA; AURKB; AURKC; PRKACA (PKA C-alpha); PRKACB (PKA C-beta); PRKACG (PKA C-gamma), PRKG1 (PKG1); PRKG2 (PKG2);
PA_426	2I16	Key_L2_141 - sample + KaB + ATP + pept. PA_426	A	BIO	VAFQGYLRQTRGC	IL10RA	Y446	JAK1
PA_427	2K16	Key_L2_142 - sample + KaB + ATP + pept. PA_427	A	BIO	RPRSLSSPTVTGC	NEDD4L	S448	SGK1 (SGK)
PA_428	2M16	Key_L2_143 - sample + KaB + ATP + pept. PA_428	A	BIO	DSDEDYEKVPLGC	SH3BP2	Y448	SYK
PA_429	2O16	Key_L2_144 - sample + KaB + ATP + pept. PA_429	A	BIO	GAGGYTQSPGGGC	RPA2	T21	PRKDC (DNA-PKcs, DNAPK)
PA_430	2A18	Key_L2_145 - sample + KaB + ATP + pept. PA_430	A	BIO	RSSDSYAVIDLGC	FRS3	T455	NTRK2 (TRKB)
PA_431	2C18	Key_L2_146 - sample + KaB + ATP + pept. PA_431	B	CON +	AVPPSPSLSRHSSPHQSEDEEEGC	consensus _ CON+	--	GSK3A; GSK3B
PA_432	2EE18	Key_L2_147 - sample + KaB + ATP + pept. PA_432	A	BIO	SSPPISPASSDGC	MYOCD	S480	GSK3B
PA_433	2G18	Key_L2_148 - sample + KaB + ATP + pept. PA_433	A	BIO	GSVEQTPKKPGGC	CDKN1B (p27, KIP1)	T187	CDK2; PKN2 (PRK2)
PA_434	2I18	Key_L2_149 - sample + KaB + ATP + pept. PA_434	A	BIO	CGGSPHNPISSVS	SMAD1	S463 (C-term)	ACVR1 (ACVR1A, ALK2); TGFBR1 (ALK5)

Table 1

PA_435	2K18	Key_L2_150 - sample + KaB + ATP + pept. PA_435	B		CON +	LRRASLGGC	consensus _ CON+	_	AURKA; AURKB; AURKC; PRKACA (PKA C-alpha); PRKACB (PKA C-beta); PRKACG (PKA C-gamma); PRKG1 (PKG1); PRKG2 (PKG2);
PA_436	2M18	Key_L2_151 - sample + KaB + ATP + pept. PA_436	A		BIO	TGSRYYKEIPLGC	PRKD1 (PKD1)	Y463	ABL1; SRC
PA_437	2O18	Key_L2_152 - sample + KaB + ATP + pept. PA_437	A		BIO	CGTHFPGFSYSASG	AKT2	S474	PDPK1
PA_438	2A20	Key_L2_153 - sample + KaB + ATP + pept. PA_438	A		BIO	RERLGTGGFGNGC	CHUK (IKK alpha)	T23	AKT1; AKT2
PA_439	2C20	Key_L2_154 - sample + KaB + ATP + pept. PA_439	A		BIO	LVNRHYAKISDGC	ZAP70	Y474	LCK
PA_440	2EE20	Key_L2_155 - sample + KaB + ATP + pept. PA_440	A		BIO	CGEPSFSEYASVQVPR	SIRPA	Y496 (C-term)	JAK2
PA_441	2G20	Key_L2_156 - sample + KaB + ATP + pept. PA_441	A		BIO	HPNDLYVEGLPGC	GTF2I	Y503	BTK
PA_442	2I20	Key_L2_157 - sample + KaB + ATP + pept. PA_442	C		CON - _ mutated BIO	LARMGALRAPVGC	E2F1 _ CON (-) _ S/T to A/V	S364	CHEK2
PA_443	2K20	Key_L2_158 - sample + KaB + ATP + pept. PA_443	A		BIO	RTKSRTWAGEKGC	CDC25A	T507	PKN2 (PRK2)
PA_444	2M20	Key_L2_159 - sample + KaB + ATP + pept. PA_444	A		BIO	ESRASTFCGTPGC	PRKCD (PKCD)	T507	PDPK1
PA_445	2O20	Key_L2_160 - sample + KaB + ATP + pept. PA_445	A		BIO	SSTSVTPDVSDGC	PTEN	T366	CSNK2A1 (CK2A1); CSNK2A2 (CK2A2)
PA_446	2B01	Key_L2_161 - sample + KaB + ATP + pept. PA_446	A		BIO	KRRRLSSLRASTGC	RPS6	S235, S236	PAK2
PA_447	2D01	Key_L2_162 - sample + KaB + ATP + pept. PA_447	A		BIO	KRKDPSSVDIKKGC	PTPN1	S242, S243	CLK1; CLK2
PA_448	2F01	Key_L2_163 - sample + KaB + ATP + pept. PA_448	A		BIO	RPRSCTWPLPRGC	FOXO1 / FOXO4	T24 / T32	AKT1, AKT2
PA_449	2H01	Key_L2_164 - sample + KaB + ATP + pept. PA_449	B		CON +	CGKRQEQIAKRRRLSSLRASTSKSGGSQK	consensus _ CON+	_	PAK1; PAK2; PRKACB (PKA C-beta); PRKACG (PKA C-gamma); RPS6KA6 (RSK4, p90RSK6, S6K-alpha-6)
PA_450	2J01	Key_L2_165 - sample + KaB + ATP + pept. PA_450	A		BIO	RKKRYTVVGNPGC	LIMK1	T508	CDC42BPA (MRCK alpha); PAK1; ROCK1
PA_451	2L01	Key_L2_166 - sample + KaB + ATP + pept. PA_451	A		BIO	DMKRLSMEIEKGC	NF2	S518	PAK1
PA_452	2N01	Key_L2_167 - sample + KaB + ATP + pept. PA_452	A		BIO	PYAGSTDENYDGC	XRCC1	T519	CSNK2A1 (CK2A1); CSNK2A2 (CK2A2)
PA_453	2P01	Key_L2_168 - sample + KaB + ATP + pept. PA_453	A		BIO	KSYDETVDIFSGC	LIMK2	T526	CDC42BPA (MRCK alpha); ROCK1
PA_454	2B03	Key_L2_169 - sample + KaB + ATP + pept. PA_454	A		BIO	RKRTHSAGTSPGC	IRS1	S527	IKBKB (IKK beta)
PA_455	2D03	Key_L2_170 - sample + KaB + ATP + pept. PA_455	E		CON - _ random	PEP(pT)IDERIDDLEGC	_	_	_
PA_456	2F03	Key_L2_171 - sample + KaB + ATP + pept. PA_456	A		BIO	MPEEYQTQDQPGC	HSP90AA1	T5 (N-term)	PRKDC (DNA-PKcs, DNAPK)
PA_457	2H03	Key_L2_172 - sample + KaB + ATP + pept. PA_457	A		BIO	GSRSRTPSLPTGC	MAPT (TAU)	T529	CDK5; GSK3B; PRKACA (PKA C-alpha); RPS6KA3 (RSK2, p90RSK2, S6K-alpha-3)
PA_458	2J03	Key_L2_173 - sample + KaB + ATP + pept. PA_458	A		BIO	CGTATEPQYQPGEN	FYN	Y531 (C-term)	CSK
PA_459	2L03	Key_L2_174 - sample + KaB + ATP + pept. PA_459	A		BIO	HSAGTSPTITHGC	IRS1	S531	IKBKB (IKK beta); MAPK8 (JNK1)
PA_460	2N03	Key_L2_175 - sample + KaB + ATP + pept. PA_460	A		BIO	LHEDSQPESQGC	TP53BP1	S25	ATM
PA_461	2P03	Key_L2_176 - sample + KaB + ATP + pept. PA_461	A		BIO	SVPTPSPLGPLGC	CSNK2A1 (CK2A1)	S362	CDK1 (CDC2)
PA_462	2B05	Key_L2_177 - sample + KaB + ATP + pept. PA_462	A		BIO	GQESEYGNITYGC	PTPN6	Y536	ABL1, INSR, LCK
PA_463	2D05	Key_L2_178 - sample + KaB + ATP + pept. PA_463	A		BIO	DEDFSSIADMDGC	RELA	S536	CHUK (IKK alpha)
PA_464	2F05	Key_L2_179 - sample + KaB + ATP + pept. PA_464	A		BIO	KFMQASEDLLKGC	NME1	S44	NME1-NME2, NME1 (NM23, NDPK-A)
PA_465	2H05	Key_L2_180 - sample + KaB + ATP + pept. PA_465	D		CON - _ mutated CON+	CKRREILARRPAFRK	consensus _ CON- _ S/T to A/V	_	AKT1; AKT2; AKT3; AURKA; CAMK1beta; CAMK1delta; CAMK1gamma; CAMK2; CAMK4; IKBKB (IKK beta); IRAK4; KSR1; KSR1(A635F); KSR1(L639F); KSR2; KSR2(R576S); PAK2, PRKACA (PKA C-alpha); PRKACB (PKA C-beta), PRKACG (PKA C-gamma); PRKCA (PKC alpha, PKCA); PRKCB (PKC beta, PKCB); PRKCD (PKC delta, PKCD); PRKCI (PKC iota, PKCI), PRKCM (PKC mu, PKCM); PRKCN (PKC nu); PRKCZ (PKC zeta); PRKD2 (PKD2); RPS6KA5 (MSK1)
PA_466	2J05	Key_L2_181 - sample + KaB + ATP + pept. PA_466	A		BIO	LKVLYSQKATPGC	CDC20	S153	BUB1

Table 1

PA_467	2L05	Key_L2_182 - sample + KaB + ATP + pept. PA_467	A	BIO	AVHPLTPLITYGC	LEF1	T155		NLK
PA_468	2N05	Key_L2_183 - sample + KaB + ATP + pept. PA_468	B	CON +	LIDSMANSFVGGC	consensus _ CON+	--		RAF1 (cRAF)
PA_469	2P05	Key_L2_184 - sample + KaB + ATP + pept. PA_469	A	BIO	STGEDSAFQEPGC	WEE1	S53		PLK1
PA_470	2B07	Key_L2_185 - sample + KaB + ATP + pept. PA_470	A	BIO	GAVTHTFCGTIGC	RPS6KB2 (S6K2)	T228		MTOR (FRAP1); PDPK1
PA_471	2D07	Key_L2_186 - sample + KaB + ATP + pept. PA_471	A	BIO	SNHDESLKKNDGC	BRCA2	S239		PLK1
PA_472	2F07	Key_L2_187 - sample + KaB + ATP + pept. PA_472	A	BIO	GALSNSESIPTGC	STAMBP	S245		BMPR1B
PA_473	2H07	Key_L2_188 - sample + KaB + ATP + pept. PA_473	A	BIO	DEWCDSGLGSLGC	NFKBIB (IKBB)	S19		CHUK (IKK alpha); IKBKB (IKK beta)
PA_474	2J07	Key_L2_189 - sample + KaB + ATP + pept. PA_474	A	BIO	CGPRPRLNTSDFQK	AKT1S1	T246 (S247)		AKT1, AKT2
PA_475	2L07	Key_L2_190 - sample + KaB + ATP + pept. PA_475	A	BIO	PIDMESQERIKGC	JUN	S249		CSNK2A1 (CK2A1); PRKDC (DNA-PKcs, DNAPK)
PA_476	2N07	Key_L2_191 - sample + KaB + ATP + pept. PA_476	A	BIO	QMEVASFLLSKGC	CDC20	S92		BUB1
PA_477	2P07	Key_L2_192 - sample + KaB + ATP + pept. PA_477	B	CON +	CGKKKKERLLDDRHDSGLDSMKDEE	consensus _ CON+	--		CHUK (IKK alpha); IKBKB (IKK beta)
PA_478	2B09	Key_L2_193 - sample + KaB + ATP + pept. PA_478	A	BIO	ARDITAWHIPPGC	IRAK1	T100		AKT1
PA_479	2D09	Key_L2_194 - sample + KaB + ATP + pept. PA_479	A	BIO	KLLGCSPALKRGC	CDC25A	S116		CDK1 (CDC2); PIM1
PA_480	2F09	Key_L2_195 - sample + KaB + ATP + pept. PA_480	A	BIO	IPINGSPRTPRGC	RB1	S249		CDK1 (CDC2)
PA_481	2H09	Key_L2_196 - sample + KaB + ATP + pept. PA_481	A	BIO	LLDEDYEKVLGGC	STAP2	Y250		JAK2, SRC
PA_482	2J09	Key_L2_197 - sample + KaB + ATP + pept. PA_482	A	BIO	FDDPSYVNVQNGC	SHC1 (p66Shc / p52Shc / p46Shc)	Y427		FLT3; FYN; INSR; LCK; ZAP70
PA_483	2L09	Key_L2_198 - sample + KaB + ATP + pept. PA_483	A	BIO	GTVTHTFCGTIGC	RPS6KB1 (S6K1)	T252		PDPK1
PA_484	2N09	Key_L2_199 - sample + KaB + ATP + pept. PA_484	A	BIO	EDTTSTFCGTPGC	SGK2	T253		PDPK1
PA_485	2P09	Key_L2_200 - sample + KaB + ATP + pept. PA_485	A	BIO	RRRAASMDNNSGC	FOXO1	S256		AKT1; PAK1
PA_486	2B11	Key_L2_201 - sample + KaB + ATP + pept. PA_486	A	BIO	NSTTSTFCGTPGC	SGK1	T256		PDPK1
PA_487	2D11	Key_L2_202 - sample + KaB + ATP + pept. PA_487	A	BIO	DTLSDSDDEDDGC	MYCN	S263		CSNK2A1 (CK2A1); CSNK2A2 (CK2A2)
PA_488	2F11	Key_L2_203 - sample + KaB + ATP + pept. PA_488	A	BIO	QLFYISQPGSSGC	MRE11A	S284		ATM
PA_489	2H11	Key_L2_204 - sample + KaB + ATP + pept. PA_489	D	CON - _ mutated CON+	KRRRLAALRAGC	consensus _ CON- _ S/T to A/V	--		CDC42BPA (MRCK alpha); CDC42BPB (MRCK beta); CHUK (IKK alpha); IKBKB (IKK beta); CLK2; PAK2; PIM1; PIM2; PIM3; PRKG1 (PKG1); PRKG2 (PKG2); ROCK1; ROCK2; RPS6KA1 (RSK1, p90RSK); RPS6KA2 (RSK3, p90RSK2, S6K-alpha-2); RPS6KA3 (RSK2, p90RSK2, S6K-alpha-3); RPS6KA4 (MSK2, S6K-alpha-4); RPS6KA5 (MSK1); RPS6KA6 (RSK4, p90RSK6, S6K-alpha-6); RPS6KB1 (S6K1, p70S6K, S6K-beta-1)
PA_490	2J11	Key_L2_205 - sample + KaB + ATP + pept. PA_490	A	BIO	SKAKKTVDKHSGC	CEBPB	T266		RPS6KA1 (RSK1, p90RSK)
PA_491	2L11	Key_L2_206 - sample + KaB + ATP + pept. PA_491	A	BIO	VHMVSTTLPVDGC	RAF1 (cRAF)	T268		RAF1 (cRAF)
PA_492	2N11	Key_L2_207 - sample + KaB + ATP + pept. PA_492	A	BIO	RSKSQSSSNCSGC	IRS1	S272		IKBKB (IKK beta)
PA_493	2P11	Key_L2_208 - sample + KaB + ATP + pept. PA_493	A	BIO	KRPERSQEESPGC	CDC25A	S279		CHEK1; CHEK2
PA_494	2B13	Key_L2_209 - sample + KaB + ATP + pept. PA_494	A	BIO	MGPRRRSRKPEAPGC	CENPA	S7 (N-term)		AURKB
PA_495	2D13	Key_L2_210 - sample + KaB + ATP + pept. PA_495	A	BIO	TGDTSSEEDEDGC	GTF2A1	S281		CSNK2A1 (CK2A1); CSNK2A2 (CK2A2); TAF1
PA_496	2F13	Key_L2_211 - sample + KaB + ATP + pept. PA_496	A	BIO	CGEVDLACTPTDVRD	CCND1	T286		GSK3B
PA_497	2H13	Key_L2_212 - sample + KaB + ATP + pept. PA_497	A	BIO	LEVWGSQEALEGC	XPA	S196		ATM; ATR; PRKDC (DNA-PKcs, DNAPK)
PA_498	2J13	Key_L2_213 - sample + KaB + ATP + pept. PA_498	A	BIO	SPNNLSPTGWSGC	RAF1 (cRAF)	S301		MAPK1 (ERK2)
PA_499	2L13	Key_L2_214 - sample + KaB + ATP + pept. PA_499	A	BIO	EFCNKSKQPGLGC	BRCA1	S308		AURKA
PA_500	2N13	Key_L2_215 - sample + KaB + ATP + pept. PA_500	A	BIO	NQEENYVTPIGGC	STAP2	Y310		JAK2; SRC

Table 1

PA_501	2P13	Key_L2_216 - sample + KaB + ATP + pept. PA_501	D		CON - _ mutated CON+	LIDAMANAFVGGC	consensus _ CON- _ S/T to A/V	_	RAF1 (cRAF)
PA_502	2B15	Key_L2_217 - sample + KaB + ATP + pept. PA_502	A		BIO	PGPSLSQGVSVGC	NBN	S343	ATM
PA_503	2D15	Key_L2_218 - sample + KaB + ATP + pept. PA_503	A		BIO	CGTRSTGEQEISVGL	CCR5	S349	GRK3 (ADRBK2)
PA_504	2F15	Key_L2_219 - sample + KaB + ATP + pept. PA_504	A		BIO	RTTSQLYDAVPIQGC	PDPK1	Y9 (N-term)	SRC
PA_505	2H15	Key_L2_220 - sample + KaB + ATP + pept. PA_505	A		BIO	SQETFSDLWKLGC	TP53	S20	ATM; ATR; CHEK1; PLK3; PRKDC (DNA-PKcs, DNAPK)
PA_506	2J15	Key_L2_221 - sample + KaB + ATP + pept. PA_506	A		BIO	RSARLSAKPAPGC	HMGN2	S29	PRKACA (PKA C-alpha); PRKCA (PKC alpha, PKCA); RPS6KA3 (RSK2, p90RSK2, S6K-alpha-3)
PA_507	2L15	Key_L2_222 - sample + KaB + ATP + pept. PA_507	A		BIO	CGEEGISQESSEEEQ	HMGA1	S99, S102, S103 (C-term end)	CSNK2A1 (CK2A1); CSNK2A2 (CK2A2)
PA_508	2N15	Key_L2_223 - sample + KaB + ATP + pept. PA_508	A		BIO	PEGHEYYRVREDGC	TYK2	Y1054, Y1055	JAK1
PA_509	2P15	Key_L2_224 - sample + KaB + ATP + pept. PA_509	A		BIO	DSEENYVPMQNGC	GAB2	Y584	FGFR1; FGFR2
PA_510	1L10	Key_L1_299 - sample + KaB + ATP + pept. PA_510	A		BIO _ Rep (lib5-8)_e9	RREILSRRPSYGC	CREB1 / CREM	S129 / S132	GSK3B; GSK3A
PA_510	2B17	Key_L2_225 - sample + KaB + ATP + pept. PA_510	A		BIO	RREILSRRPSYGC	CREB1 / CREM	S129 / S132	GSK3B; GSK3A
PA_510	2L10	Key_L2_226 - sample + KaB + ATP + pept. PA_510	A		BIO _ Rep (lib5-8)_i9	RREILSRRPSYGC	CREB1 / CREM	S129 / S132	GSK3B; GSK3A
PA_511	2D17	Key_L2_227 - sample + KaB + ATP + pept. PA_511	A		BIO	KIGEGTYGVVYKGC	CDK1 (CDC2); CDK2	T14, Y15	PKMYT1 (MYT1); LYNA; LYNB; STK10 (LCK); WEE1 (WEE1A); WEE2 (WEE1B)
PA_512	2F17	Key_L2_228 - sample + KaB + ATP + pept. PA_512	B		CON +	CGGGGPATPKKAKKL	consensus _ CON+	_	CDK1 (CDC2); CDK2; CDK3; CDK5; PRKACA (PKA C-alpha); PRKACB (PKA C-beta); PRKACG (PKA C-gamma)
PA_513	2H17	Key_L2_229 - sample + KaB + ATP + pept. PA_513	A		BIO	GSSCISPTIVQGC	RAF1 (cRAF)	S29	MAPK1 (ERK2)
PA_515	2L17	Key_L2_230 - sample + KaB + ATP + pept. PA_515	A		BIO	RKRPATDDSSTGC	CDKN1B (p27, KIP1)	T157	AKT1; PKN2 (PRK2)
PA_516	2N17	Key_L2_231 - sample + KaB + ATP + pept. PA_516	A		BIO	SDEHFSPGSHPGC	LEF1	S166	NLK
PA_518	2B19	Key_L2_232 - sample + KaB + ATP + pept. PA_518	A		BIO	GGDDIYEDIIKGC	VAV2	Y172	EGFR; FGFR1; FGFR2
PA_519	2D19	Key_L2_233 - sample + KaB + ATP + pept. PA_519	A		BIO	TDNEDYEHDDEGC	SH3BP2	Y174	SYK
PA_520	2F19	Key_L2_234 - sample + KaB + ATP + pept. PA_520	C		CON - _ mutated BIO	GQLIDAMANAFGC	MAP2K1 (MEK1) _ CON (-) _ S/T to A/V	S218	ARAF; BRAF; RAF1 (cRAF)
PA_521	2H19	Key_L2_235 - sample + KaB + ATP + pept. PA_521	A		BIO	LSPVRSPKKKGGC	RB1	S612	CDK2
PA_522	2J19	Key_L2_236 - sample + KaB + ATP + pept. PA_522	A		BIO	PHGSVTQSQGSGC	CHEK2	T26	ATM; ATR; PLK1
PA_523	2L19	Key_L2_237 - sample + KaB + ATP + pept. PA_523	A		BIO	DVDQGSLCTSFGC	CHUK (IKK alpha)	S176	MAP3K14 (NIK); PRKCQ (PKC theta)
PA_524	2N19	Key_L2_238 - sample + KaB + ATP + pept. PA_524	A		BIO	NVVPLYDLLLEGC	ESR1	Y537	LCK; SRC
PA_525	2P19	Key_L2_239 - sample + KaB + ATP + pept. PA_525	A		BIO	HKEDVYENLHTGC	PTPN6	Y564	ABL1; LCK; LYNA; LYNB
PA_526	2B02	Key_L2_240 - sample + KaB + ATP + pept. PA_526	A		BIO	EERRKSHEAEVGC	STMN1	S63	CSNK2A1 (CK2A1); PRKACA (PKA C-alpha)
PA_527	2D02	Key_L2_241 - sample + KaB + ATP + pept. PA_527	A		BIO	AWLSDSPLFDLGC	RB1	S567	CDK2
PA_528	2F02	Key_L2_242 - sample + KaB + ATP + pept. PA_528	A		BIO	RFRKETNNAAIGC	GMFB	T27	RPS6KA1 (RSK1, p90RSK)
PA_529	2H02	Key_L2_243 - sample + KaB + ATP + pept. PA_529	A		BIO	KTRDQYLMWLTGC	PIK3R1	Y580	INSR
PA_530	2L02	Key_L2_244 - sample + KaB + ATP + pept. PA_530	A		BIO	DNEYFYVDFREGC	FLT3	Y591	FLT3
PA_531	2N02	Key_L2_245 - sample + KaB + ATP + pept. PA_531	A		BIO	DFGLATVKSRWGC	BRAF	T599	PKN2 (PRK2)
PA_532	2P02	Key_L2_246 - sample + KaB + ATP + pept. PA_532	A		BIO	MSSSPLSKKRRGC	UBA1	S4 (N-term)	CDK1 (CDC2)
PA_533	2B04	Key_L2_247 - sample + KaB + ATP + pept. PA_533	B		CON +	CGKKYSPTSPSYSPTSPSYSPTSPS	consensus _ CON+	_	CDK7; CDK8; CDK9; CDK11
PA_534	2J04	Key_L2_248 - sample + KaB + ATP + pept. PA_534	A		BIO	NTEDQYSLVEDGC	PIK3R1	Y607	INSR
PA_535	2L04	Key_L2_249 - sample + KaB + ATP + pept. PA_535	A		BIO	LEQHGSQPSNSGC	BRCA1	S1423	ATM; ATR
PA_536	2N04	Key_L2_250 - sample + KaB + ATP + pept. PA_536	A		BIO	HTDDGYMPMSPGC	IRS1	Y612	JAK1
PA_537	2P04	Key_L2_251 - sample + KaB + ATP + pept. PA_537	A		BIO	DSGVETSFRKLSGC	NFKB1	T931, S932	CHUK (IKK alpha)

Table 1

PA_538	2B06	Key_L2_252 - sample + KaB + ATP + pept. PA_538	A	BIO	ESDGGYMDMSKGC	PDGFRB	Y740	FGFR1; FGFR2; PDGFRB
PA_539	2D06	Key_L2_253 - sample + KaB + ATP + pept. PA_539	A	BIO	VDAAVTPEERHGC	APP	T744	CDK5; GSK3B
PA_540	2J06	Key_L2_254 - sample + KaB + ATP + pept. PA_540	A	BIO	MRRSNSSGNLHGC	TLK1	S743	CHEK1
PA_541	2N06	Key_L2_255 - sample + KaB + ATP + pept. PA_541	A	BIO	RYRDVSPFDHSGC	PTPN1	S50	AKT1; CLK1; CLK2
PA_542	2P06	Key_L2_256 - sample + KaB + ATP + pept. PA_542	C	CON - _ mutated BIO	ELDQGALCVAFGC	IKBKB (IKK beta) _ CON (-) _ S/T to A/V	S177	CHUK (IKK alpha); MAP3K14 (NIK); MAP3K7 (MEKK7, TAK1); PRKCQ (PKC theta); PRKCZ (PKC zeta)
PA_543	2B08	Key_L2_257 - sample + KaB + ATP + pept. PA_543	A	BIO	LLSELSRRRIRGC	EIF2S1	S52	EIF2AK1; EIF2AK2; EIF2AK3 (PEK); PRKCD (PKC delta, PKCD); PRKRIR (THAP12, DAP4, P52rIPK)
PA_544	2D08	Key_L2_258 - sample + KaB + ATP + pept. PA_544	A	BIO	PSEVPTPKRPRGC	HMGA1	T53	CDK1 (CDC2)
PA_545	2J08	Key_L2_259 - sample + KaB + ATP + pept. PA_545	A	BIO	QVSRTSGGAGGGC	DES	S60	AURKB
PA_546	2N08	Key_L2_260 - sample + KaB + ATP + pept. PA_546	A	BIO	PTPPLSPSRRSGC	MYC	S62 (T58)	MAPK8 (JNK1)
PA_547	2P08	Key_L2_261 - sample + KaB + ATP + pept. PA_547	A	BIO	LARRPSYRKILGC	ATF1	S63	CAMK1; CAMK2G; PRKACA (PKA C-alpha); RPS6KA4 (MSK2, S6K-alpha-4); RPS6KA5 (MSK1)
PA_548	2B10	Key_L2_262 - sample + KaB + ATP + pept. PA_548	A	BIO	MSETVPPAPAASGC	HIST1H1A	S2 or T5 (N-term end)	CDK1 (CDC2)
PA_550	2H10	Key_L2_263 - sample + KaB + ATP + pept. PA_550	A	BIO	NIHGSDSVESGC	NME1	S120	NME1-NME2, NME1 (NM23, NDPK-A)
PA_551	2N10	Key_L2_264 - sample + KaB + ATP + pept. PA_551	A	BIO	EPNPNSPANSQGC	UBE2A	S120	CDK1 (CDC2); CDK2
PA_552	2P10	Key_L2_265 - sample + KaB + ATP + pept. PA_552	A	BIO	SPMETSGCAPAGC	CCNB1	S133	PLK1
PA_553	2B12	Key_L2_266 - sample + KaB + ATP + pept. PA_553	A	BIO	LTIDRYLAIVHGC	CCR2	Y139	JAK2
PA_554	2D12	Key_L2_267 - sample + KaB + ATP + pept. PA_554	A	BIO	RKGHEYTNIKYGC	PTPN11	Y546	PDGFRB
PA_555	2F12	Key_L2_268 - sample + KaB + ATP + pept. PA_555	B	CON +	KRRRLSSLRAGC	consensus _ CON+	_	CDC42BPA (MRCK alpha); CDC42BPB (MRCK beta); CHUK (IKK alpha); IKBKB (IKK beta); CLK2; PAK2; PIM1; PIM2; PIM3; PRKG1 (PKG1); PRKG2 (PKG2); ROCK1; ROCK2; RPS6KA1 (RSK1, p90RSK); RPS6KA2 (RSK3, p90RSK2, S6K-alpha-2); RPS6KA3 (RSK2, p90RSK2, S6K-alpha-3); RPS6KA4 (MSK2, S6K-alpha-4); RPS6KA5 (MSK1); RPS6KA6 (RSK4, p90RSK6, S6K-alpha-6); RPS6KB1 (S6K1, p70S6K, S6K-beta-1)
PA_556	2N12	Key_L2_269 - sample + KaB + ATP + pept. PA_556	A	BIO	KILRKSPHLEKGC	NSUN2	S139	AURKB
PA_557	2P12	Key_L2_270 - sample + KaB + ATP + pept. PA_557	A	BIO	GEGTESTVITGGC	TPT1	S54	PLK1
PA_558	2B14	Key_L2_271 - sample + KaB + ATP + pept. PA_558	A	BIO	RSGQRTASVLWGC	IRAK1	T56	AKT1; IRAK1
PA_559	2D14	Key_L2_272 - sample + KaB + ATP + pept. PA_559	A	BIO	QEDNDYINASLGC	PTPN1	S66	EGFR; INSR
PA_560	2F14	Key_L2_273 - sample + KaB + ATP + pept. PA_560	A	BIO	RSARLSAKPPAGC	HMGN1	S25	PRKACA (PKA C-alpha); PRKCA (PKC alpha, PKCA); RPS6KA3 (RSK2, p90RSK2, S6K-alpha-3)
PA_561	2H14	Key_L2_274 - sample + KaB + ATP + pept. PA_561	A	BIO	TGSVDYLALDFGC	GAB2	Y614	ZAP70
PA_563	2L14	Key_L2_275 - sample + KaB + ATP + pept. PA_563	A	BIO	CGNACTLTTSPRLPV	RAF1 (cRAF)	S642 (C-term)	MAPK1 (ERK2)
PA_564	2N14	Key_L2_276 - sample + KaB + ATP + pept. PA_564	C	CON - _ mutated BIO	CGGKKAVQAAQEF	H2AFX _ CON (-) _ S/T to A/V	S140	ATM
PA_565	2P14	Key_L2_277 - sample + KaB + ATP + pept. PA_565	A	BIO	STNADSQSSSDGC	DCLRE1C	S645	ATM
PA_566	2B16	Key_L2_278 - sample + KaB + ATP + pept. PA_566	A	BIO	DERVDYVVVDQGC	GAB1	Y659	EGFR; INSR; MET
PA_567	2D16	Key_L2_279 - sample + KaB + ATP + pept. PA_567	A	BIO	EPKRRSARLSAGC	HMGN1	S21	PRKACA (PKA C-alpha); PRKCA (PKC alpha, PKCA); RPS6KA3 (RSK2, p90RSK2, S6K-alpha-3)
PA_568	2F16	Key_L2_280 - sample + KaB + ATP + pept. PA_568	A	BIO	DSGLGSLGPDAGC	NFKBIB (IKBB)	S23	CHUK (IKK alpha); IKBKB (IKK beta)
PA_569	2H16	Key_L2_281 - sample + KaB + ATP + pept. PA_569	D	CON - _ mutated CON+	CGKKKKERLLDDRHDAGLDAMKDEE	consensus _ CON- _ S/T to A/V	_	CHUK (IKK alpha); IKBKB (IKK beta)
PA_570	2J16	Key_L2_282 - sample + KaB + ATP + pept. PA_570	A	BIO	FELILSPRSKEGC	STMN1	S25	CDK1 (CDC2); MAPK3 (ERK1)

Table 1

PA_571	2L15	Key_L2_283 - sample + KaB + ATP + pept. PA_571	A		BIO	PGADLSQYKMDGC	RBBP8	S664	ATM
PA_572	2P16	Key_L2_284 - sample + KaB + ATP + pept. PA_572	A		BIO	EEDTEYMTPSSGC	CBL	Y700	EGFR; FGFR1; FGFR2; STK10 (LOK)
PA_573	2B16	Key_L2_285 - sample + KaB + ATP + pept. PA_573	A		BIO	NLLPMSPEEFDGC	STAT1	S727	CAMK2G; PRKCD (PKC delta, PKCD); RPS6KA5 (MSK1)
PA_574	2D16	Key_L2_286 - sample + KaB + ATP + pept. PA_574	A		BIO	GDRTSYFCGTPGC	PKN1 (PRK1) / PKN2 (PRK2)	T774 / T816	PDPK1; PDK1
PA_575	2F16	Key_L2_287 - sample + KaB + ATP + pept. PA_575	A		BIO	RYHKRTSSAVWNSGC	INCENP	T892, S893, S894	AURKB
PA_576	2H16	Key_L2_288 - sample + KaB + ATP + pept. PA_576	D		CON - _ mutated CON+	KRPRAAAFAEGC	consensus _ CON- _ S/T to A/V	--	AKT1, AKT2; AKT3; PAK4; PAK7; SGK1 (SGK); SGK2
PA_577	2J16	Key_L2_289 - sample + KaB + ATP + pept. PA_577	A		BIO	VQTTPSKPGGDGC	CDC20	S72	BUB1
PA_578	2L16	Key_L2_290 - sample + KaB + ATP + pept. PA_578	A		BIO	YSRALSRQLSSGC	HSPB1	S78	MAPKAPK2 (MK2); MAPKAPK3 (MK3)
PA_579	2N16	Key_L2_291 - sample + KaB + ATP + pept. PA_579	A		BIO	PSPPPSPSQQIGC	SGK1	S78	MAPK7 (ERK5)
PA_580	2P16	Key_L2_292 - sample + KaB + ATP + pept. PA_580	C		CON - _ mutated BIO	CGLMFKVEGPDAD	TP53 _ CON (-) _ S/T to A/V	S392	CDK2; CDK7; CDK9; CSNK2A1 (CK2A1); EIF2AK2; MAPK14 (p38a); NUAK1; STK11 (LKB)
PA_581	2B20	Key_L2_293 - sample + KaB + ATP + pept. PA_581	A		BIO	LSRQLSSGVSEGC	HSPB1	S82	MAPKAPK2 (MK2); MAPKAPK3 (MK3)
PA_582	2D20	Key_L2_294 - sample + KaB + ATP + pept. PA_582	A		BIO	MKALSPVRGCYEGC	ID3	S5	CDK2
PA_583	2F20	Key_L2_295 - sample + KaB + ATP + pept. PA_583	A		BIO	IPGVTSPSSDEGC	EIF4EBP1 (4EBP1)	S83	MAPK1 (ERK2); MTOR (FRAP1)
PA_584	2H20	Key_L2_296 - sample + KaB + ATP + pept. PA_584	A		BIO	RGRGSSVGGGSGC	MAP3K5 (ASK1)	S83	AKT1
PA_585	2J20	Key_L2_297 - sample + KaB + ATP + pept. PA_585	A		BIO	LSSGVSEIRHTGC	HSPB1	S86	PKN2 (PRK2)
PA_586	2L20	Key_L2_298 - sample + KaB + ATP + pept. PA_586	A		BIO	GHITTPPTQGC	JUN	T91	MAPK8 (JNK1); MAPK9 (JNK2)
PA_587	1H04	Key_L1_300 - sample + KaB + ATP + pept. PA_587	A		BIO _ Rep (lib5-8)_e6	RGRLPSKPKQPGC	NR4A1	S351	AKT1; RPS6KA1 (RSK1, p90RSK); RPS6KA3 (RSK2, p90RSK2, S6K-alpha-3); RPS6KA5 (MSK1)
PA_587	2H04	Key_L2_299 - sample + KaB + ATP + pept. PA_587	A		BIO _ Rep (lib5-8)_i6	RGRLPSKPKQPGC	NR4A1	S351	AKT1; RPS6KA1 (RSK1, p90RSK); RPS6KA3 (RSK2, p90RSK2, S6K-alpha-3); RPS6KA5 (MSK1)
PA_587	2N20	Key_L2_300 - sample + KaB + ATP + pept. PA_587	A		BIO	RGRLPSKPKQPGC	NR4A1	S351	AKT1, RPS6KA1 (RSK1, p90RSK); RPS6KA3 (RSK2, p90RSK2, S6K-alpha-3); RPS6KA5 (MSK1)
PA_588	2P20	Key_L2_301 - sample + KaB + ATP + pept. PA_588	A		BIO	SEGLPTPTKMTGC	RB1	T821	CDK2
PA_589	1C13	Key_L1_301 - sample + KaB + ATP + pept. PA_589	A		BIO_nsPV	DFGLATVKSRWGC	BRAF	T599 _ p.V600E _ COSMIC prevalence: 22678 x	PKN2 (PRK2)
PA_590	1EE13	Key_L1_302 - sample + KaB + ATP + pept. PA_590	A		BIO_nsPV	DFGLATKKSRWGC	BRAF	T599 _ p.V600K _ COSMIC prevalence: 472 x	PKN2 (PRK2)
PA_591	1L04	Key_L1_303 - sample + KaB + ATP + pept. PA_591	A		BIO_nsPV	DFGLATVESRWGC	BRAF	T599 _ p.K601E _ COSMIC prevalence: 77 x	PKN2 (PRK2)
PA_592	1F12	Key_L1_304 - sample + KaB + ATP + pept. PA_592	C		CON - _ mutated BIO	DFGLAGVKSRWGC	BRAF _ CON (-) _ T to G	T599	PKN2 (PRK2)
PA_593	1D04	Key_L1_305 - sample + KaB + ATP + pept. PA_593	A		BIO_nsPV	KRPSQTSMTDFYGC	CDKN1A (p21, WAF1, CIP1)	S146 (+T145) _ p.R143W _ COSMIC prevalence: 2x	AKT1; PIM1; PIM2; PRKCA (PKC alpha, PKCA); NUAK1; LATS2
PA_594	2J17	Key_L2_302 - sample + KaB + ATP + pept. PA_594	A		BIO_nsPV	RPSSCTWPLPRGC	FOXO1	T24 _ p.R21C _ COSMIC prevalence: 1x	AKT1
PA_595	2R17	Key_L2_303 - sample + KaB + ATP + pept. PA_595	A		BIO	TPPPGTRVRAMGC	TP53	T155	CSNK2A1 (CK2A1)
PA_596	2F10	Key_L2_304 - sample + KaB + ATP + pept. PA_596	A		BIO_nsPV	TPPPGTRVRAMGC	TP53	T155 _ p.V157F _ COSMIC prevalence: 164 x	CSNK2A1 (CK2A1)
PA_597	2J14	Key_L2_305 - sample + KaB + ATP + pept. PA_597	A		BIO_nsPV	TPPPGTRVVAMGC	TP53	T155 _ p.R156P _ COSMIC prevalence: 24 x	CSNK2A1 (CK2A1)
PA_598	2D10	Key_L2_306 - sample + KaB + ATP + pept. PA_598	A		BIO_nsPV	HEQWFTKDPGPGC	TP53	T55 _ p.E56K _ COSMIC prevalence: 3 x	MAPK1 (ERK2)
PA_599	2K19	Key_L2_307 - sample + KaB + ATP + pept. PA_599	A		BIO	HSGATTTAPSLGC	CTNNB1	T41	GSK3B
PA_600	1K19	Key_L1_306 - sample + KaB + ATP + pept. PA_600	A		BIO_nsPV	HSGATATAPSLGC	CTNNB1	T41 _ p.T41A _ COSMIC prevalence: 828 x	GSK3B
PA_601	2D04	Key_L2_308 - sample + KaB + ATP + pept. PA_601	A		BIO_nsPV	HSGATTTAPFLGC	CTNNB1	T41 _ p.S45F _ COSMIC prevalence: 518 x	GSK3B

WHAT IS CLAIMED IS:

1. A method of determining the phosphorylation activity profile of a sample comprising one or more kinases, the method comprising:

incubating the sample with a panel of sensor peptides comprising a diversity of biological sensor peptides, wherein each biological sensor peptide comprises a substrate region phosphorylated by a kinase, and the diversity of biological sensor peptides comprises biological sensor peptides for different kinases; and further, wherein members of the panel of peptides are distributed into separate reaction mixtures to assess phosphorylation activity, such that each reaction mixture represents one biological sensor peptide; and

measuring phosphorylation activity for each peptide in the separate reaction mixtures, thereby determining the phosphorylation activity profile of the sample.

2. The method of claim 1, further comprising a plurality of mutated control sensor peptides.

3. The method of claim 1 or 2, wherein the step of measuring phosphorylation activity comprises detecting ATP consumption.

4. The method of claim 1, 2, or 3, further comprising normalizing the phosphorylation activity measured in each reaction mixture and assigning the activity to a subfamily or to a kinase based on the pattern of phosporylation activity.

5. The method of any one of claims 1 to 4, wherein the panel comprises biological sensor peptides for kinases that are members of at least two different kinase subfamilies.

6. The method of any one of claims 1 to 4, wherein the panel of sensor peptides comprises biological sensor peptides for kinases that are members of the ABL, AKT, HER, MAPK and SFK kinase subfamilies.

7. The method of claim 6, wherein the panel of sensor peptides comprise biological sensor peptides for kinases that are members of the ABL1, AKT1, EGFR, MAPK1/ERK2, MAPK14/p38a, HCK, and SRC subfamilies.

8. The method of claim 6, wherein the panel of sensor peptides comprises biological sensor peptides for BLK, BRK, FGR, FRK, HCK, LCK, LYN A,

SRMS, YES1, ABL1T315I, EGFR, JAK2, CSK, AKT1, AKT2, AKT3, MAPK1/ERK2, and MAPK14/p38a kinases.

9. The method of any one of claims 1 to 8, wherein the panel comprises at least three biological sensor peptides for each kinase.

10. The method of claim 9, wherein the panel comprises 4, 5, 6, 7, 8, 9, or 10 biological sensor peptides for each kinase.

11. The method of any one of claims 1 to 10, wherein the individual sensor peptides are 9 to 21 amino acids in length.

12. The method of claim 11, wherein the individual sensor peptides are from 9 to 15 amino acids in length.

13. The method of claim 12, wherein the individual sensor peptides are 11 amino acids in length.

14. The method of any one of claims 1 to 13, wherein the panel comprises at least 10, at least 20, at least 30, at least 40, at least 50, at least 60, at least 70, at least 80, or at least 90 biological sensor peptides having a sequence as shown in Table 1 for the peptide id of a biological sensor peptide shown in Fig. 4.

15. The method of claim 14, wherein the panel comprises at least 100 sensor peptides, or at least 110, at least 120, at least 130, at least 140, or 151 biological sensor peptides having a sequence as shown in Table 1 for the peptide id of a biological sensor peptide shown in Fig. 4.

16. The method of claim 15, wherein the panel comprises at leaset 10, at least 20, at least 30, at least 40, at least 50, at least 60, or 63 reference peptides as identified in Fig. 4.

17. The method of claim 15, wherein the panel comprises the 228 peptides as identified in Fig. 4.

18. The method of any one of claims 1 to 17, wherein the sample comprises cancer cells.

19. The method of claim 18, wherein the cancer cells are from a solid tumor.

20. The method of claim 19, wherein the solid tumor is a breast tumor, a colorectal tumor, a melanoma, or a lung tumor.

21. The method of claim 19 or 20, wherein the sample comprises metastatic cancer cells.

22. The method of claim 18, wherein the cancer cells are from a hematological cancer.

23. The method of any one of claims 18 to 22, wherein the cancer cells are from a patient that has been treated with a cancer therapeutic agent.

24. The method of claim 23, wherein the therapeutic agent is a kinase inhibitor.

25. The method of any one of claims 18 to 22, wherein the cancer cells are from a patient that has not been treated with a cancer therapeutic agent.

26. A panel comprising a plurality of biological sensor peptides to evaluate phosphorylation activity of two or more different kinases.

27. The panel of claim 26, further comprising a plurality of control mutated sensor peptides.

28. The panel of claim 26 or 27, wherein the panel comprises 4, 5, 6, 7, 8, 9, or 10 biological sensor peptide for each kinase.

29. The panel of any one of claims to 26 to 28, wherein the individual sensor peptides are 9 to 21 amino acids in length.

30. A panel of biological sensor peptides to evaluate phosphorylation activity, wherein the panel comprises at least four biological sensor peptides for each of kinase families ABL, AKT, HER, MAPK and SFK.

31. The panel of claim 30, wherein the panel of sensor peptides comprises at least four biological sensor peptides for each of kinase subfamilies ABL1, AKT1, EGFR, MAPK1/ERK2, MAPK14/p38a, HCK, and SRC.

32. The panel of claim 30, wherein the panel of sensor peptides comprises at least three biological sensor peptides for each kinase BLK, BRK, FGR, FRK, HCK, LCK, LYN A, SRMS, YES1, ABL1T315I, EGFR, JAK2, CSK, AKT1, AKT2, AKT3, MAPK1/ERK2, and MAPK14/p38a.

33. The panel of claim 32, wherein the panel comprises 4, 5, 6, 7, 8, 9, or 10 biological sensor peptide for each kinase.

34. The panel of any one of claims 30 to 33, wherein the individual sensor peptides are 9 to 21 amino acids in length.

35. The panel of claim 34, wherein the individual sensor peptides are from 9 to 15 amino acids in length.

36. The panel of claim 35, wherein the individual sensor peptides are 11 amino acids in length.

37. The panel of any one of claims 30 to 36, wherein the panel comprises at least 10, at least 20, at least 30, at least 40, at least 50, at least 60, at least 70, at least 80, or at least 90 biological sensor peptides having a sequence as shown in Table 1 for the peptide id of a biological sensor peptide shown in Fig. 4.

38. The panel of claim 37, wherein the panel comprises at least 100 sensor peptides, or at least 110, at least 120, at least 130, at least 140, or 151 biological sensor peptides having a sequence as shown in Table 1 for the peptide id of a biological sensor peptide shown in Fig. 4.

39. The panel of claim 38, wherein the panel comprises at least 10, at least 20, at least 30, at least 40, at least 50, at least 60, or 63 reference peptides as identified in Fig. 4.

40. The panel of claim 38, wherein the panel comprises the 228 peptides shown in Fig. 4.

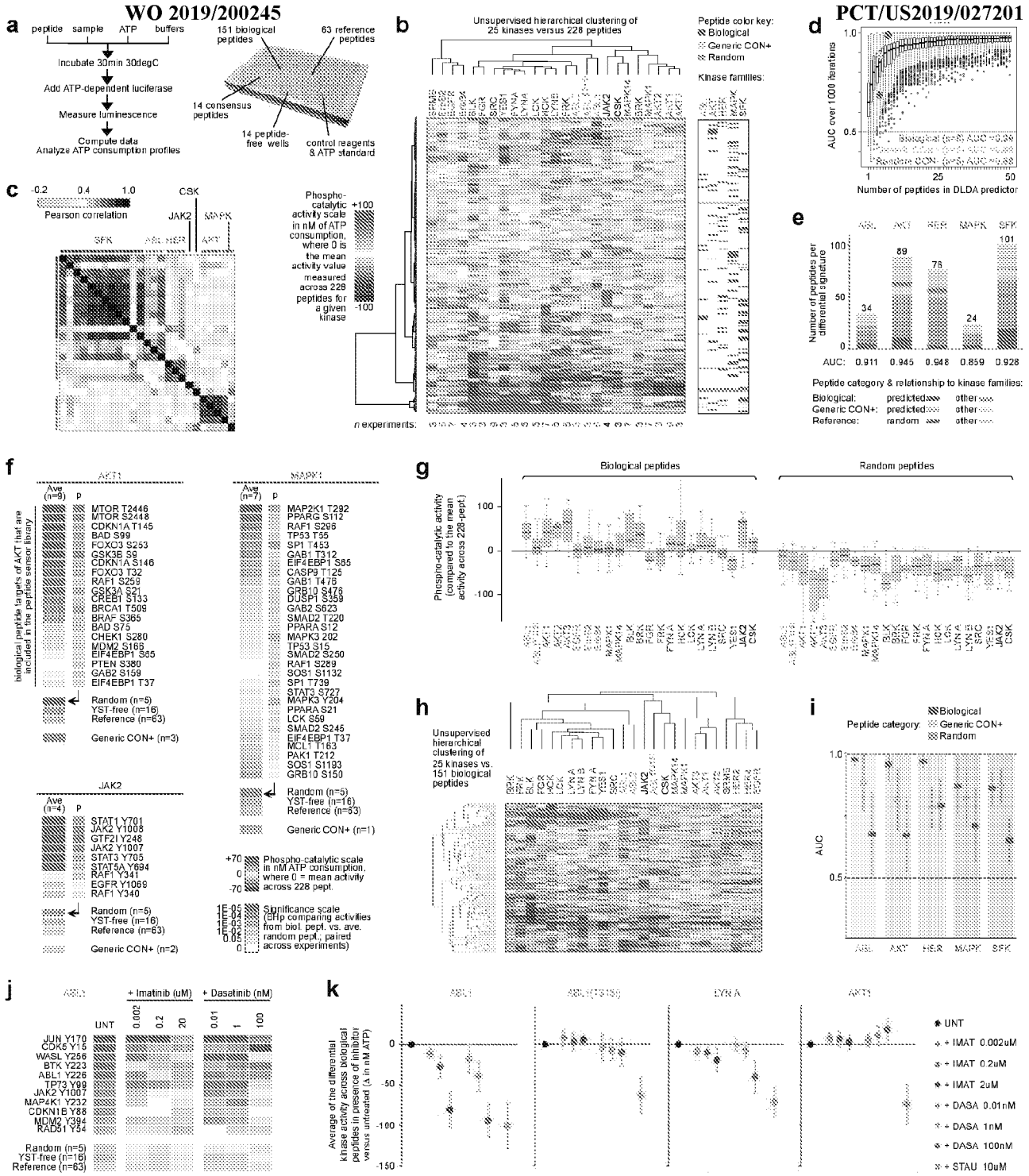
WO 2019/200245
PCT/US2019/027201
a
peptide sample ATP buffers
Incubate 30min 30degC
Add ATP-dependent luciferase
Measure luminescence
Compute data
Analyze ATP consumption profiles
151 biological peptides
63 reference peptides
14 consensus peptides
14 peptide-free wells
control reagents & ATP standard
b
Unsupervised hierarchical clustering of 25 kinases versus 228 peptides
Peptide color key:
Biological
Generic CON+
Random
Kinase families:
Phospho-catalytic activity scale in nM of ATP consumption, where 0 is the mean activity value measured across 228 peptides for a given kinase
n experiments:
c
Pearson correlation
d
AUC over 1000 iterations
Number of peptides in DLDA predictor
e
Number of peptides per differential signature
AUC: 0.911 0.945 0.948 0.859 0.928
Peptide category & relationship to kinase families:
Biological: predicted other
Generic CON+: predicted other
Reference: random other
f
AKT1
MAPK1
JAK2
biological peptide targets of AKT that are included in the peptide sensor library
Random (n=5)
YST-free (n=16)
Reference (n=63)
Generic CON+ (n=3)
Generic CON+ (n=1)
Generic CON+ (n=2)
Phospho-catalytic scale in nM ATP consumption, where 0 = mean activity across 228 pept.
Significance scale (BHp comparing activities from biol. pept. vs. ave. random pept., paired across experiments)
g
Biological peptides
Random peptides
Phospho-catalytic activity (compared to the mean activity across 228-pept.)
h
Unsupervised hierarchical clustering of 25 kinases vs. 151 biological peptides
i
Peptide category:
Biological
Generic CON+
Random
AUC
j
ABL1
+ Imatinib (uM)
+ Dasatinib (nM)
UNT
Random (n=5)
YST-free (n=16)
Reference (n=63)
k
ABL1
ABL1(T315I)
LYN A
AKT1
Average of the differential kinase activity across biological peptides in presence of inhibitor versus untreated (Δ in nM ATP)
UNT
+ IMAT 0.002uM
+ IMAT 0.2uM
+ IMAT 2uM
+ DASA 0.01nM
+ DASA 1nM
+ DASA 100nM
+ STAU 10uM

Fig. 1

WO 2019/200245

PCT/US2019/027201

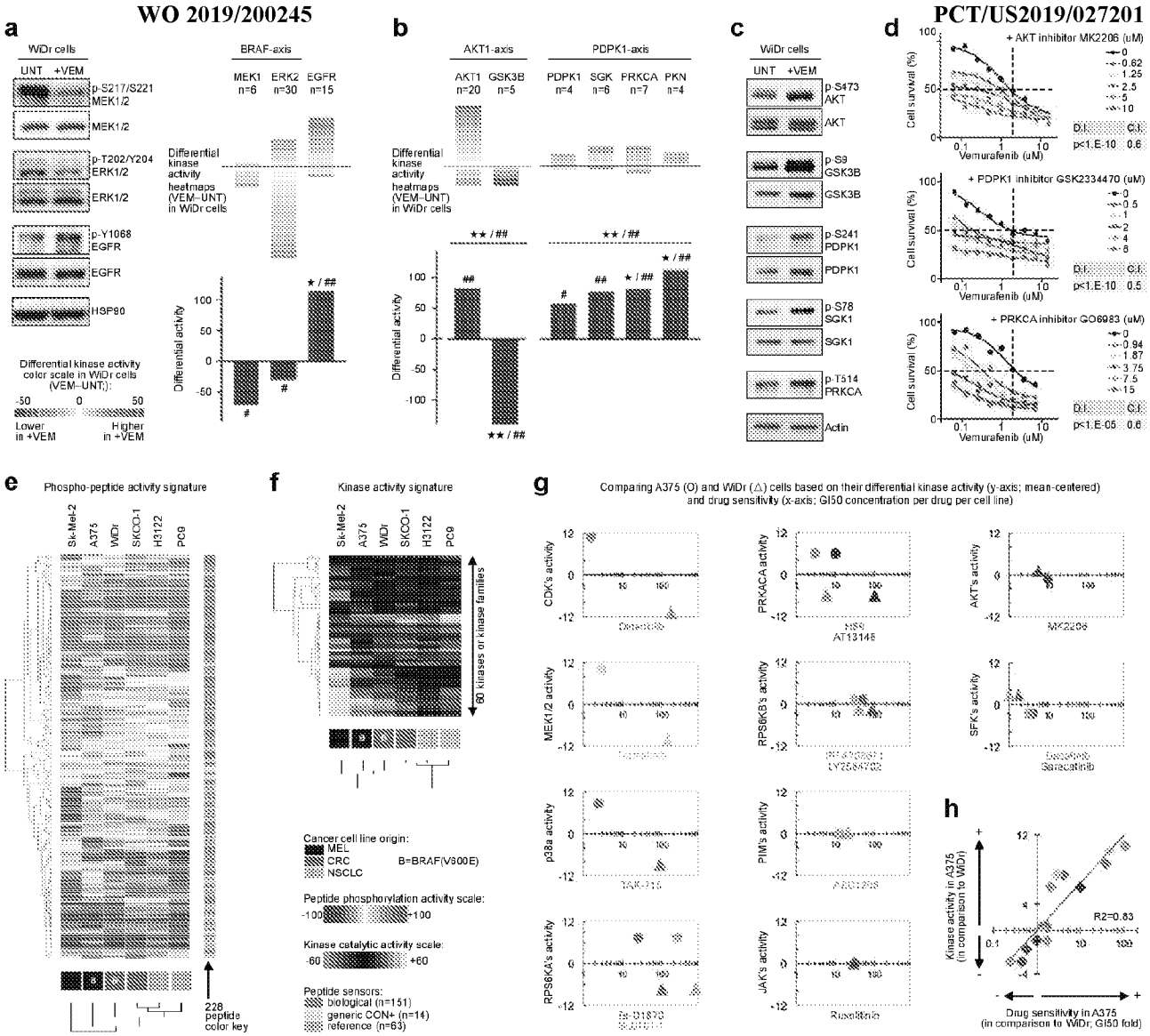

Fig. 2

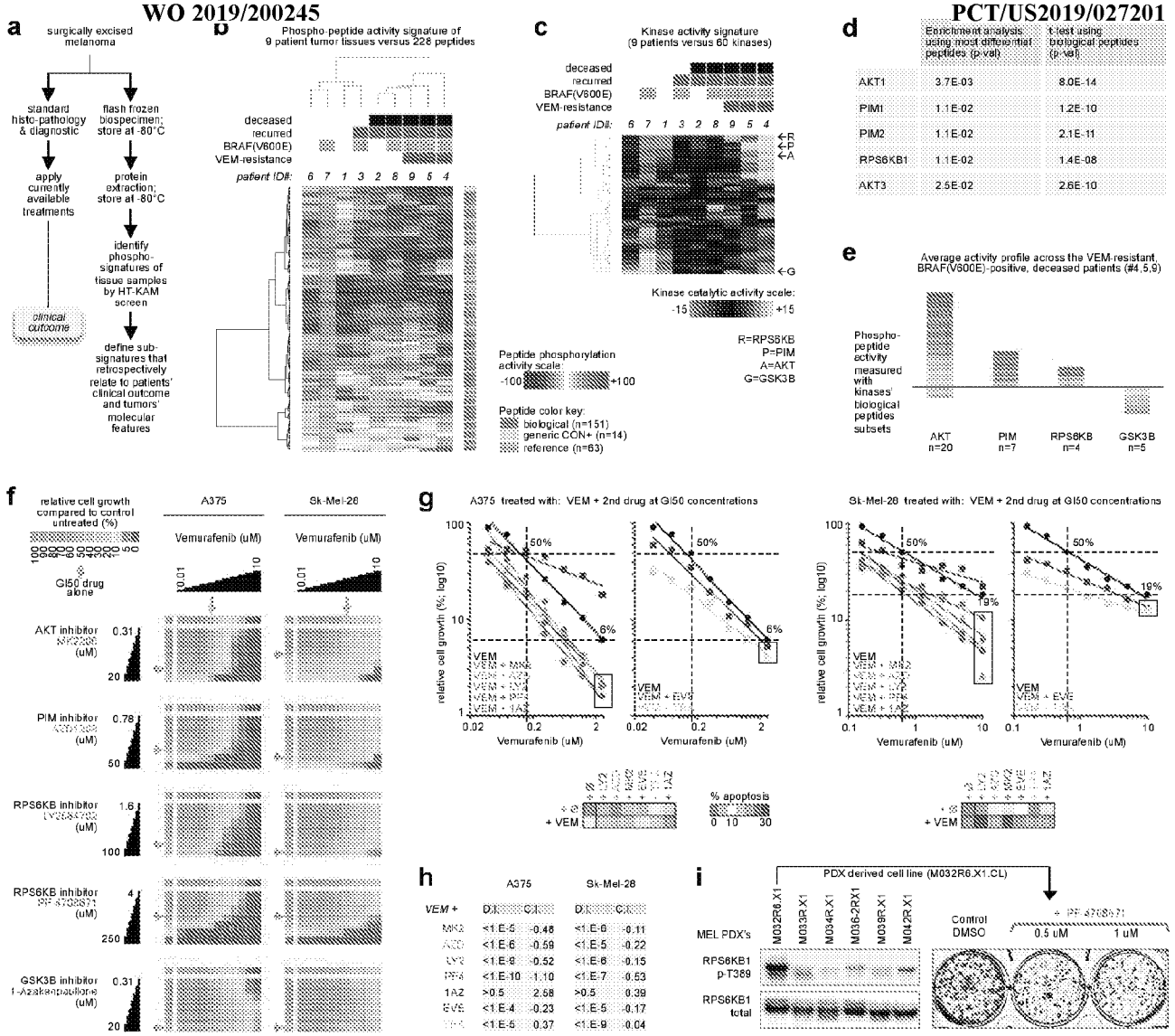
a
surgically excised melanoma
standard histo-pathology & diagnostic
flash frozen biospecimen; store at -80°C
apply currently available treatments
protein extraction; store at -80°C
identify phospho-signatures of tissue samples by HT-KAM screen
clinical outcome
define sub-signatures that retrospectively relate to patients' clinical outcome and tumors' molecular features
b
Phospho-peptide activity signature of 9 patient tumor tissues versus 228 peptides
deceased
recurred
BRAF(V600E)
VEM-resistance
patient ID#: 6 7 1 3 2 8 9 5 4
Peptide phosphorylation activity scale:
-100 +100
Peptide color key:
biological (n=151)
generic CON+ (n=14)
reference (n=63)
c
Kinase activity signature (9 patients versus 60 kinases)
deceased
recurred
BRAF(V600E)
VEM-resistance
patient ID#: 6 7 1 3 2 8 9 5 4
R
P
A
G
Kinase catalytic activity scale:
-15 +15
R=RPS6KB
P=PIM
A=AKT
G=GSK3B
d
Enrichment analysis using most differential peptides (p-val)
t-test using biological peptides (p-val)
AKT1 3.7E-03 8.0E-14
PIM1 1.1E-02 1.2E-10
PIM2 1.1E-02 2.1E-11
RPS6KB1 1.1E-02 1.4E-08
AKT3 2.5E-02 2.6E-10
e
Average activity profile across the VEM-resistant, BRAF(V600E)-positive, deceased patients (#4,5,9)
Phospho-peptide activity measured with kinases' biological peptides subsets
AKT n=20
PIM n=7
RPS6KB n=4
GSK3B n=5
f
relative cell growth compared to control untreated (%)
A375
Sk-Mel-28
Vemurafenib (uM)
GI50 drug alone
AKT inhibitor
PIM inhibitor
RPS6KB inhibitor
RPS6KB inhibitor
GSK3B inhibitor
(uM)
g
A375 treated with: VEM + 2nd drug at GI50 concentrations
Sk-Mel-28 treated with: VEM + 2nd drug at GI50 concentrations
relative cell growth (%; log10)
Vemurafenib (uM)
50%
6%
19%
VEM
% apoptosis
0 10 30
+ VEM
h
A375
Sk-Mel-28
VEM +
D.I.
C.I.
MK2 <1.E-5 -0.48 <1.E-6 -0.11
1AZ >0.5 2.58 >0.5 0.39
EVE <1.E-4 -0.23 <1.E-5 -0.17
<1.E-5 0.37 <1.E-9 0.04
i
PDX derived cell line (M032R6.X1.CL)
M032R6.X1
M033R.X1
M034R.X1
M036-2RX1
M039R.X1
M042R.X1
MEL PDX's
RPS6KB1 p-T389
RPS6KB1 total
Control DMSO
+ PF-4708671
0.5 uM
1 uM

Fig. 3

a

Peptide probe ID	Peptide category: A=biological; B=genetic (standard 'CON-1'), C=mutated biological, D=mutated genetic, E=random; (C+D+E= reference probes)	Origin of peptide probes (i.e. name of biological substrate protein (102 distinct substrate proteins); or description of control peptide); (1' is placed between distinct proteins containing the same sequence; common protein names are between brackets)	Phospho-residue target (151 distinct biological peptide sequences established from 187 different biological substrate target sites, and corresponding to 478 distinct kinase-substrate-residue target sites; or description of control); (1' is placed between distinct residue sites from different proteins; only the phospho-residue location from the main isoform of the protein substrate is indicated)	Kinase enzymes (140 different kinases associated with biological target sites, without counting kinases associated with standard CON-1 generic probes); (1' is placed between distinct protein kinases that target the same protein substrate site; 1' is placed between distinct groups of kinases that target the respective protein substrate sites listed in previous columns)
PA_002	A	FCGR2A	Y304	BLK; FYN; LYN; SYK
PA_001	A	FCGR2B	Y292	BLK; LYN
PA_003	A	KHDRBS1 (SAM68)	Y435	BRK (PTK6)
PA_004	A	BRK (PTK6)	Y342	BRK (PTK6)
PA_006	A	KHDRBS1 (SAM68)	Y440	BRK (PTK6)
PA_007	A	SNCA	Y125	FGR; FYN; LYN; PTK2B (FAK2); SYK
PA_006	A	SRC	Y530	FGR; CSK
PA_005	A	FGR	Y412	FGR
PA_008	A	FOS	S133	FRK
PA_009	A	FOS	T232	FRK
PA_108	A	CBL	Y731	EGFR; FYN; HCK
PA_012	A	FYN / SRC / YES1	Y420 / Y419 / Y426	FYN / SRC / YES1
PA_076	A	GRB10	Y87	FYN; SRC; TEC
PA_033	A	CDK5	Y15	FYN; ABL1; EPHA4
PA_010	A	CDH9A	Y199	FYN
PA_011	A	CTNNB1	Y142	FYN; FGFR2; FGFR3; NTRK1
PA_087	A	GRIN2B	Y1252	FYN
PA_088	A	PSEN	Y363	FYN
PA_015	A	HCK / LCK / LYN	Y411 / Y394 / Y397	HCK / LCK / LYN
PA_106	A	PLCG1	Y771	EGFR; ERBB4; HCK; LYN; SYK
PA_029	A	STAT5	Y705	SRC; HCK; FGFR3; FGFR4; JAK1; JAK2; ALK; FER; RET;
PA_013	A	CSF3R	Y752	HCK
PA_014	A	ELMO1	Y720	HCK
PA_089	A	PLCG1	Y1253	HCK
PA_070	A	RASGEF1	Y594	HCK
PA_107	A	RASA1	Y460	EGFR; ERBB4; LCK
PA_109	A	STAT1	Y701	EGFR; LCK; FGFR4; FDFR4; JAK1; JAK2; JAK3; TYK2; KIT
PA_016	A	DOK1	Y174	LCK
PA_017	A	PRKCD	Y334	LCK
PA_018	A	ZAP70	Y492	LCK
PA_071	A	ITK	Y512	LCK
PA_072	A	PIK3R1 (GRB1)	Y688	LCK
PA_019	A	CDKN1B (p27, KIP1)	Y88	LYN, ABL1
PA_020	A	PRKCD	Y64	LYN
PA_073	A	SYK	Y131	LYN, STK
PA_021	A	ABL1	Y239	SRC, ABL1
PA_028	A	RAF1 (CRAF)	Y341	SRC; JAK2
PA_075	A	GTF2I	Y248	SRC; JAK2, BTK
PA_022	A	AKT1	Y326	SRC
PA_023	A	BCAR1	Y234	SRC
PA_024	A	GRB2	Y160	SRC; ALK
PA_025	A	EGFR	Y944	SRC
PA_026	A	AFAP1	Y94	SRC
PA_027	A	TERT	Y707	SRC
PA_074	A	FGFR3	Y773	SRC
PA_146	A	EGFR	Y869	SRC
PA_168	A	AKT1	Y315	SRC; RET
PA_030	A	CD46	Y344	YES1
PA_086	A	JAK2	Y1007	ABL1; JAK2
PA_031	A	MDM2	Y394	ABL1
PA_032	A	BTK	Y223	ABL1; BTK; ITK; TEC
PA_085	A	MAP4K1	Y252	ABL1
PA_087	A	JUN	Y170	ABL1
PA_088	A	RAD51	Y54	ABL1
PA_089	A	TP73	Y99	ABL1
PA_090	A	WASL	Y256	ABL1; PTK2 (FAK1); TNK2 (ACK1)
PA_120	A	ERBB2	Y1248	EGFR; ERBB2
PA_122	A	STAT5A / STAT5B	Y694 / Y699	ERBB4; JAK2; JAK3; BTK; SYK / EGFR; JAK2
PA_121	A	EGFR	Y1197	EGFR; ERBB4
PA_144	A	EGFR	Y1068	EGFR; JAK2
PA_110	A	GAB1	Y627	EGFR; MET; INSR
PA_111	A	GAB1	Y472	EGFR; MET; INSR
PA_112	A	MUC1	Y1229	EGFR; ZAP70
PA_113	A	PLCG1	Y472	EGFR
PA_114	A	STAT3B	Y740	EGFR
PA_115	A	CBL	Y774	EGFR; SYK
PA_116	A	PKIA	Y9	EGFR
PA_117	A	ERBB2	Y1023	ERBB2
PA_123	A	ABI1	Y213	ERBB4
PA_124	A	BCAR1	Y864	ERBB4; PTK2 (FAK1)
PA_125	A	CDK6	Y24	ERBB4;
PA_126	A	NFKBIA (IKBA)	Y305	ERBB4
PA_127	A	SYK	Y525	ERBB4; SYK
PA_116	A	PABPC1	Y54	
PA_119	A	TEK (TIE2)	Y1048	ERBB4
PA_153	A	RAF1 (CRAF)	Y340	JAK2
PA_175	A	JAK2	Y1008	JAK2
PA_200	A	FOXO3 / FOXO1	T32 / T24	AKT1; AKT2; SGK (SGK1); PIM1 / AKT1 ; AKT2; SGK (SGK1)
PA_182	A	GSK3B	S9	AKT1; AKT3; AURKA; MAPK6; PRKACA; PRKCA; PRKCB; PRKCD; PRKCG; PRKCH; RPS6KA1 (RSK1); RPS6KA3 (RSK2); RPS6KB1 (S6K p70S6K alpha); RPS6KB2 (S6K2 p70 S6K beta); SGK1 (SGK3);
PA_189	A	BAD	S75	AKT1; AKT3; PIM1; PIM2; PIM3; PKN2; RPS6KA1 (RSK1); RPS6KA2 (RSK3); RPS6KA3 (RSK2); PLK1; PIK2; PAK4; PAK7 (PAK5); ARAF; BRAF; RAF1 (CRAF); PRKACA; PRKCE; PRKCG; PRKCD; PRKD1
PA_189	A	BAD	S99	AKT1; AKT3; PIM1; PIM2; PIM3; PAK1; RPS6KA1 (RSK1); RPS6KA3 (RSK2); RPS6KB1 (S6K p70S6K alpha); ARAF; BRAF; RAF1 (CRAF); PRKACA; PRKCE; PRKCD; PRKD1
PA_201	A	MTOR (FRAP1)	S2448	AKT1; AKT3; RPS6KB1 (S6K p70 S6K alpha); RPS6KB2 (S6K2 p70 S6K beta)
PA_202	A	MTOR (FRAP1)	T2446	AKT1; AKT3; RPS6KB1 (S6K p70 S6K alpha)
PA_187	A	EIF4EBP1 (4EBP1)	S65	AKT1; MAPK1 (ERK2);MAPK14 (p38a); MTOR (FRAP1); RPS6KA5 (MSK1); DYRK2
PA_158	A	EIF4EBP1 (4EBP1)	T37	AKT1; MAPK1 (ERK2);MAPK14 (p38a); MTOR (FRAP1); GSK3B
PA_152	A	RAF1 (CRAF)	S259	AKT1; PRKACA; RAF1 (CRAF)
PA_157	A	BRAF	S365	AKT1; SGK (SGK1)
PA_183	A	GSK3A	S21	AKT1; KDR; PRKACA; PRKCA; PRKCB; PRKCD; PRKCG; PRKCH; PRKD3; RPS6KB2 (S6K2); SGK (SGK1); SGK1 (SGK3)
PA_191	A	BRCA1	T509	AKT1
PA_193	A	CDKN1A (p21; WAF1; CIP1)	S146	AKT1; PIM1; PIM2; PRKCA; NUAK1; LATS2
PA_194	A	CDKN1A (p21; WAF1; CIP1)	T145	AKT1; DAPK3 (ZIPK); PIM1; PIM2
PA_185	A	CHEK1	S280	AKT1
PA_196	A	CREB1 / CREM	S133 / S108	AKT1; ATM; CAMK1; CAMK2D; CAMK2G; CAMK4; CDK1; MAPK6; MAPKAPK2; PRKACA; PRKCA; PRKCE; PRKD1; PRKCD (PKC); RPS6KA1 (RSK1); RPS6KA2 (RSK3); RPS6KA3 (RSK2); RPS6KA4 (MSK2); RPS6KA5 (MSK1); SGK (SGK1); TSSK4 / CAMK2D; CAMK2G; CDK1; PRKACA; PRKCA
PA_199	A	FOXO3	S253	AKT1; MAPKAPK5; PIM1; SGK1
PA_205	A	GABZ	S159	AKT1
PA_211	A	MDM2	S166	AKT1; CSNK1D; DAPK3 (ZIPK); MAPKAPK2; PIM1; SGK1
PA_219	A	PTEN	S380	AKT1; CSNK2A1; PLK1; PRKCZ; SGK1; STK11
PA_163	A	MAPK1 (ERK2) / MAPK3 (ERK1)	Y187 / Y204	MAPK1 (ERK2); MAPK3 (ERK1); MAP3K1 (MEK1); MAP2K2 (MEK2); RET / MAPK3 (ERK1); MAP2K1 (MEK1); MAP2K2 (MEK2); RET
PA_164	A	MAPK1 (ERK2) / MAPK3 (ERK1)	T185 / T202	MAPK1 (ERK2); MAP2K1 (MEK1); MAP2K2 (MEK2) / MAPK3 (ERK1); MAP2K1 (MEK1),MAP2K2 (MEK2)
PA_172	A	SP1	T739	MAPK1 (ERK2); MAPK3 (ERK1); MAPK8 (JNK1); CDK1
PA_173	A	SP1	T453	MAPK1 (ERK2); MAPK3 (ERK1)
PA_179	A	CASP9	T125	MAPK1 (ERK2); MAPK3 (ERK1); MAP3K1 (MEK1); MAP2K2 (MEK2); CDK1
PA_181	A	STAT3	S727	MAPK1 (ERK2); MAPK3 (ERK1); MAPK8 (JNK1); MAPK9 (JNK2); CDK5; DAPK3 (ZIPK); DYRK2; INAK1; NEK6; NLK; PRKCD; PRKCE; RPS6KA3 (RSK2); RPS6KA5 (MSK1)
PA_203	A	GAB1	T312	MAPK1 (ERK2); MAPK3 (ERK1)
PA_204	A	GAB1	T476	MAPK1 (ERK2); MAPK3 (ERK1)
PA_206	A	GAB2	S623	MAPK1 (ERK2); MAPK3 (ERK1)
PA_209	A	LCK	S59	MAPK1 (ERK2); MAPK3 (ERK1)
PA_210	A	PPARA	S12	MAPK1 (ERK2); MAPK3 (ERK1)
PA_217	A	PPARA	S21	MAPK1 (ERK2); MAPK3 (ERK1)
PA_148	A	SMAD2	S250	MAPK1 (ERK2)
PA_149	A	SMAD2	S245	MAPK1 (ERK2)
PA_150	A	SMAD2	T220	MAPK1 (ERK2)
PA_154	A	RAF1 (CRAF)	S289	MAPK1 (ERK2)
PA_155	A	RAF1 (CRAF)	S296	MAPK1 (ERK2)
PA_161	A	MAP2K1 (MEK1)	T292	MAPK1 (ERK2); RAF1 (CRAF); CDK1
PA_177	A	DUSP1	S359	MAPK1 (ERK2)
PA_207	A	GRB10	S150	MAPK1 (ERK2); MTOR (FRAP1)
PA_208	A	GRB10	S476	MAPK1 (ERK2); MTOR (FRAP1)
PA_210	A	MLL1	T163	MAPK1 (ERK2); MAPK9 (JNK1); GSK3A; GSK3B
PA_215	A	PAK1	T212	MAPK1 (ERK2); CDK5
PA_218	A	PPARG	S112	MAPK1 (ERK2); MAPK8 (JNK1); CDK9
PA_222	A	SOS1	S1132	MAPK1 (ERK2)
PA_223	A	SOS1	S1193	MAPK1 (ERK2)
PA_224	A	TP53	S15	MAPK1 (ERK2); ATM; ATR; CHEK1; CHEK2; PRKDC (DNAPK); CDK8; DYRK1A; NUAK1; PRKAA1 (AMPK); SMG1; STK11; TP53RK (PRPK)
PA_225	A	TP53	T55	MAPK1 (ERK2); GRK5; TAF1
PA_179	A	CDC25C	S216	MAPK14 (p38a); CHEK1; CHEK2; BRSK1; BRSK2; MARK3; PKN1; PLK3
PA_180	A	JUN / JUNB	T91 / T102	MAPK14 (p38a); MAPK8 (JNK1); MAPK9 (JNK2) / MAPK8 (JNK1)
PA_188	A	ATF2 (CREB2)	T71	MAPK14 (p38a); MAPK8 (JNK1); MAPK9 (JNK2); MAPK11 (p38b2); MAPK12 (p38g); PLK3
PA_220	A	RPS6KA4 (MSK2)	T568	MAPK14 (p38a); MAP3K1 (MEK1)
PA_221	A	RPS6KA4 (MSK2)	S343	MAPK14 (p38a); MAP3K1 (MEK1)
PA_226	A	TP53	S392	MAPK14 (p38a); CDK2; CDK7; CDK9; CSNK2A1; EIF2AK2; NUAK1; STK11
PA_151	A	SMAD2	T8	MAPK3 (ERK1)

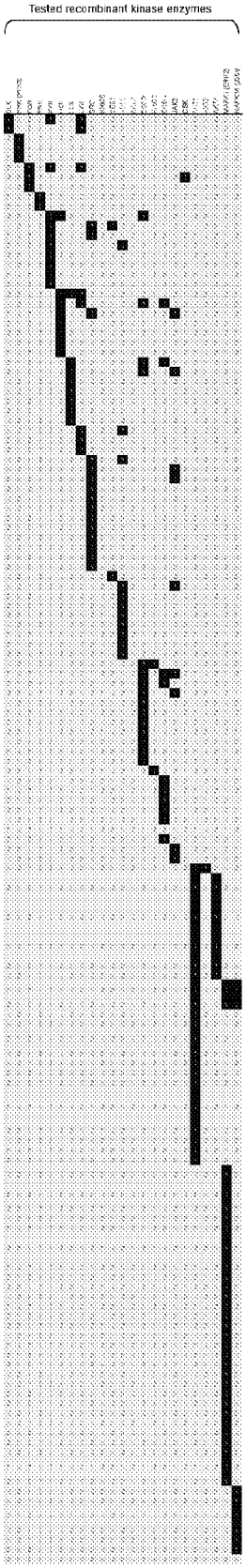

Fig. 4 (part 1)

Peptide probe ID	Peptide category: A=biological; B=generic (standard 'CON-'); C=mutated biological; D=mutated generic; E=random; (C+D+E= 'reference' probes)	Origin of peptide probes (i.e. name of biological substrate protein (102 distinct substrate proteins); or description of control peptide); (* is placed between distinct proteins containing the same sequence; common protein names are between brackets)	Phospho-residue target (151 distinct biological peptide sequences associated from 147 different biological substrate target sites, and corresponding to 418 distinct kinase-substrate+residue target site; or description of controls); (* is placed between distinct residue sites from different proteins; only the phospho-residue location from the main isoform of the protein substrate is indicated)	Kinase enzymes (149 different kinases associated with biological target sites, without counting kinases associated with standard CON+generic probes); (* is placed between distinct protein kinases that target the same protein substrate site; * is placed between distinct groups of kinases that target the respective protein substrate sites listed in pre-ious columns)
PA_145	A	EGFR	T678	PRKCA; PRKCD; PRKD1 (PKD); PKN1, PKN3
PA_147	A	SMAD2	S465	TGFBR1; ACVR1B; BMPR1B
PA_156	A	RAF1 (CRAF)	S338	MAPK3K1 (MEK1); PAK1; PAK2; PAK3; PAK7 (PAK5); RAF1 (CRAF)
PA_158	A	MAP2K1 (MEK1) / MAP2K2 (MEK2)	S218 / S222	ARAF; BRAF; RAF1 (CRAF); MAP3K1 (MEKK1); MAP3K8 (COT) / BRAF; MAP3K8 (COT)
PA_159	A	MAP2K1 (MEK1) / MAP2K2 (MEK2)	S222 / S226	ARAF; BRAF; RAF1 (CRAF); MAP3K1 (MEKK1); MAP3K8 (COT); PDPK1 / BRAF; MAP3K8 (COT); PDPK1
PA_160	A	MAP2K1 (MEK1)	T386	RAF1 (CRAF); CDK1; CDK5
PA_162	A	MAP2K1 (MEK1)	S298	PAK1
PA_165	A	MAPK1 (ERK2)	S29	RAF1 (CRAF)
PA_166	A	AKT1 / AKT2 / AKT3	S473 / S474 / S472	IKBKE; TBK1; ILK; LRRK2; MAPKAPK2; MTOR; PRKDC (DNAPK); PDK1; PDPK1; PRKCA; PRKCB; PRKCD; PRKD1 (PKD); PIKFYVE (PIKfyve); PDPK1 / PRKCD; PRKCZ
PA_167	A	AKT1 / AKT2 / AKT3	T308 / T309 / T305	IKBKE; TBK1; CAMKK1; PDK1; PDPK1; PRKDA; PRKCD; PRKCZ; PRKD1 (PKD) / PDPK1 / PDPK1; PRKCZ
PA_169	A	CDC25C	T48	CDK1 (CDC2)
PA_171	A	CDC25C	S214	CDK1 (CDC2)
PA_174	A	SRC	S17	PRKACA
PA_175	A	JAK1	Y1034	JAK3; JAK1
PA_176	A	JAK1	Y1035	JAK3; JAK1
PA_182	A	ERK5A1	S386	CHEK2
PA_212	A	MYC	T58	GSK3B; CSNK2A1; CSNK2A2
PA_213	A	NFKB1	S907	GSK3B
PA_214	A	NOTCH2	S2070	GSK3B
PA_040	B	generic pept. probe _ CON (+) #01	_ (YVGEFPKKKAA)	all TKs (>96 Tyrosine Kinases)
PA_241	B	generic pept. probe _ CON (+) #02	_ (EEEEY)~46	all TKs (>96 Tyrosine Kinases)
PA_084	B	generic pept. probe _ CON (+) #03	_ (KVVVGVTGEGIKEVK)	all 11 SFKs (BLK; BRK; FRK; FGR; FYN; HCK; LCK; LYNA/B; SRC; SRMS; YES1)
PA_249	B	generic pept. probe _ CON (+) #04 (seq derived from CDK1)	_ (KVEKIGEGTYGVVYK-amid)	all 11 SFKs (BLK; BRK; FRK; FGR; FYN; HCK; LCK; LYNA/B; SRC; SRMS; YES1)
PA_093	B	generic pept. probe _ CON (+) #05	_ (EGIVGVL)	6 SFKs (FYN; HCK; LCK; LYNA/B; SRC)
PA_097	B	generic pept. probe _ CON (+) #06	_ (EFRIYDFLPAKKK)	2 SFKs (LYNB; SRMS); 10 EPHs (EphA1; EphA2; EphA3; EphA4; EphA5; EphB1; EphB2; EphB3; EphB4); 5 RTKs (PDGFRB; MERTK; NTRK2; NTRK3; TYR(Q3)); 4 NRTKs (FES; ITK; PTK2B; TXK)
PA_095	B	generic pept. probe _ CON (+) #07	_ (EAIYAAP)	all 2 ABLs and 3 ABL mutants (ABL1; ABL2; ABL1(Q252H); ABL1(T315I); ABL1(I1499F)); 4 RTKs and 1 RTK mutant (FLT3; KIT; MET; RET; FLT3(D835Y)); 1 NRTK (BTK)
PA_096	B	generic pept. probe _ CON (+) #08	_ (EAIYAAPFAKKK)	all 2 ABLs (ABL1, ABL2)
PA_242	B	generic pept. probe _ CON (+) #09 (seq derived from ABL1)	_ (EAIYAAPFAK)	all 2 ABLs (ABL1, ABL2)
PA_099	B	generic pept. probe _ CON (+) #10	_ (EPLYWSFPA)	EGFR; 3 FGFRs and 1 FGFR mutant (FGFR2; FGFR3; FGFR4; FGFR2(N549H)); 2 RTKs (PDGFRA; VEGFR2); 2 NRTKs (FER; SYK)
PA_184	B	generic pept. probe _ CON (+) #11	_ (KRPRAASFAE)	all 3 AKTs (AKT1; AKT2; AKT3)
PA_185	B	generic pept. probe _ CON (+) #12	_ (RPRAATPFE)	all 3 AKTs (AKT1; AKT2; AKT3); SGK1
PA_186	B	generic pept. probe _ CON (+) #13	_ (PRTSSFAE)	all 3 AKTs (AKT1; AKT2; AKT3); SGK1; RPS6KA5
PA_187	B	generic pept. probe _ CON (+) #14	_ (IPTSPITTTYF)	6 MAPKs (MAPK1/ERK2; MAPK3/ERK1; MAPK11/p38β; MAPK12/p38γ; MAPK13/p38δ; MAPK14/p38α); CDK8; IRAK4
PA_041	C	SRC _ PA_506 CON (-) _ Y to G	Y530 _ Y to G	FGR; CSK
PA_042	C	SRC _ PA_506 CON (-) _ Y to pY	Y530 _ Y to pY	FGR; CSK
PA_039	C	FYN / SRC / YES1 _ PA_012 CON (-) _ Y to G	Y420 / V419 / V426 _ Y to G	FYN / SRC / YES1
PA_040	C	FYN / SRC / YES1 _ PA_012 CON (-) _ Y to pY	Y420 / Y419 / Y426 _ Y to pY	FYN / SRC / YES1
PA_079	C	GRB10 _ PA_074 CON (-) _ Y to G	Y67 _ Y to G	FYN; SRC; TEC
PA_083	C	GRB10 _ PA_074 CON (-) _ Y to pY	Y67 _ Y to pY	FYN; SRC; TEC
PA_077	C	GRIN2B _ PA_067 CON (-) _ Y to G	Y1252 _ Y to G	FYN
PA_081	C	GRIN2B _ PA_067 CON (-) _ Y to pY	Y1252 _ Y to pY	FYN
PA_043	C	STAT3 _ PA_029 CON (-) _ Y to G	Y705 _ Y to G	SRC; HCK; FGFR3; FGFR4; JAK1; JAK2; ALK; FER; RET;
PA_044	C	STAT3 _ PA_029 CON (-) _ Y to pY	Y705 _ Y to pY	SRC; HCK; FGFR3; FGFR4; JAK1; JAK2; ALK; FER; RET;
PA_129	C	STAT1 _ PA_156 CON (-) _ Y to G	Y701 _ Y to G	EGFR; LCK; FGFR4; FGFR4; JAK1; JAK2; JAK3; TYK2; KIT
PA_130	C	STAT1 _ PA_156 CON (-) _ Y to pY	Y701 _ Y to pY	EGFR; LCK; FGFR4; FGFR4; JAK1; JAK2; JAK3; TYK2; KIT
PA_075	C	PIK3R1 (GRB1) _ PA_372 CON (-) _ Y to G	Y688 _ Y to G	LCK
PA_082	C	PIK3R1 (GRB1) _ PA_372 CON (-) _ Y to pY	Y688 _ Y to pY	LCK
PA_069	C	SYK _ PA_073 CON (-) _ Y to G	Y131 _ Y to G	LYN; SYK
PA_084	C	SYK _ PA_073 CON (-) _ Y to pY	Y131 _ Y to pY	LYN; SYK
PA_045	C	ABL1 _ PA_021 CON (-) _ Y to G	Y226 _ Y to G	SRC; ABL1
PA_046	C	ABL1 _ PA_021 CON (-) _ Y to pY	Y226 _ Y to pY	SRC; ABL1
PA_047	C	EGFR _ PA_025 CON (-) _ Y to G	Y944 _ Y to G	SRC
PA_048	C	EGFR _ PA_025 CON (-) _ Y to pY	Y944 _ Y to pY	SRC
PA_227	C	EGFR _ PA_148 CON (-) _ Y to pY	Y869 _ Y to pY	SRC
PA_228	C	EGFR _ PA_148 CON (-) _ Y to G	Y869 _ Y to G	SRC
PA_091	C	RAD51 _ PA_066 CON (-) _ Y to G	Y54 _ Y to G	ABL1
PA_092	C	RAD51 _ PA_066 CON (-) _ Y to pY	Y54 _ Y to pY	ABL1
PA_129	C	GAB1 _ PA_118 CON (-) _ Y to G	Y627 _ Y to G	EGFR; MET; INSR
PA_130	C	PLCG1 _ PA_113 CON (-) _ Y to G	Y472 _ Y to G	EGFR
PA_137	C	GAB1 _ PA_118 CON (-) _ Y to pY	Y627 _ Y to pY	EGFR; MET; INSR
PA_138	C	PLCG1 _ PA_113 CON (-) _ Y to pY	Y472 _ Y to pY	EGFR
PA_131	C	ERBB2 _ PA_117 CON (-) _ Y to G	Y1023 _ Y to G	ERBB2
PA_139	C	ERBB2 _ PA_117 CON (-) _ Y to pY	Y1023 _ Y to pY	ERBB2
PA_154	C	BCAR1 _ PA_124 CON (-) _ Y to G	Y864 _ Y to G	ERBB4; PTK2 (FAK1)
PA_155	C	NFKBIA (IKBA) _ PA_126 CON (-) _ Y to G	Y305 _ Y to G	ERBB4
PA_142	C	BCAR1 _ PA_124 CON (-) _ Y to pY	Y864 _ Y to pY	ERBB4; PTK2 (FAK1)
PA_143	C	NFKBIA (IKBA) _ PA_126 CON (-) _ Y to pY	Y305 _ Y to pY	ERBB4
PA_132	C	PABPC1 _ PA_115 CON (-) _ Y to G	Y34 _ Y to G	
PA_140	C	PABPC1 _ PA_115 CON (-) _ Y to pY	Y34 _ Y to pY	
PA_133	C	TEK (TIE2) _ PA_119 CON (-) _ Y to G	Y1046 _ Y to G	ERBB4
PA_141	C	TEK (TIE2) _ PA_119 CON (-) _ Y to pY	Y1046 _ Y to pY	ERBB4
PA_252	C	GSK3B _ PA_162 CON (-) _ S to pS	S9 _ S to pS	AKT1; AKT3; AURKA; MAPKAPK5; PRKACA; PRKCB; PRKCD; PRKCG; PRKCH; RPS6KA1 (RSK1); RPS6KA3 (RSK3); RPS6KB1 (S6K; p70S6K-alpha); RPS6KB2 (S6K2; p70S6K-beta); SGK1 (SGK3);
PA_253	C	BAD _ PA_160 CON (-) _ S/S to pS/pS	S99 _ S/S to pS/pS	AKT1; AKT3; PIM1; PIM2; PIM3; PAK1; RPS6KA1 (RSK1); RPS6KA3 (RSK3); RPS6KB1 (S6K; p70S6K-alpha); ARAF; BRAF; RAF1 (CRAF); PRKACA; PRKCE; PRKCI; PRKCG; PRKD1
PA_234	C	MTOR (FRAP1) _ PA_102 CON (-) _ T/S to pT/pS	T2446 (& S2448) _ T/S to pT/pS	AKT1; AKT3; RPS6KB1 (S6K; p70 S6K-alpha); RPS6KB2 (S6K2; p70 S6K-beta)
PA_237	C	MDM2 _ PA_211 CON (-) _ S/T to pS/pT	S166 _ S/T to pS/pT	AKT1; CSNK1D; DAPK3 (ZIPK); MAPKAPK2; PIM1; SGK1
PA_238	C	MDM2 _ PA_211 CON (-) _ S/T to S/T	S166 _ S/T to S/T	AKT1; CSNK1D; DAPK3 (ZIPK); MAPKAPK2; PIM1; SGK1
PA_229	C	MAPK1 (ERK2) / MAPK3 (ERK1) _ PA_163 CON (-) _ T/Y to pT/pY	Y187 / Y204 (& T185 / T202) _ T/Y to pT/pY	MAPK1 (ERK2); MAPK3 (ERK1); MAP3K1 (MEK1); MAP2K2 (MEK2); RET / MAPK3 (ERK1); MAP2K1 (MEK1); MAP2K2 (MEK2); RET
PA_230	C	MAPK1 (ERK2) / MAPK3 (ERK1) _ PA_163 CON (-) _ T/Y to S/S	Y187 / Y204 (& T185 / T202) _ T/Y to S/S	MAPK1 (ERK2); MAPK3 (ERK1); MAP3K1 (MEK1); MAP2K2 (MEK2); RET / MAPK3 (ERK1); MAP2K1 (MEK1); MAP2K2 (MEK2); RET
PA_231	C	MAPK1 (ERK2) / MAPK3 (ERK1) _ PA_164 CON (-) _ T to pT	T185 / T202 _ T to pT	MAPK1 (ERK2); MAP2K1 (MEK1); MAP2K2 (MEK2) / MAPK3 (ERK1); MAP2K1 (MEK1); MAP2K2 (MEK2)
PA_235	C	LCK _ PA_209 CON (-) _ S to pS	S59 _ S to pS	MAPK1 (ERK2); MAPK3 (ERK1)
PA_236	C	LCK _ PA_209 CON (-) _ S to S	S59 _ S to S	MAPK1 (ERK2); MAPK3 (ERK1)
PA_239	C	PAK1 _ PA_215 CON (-) _ T/T to pT/pT	T212 _ T/T to pT/pT	MAPK1 (ERK2); CDK5
PA_051	D	generic pept. probe _ PA_049 CON (-) _ Y to T	_	all TKs (>96 Tyrosine Kinases)
PA_055	D	generic pept. probe _ PA_049 CON (-) _ Y to G	_	all TKs (>96 Tyrosine Kinases)
PA_057	D	generic pept. probe _ PA_049 CON (-) _ (level seq /technical control _ Y to pY	_	all TKs (>96 Tyrosine Kinases)
PA_100	D	generic pept. probe _ PA_095 CON (-) _ Y to G	_	5 SFKs (FYN; HCK; LCK; LYNA/B; SRC)
PA_103	D	generic pept. probe _ PA_095 CON (-) _ Y to pY	_	5 SFKs (FYN; HCK; LCK; LYNA/B; SRC)
PA_101	D	generic pept. probe _ PA_095 CON (-) _ Y to G	_	all 2 ABLs and 3 ABL mutants (ABL1; ABL2; ABL1(Q252H); ABL1(T315I); ABL1(I1499F)); 4 RTKs and 1 RTK mutant (FLT3; KIT; MET; RET; FLT3(D835Y)); 1 NRTK (BTK)
PA_104	D	generic pept. probe _ PA_095 CON (-) _ Y to pY	_	all 2 ABLs and 3 ABL mutants (ABL1; ABL2; ABL1(Q252H); ABL1(T315I); ABL1(I1499F)); 4 RTKs and 1 RTK mutant (FLT3; KIT; MET; RET; FLT3(D835Y)); 1 NRTK (BTK)
PA_102	D	generic pept. probe _ PA_099 CON (-) _ Y to G	_	EGFR; 3 FGFRs and 1 FGFR mutant (FGFR2; FGFR3; FGFR4; FGFR2(N549H)); 2 RTKs (PDGFRA; VEGFR2); 2 NRTKs (FER; SYK)
PA_105	D	generic pept. probe _ PA_099 CON (-) _ Y to pY	_	EGFR; 3 FGFRs and 1 FGFR mutant (FGFR2; FGFR3; FGFR4; FGFR2(N549H)); 2 RTKs (PDGFRA; VEGFR2); 2 NRTKs (FER; SYK)
PA_034	E	(control) CON (-) _ poly A	_	-
PA_035	E	(control) CON (-) _ poly A _ Y to pY	_	
PA_056	E	(control) CON (-) _ poly G	_	.
PA_037	E	(control) CON (-) _ poly G _ Y to pY	_	-
PA_038	E	(control) CON (-) _ poly E	_	-

Biological peptides (continued)

Generic peptides

Reference peptides

Fig. 4

(part 2)

b

Peptide category | Peptide code | Relationship between peptides and tested recombinant kinase enzymes

A	Biological peptide identified from a substrate residue location phosphorylated by the indicated kinase (i.e. PhosphoAtlas database)	Biological peptides (n=151)
A	Biological peptide not anticipated to be targeted by the indicated kinase	
B	Generic peptide (homemade or commercial or standard) specifically targeted by the indicated kinase	Generic peptides (n=14)
B	Generic peptide not predicted to be targeted by the indicated kinase	
C	Mutated biological peptide originally anticipated to be targeted by the indicated kinase	Reference peptides (n=63)
C	Mutated biological peptide originally not anticipated to be targeted by the indicated kinase	
D	Mutated generic peptide originally predicted to be targeted by the indicated kinase	
D	Mutated generic peptide originally not predicted to be targeted by the indicated kinase	
E	Random peptide sequences (n=5)	

c

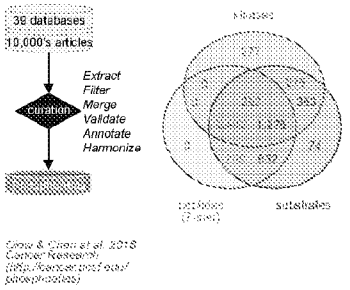

Gray & Chen et al. 2018 Cancer Research (http://cancerres.aacrjournals.org/phosphoatlas)

d

Biological peptides available in PhosphoAtlas with the potential to be used for kinase activity assays:

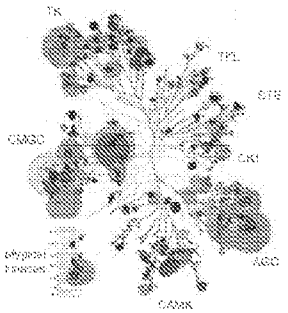

Number of different peptide sequences: **2,452**
Average % of unique peptide set per kinase: **50.81%**

Generic positive control peptides publicly available and commonly used for kinase activity assays:

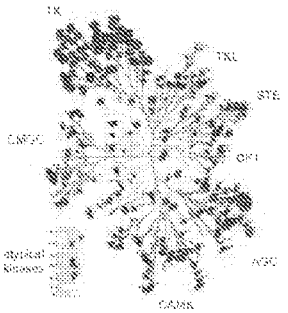

Number of different peptide sequences: **162**
Average % of unique* peptide set per kinase: **0.03%**

Kinome-tree** legend:

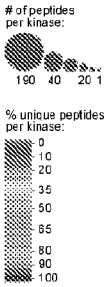

* *uniqueness of generic positive control peptides is defined for 399 kinases as advertised/published by manufacturers.*

** *kinome-trees represent the phylogenic tree for the 518 human kinases defined in Manning G. 2002 Science.*

Illustration reproduced courtesy of Cell Signaling Technology, Inc. (www.cellsignal.com)

e

Descriptive characteristics of the 151 biological peptides included in the peptide probe library

Biological peptides are established from 102 distinct biological substrate proteins

Biological peptides are established from 167 different biological substrate residue target locations

Biological peptides are established from biological substrate residue target locations phosphorylated by 149 distinct kinases

Biological peptides relate to 479 unique phospho-catalytic dyads (i.e. kinase-substrate-residue)

f

Organization/content of each 384-well kinase assay plate

151 wells, each containing a different biological peptide + kinase assay buffer + ATP (100µM) + recombinant kinase or cell extract or tissue homogenate; additional subset of duplicated wells; randomly assigned location	Section 1
14 wells, each containing a different generic peptide + kinase assay buffer + ATP (100µM) + recombinant kinase or cell extract or tissue extract; additional subset of duplicated wells; randomly assigned location	
63 wells, each containing a different reference peptide + kinase assay buffer + ATP (100µM) + recombinant kinase or cell extract or tissue extract; additional subset of duplicated wells; randomly assigned location	
16 wells containing kinase assay buffer + ATP (100µM) + recombinant kinase or cell extract or tissue extract (i.e. without peptide); randomly assigned location	
16 wells containing kinase assay buffer + ATP (100µM) (i.e. without peptide, without sample)	Section 2
16 wells containing kinase assay buffer alone (i.e. without peptide, without sample, without ATP)	
32 wells containing ATP serial dilution in kinase assay buffer (each concentration tested in duplicate); to establish ATP standard curve to identify the ATP consumption (i.e. kinase activity)	

note 1: the organization and well content of each 384-well plate is identical across all experimental plates
note 2: samples (i.e. recombinant kinase or cell extract) may additionally contain inhibitor

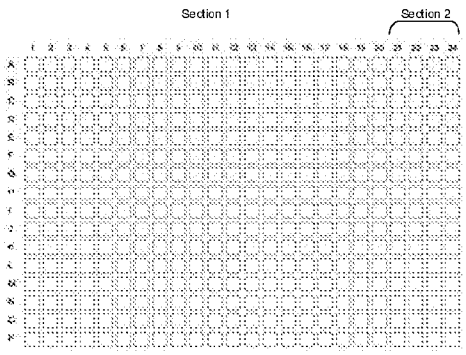

Semi-automated liquid dispensing (Biomek FX)

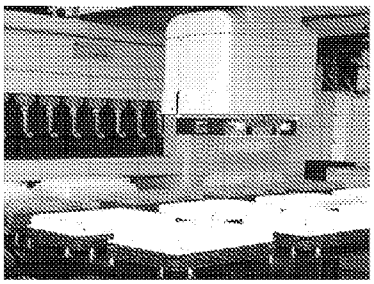

Fig. 4

(part 3)

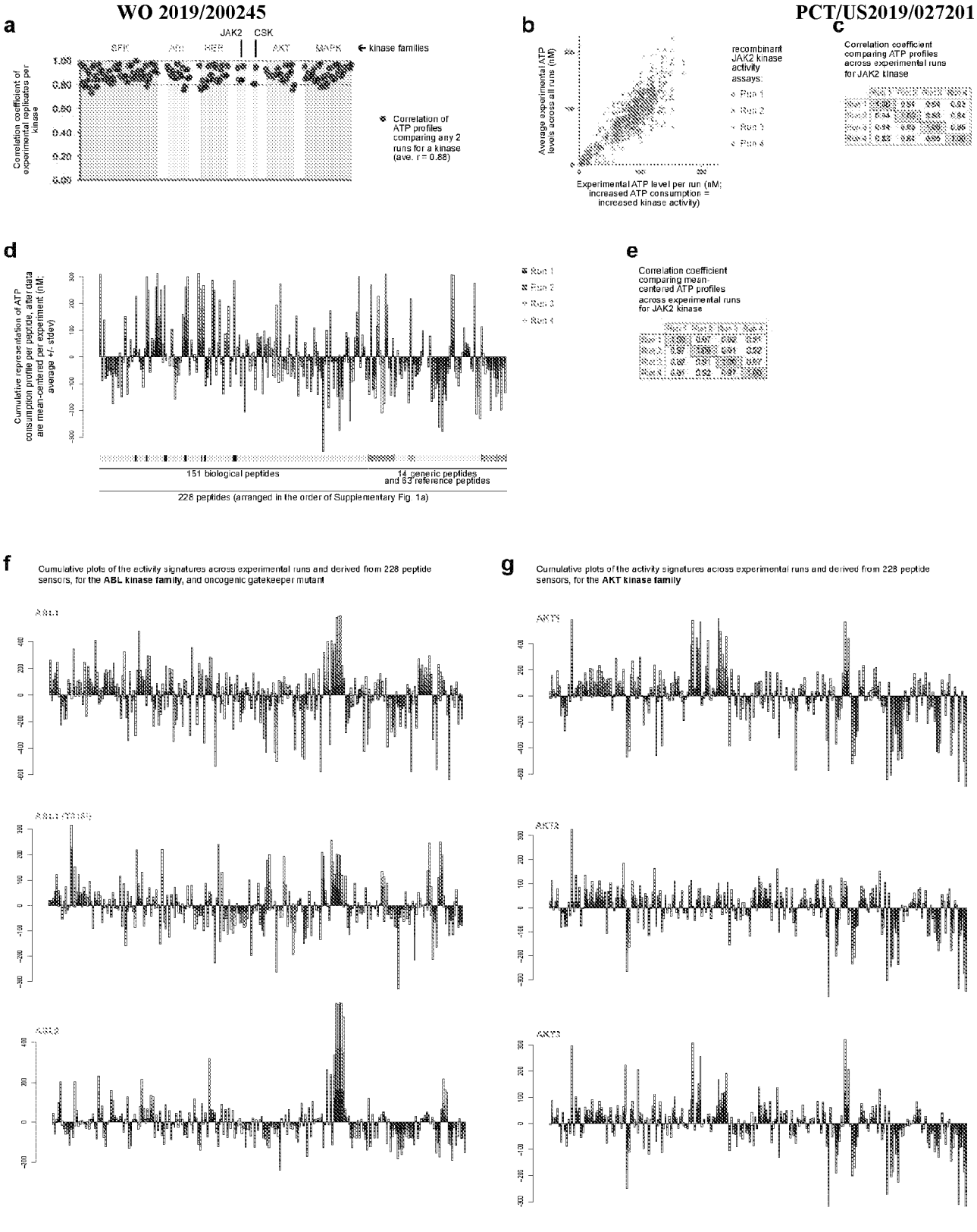
a
JAK2
CSK
SFK
ABL
HER
AKT
MAPK
kinase families
Correlation coefficient of experimental replicates per kinase
Correlation of ATP profiles comparing any 2 runs for a kinase (ave. r = 0.88)
b
Average experimental ATP levels across all runs (nM)
recombinant JAK2 kinase activity assays:
Run 1
Run 2
Run 3
Run 4
Experimental ATP level per run (nM; increased ATP consumption = increased kinase activity)
c
Correlation coefficient comparing ATP profiles across experimental runs for JAK2 kinase
d
Cumulative representation of ATP consumption profile per peptide, after data are mean-centered per experiment (nM; average +/- stdev)
Run 1
Run 2
Run 3
Run 4
151 biological peptides
14 generic peptides and 63 reference peptides
228 peptides (arranged in the order of Supplementary Fig. 1a)
e
Correlation coefficient comparing mean-centered ATP profiles across experimental runs for JAK2 kinase
f
Cumulative plots of the activity signatures across experimental runs and derived from 228 peptide sensors, for the ABL kinase family, and oncogenic gatekeeper mutant
ABL1
ABL1 (T315I)
ABL2
g
Cumulative plots of the activity signatures across experimental runs and derived from 228 peptide sensors, for the AKT kinase family
AKT1
AKT2
AKT3

Fig. 5 **(part 1)**

h

Cumulative plots of the activity signatures across experimental runs and derived from 228 peptide sensors, for the **SRC kinase family**, and isoforms

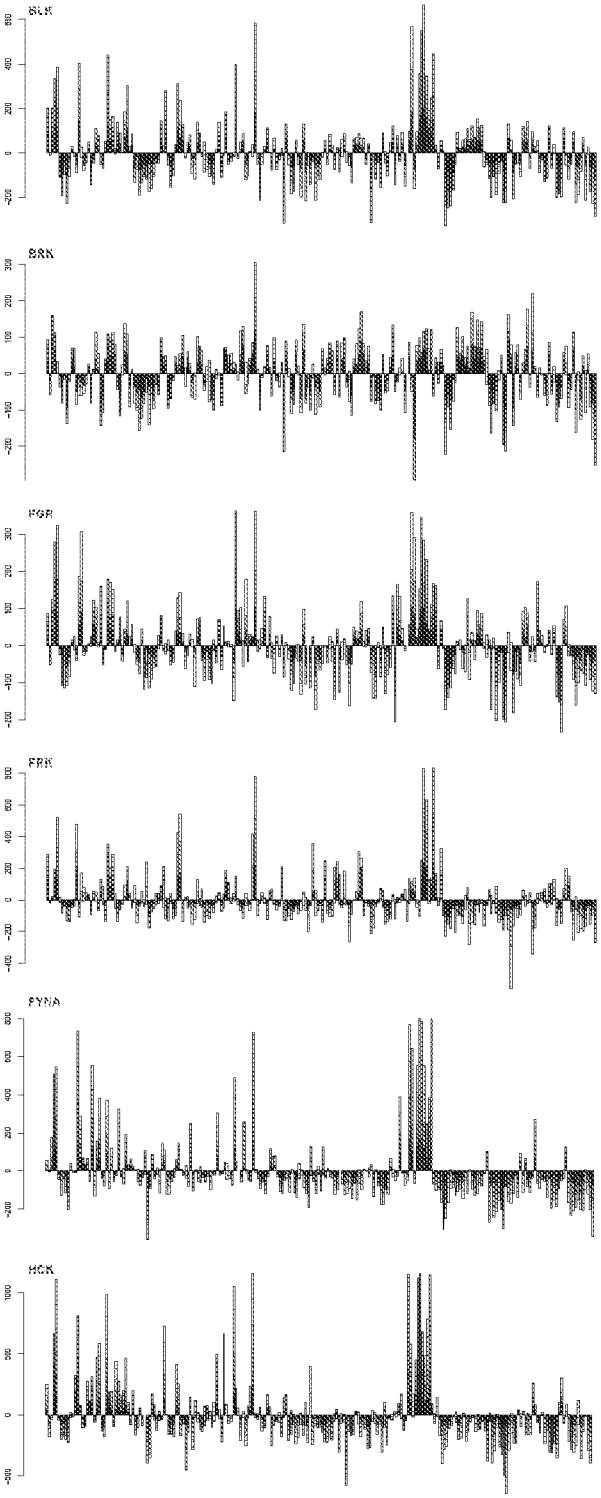

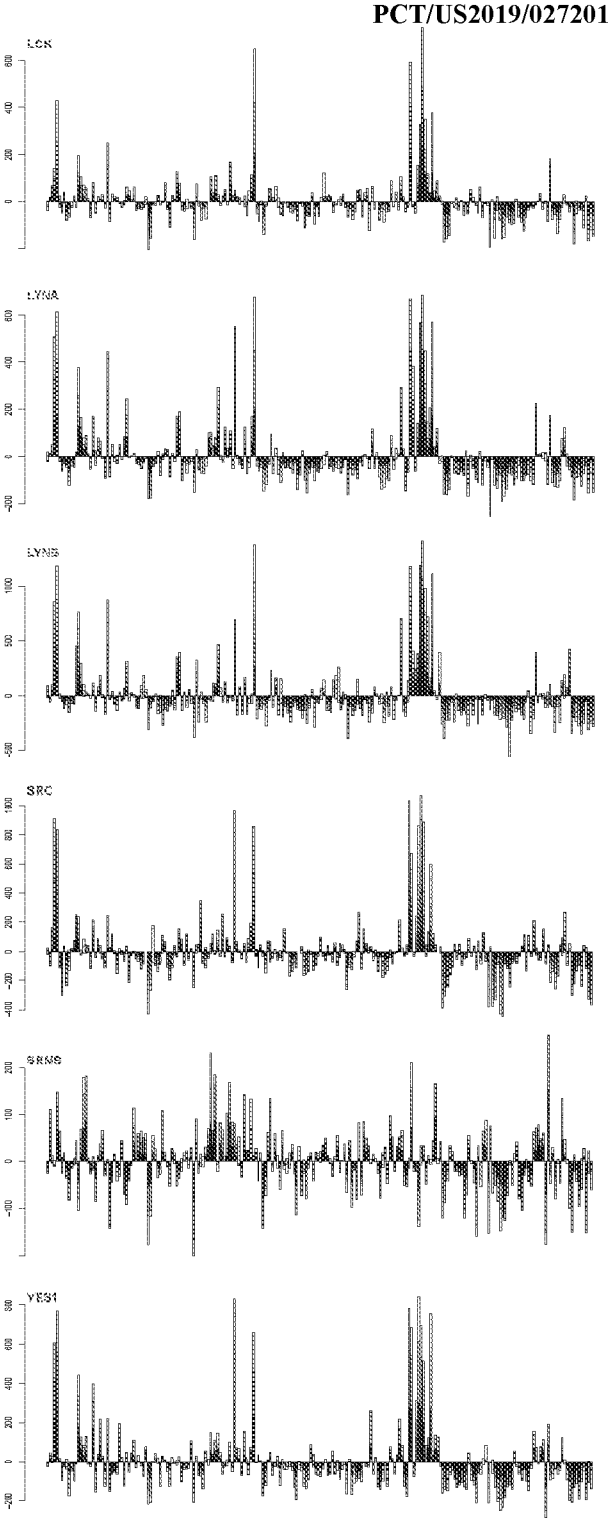

Fig. 5

(part 2)

i

Cumulative plots of the activity signatures across experimental runs and derived from 228 peptide sensors, for the **HER kinase family**

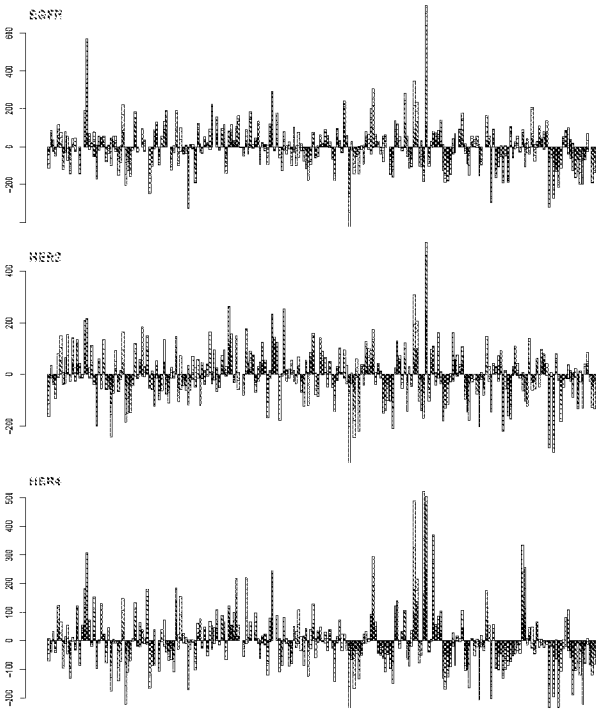

j

Cumulative plots of the activity signatures across experimental runs and derived from 228 peptide sensors, for the **MAPK kinase family**

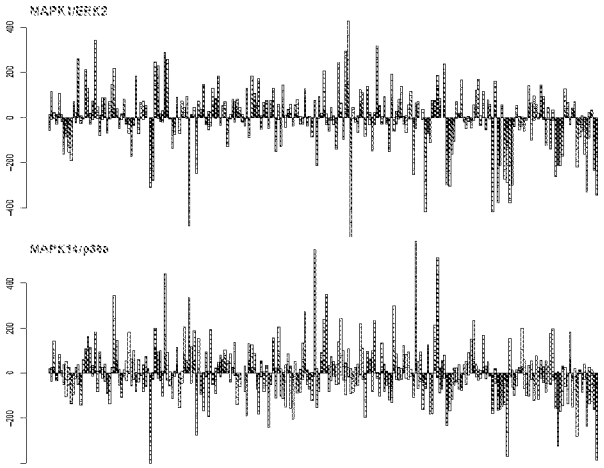

k

Cumulative plots of the activity signatures across experimental runs and derived from 228 peptide sensors, for the **CSK kinase**

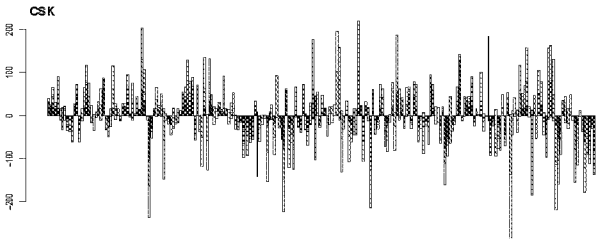

l

Cumulative plots of the activity signatures across experimental runs and derived from 228 peptide sensors, for all **25 recombinant kinases**

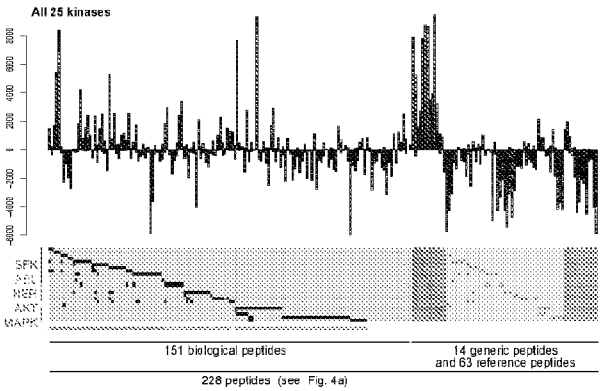

Fig. 5 **(part 3)**

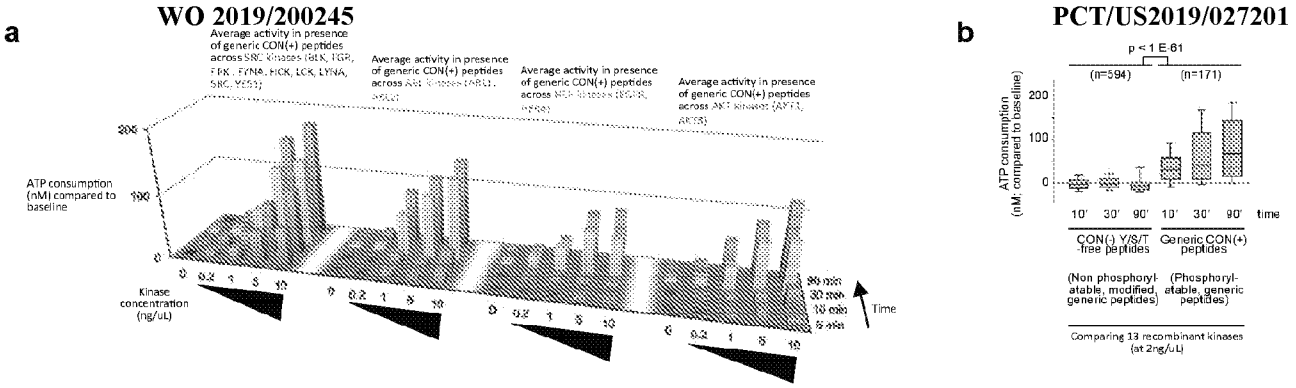
a
WO 2019/200245
Average activity in presence of generic CON(+) peptides across SRC Kinases (BLK, FGR, FRK, FYN A, HCK, LCK, LYN A, SRC, YES1)
Average activity in presence of generic CON(+) peptides across ABL Kinases (ABL1, ABL2)
Average activity in presence of generic CON(+) peptides across MET Kinases (MET, RON)
Average activity in presence of generic CON(+) peptides across AKT Kinases (AKT1, AKT3)
ATP consumption (nM) compared to baseline
200
100
0
Kinase concentration (ng/uL)
0 0.2 1 5 10
Time
b
PCT/US2019/027201
p < 1 E-61
(n=594)
(n=171)
ATP consumption (nM, compared to baseline)
200
100
0
10' 30' 90' 10' 30' 90' time
CON(-) Y/S/T -free peptides
Generic CON(+) peptides
(Non phosphoryl-atable, modified, generic peptides)
(Phosphoryl-atable, generic peptides)
Comparing 13 recombinant kinases (at 2ng/uL)

Fig. 6

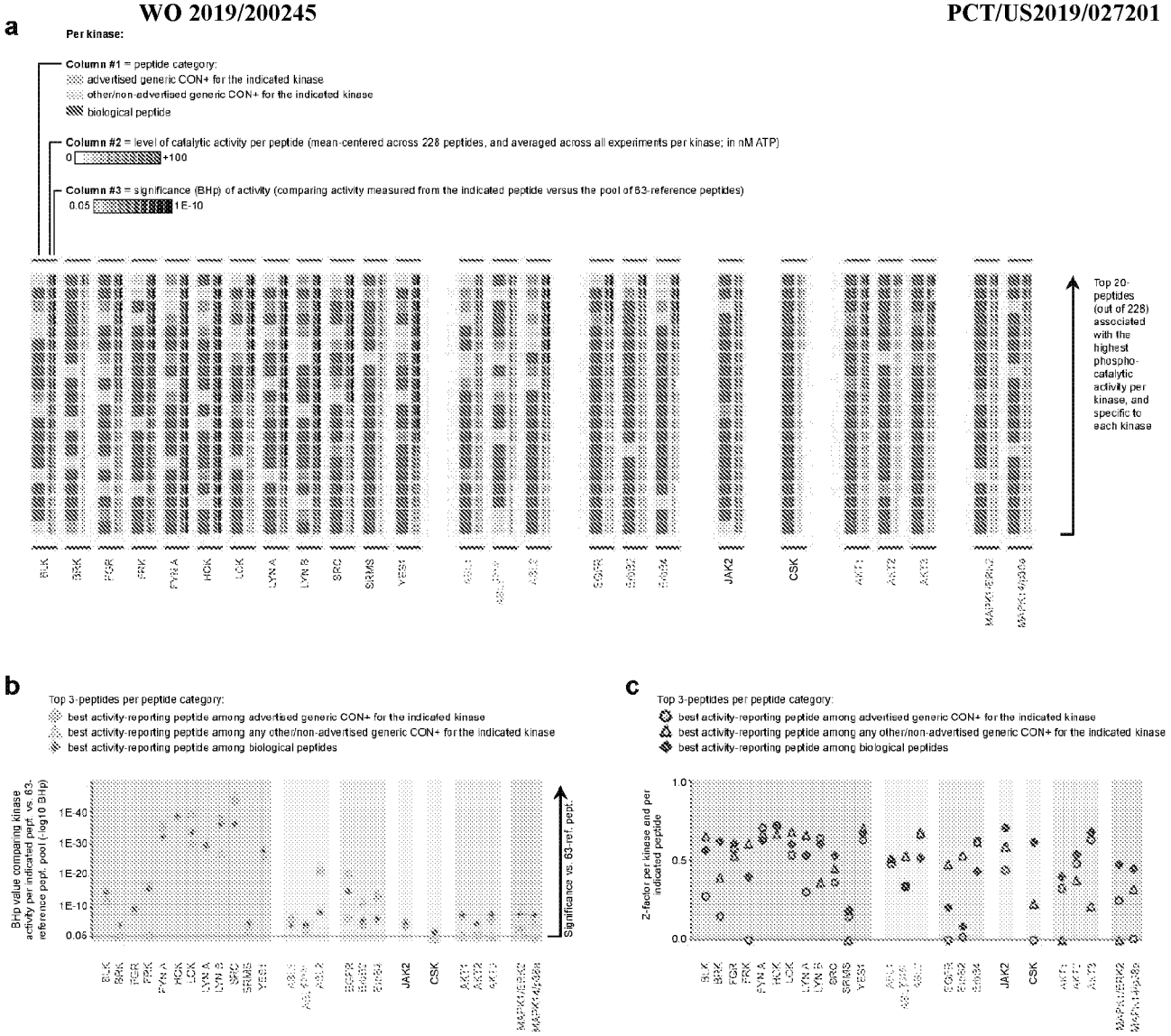
a
Per kinase:
Column #1 = peptide category:
advertised generic CON+ for the indicated kinase
other/non-advertised generic CON+ for the indicated kinase
biological peptide
Column #2 = level of catalytic activity per peptide (mean-centered across 228 peptides, and averaged across all experiments per kinase; in nM ATP)
0
+100
Column #3 = significance (BHp) of activity (comparing activity measured from the indicated peptide versus the pool of 63-reference peptides)
0.05
1E-10
Top 20-peptides (out of 228) associated with the highest phospho-catalytic activity per kinase, and specific to each kinase
BLK
BRK
FGR
FRK
FYN A
HCK
LCK
LYN A
LYN B
SRC
SRMS
YES1
EGFR
ErbB2
ErbB4
JAK2
CSK
AKT1
AKT2
AKT3
MAPK1/ERK2
MAPK14/p38a
b
Top 3-peptides per peptide category:
best activity-reporting peptide among advertised generic CON+ for the indicated kinase
best activity-reporting peptide among any other/non-advertised generic CON+ for the indicated kinase
best activity-reporting peptide among biological peptides
BHp value comparing kinase activity per indicated pept. vs. 63-reference pept. pool (-log10 BHp)
1E-40
1E-30
1E-20
1E-10
0.05
Significance vs. 63-ref. pept.
c
Top 3-peptides per peptide category:
best activity-reporting peptide among advertised generic CON+ for the indicated kinase
best activity-reporting peptide among any other/non-advertised generic CON+ for the indicated kinase
best activity-reporting peptide among biological peptides
Z-factor per kinase and per indicated peptide
1.0
0.5
0.0

Fig. 7

a

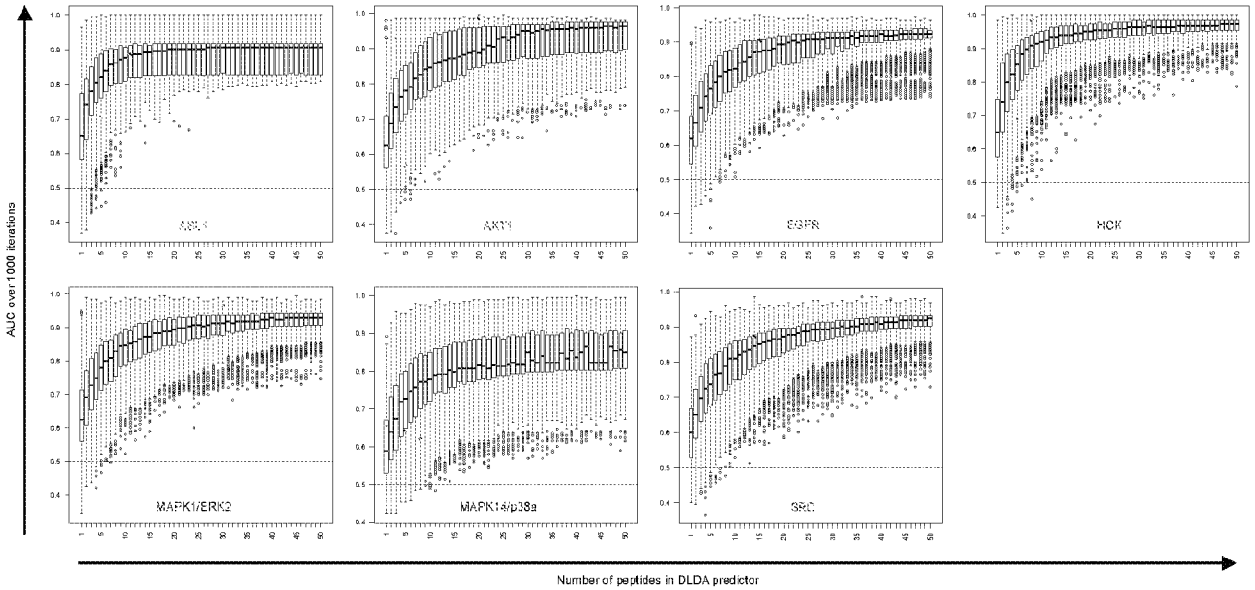
AUC over 1000 iterations
AKT1
EGFR
HCK
MAPK1/ERK2
MAPK14/p38a
SRC
Number of peptides in DLDA predictor

b

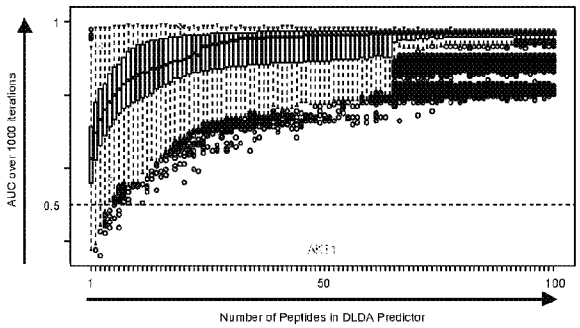
AUC over 1000 iterations
1
0.5
AKT1
1
50
100
Number of Peptides in DLDA Predictor

c

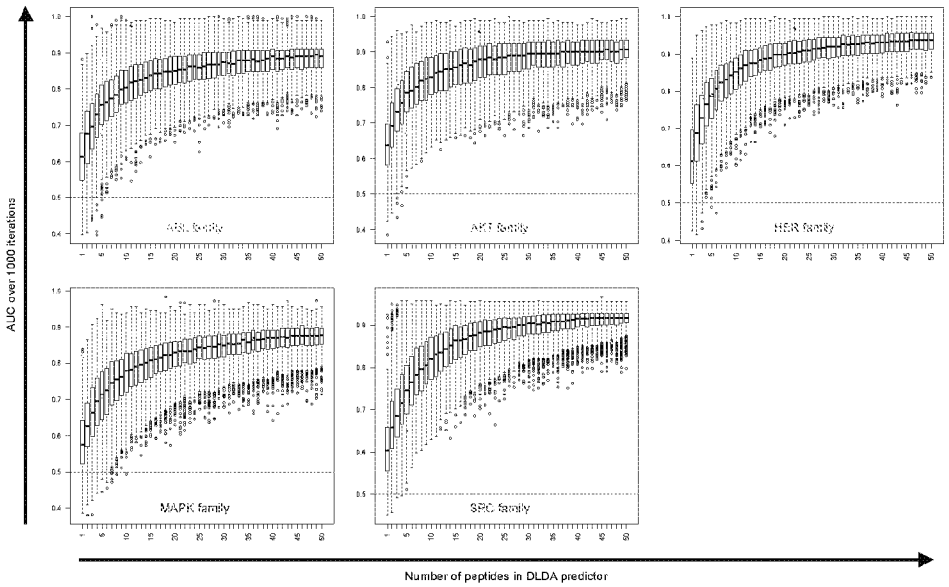
AUC over 1000 iterations
ABL family
AKT family
HER family
MAPK family
SRC family
Number of peptides in DLDA predictor

Fig. 8

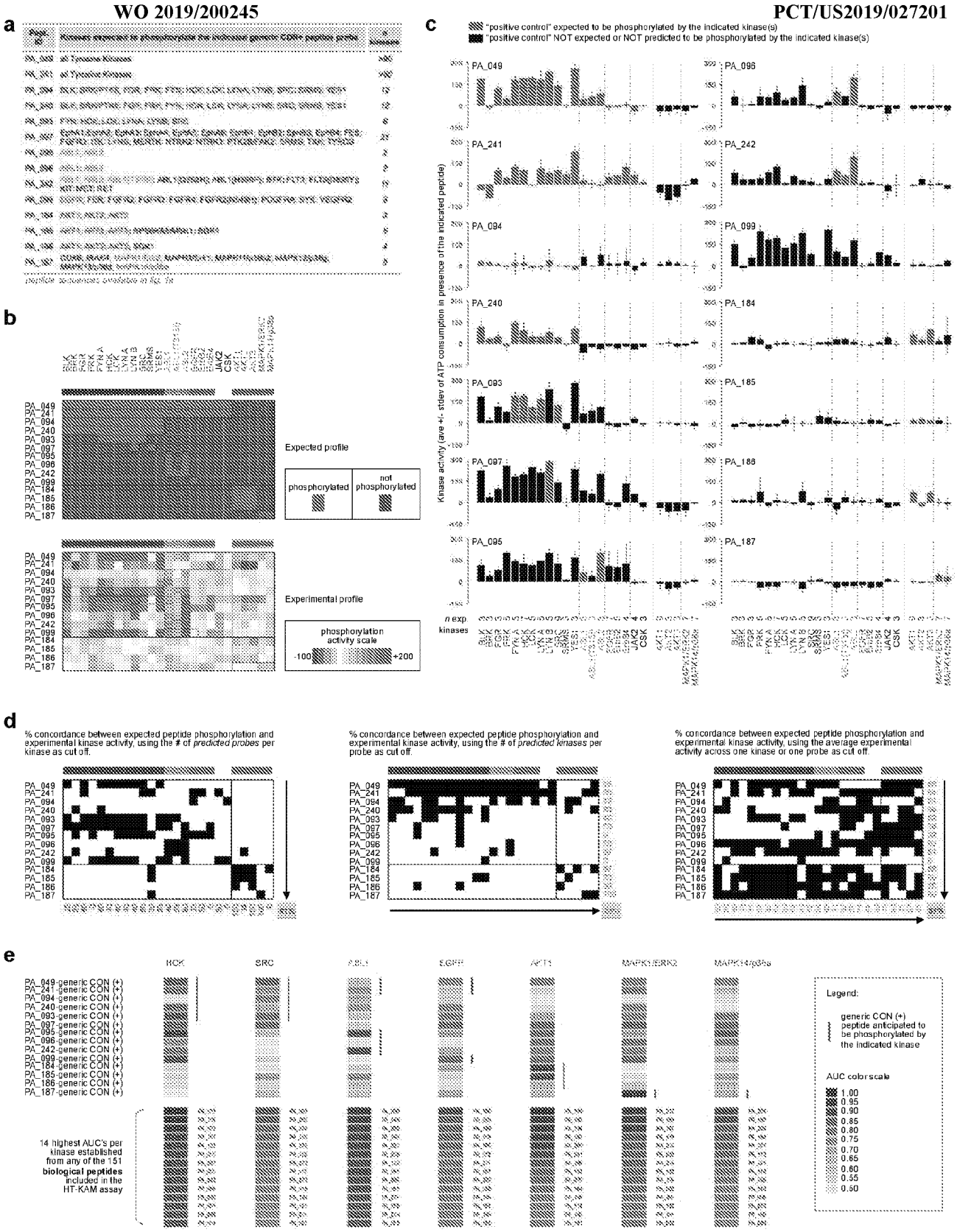
a
b
Expected profile
phosphorylated
not phosphorylated
Experimental profile
phosphorylation activity scale
-100
+200
c
"positive control" expected to be phosphorylated by the indicated kinase(s)
"positive control" NOT expected or NOT predicted to be phosphorylated by the indicated kinase(s)
Kinase activity (ave +/- stdev of ATP consumption in presence of the indicated peptide)
n exp. kinases
d
% concordance between expected peptide phosphorylation and experimental kinase activity, using the # of predicted probes per kinase as cut off.
% concordance between expected peptide phosphorylation and experimental kinase activity, using the # of predicted kinases per probe as cut off.
% concordance between expected peptide phosphorylation and experimental kinase activity, using the average experimental activity across one kinase or one probe as cut off.
e
14 highest AUC's per kinase established from any of the 151 biological peptides included in the HT-KAM assay
Legend:
generic CON (+) peptide anticipated to be phosphorylated by the indicated kinase
AUC color scale
1.00
0.95
0.90
0.85
0.80
0.75
0.70
0.65
0.60
0.55
0.50

Fig. 9

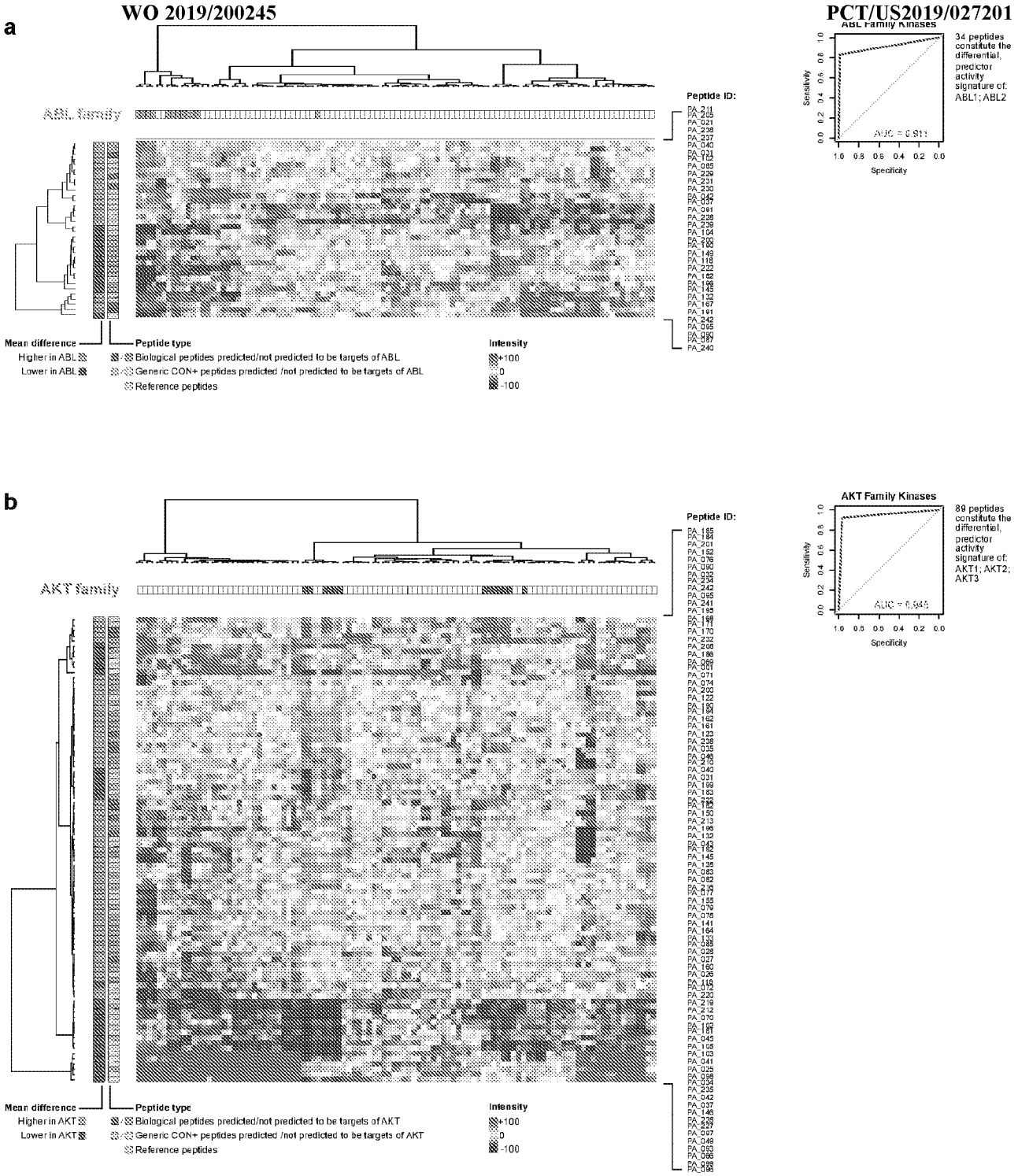
a
ABL family
Peptide ID:
Mean difference
Higher in ABL
Lower in ABL
Peptide type
Biological peptides predicted/not predicted to be targets of ABL
Generic CON+ peptides predicted /not predicted to be targets of ABL
Reference peptides
Intensity
+100
0
-100
ABL Family Kinases
Sensitivity
Specificity
AUC = 0.913
34 peptides constitute the differential, predictor activity signature of: ABL1; ABL2
b
AKT family
Peptide ID:
Mean difference
Higher in AKT
Lower in AKT
Peptide type
Biological peptides predicted/not predicted to be targets of AKT
Generic CON+ peptides predicted /not predicted to be targets of AKT
Reference peptides
Intensity
+100
0
-100
AKT Family Kinases
Sensitivity
Specificity
AUC = 0.945
89 peptides constitute the differential, predictor activity signature of: AKT1; AKT2; AKT3

Fig. 10

(part 1)

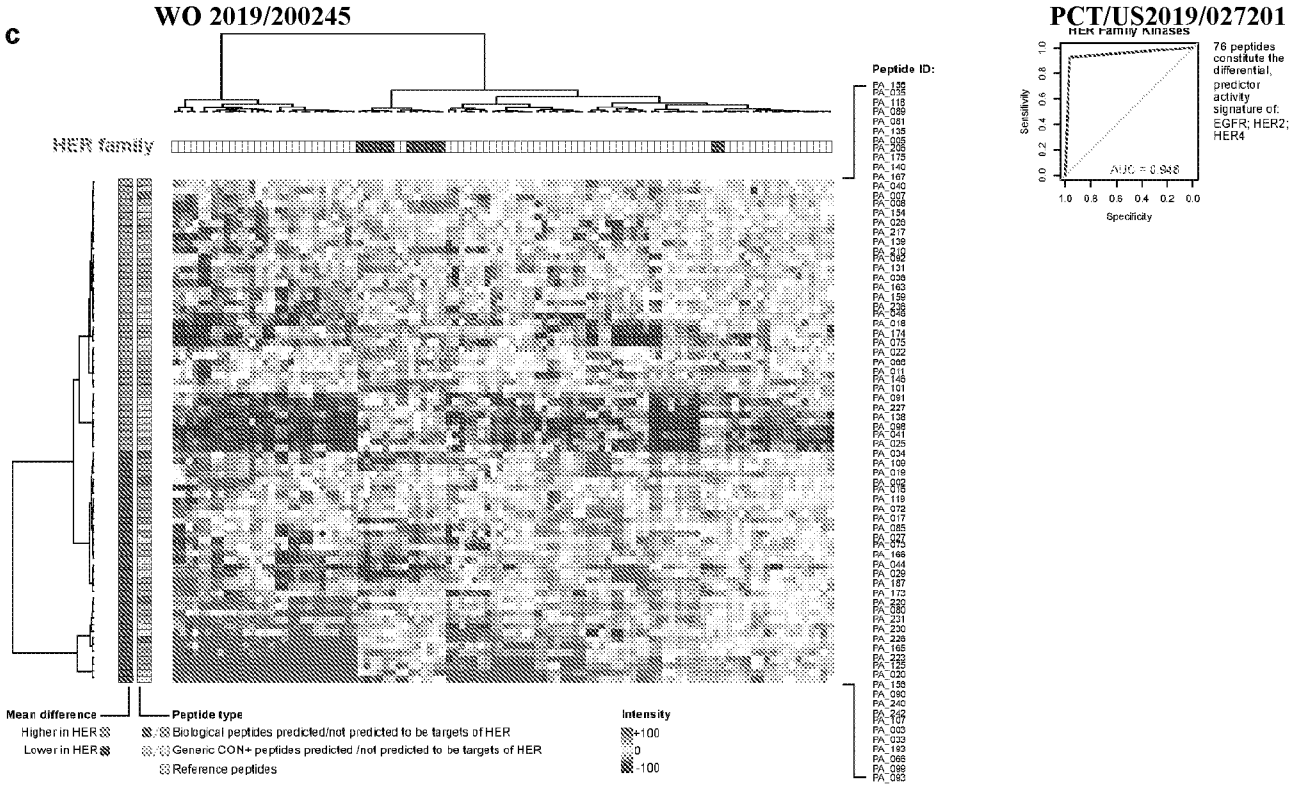
c
HER family
Peptide ID:
Mean difference
Higher in HER
Lower in HER
Peptide type
Biological peptides predicted/not predicted to be targets of HER
Generic CON+ peptides predicted /not predicted to be targets of HER
Reference peptides
Intensity
+100
0
-100
HER Family Kinases
Sensitivity
Specificity
AUC = 0.948
76 peptides constitute the differential, predictor activity signature of: EGFR; HER2; HER4

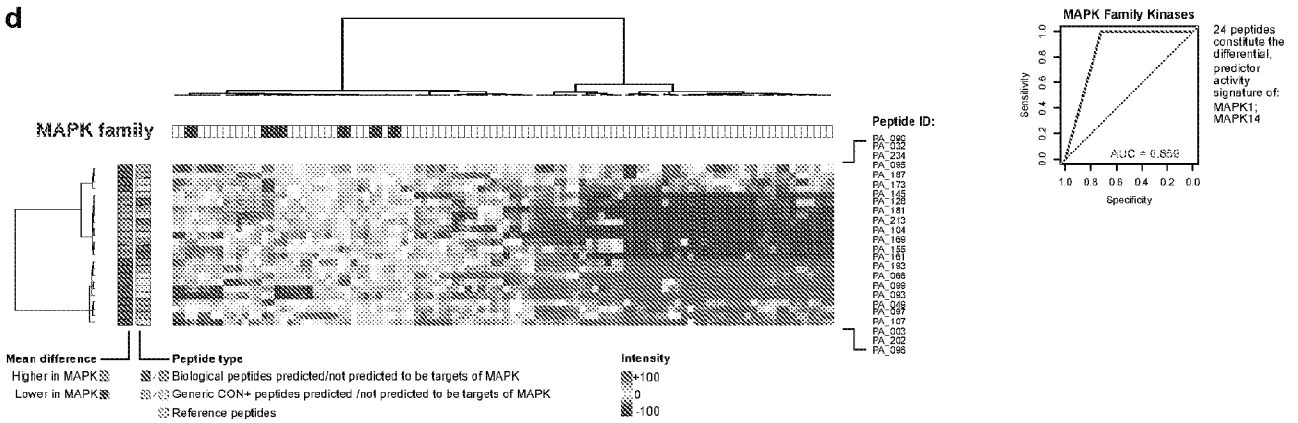
d
MAPK family
Peptide ID:
Mean difference
Higher in MAPK
Lower in MAPK
Peptide type
Biological peptides predicted/not predicted to be targets of MAPK
Generic CON+ peptides predicted /not predicted to be targets of MAPK
Reference peptides
Intensity
+100
0
-100
MAPK Family Kinases
Sensitivity
Specificity
AUC = 0.859
24 peptides constitute the differential, predictor activity signature of: MAPK1; MAPK14

Fig. 10 (part 2)

e

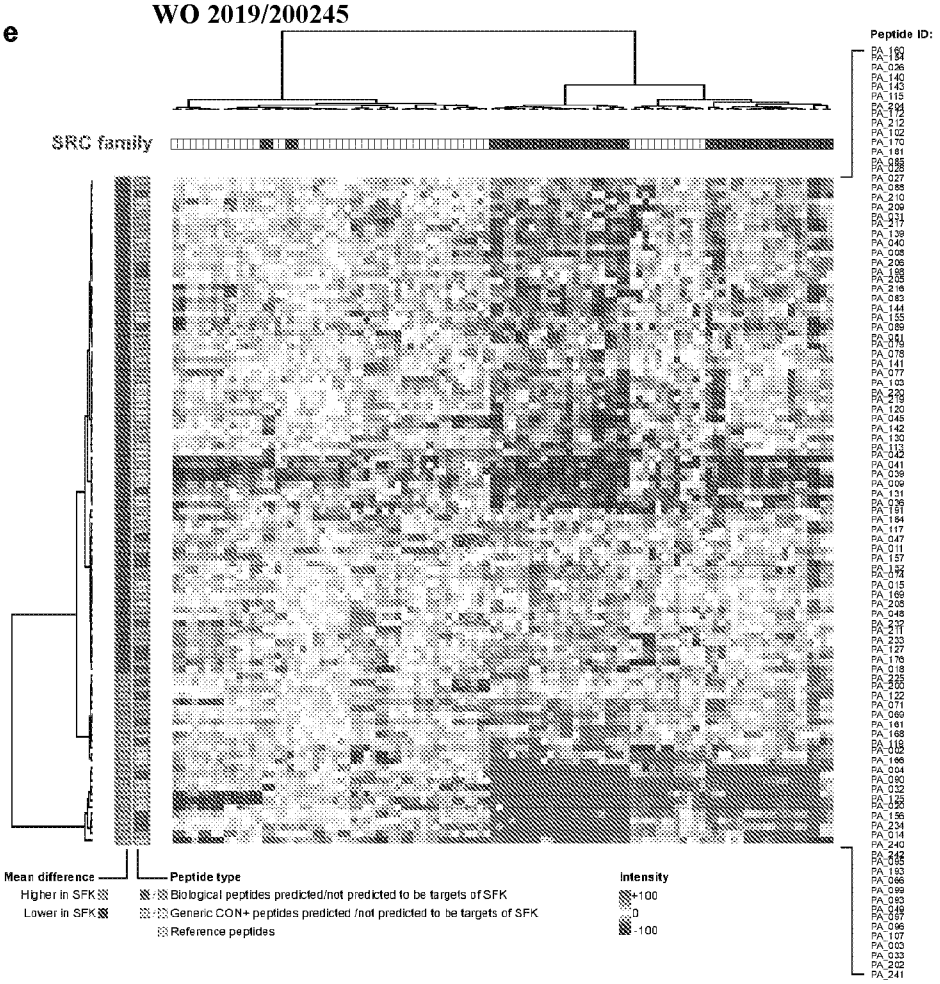

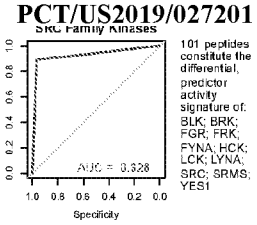

Fig. 10 (part 3)

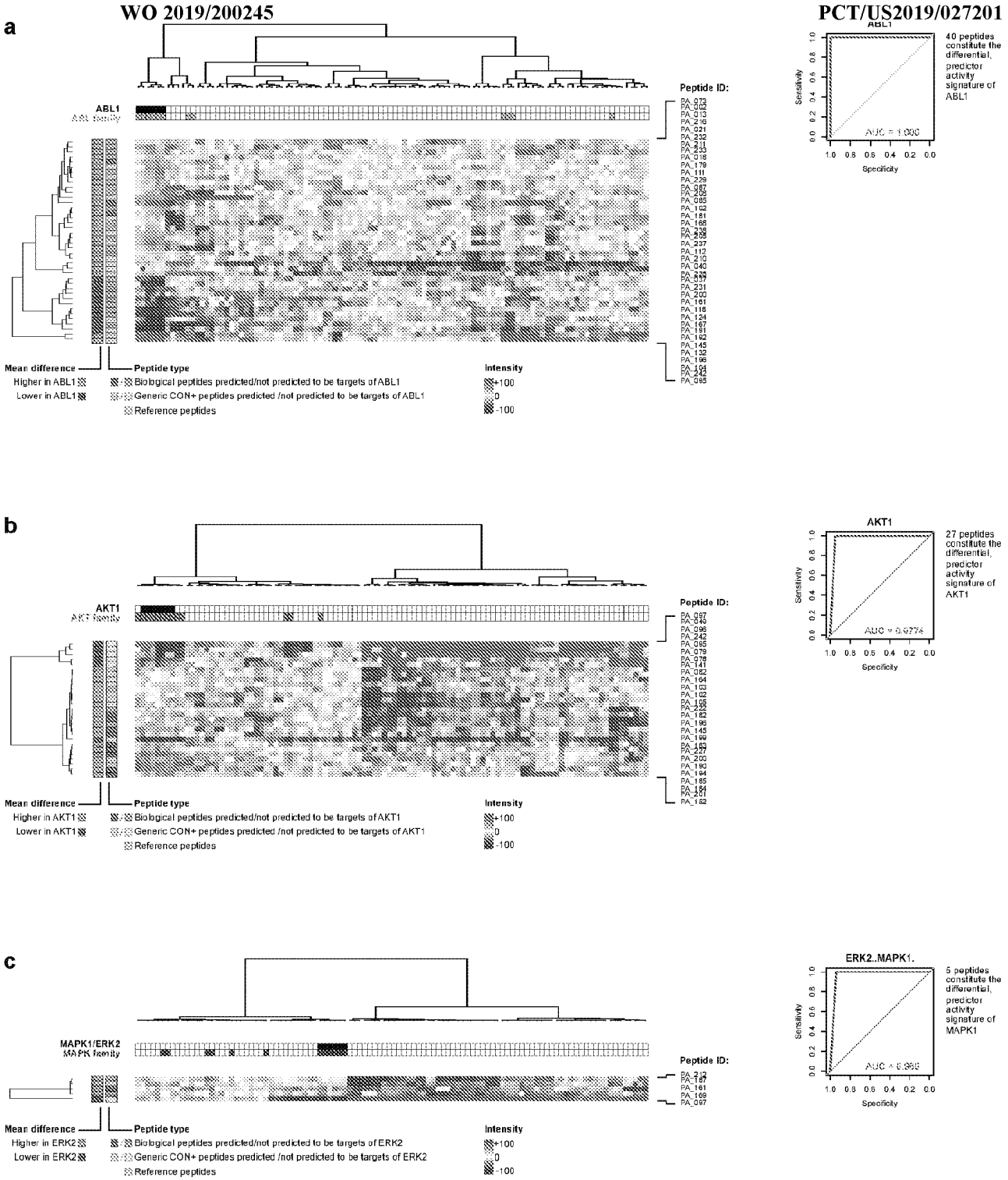
a
ABL1
ABL family
Peptide ID:
Mean difference
Higher in ABL1
Lower in ABL1
Peptide type
Biological peptides predicted/not predicted to be targets of ABL1
Generic CON+ peptides predicted /not predicted to be targets of ABL1
Reference peptides
Intensity
+100
0
-100
ABL1
Sensitivity
Specificity
AUC = 1.000
40 peptides constitute the differential, predictor activity signature of ABL1
b
AKT1
AKT family
Peptide ID:
Mean difference
Higher in AKT1
Lower in AKT1
Peptide type
Biological peptides predicted/not predicted to be targets of AKT1
Generic CON+ peptides predicted /not predicted to be targets of AKT1
Reference peptides
Intensity
+100
0
-100
AKT1
Sensitivity
Specificity
AUC = 0.9774
27 peptides constitute the differential, predictor activity signature of AKT1
c
MAPK1/ERK2
MAPK family
Peptide ID:
Mean difference
Higher in ERK2
Lower in ERK2
Peptide type
Biological peptides predicted/not predicted to be targets of ERK2
Generic CON+ peptides predicted /not predicted to be targets of ERK2
Reference peptides
Intensity
+100
0
-100
ERK2..MAPK1.
Sensitivity
Specificity
AUC = 0.968
5 peptides constitute the differential, predictor activity signature of MAPK1

Fig. 11 (part 1)

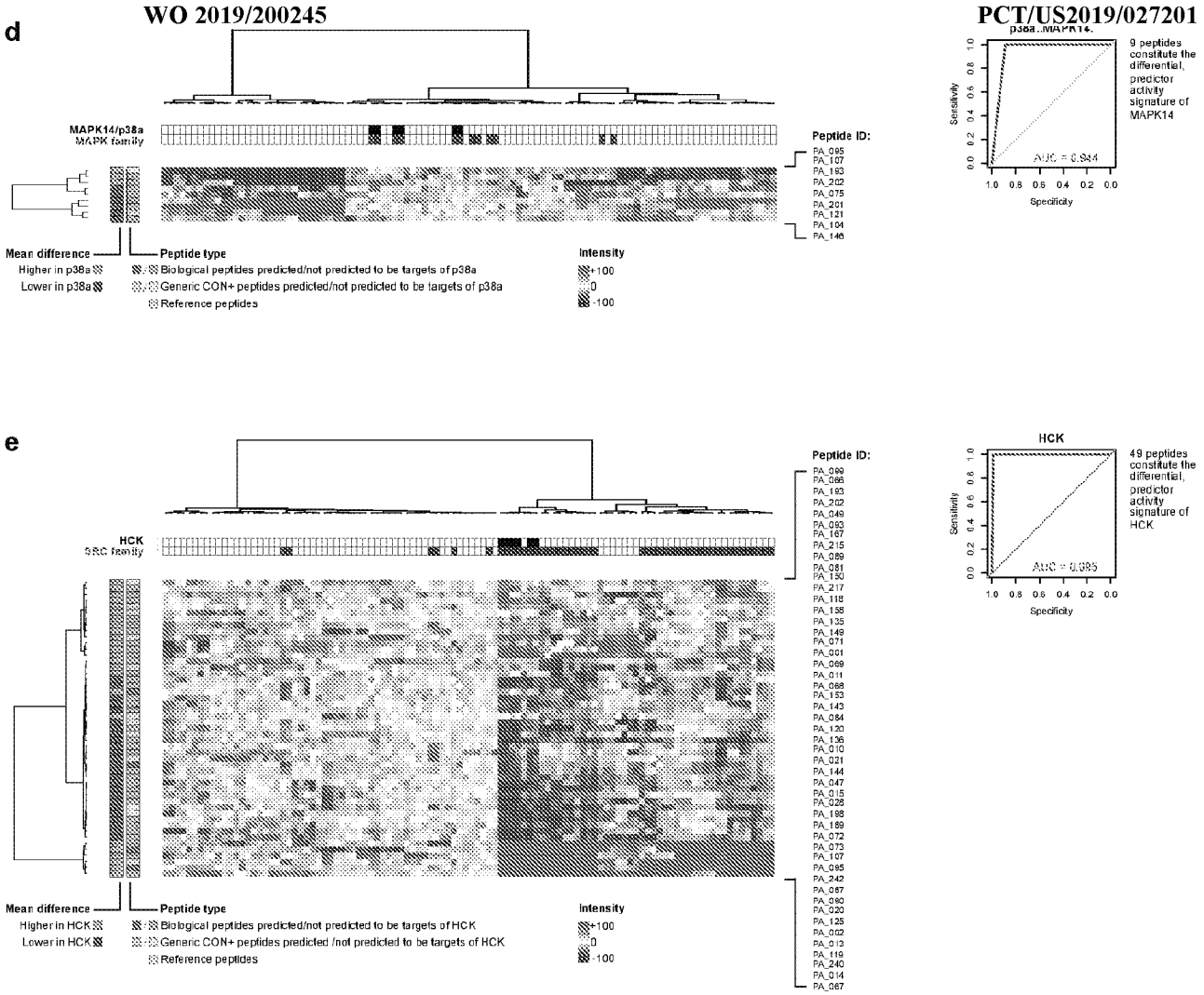
d
MAPK14/p38a
MAPK family
Peptide ID:
PA_095
PA_107
PA_193
PA_202
PA_075
PA_201
PA_121
PA_104
PA_146
Mean difference
Higher in p38a
Lower in p38a
Peptide type
Biological peptides predicted/not predicted to be targets of p38a
Generic CON+ peptides predicted/not predicted to be targets of p38a
Reference peptides
Intensity
+100
0
-100
p38a.MAPK14
Sensitivity
Specificity
AUC = 0.984
9 peptides constitute the differential, predictor activity signature of MAPK14
e
HCK
SRC family
Peptide ID:
PA_099
PA_066
PA_193
PA_202
PA_049
PA_093
PA_167
PA_215
PA_089
PA_081
PA_150
PA_217
PA_118
PA_158
PA_135
PA_149
PA_071
PA_001
PA_069
PA_011
PA_068
PA_153
PA_143
PA_084
PA_120
PA_136
PA_010
PA_021
PA_144
PA_047
PA_015
PA_028
PA_198
PA_189
PA_072
PA_073
PA_107
PA_095
PA_242
PA_087
PA_090
PA_020
PA_125
PA_002
PA_013
PA_119
PA_240
PA_014
PA_067
Mean difference
Higher in HCK
Lower in HCK
Peptide type
Biological peptides predicted/not predicted to be targets of HCK
Generic CON+ peptides predicted /not predicted to be targets of HCK
Reference peptides
Intensity
+100
0
-100
HCK
Sensitivity
Specificity
AUC = 0.985
49 peptides constitute the differential, predictor activity signature of HCK
f
Number of differential peptides
40
27
5
9
49
ABL1
AKT1
ERK2
p38a
HCK
Peptide category:
Biological; predicted
Biological; other
Generic CON+; predicted
Generic CON+; other
Random CON-
Reference; other

Fig. 11 (part 2)

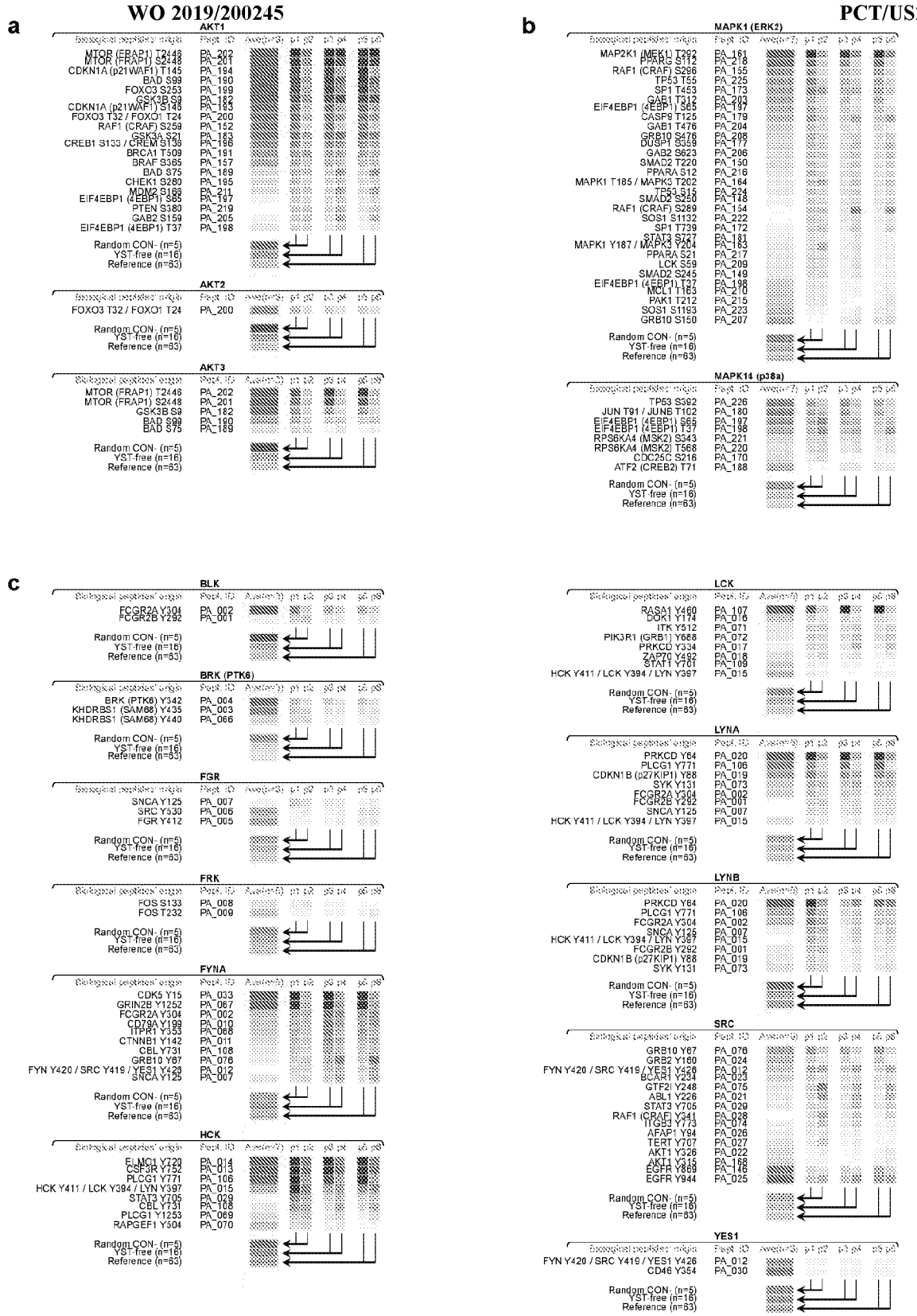
a
AKT1
MTOR (FRAP1) T2448 PA_202
MTOR (FRAP1) S2448 PA_201
CDKN1A (p21WAF1) T145 PA_194
BAD S99 PA_190
FOXO3 S253 PA_199
GSK3B S9 PA_182
CDKN1A (p21WAF1) S146 PA_193
FOXO3 T32 / FOXO1 T24 PA_200
RAF1 (CRAF) S259 PA_152
GSK3A S21 PA_183
CREB1 S133 / CREM S136 PA_196
BRCA1 T509 PA_191
BRAF S365 PA_157
BAD S75 PA_189
CHEK1 S280 PA_195
MDM2 S166 PA_211
EIF4EBP1 (4EBP1) S65 PA_197
PTEN S380 PA_219
GAB2 S159 PA_205
EIF4EBP1 (4EBP1) T37 PA_198
Random CON- (n=5)
YST-free (n=16)
Reference (n=63)
AKT2
FOXO3 T32 / FOXO1 T24 PA_200
Random CON- (n=5)
YST-free (n=16)
Reference (n=63)
AKT3
MTOR (FRAP1) T2448 PA_202
MTOR (FRAP1) S2448 PA_201
GSK3B S9 PA_182
BAD S99 PA_190
BAD S75 PA_189
Random CON- (n=5)
YST-free (n=16)
Reference (n=63)
b
MAPK1 (ERK2)
MAP2K1 (MEK1) T292 PA_161
PPARG S112 PA_216
RAF1 (CRAF) S296 PA_155
TP53 T55 PA_225
SP1 T453 PA_173
GAB1 T312 PA_203
EIF4EBP1 (4EBP1) S65 PA_197
CASP9 T125 PA_179
GAB1 T476 PA_204
GRB10 S476 PA_208
DUSP1 S359 PA_177
GAB2 S623 PA_206
SMAD2 T220 PA_150
PPARA S12 PA_216
MAPK1 T185 / MAPK3 T202 PA_164
TP53 S15 PA_224
SMAD2 S250 PA_148
RAF1 (CRAF) S289 PA_154
SOS1 S1132 PA_222
SP1 T739 PA_172
STAT3 S727 PA_181
MAPK1 Y187 / MAPK3 Y204 PA_163
PPARA S21 PA_217
LCK S59 PA_209
SMAD2 S245 PA_149
EIF4EBP1 (4EBP1) T37 PA_198
MCL1 T163 PA_210
PAK1 T212 PA_215
SOS1 S1193 PA_223
GRB10 S150 PA_207
Random CON- (n=5)
YST-free (n=16)
Reference (n=63)
MAPK14 (p38a)
TP53 S392 PA_226
JUN T91 / JUNB T102 PA_180
EIF4EBP1 (4EBP1) S65 PA_197
EIF4EBP1 (4EBP1) T37 PA_198
RPS6KA4 (MSK2) S343 PA_221
RPS6KA4 (MSK2) T568 PA_220
CDC25C S216 PA_170
ATF2 (CREB2) T71 PA_188
Random CON- (n=5)
YST-free (n=16)
Reference (n=63)
c
BLK
FCGR2A Y304 PA_002
FCGR2B Y292 PA_001
Random CON- (n=5)
YST-free (n=16)
Reference (n=63)
BRK (PTK6)
BRK (PTK6) Y342 PA_004
KHDRBS1 (SAM68) Y435 PA_003
KHDRBS1 (SAM68) Y440 PA_066
Random CON- (n=5)
YST-free (n=16)
Reference (n=63)
FGR
SNCA Y125 PA_007
SRC Y530 PA_006
FGR Y412 PA_005
Random CON- (n=5)
YST-free (n=16)
Reference (n=63)
FRK
FOS S133 PA_008
FOS T232 PA_009
Random CON- (n=5)
YST-free (n=16)
Reference (n=63)
FYNA
CDK5 Y15 PA_033
GRIN2B Y1252 PA_067
FCGR2A Y304 PA_002
CD79A Y199 PA_010
ITPR1 Y353 PA_068
CTNNB1 Y142 PA_011
CBLY731 PA_108
GRB10 Y67 PA_076
FYN Y420 / SRC Y419 / YES1 Y426 PA_012
SNCA Y125 PA_007
Random CON- (n=5)
YST-free (n=16)
Reference (n=63)
HCK
EIMC1 Y720 PA_014
CSF3R Y752 PA_013
PLCG1 Y771 PA_106
HCK Y411 / LCK Y394 / LYN Y397 PA_015
STAT3 Y705 PA_029
CBLY731 PA_108
PLCG1 Y1253 PA_069
RAPGEF1 Y504 PA_070
Random CON- (n=5)
YST-free (n=16)
Reference (n=63)
LCK
RASA1 Y460 PA_107
DOK1 Y174 PA_016
ITK Y512 PA_071
PIK3R1 (GRB1) Y688 PA_072
PRKCD Y334 PA_017
ZAP70 Y492 PA_018
STAT1 Y701 PA_109
HCK Y411 / LCK Y394 / LYN Y397 PA_015
Random CON- (n=5)
YST-free (n=16)
Reference (n=63)
LYNA
PRKCD Y64 PA_020
PLCG1 Y771 PA_106
CDKN1B (p27KIP1) Y88 PA_019
SYK Y131 PA_073
FCGR2A Y304 PA_002
FCGR2B Y292 PA_001
SNCA Y125 PA_007
HCK Y411 / LCK Y394 / LYN Y397 PA_015
Random CON- (n=5)
YST-free (n=16)
Reference (n=63)
LYNB
PRKCD Y64 PA_020
PLCG1 Y771 PA_106
FCGR2A Y304 PA_002
SNCA Y125 PA_007
HCK Y411 / LCK Y394 / LYN Y397 PA_015
FCGR2B Y292 PA_001
CDKN1B (p27KIP1) Y88 PA_019
SYK Y131 PA_073
Random CON- (n=5)
YST-free (n=16)
Reference (n=63)
SRC
GRB10 Y67 PA_076
GRB2 Y160 PA_024
FYN Y420 / SRC Y419 / YES1 Y426 PA_012
BCAR1 Y234 PA_023
GTF2I Y248 PA_075
ABL1 Y226 PA_021
STAT3 Y705 PA_029
RAF1 (CRAF) Y341 PA_028
ITGB3 Y773 PA_074
AFAP1 Y94 PA_026
TERT Y707 PA_027
AKT1 Y326 PA_022
AKT1 Y315 PA_168
EGFR Y869 PA_146
EGFR Y944 PA_025
Random CON- (n=5)
YST-free (n=16)
Reference (n=63)
YES1
FYN Y420 / SRC Y419 / YES1 Y426 PA_012
CD46 Y364 PA_030
Random CON- (n=5)
YST-free (n=16)
Reference (n=63)

Fig. 12 (part 1)

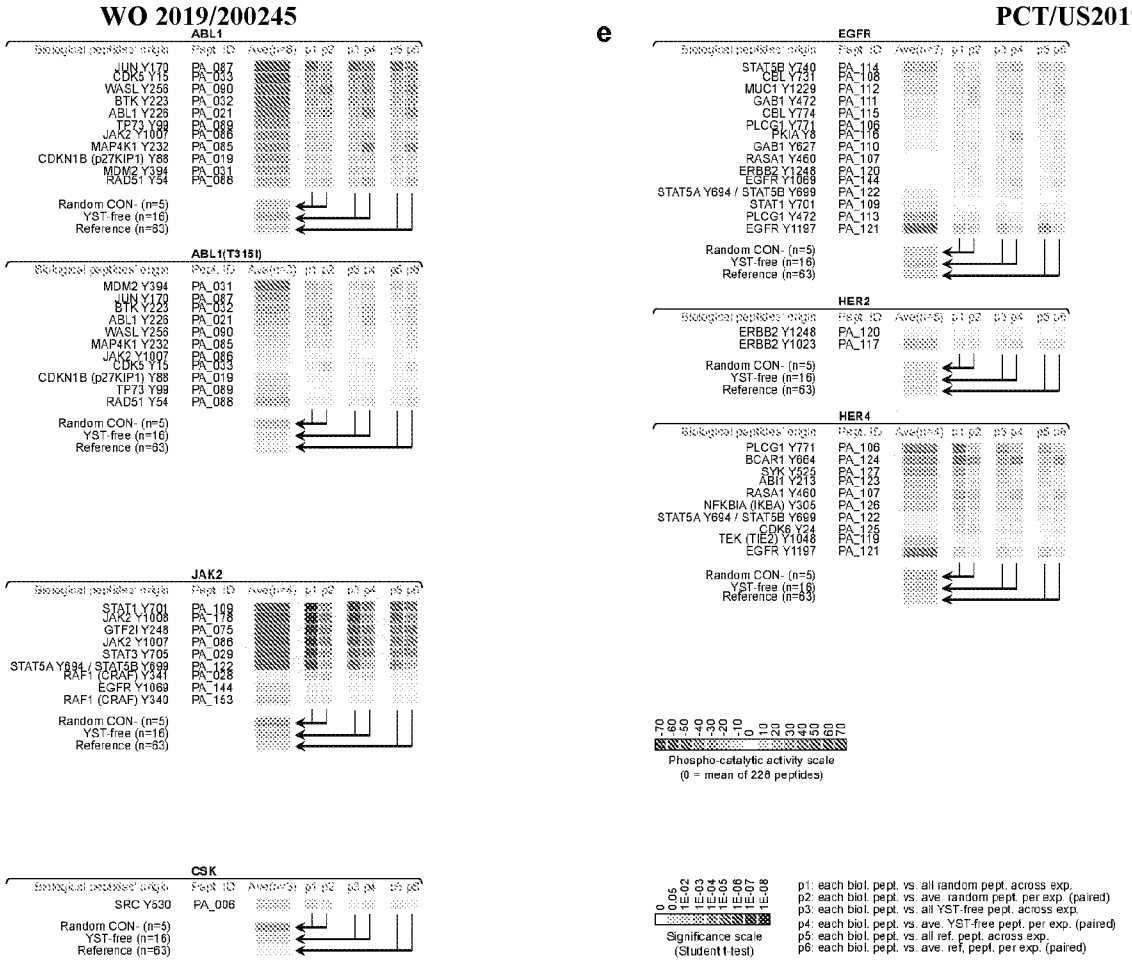
d
ABL1
Biological peptides' origin
Pept. ID
Ave(n=5)
p1 p2
p3 p4
p5 p6
JUN Y170 PA_087
CDK5 Y15 PA_033
WASL Y256 PA_090
BTK Y223 PA_032
ABL1 Y226 PA_021
TP73 Y99 PA_089
JAK2 Y1007 PA_086
MAP4K1 Y232 PA_085
CDKN1B (p27KIP1) Y88 PA_019
MDM2 Y394 PA_031
RAD51 Y54 PA_088
Random CON- (n=5)
YST-free (n=16)
Reference (n=63)
ABL1(T315I)
MDM2 Y394 PA_031
JUN Y170 PA_087
BTK Y223 PA_032
ABL1 Y226 PA_021
WASL Y256 PA_090
MAP4K1 Y232 PA_085
JAK2 Y1007 PA_086
CDK5 Y15 PA_033
CDKN1B (p27KIP1) Y88 PA_019
TP73 Y99 PA_089
RAD51 Y54 PA_088
Random CON- (n=5)
YST-free (n=16)
Reference (n=63)
e
EGFR
STAT5B Y740 PA_114
CBL Y731 PA_108
MUC1 Y1229 PA_112
GAB1 Y472 PA_111
CBL Y774 PA_115
PLCG1 Y771 PA_106
PKIA Y8 PA_116
GAB1 Y627 PA_110
RASA1 Y460 PA_107
ERBB2 Y1248 PA_120
EGFR Y1069 PA_144
STAT5A Y694 / STAT5B Y699 PA_122
STAT1 Y701 PA_109
PLCG1 Y472 PA_113
EGFR Y1197 PA_121
Random CON- (n=5)
YST-free (n=16)
Reference (n=63)
HER2
ERBB2 Y1248 PA_120
ERBB2 Y1023 PA_117
Random CON- (n=5)
YST-free (n=16)
Reference (n=63)
HER4
PLCG1 Y771 PA_106
BCAR1 Y664 PA_124
SYK Y525 PA_127
ABI1 Y213 PA_123
RASA1 Y460 PA_107
NFKBIA (IKBA) Y305 PA_126
STAT5A Y694 / STAT5B Y699 PA_122
CDK6 Y24 PA_125
TEK (TIE2) Y1048 PA_119
EGFR Y1197 PA_121
Random CON- (n=5)
YST-free (n=16)
Reference (n=63)
f
JAK2
STAT1 Y701 PA_109
JAK2 Y1008 PA_178
GTF2I Y248 PA_075
JAK2 Y1007 PA_086
STAT3 Y705 PA_029
STAT5A Y694 / STAT5B Y699 PA_122
RAF1 (CRAF) Y341 PA_028
EGFR Y1069 PA_144
RAF1 (CRAF) Y340 PA_153
Random CON- (n=5)
YST-free (n=16)
Reference (n=63)
g
CSK
SRC Y530 PA_006
Random CON- (n=5)
YST-free (n=16)
Reference (n=63)
70 60 50 40 30 20 10 0 10 20 30 40 50 60 70
Phospho-catalytic activity scale
(0 = mean of 228 peptides)
0 0.05 1E-02 1E-03 1E-04 1E-05 1E-06 1E-07 1E-08
Significance scale
(Student t-test)
p1: each biol. pept. vs. all random pept. across exp.
p2: each biol. pept. vs. ave. random pept. per exp. (paired)
p3: each biol. pept. vs. all YST-free pept. across exp.
p4: each biol. pept. vs. ave. YST-free pept. per exp. (paired)
p5: each biol. pept. vs. all ref. pept. across exp.
p6: each biol. pept. vs. ave. ref. pept. per exp. (paired)

Fig. 12 (part 2)

h

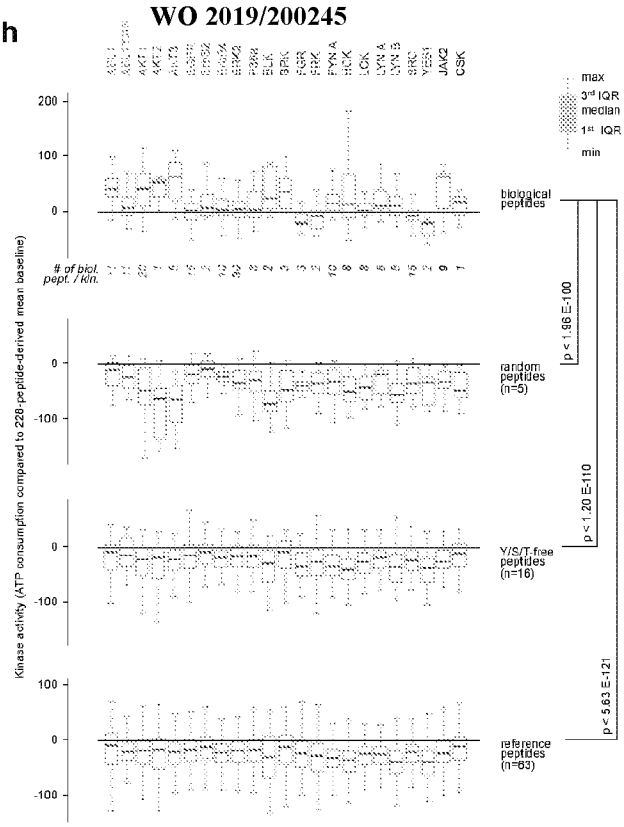

i

Kinase family	Kinase	# of biol. pept. per kinase	Significance (t-test) comparing all experimental pep. kinases: all biol. pept. vs. all (63) reference pept.	all biol. pept. vs. all (16) Y/S/T-free pept.	all biol. pept. vs. all (63) reference pept.
ABL	ABL1	11	1.75E-06	1.31E-13	3.33E-13
	ABL1(T315I)	11	1.23E-01	3.03E-01	1.03E-01
	ABL2	2	n.a.	n.a.	n.a.
AKT	AKT1	10	4.79E-06	1.39E-24	3.84E-11
	AKT2	1	2.20E-02	2.23E-02	3.06E-02
	AKT3	5	4.40E-02	9.53E-10	6.62E-11
ERBB	EGFR	15	4.59E-01	1.05E-01	3.65E-01
	ERBB2	2	7.01E-02	2.16E-02	3.92E-02
	ERBB4	10	5.93E-03	7.44E-04	4.33E-03
MAPK	ERK2	10	1.83E-09	9.81E-10	6.55E-11
	p38	8	4.29E-05	4.79E-03	4.05E-04
SRC	BLK	2	8.12E-05	3.02E-03	7.33E-03
	BRK	3	2.12E-04	9.45E-03	6.30E-03
	FGR	3	4.93E-01	9.77E-01	3.37E-01
	FRK	2	4.55E-01	9.07E-01	7.30E-01
	FYN A	10	2.89E-08	1.05E-19	2.09E-21
	HCK	8	8.29E-11	3.61E-15	8.42E-22
	LCK	8	4.92E-04	9.57E-05	8.36E-06
	LYN A	9	2.62E-07	1.12E-13	8.77E-15
	LYN B	9	9.65E-10	5.28E-04	8.87E-07
	SRC	15	5.97E-05	1.67E-02	1.32E-01
	SRMS	0	n.a.	n.a.	n.a.
	YES1	2	5.80E-01	9.41E-01	3.25E-01
	JAK2	2	7.80E-09	2.85E-13	7.22E-13
	CSK	1	5.23E-02	4.80E-01	8.00E-01

Significance (t-test) comparing all experimental pep. kinases

j

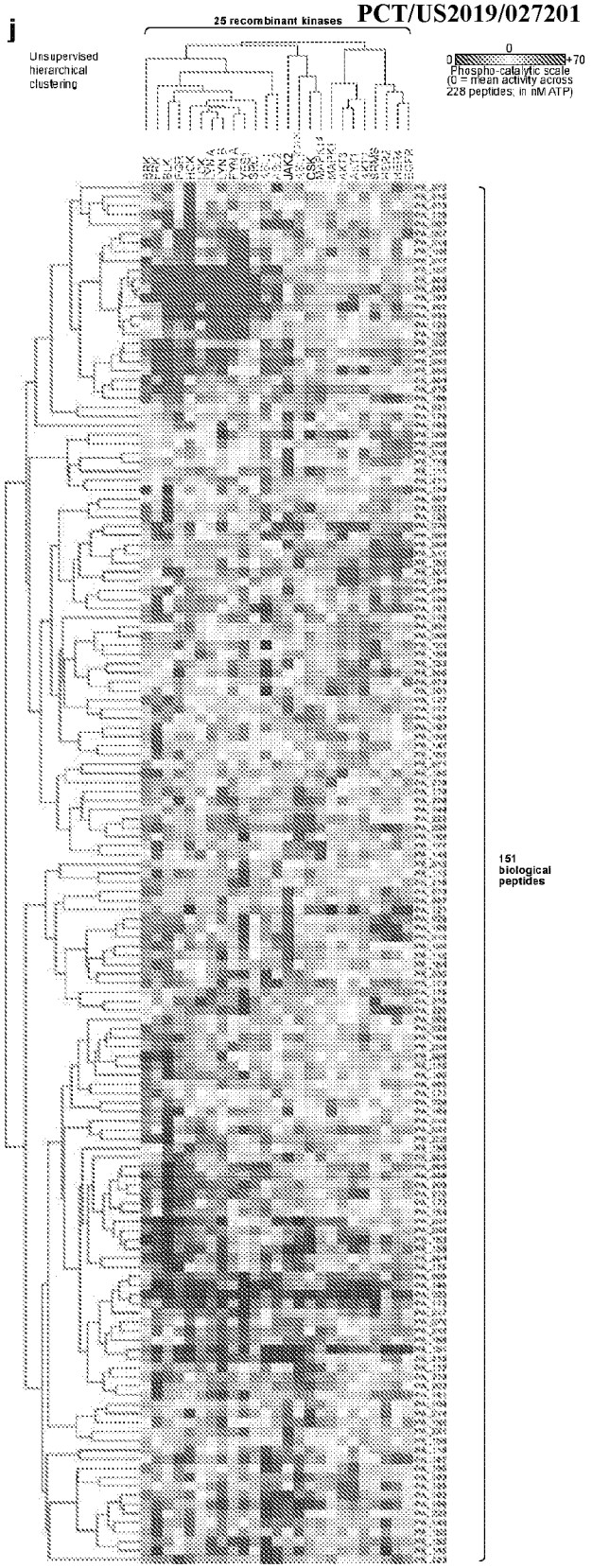

Fig. 12 (part 3)

a

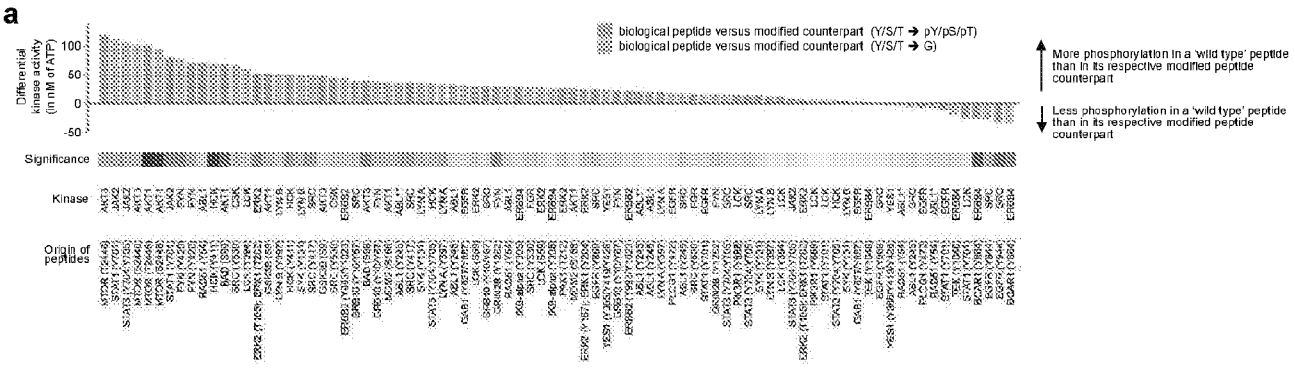

b

Comparison of Tyrosine Kinases' activity profiles, measured in presence of different peptide classes (Student t-test, unpaired)	Y-free Reference peptides; 4772 data points; Ave. activity = -15.9	Y-free Biological peptides; 1496 data points; Ave. activity = -6.6
Biological target peptides of Tyr. Kin.; 691 data points; Ave. activity = 11.1	8.81E-65	2.70E-41

Comparison of Serine/Threonine Kinases' activity profiles, measured in presence of different peptide classes (Student t-test, unpaired)	S/T-free Reference peptides; 906 data points; Ave. activity = -18.1	S/T-free Biological peptides; 735 data points; Ave. activity = 2.1
Biological target peptides of Ser/Thr. Kin.; 499 data points; Ave. activity = 30.9	1.57E-55	2.37E-16

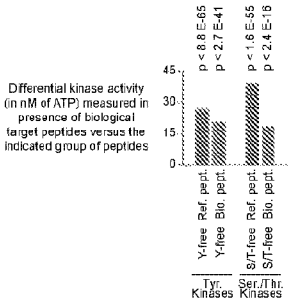

c

Comparison of Tyrosine Kinases' activity profiles, measured in presence of different peptide classes (Student t-test; unpaired)	Y- Ref. pept. (n=63); 4772 data points; Ave. activity = -15.9	Y+ Ref. pept. (n=10); 894 data points; Ave. activity = -11.2	Y- Bio&Con pept. (n=54); 4830 data points; Ave. activity = -6.6
Y+ Bio&Con pept. (n=111); 10391 data points; Ave. activity = 18.7	0.00E+00	1.62E-68	8.81E-217

Comparison of Serine/Threonine Kinases' activity profiles, measured in presence of different peptide classes (Student t-test; unpaired)	S/T- Ref. pept. (n=59); 820 data points; Ave. activity = -20.8	S/T+ Ref. pept. (n=34); 992 data points; Ave. activity = -8.2	S/T- Bio&Con pept. (n=34); 966 data points; Ave. activity = 2.6
S/T+ Bio&Con pept. (n=131); 3734 data points; Ave. activity = 12.3	1.68E-111	1.90E-47	6.68E-39

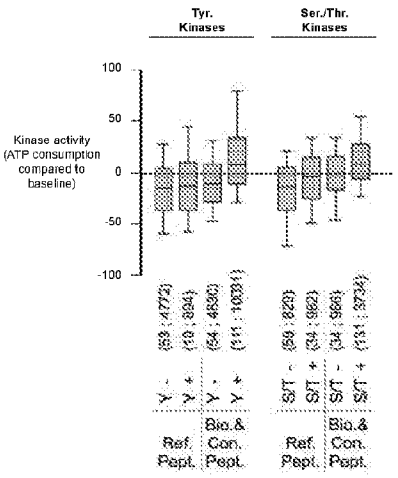

Fig. 13

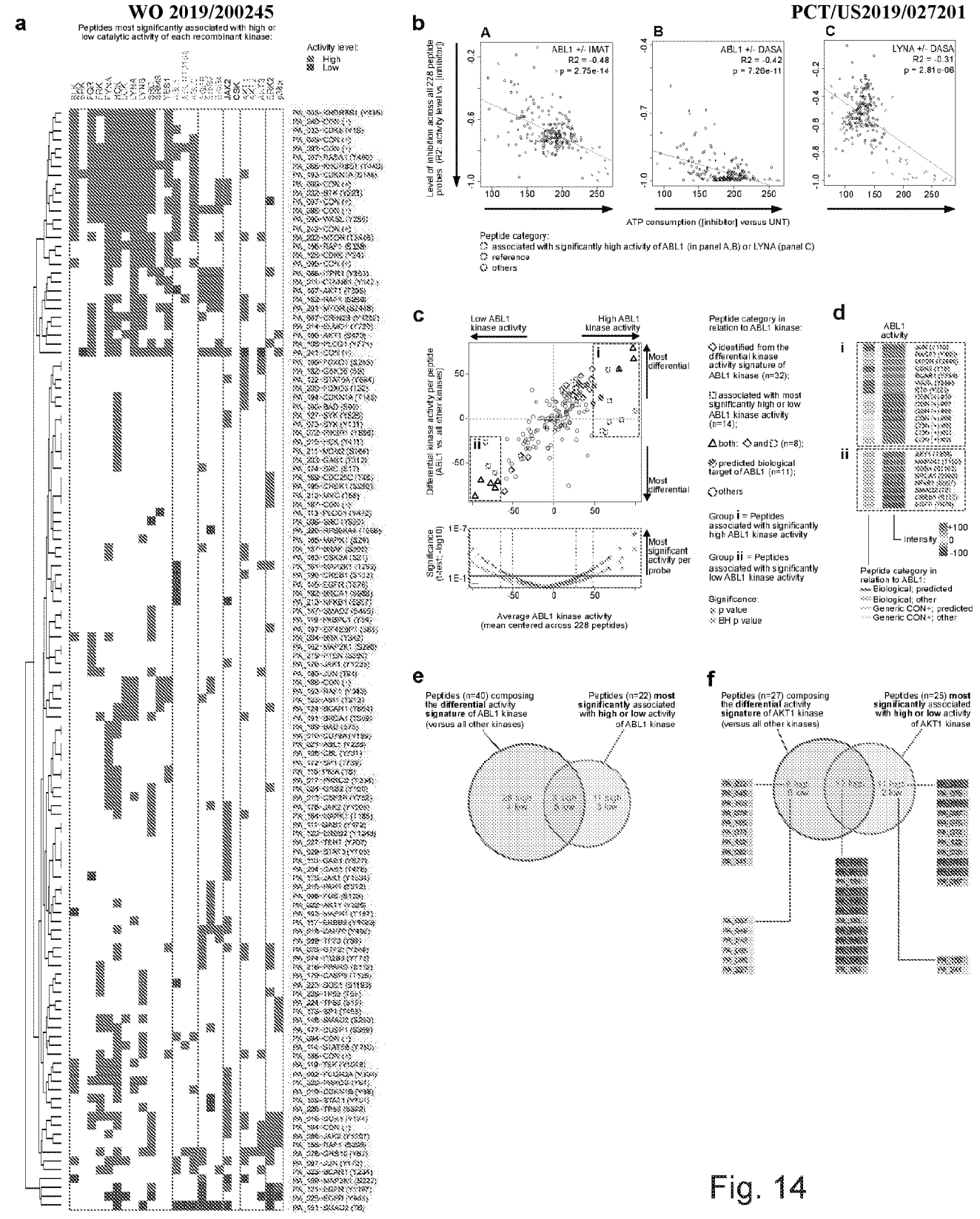
a
Peptides most significantly associated with high or low catalytic activity of each recombinant kinase:
Activity level:
High
Low
b
A
ABL1 +/- IMAT
R2 = -0.48
p = 2.75e-14
B
ABL1 +/- DASA
R2 = -0.42
p = 7.20e-11
C
LYNA +/- DASA
R2 = -0.31
p = 2.81e-06
Level of inhibition across all 228 peptide probes (R2: activity level vs. [inhibitor])
ATP consumption ([inhibitor] versus UNT)
Peptide category:
associated with significantly high activity of ABL1 (in panel A,B) or LYNA (panel C)
reference
others
c
Low ABL1 kinase activity
High ABL1 kinase activity
Differential kinase activity per peptide (ABL1 vs. all other kinases)
Most differential
Most differential
Significance (t-test, -log10)
Most significant activity per probe
Average ABL1 kinase activity (mean centered across 228 peptides)
Peptide category in relation to ABL1 kinase:
identified from the differential kinase activity signature of ABL1 kinase (n=32);
associated with most significantly high or low ABL1 kinase activity (n=14);
both: and (n=8);
predicted biological target of ABL1 (n=11);
others
Group i = Peptides associated with significantly high ABL1 kinase activity
Group ii = Peptides associated with significantly low ABL1 kinase activity
Significence:
p value
BH p value
d
ABL1 activity
Intensity
+100
0
-100
Peptide category in relation to ABL1:
Biological; predicted
Biological; other
Generic CON+; predicted
Generic CON+; other
e
Peptides (n=40) composing the differential activity signature of ABL1 kinase (versus all other kinases)
Peptides (n=22) most significantly associated with high or low activity of ABL1 kinase
f
Peptides (n=27) composing the differential activity signature of AKT1 kinase (versus all other kinases)
Peptides (n=25) most significantly associated with high or low activity of AKT1 kinase

Fig. 14

a

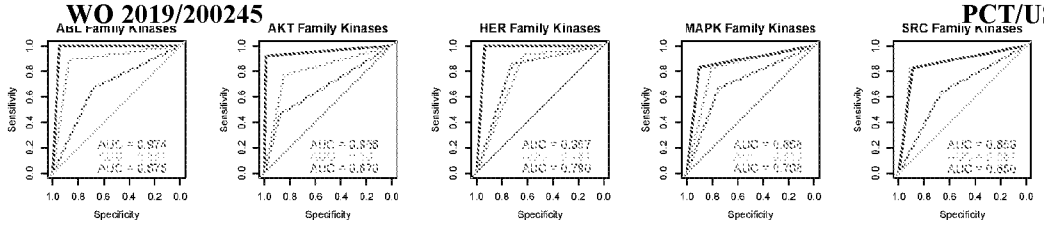
AKT Family Kinases
HER Family Kinases
MAPK Family Kinases
SRC Family Kinases
Sensitivity
Specificity

b

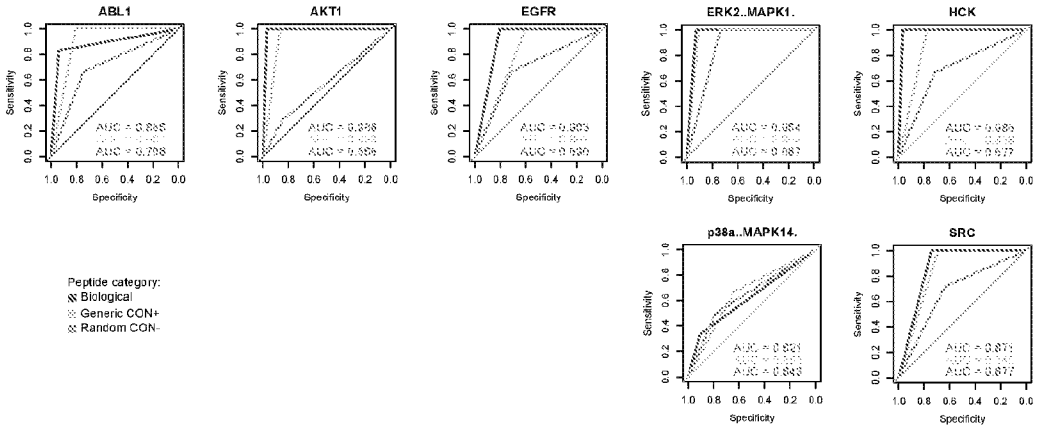
ABL1
AKT1
EGFR
ERK2..MAPK1.
HCK
p38a..MAPK14.
SRC
Sensitivity
Specificity
Peptide category:
Biological
Generic CON+
Random CON-

c

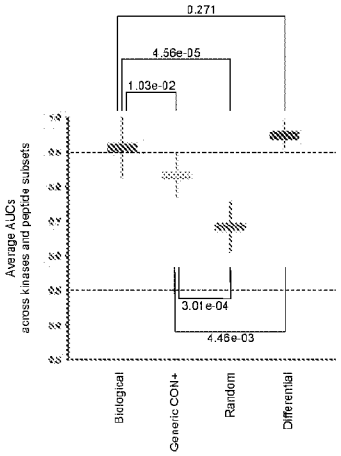
0.271
4.56e-05
1.03e-02
3.01e-04
4.46e-03
Average AUCs
across kinases and peptide subsets
Biological
Generic CON+
Random
Differential

Fig. 15

a

IC50 values	Imatinib (uM)	Dasatinib (nM)	Staurosporine (uM)
ABL1	~0.2	~1	~0.4
ABL1 (T315I)	No effect	No or limited effect	~0.35
LYN A	100	~9	~0.02
AKT1	No effect	No effect	~0.04

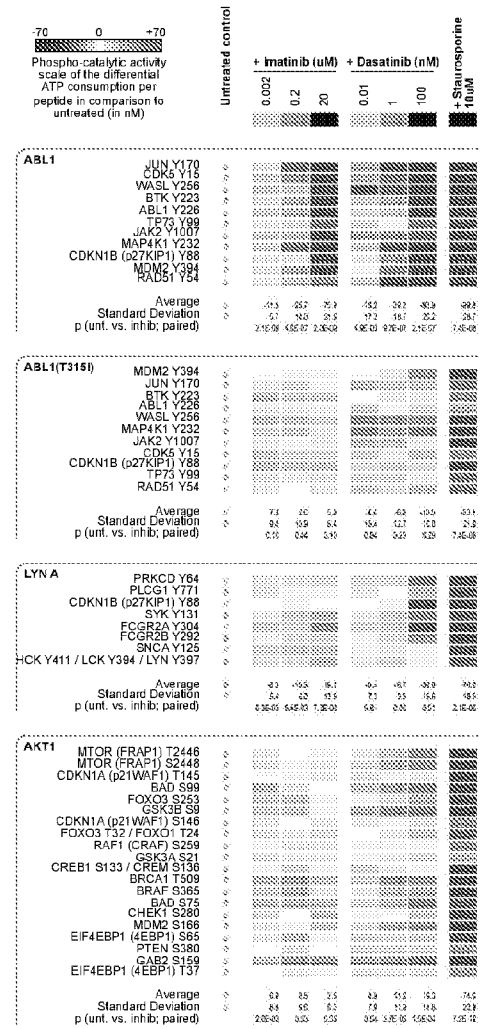

d

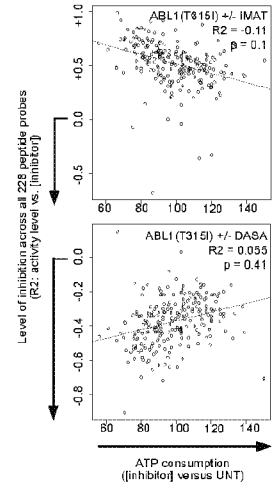

e

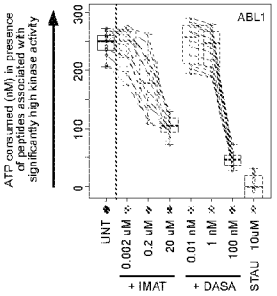

b

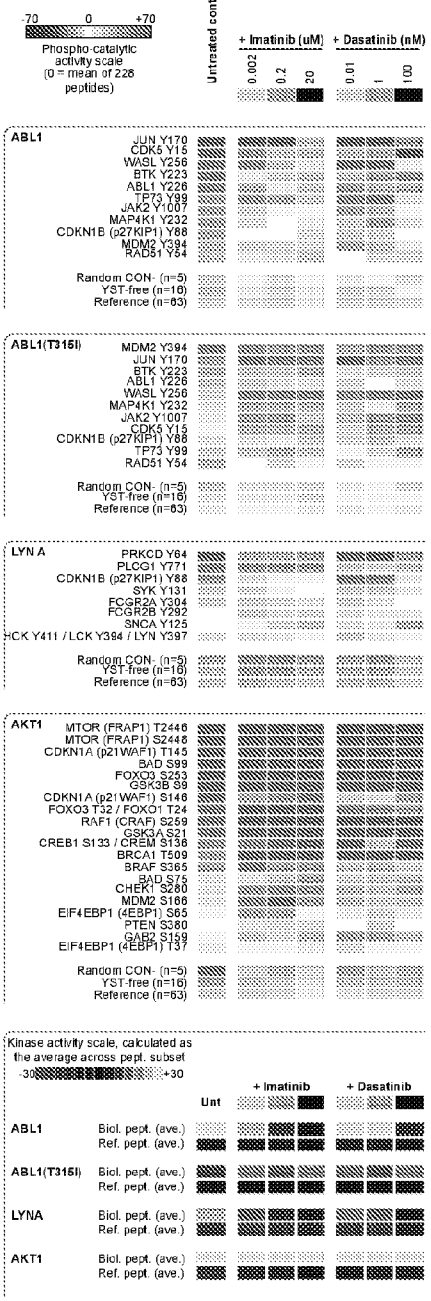

Fig. 16

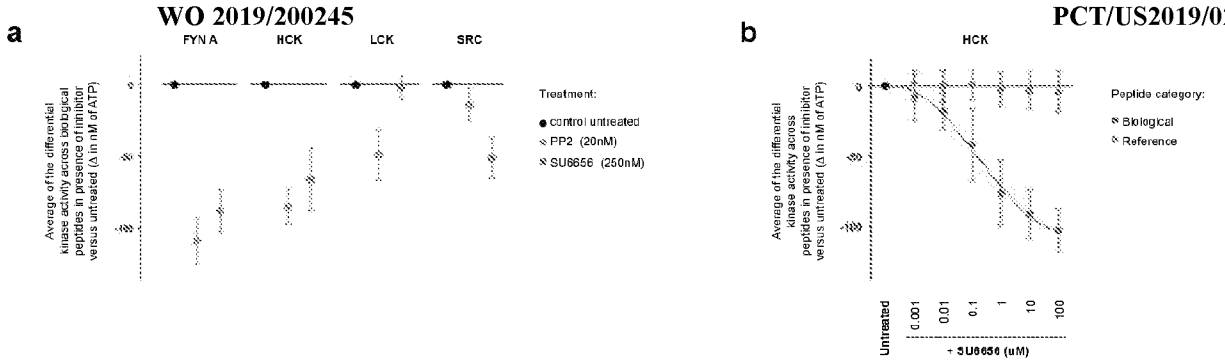
a
FYN A
HCK
LCK
SRC
Average of the differential kinase activity across biological peptides in presence of inhibitor versus untreated (Δ in nM of ATP)
0
-100
-200
Treatment:
control untreated
PP2 (20nM)
SU6656 (250nM)
b
HCK
Average of the differential kinase activity across peptides in presence of inhibitor versus untreated (Δ in nM of ATP)
0
-100
-200
Untreated
0.001
0.01
0.1
1
10
100
+ SU6656 (uM)
Peptide category:
Biological
Reference

Fig. 17

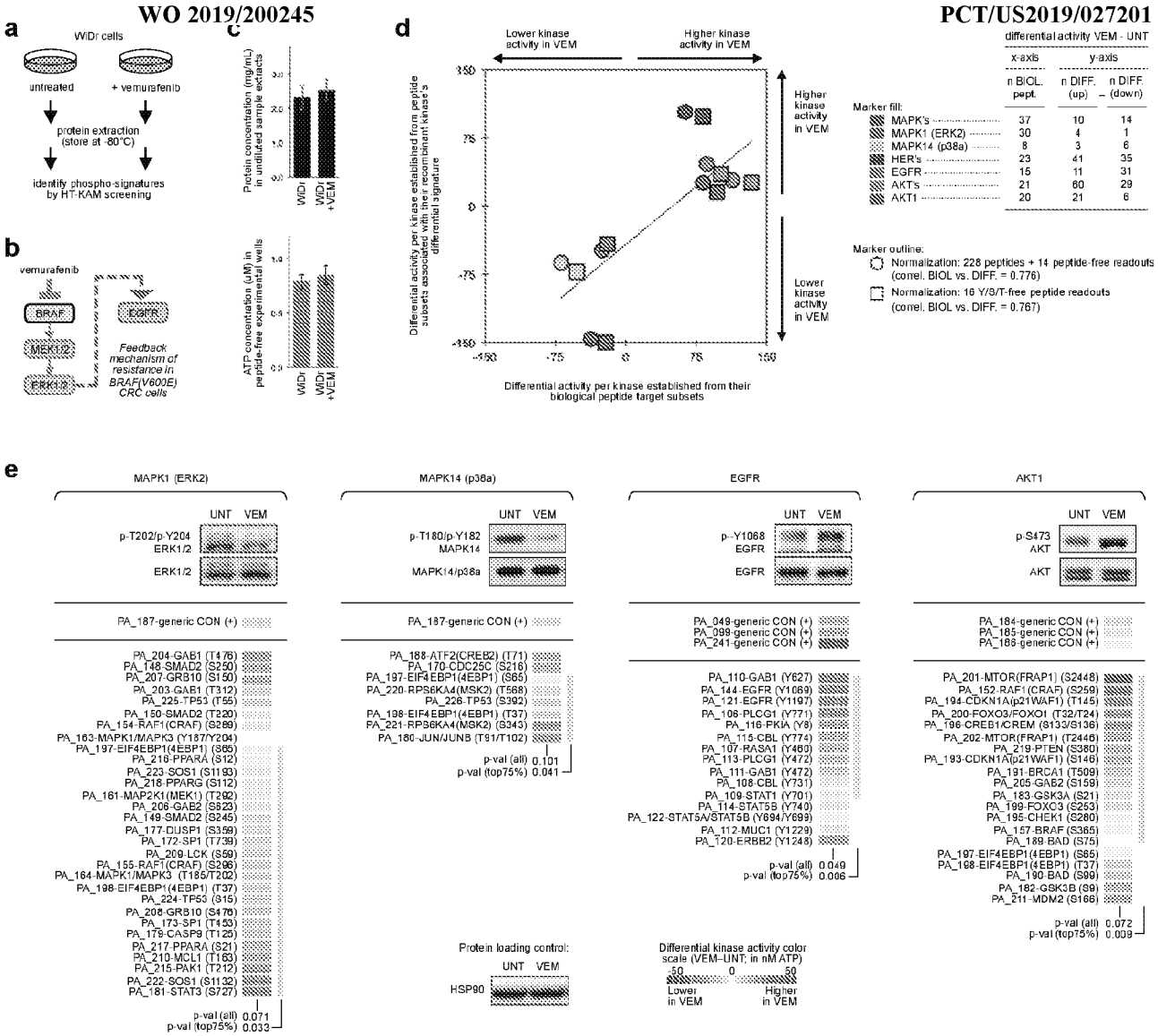
a
WiDr cells
untreated
+ vemurafenib
protein extraction (store at -80°C)
identify phospho-signatures by HT-KAM screening
c
Protein concentration (mg/mL) in undiluted sample extracts
WiDr
WiDr +VEM
b
vemurafenib
BRAF
EGFR
MEK1/2
ERK1/2
Feedback mechanism of resistance in BRAF(V600E) CRC cells
ATP concentration (uM) in peptide-free experimental wells
d
Lower kinase activity in VEM
Higher kinase activity in VEM
Differential activity per kinase established from peptide subsets associated with their recombinant kinase's differential signature
Differential activity per kinase established from their biological peptide target subsets
differential activity VEM - UNT
x-axis
y-axis
n BIOL. pept.
n DIFF. (up)
n DIFF. (down)
Marker fill:
MAPK's 37 10 14
MAPK1 (ERK2) 30 4 1
MAPK14 (p38a) 8 3 6
HER's 23 41 35
EGFR 15 11 31
AKT's 21 60 29
AKT1 20 21 6
Marker outline:
Normalization: 228 peptides + 14 peptide-free readouts (correl. BIOL vs. DIFF. = 0.776)
Normalization: 16 Y/S/T-free peptide readouts (correl. BIOL vs. DIFF. = 0.767)
e
MAPK1 (ERK2)
MAPK14 (p38a)
EGFR
AKT1
UNT VEM
p-T202/p-Y204 ERK1/2
ERK1/2
p-T180/p-Y182 MAPK14
MAPK14/p38a
p-Y1068 EGFR
EGFR
p-S473 AKT
AKT
PA_187-generic CON (+)
PA_204-GAB1 (T476)
PA_148-SMAD2 (S250)
PA_207-GRB10 (S150)
PA_203-GAB1 (T312)
PA_225-TP53 (T55)
PA_150-SMAD2 (T220)
PA_154-RAF1(CRAF) (S289)
PA_163-MAPK1/MAPK3 (Y187/Y204)
PA_197-EIF4EBP1(4EBP1) (S65)
PA_216-PPARA (S12)
PA_223-SOS1 (S1193)
PA_218-PPARG (S112)
PA_161-MAP2K1(MEK1) (T292)
PA_206-GAB2 (S323)
PA_149-SMAD2 (S245)
PA_177-DUSP1 (S359)
PA_172-SP1 (T739)
PA_209-LCK (S59)
PA_155-RAF1(CRAF) (S296)
PA_164-MAPK1/MAPK3 (T185/T202)
PA_198-EIF4EBP1(4EBP1) (T37)
PA_224-TP53 (S15)
PA_208-GRB10 (S476)
PA_173-SP1 (T453)
PA_179-CASP9 (T125)
PA_217-PPARA (S21)
PA_210-MCL1 (T163)
PA_215-PAK1 (T212)
PA_222-SOS1 (S1132)
PA_181-STAT3 (S727)
p-val (all) 0.071
p-val (top75%) 0.033
PA_187-generic CON (+)
PA_188-ATF2(CREB2) (T71)
PA_170-CDC25C (S216)
PA_197-EIF4EBP1(4EBP1) (S65)
PA_220-RPS6KA4(MSK2) (T568)
PA_226-TP53 (S392)
PA_198-EIF4EBP1(4EBP1) (T37)
PA_221-RPS6KA4(MSK2) (S343)
PA_180-JUN/JUNB (T91/T102)
p-val (all) 0.101
p-val (top75%) 0.041
PA_049-generic CON (+)
PA_099-generic CON (+)
PA_241-generic CON (+)
PA_110-GAB1 (Y627)
PA_144-EGFR (Y1069)
PA_121-EGFR (Y1197)
PA_106-PLCG1 (Y771)
PA_116-PKIA (Y8)
PA_115-CBL (Y774)
PA_107-RASA1 (Y460)
PA_113-PLCG1 (Y472)
PA_111-GAB1 (Y472)
PA_108-CBL (Y731)
PA_109-STAT1 (Y701)
PA_114-STAT5B (Y740)
PA_122-STAT5A/STAT5B (Y694/Y699)
PA_112-MUC1 (Y1229)
PA_120-ERBB2 (Y1248)
p-val (all) 0.049
p-val (top75%) 0.006
PA_184-generic CON (+)
PA_185-generic CON (+)
PA_186-generic CON (+)
PA_201-MTOR(FRAP1) (S2448)
PA_152-RAF1(CRAF) (S259)
PA_194-CDKN1A(p21WAF1) (T145)
PA_200-FOXO3/FOXO1 (T32/T24)
PA_196-CREB1/CREM (S133/S136)
PA_202-MTOR(FRAP1) (T2446)
PA_219-PTEN (S380)
PA_193-CDKN1A(p21WAF1) (S146)
PA_191-BRCA1 (T509)
PA_205-GAB2 (S159)
PA_183-GSK3A (S21)
PA_199-FOXO3 (S253)
PA_195-CHEK1 (S280)
PA_157-BRAF (S365)
PA_189-BAD (S75)
PA_197-EIF4EBP1(4EBP1) (S65)
PA_198-EIF4EBP1(4EBP1) (T37)
PA_190-BAD (S99)
PA_182-GSK3B (S9)
PA_211-MDM2 (S166)
p-val (all) 0.072
p-val (top75%) 0.009
Protein loading control:
HSP90
Differential kinase activity color scale (VEM–UNT; in nM ATP)
-50 0 50
Lower in VEM
Higher in VEM
f
Lower amount of phospho-protein in VEM
Higher amount of phospho-protein in VEM
Higher kinase activity in VEM
Lower kinase activity in VEM
Mean differential activity per kinase established from tier generic positive control peptides, or biological peptides, or most differential peptides
Change (fold) in phospho-protein amount established from western blot detection, and normalized to HSP90 and non-phospho-protein (centered on -1 or +1 fold)
Symbol and number of peptides per peptide category and per kinase
CON+
BIOL.
DIFF. (up;down)
Marker fill:
MEK1 n.a. 6 n.t
MAPK1 (ERK2) 1 30 (4;1)
MAPK14 (p38a) 1 8 (3;6)
EGFR 3 15 (11;31)
AKT1 3 20 (21;6)
GSK3B n.a. 5 n.t
RPS6KB1 n.a. 4 n.t
PDPK1 n.a. 4 n.t
SGK1 2 6 n.t
PRKCA n.a. 7 n.t
PKN's n.a. 4 n.t
RPS6KA's 1 7 n.t
Correl. kin. activity vs. prot. amount: 0.464 0.744 0.831
Trend line: dash (-) solid (+) not shown
normalization: 228 peptides + 13 peptide-free readouts;
n.a. not available;
n.t. not tested
g
vemurafenib
AKT1
PDPK1
GSK3B
PKN1
SGK
PRKCA

Fig. 18

a

Peptides from the EGFR pathway:

- ** * PA_146-EGFR (Y869)
- ** ** PA_144-EGFR (Y1069)
- * PA_121-EGFR (Y1197)
- PA_145-EGFR (T678)
- PA_025-EGFR (Y944)
- ** ** PA_069-PLCG1 (Y1253)
- PA_106-PLCG1 (Y771)
- PA_113-PLCG1 (Y472)
- ** * PA_110-GAB1 (Y627)
- ** PA_204-GAB1 (T476)
- PA_111-GAB1 (Y472)
- PA_203-GAB1 (T312)
- * PA_115-CBL (Y774)
- PA_108-CBL (Y731)
- PA_207-GRB10 (S150)
- PA_076-GRB10 (Y67)
- PA_208-GRB10 (S476)

Significance of the differential activities (VEM–UNT) measured in presence of individual peptides and across all experimental repeats:
p-val<0.05: #
p-val<0.01: ##

Differential kinase activity color scale (VEM–UNT):

-50 0 50

Lower in VEM — Higher in VEM

b

Peptides from the TGFBR pathway:

- * PA_147-SMAD2 (S465)
- PA_148-SMAD2 (S250)
- PA_151-SMAD2 (T8)
- PA_150-SMAD2 (T220)
- PA_149-SMAD2 (S245)

c

Peptides from transcription factors:

- ** PA_198-CREB1/CREM (S133/S136)
- PA_188-ATF2(CREB2) (T71)
- PA_200-FOXO3/FOXO1 (T32/T24)
- PA_199-FOXO3 (S253)
- PA_009-FOS (T232)
- PA_008-FOS (S133)
- PA_109-STAT1 (Y701)
- PA_114-STAT5B (Y740)
- PA_122-STAT5A/STAT5B (Y694/Y699)
- * PA_029-STAT3 (Y705)
- ** PA_181-STAT3 (S727)
- PA_172-SP1 (T739)
- PA_173-SP1 (T453)
- * PA_087-JUN (Y170)
- PA_180-JUN/JUNB (T91/T102)
- ** PA_213-NFKB1 (S907)
- ** PA_212-MYC (T58)

d

Peptides from kinases:

- ** ** PA_201-MTOR(FRAP1) (S2448)
- PA_202-MTOR(FRAP1) (T2446)

UNT VEM

p-S2448 MTOR

MTOR

- * PA_086-JAK2 (Y1007)
- * PA_175-JAK1 (Y1034)
- PA_176-JAK1 (Y1035)
- PA_178-JAK2 (Y1008)

e

Peptides from phosphatases:

- PA_171-CDC25C (S214)
- PA_170-CDC25C (S216)
- PA_169-CDC25C (T48)
- PA_219-PTEN (S380)

Fig. 19

a

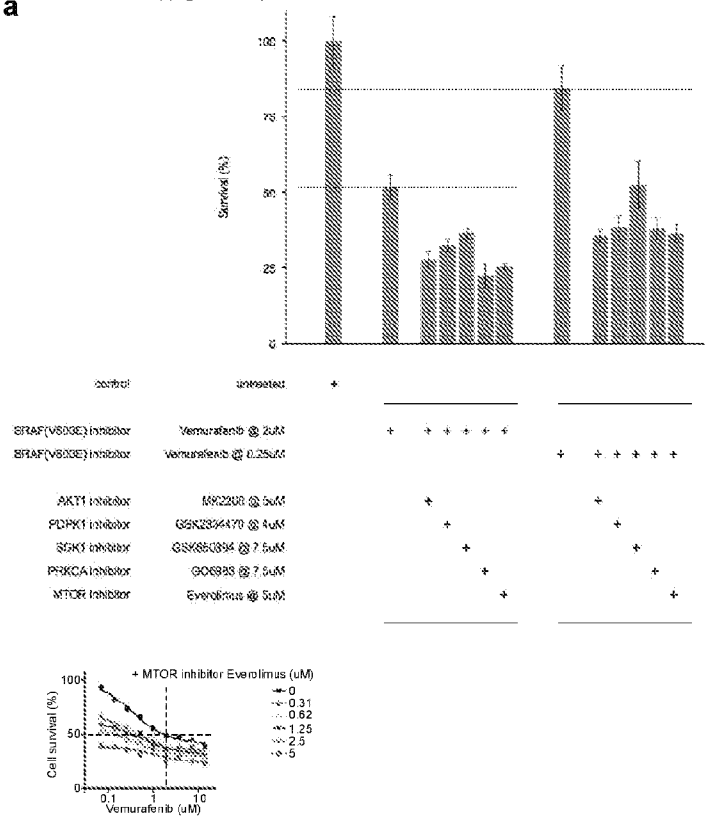

b

Characteristics of WiDr cell response to:

	Drug alone	Vemurafenib combined with the indicated inhibitor	
	(IC50; uM)	Drug interaction (two-way ANOVA p-val)	Combination index (@ IC50 concentrations)
AKT1 inhibitor	5.5	p<1E-10	0.6
PDPK1 inhibitor	4.5	p<1E-10	0.5
SGK1 inhibitor	12.5	p<1E-04	0.8
PRKCA inhibitor	15	p<1E-05	0.6
MTOR inhibitor	5	p<1E-05	0.7

c

Tested and validated inhibitors and BRAF(V600E) cell lines

Kinase targets	Inhibitors	Cell lines (§)
AKT1	MK2206	WiDr, HT29, RKO1
EGFR	Gefitinib (⌘)	WiDr, HT29
BRAF(V600E)	Vemurafenib (PLX4032)	WiDr, HT29, RKO1, 8505C
MTOR	Everolimus (RAD001)	WiDr, 8505C
PDPK1	GSK2334470, OSU-03012	WiDr, HT29
PRKCA	GO6983, Sotrastaurin	WiDr
SGK1	GSK650394	WiDr, HT29

⌘ used as control based on Prahallad A et al. 2012 Nature, and Corcoran RB et al. 2012 Cancer Discovery; § inhibitor effects we measured in the indicated cell lines were further corroborated using data from Garnett MJ 2012 Nature and Yang W 2013 NAR.

Fig. 20

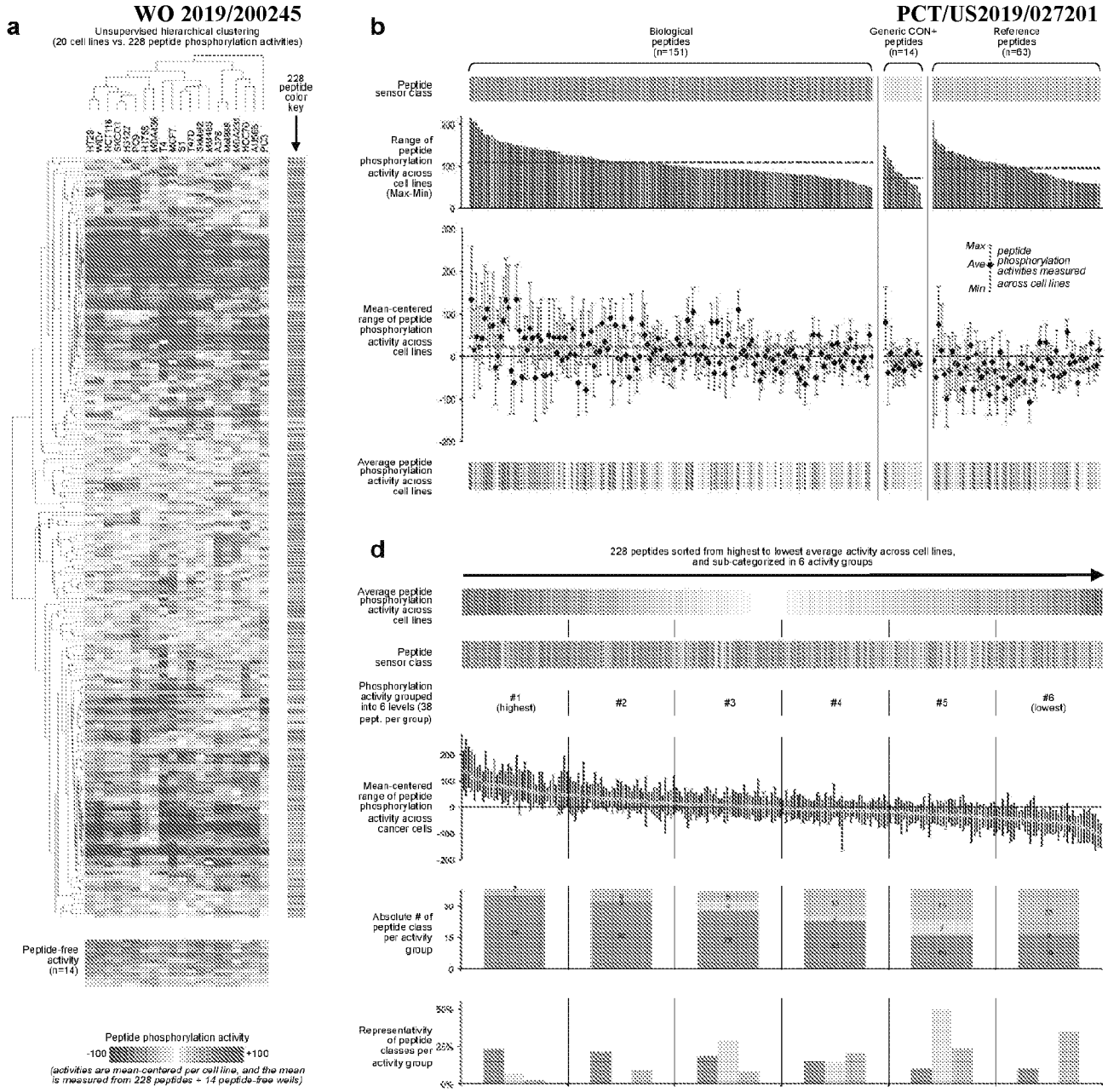

c

Measurements across cell lines & pept. class	Biol. pept.	CON+ pept.	Ref. pept.
Ave. range of activity (max-min)	100	77	99
Ave. level of activity	+15.5	-8.7	-25.8
% individual activity values above cells mean activity (i.e. >0)	62%	34%	26%

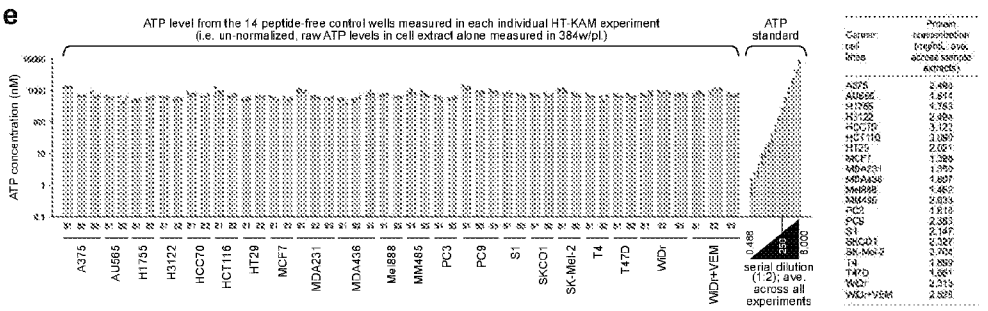

Fig. 21

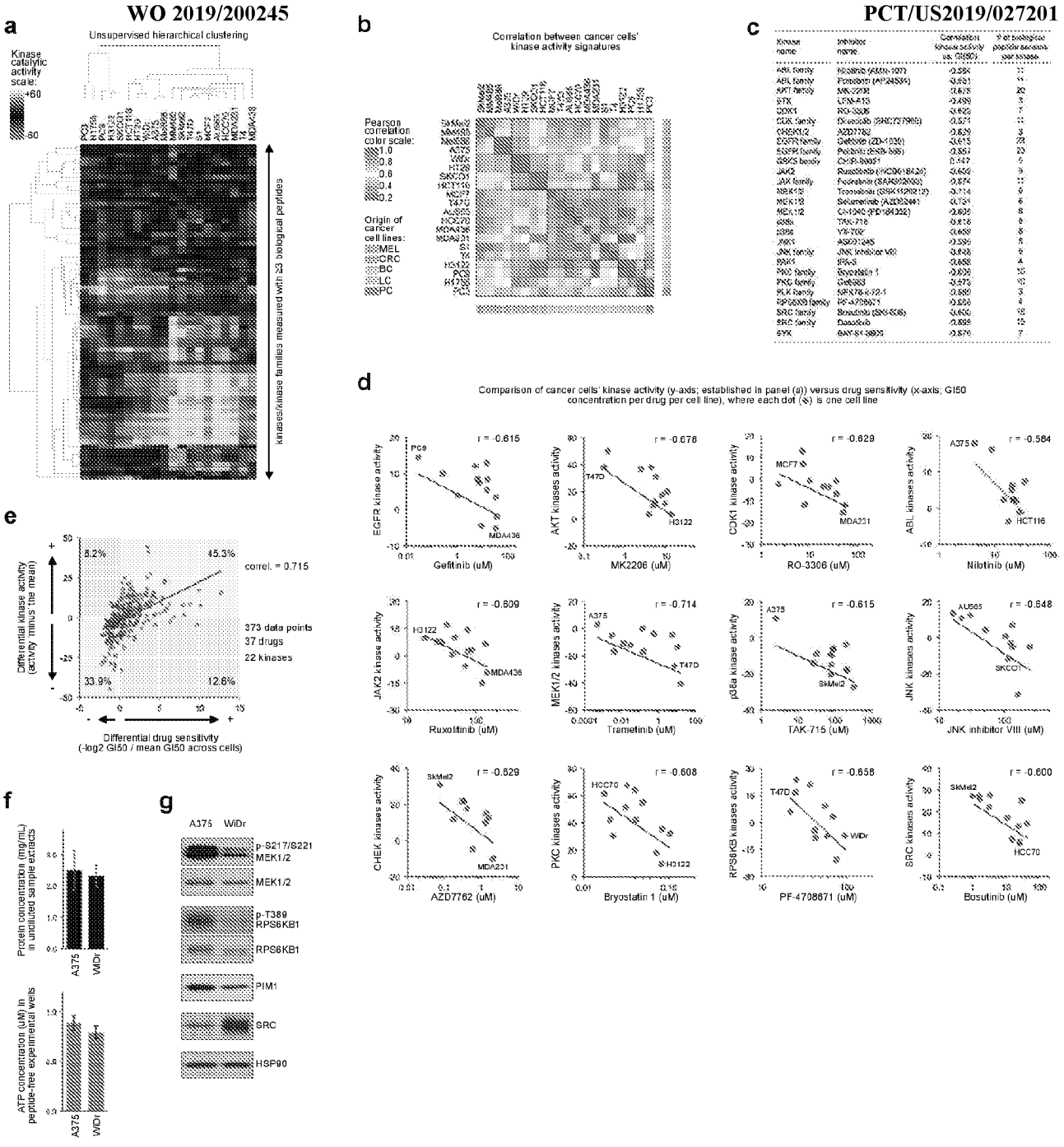
a
Unsupervised hierarchical clustering
Kinase catalytic activity scale:
+60
-60
kinases/kinase families measured with ≥3 biological peptides
b
Correlation between cancer cells' kinase activity signatures
Pearson correlation color scale:
1.0
0.8
0.6
0.4
0.2
Origin of cancer cell lines:
MEL
CRC
BC
LC
PC
c
d
Comparison of cancer cells' kinase activity (y-axis; established in panel (a)) versus drug sensitivity (x-axis; GI50 concentration per drug per cell line), where each dot (●) is one cell line
EGFR kinase activity
Gefitinib (uM)
r = -0.615
AKT kinases activity
MK2206 (uM)
r = -0.678
CDK1 kinase activity
RO-3306 (uM)
r = -0.629
ABL kinases activity
Nilotinib (uM)
r = -0.584
JAK2 kinase activity
Ruxolitinib (uM)
r = -0.609
MEK1/2 kinases activity
Trametinib (uM)
r = -0.714
p38a kinase activity
TAK-715 (uM)
r = -0.615
JNK kinases activity
JNK inhibitor VIII (uM)
r = -0.648
CHEK kinases activity
AZD7762 (uM)
r = -0.629
PKC kinases activity
Bryostatin 1 (uM)
r = -0.608
RPS6KB kinases activity
PF-4708671 (uM)
r = -0.658
SRC kinases activity
Bosutinib (uM)
r = -0.600
e
Differential kinase activity (activity minus the mean)
Differential drug sensitivity (-log2 GI50 / mean GI50 across cells)
8.2%
45.3%
33.9%
12.6%
correl. = 0.715
373 data points
37 drugs
22 kinases
f
Protein concentration (mg/mL) in undiluted sample extracts
ATP concentration (uM) in peptide-free experimental wells
A375
WiDr
g
A375
WiDr
p-S217/S221 MEK1/2
MEK1/2
p-T389 RPS6KB1
RPS6KB1
PIM1
SRC
HSP90

Fig. 22

a

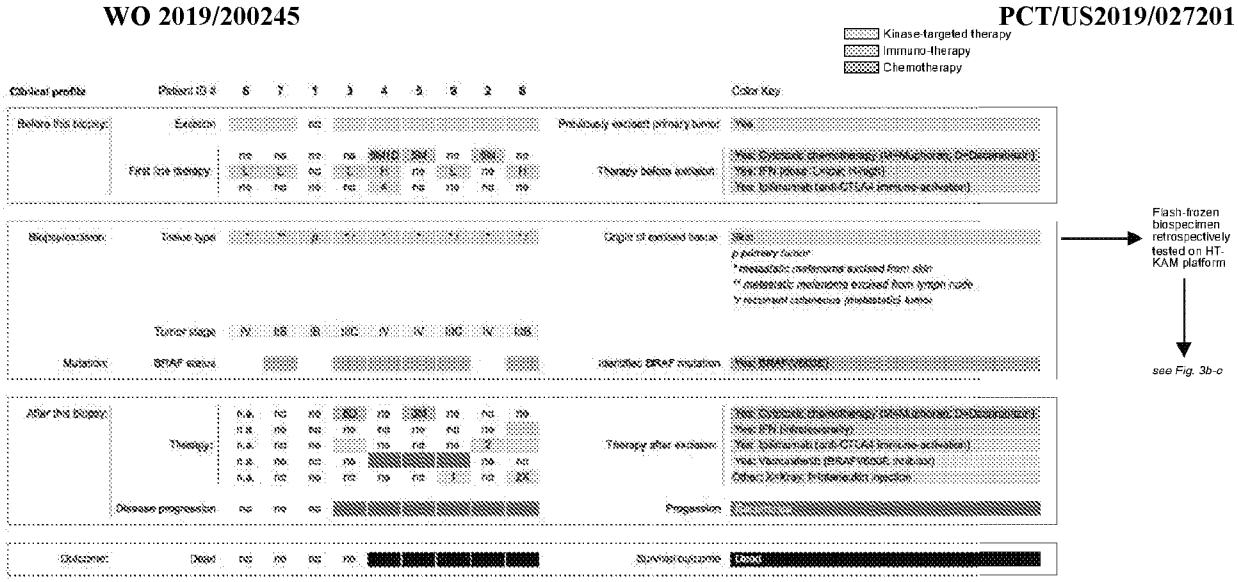
Kinase-targeted therapy
Immuno-therapy
Chemotherapy
Clinical profile
Color Key
Before this biopsy:
Excision
Previously excised primary tumor
First line therapy
Therapy before excision
Biopsy/excision
Tissue type
Origin of excised tissue
Tumor stage
Mutation
BRAF status
Identified BRaF mutation
After this biopsy:
Therapy
Therapy after excision
Disease progression
Progression
Outcome
Dead
Survival outcome
Flash-frozen biospecimen retrospectively tested on HT-KAM platform
see Fig. 3b-c

b

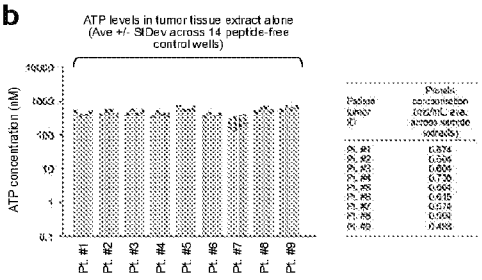
ATP levels in tumor tissue extract alone
(Ave +/- StDev across 14 peptide-free control wells)
ATP concentration (nM)
Pt. #1
Pt. #2
Pt. #3
Pt. #4
Pt. #5
Pt. #6
Pt. #7
Pt. #8
Pt. #9

Fig. 23

a

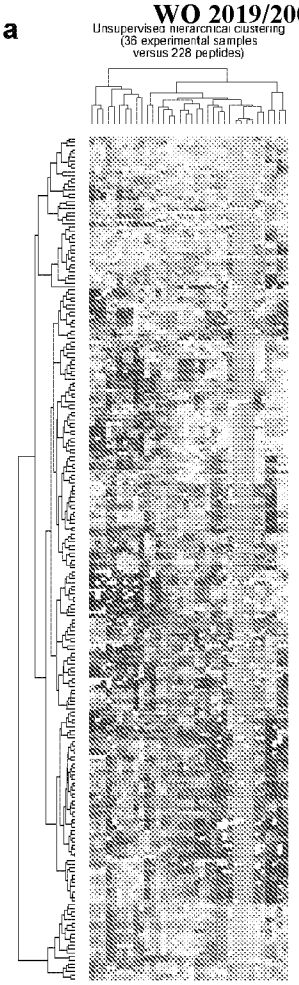

b

Technical variables	PC1: F-stat pval	PC2: F-stat pval
Patient	1.44E-06	0.226
Date of experiment	0.0938	0.171

Clinical variables	PC1: F-stat pval	PC2: F-stat pval
Survival	5.14E-06	0.028
Recurrence	2.31E-07	0.0815
BRAF status	0.0741	0.113

c

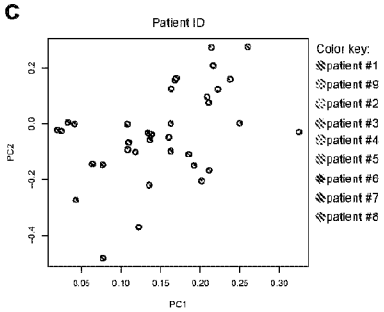

d

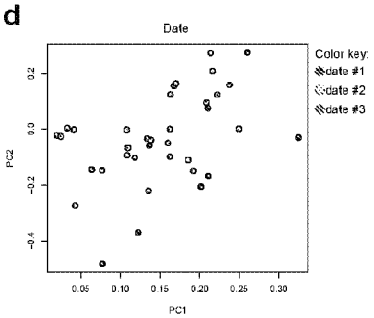

e

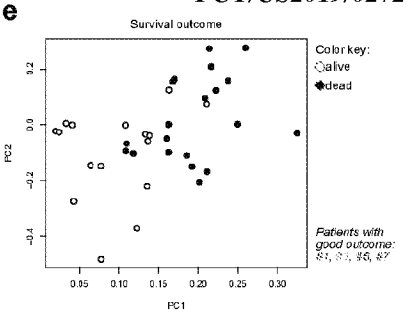

f

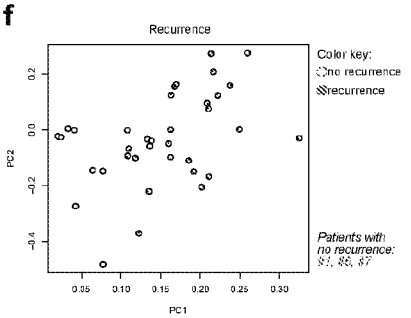

g

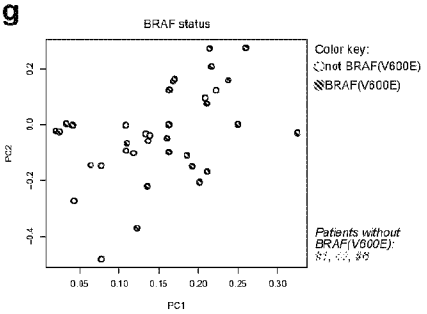

h

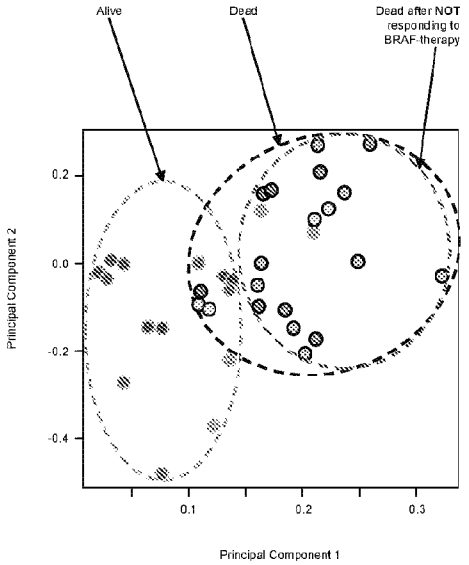

Patient color key:	vemurafenib treated:	vemurafenib resistant:
#1		
#9	Yes	Yes
#2 *		
#3		
#4 *	Yes	Yes
#5	Yes	Yes
#6		
#7		
#8 *		

* ipilimumab resistant

Fig. 24

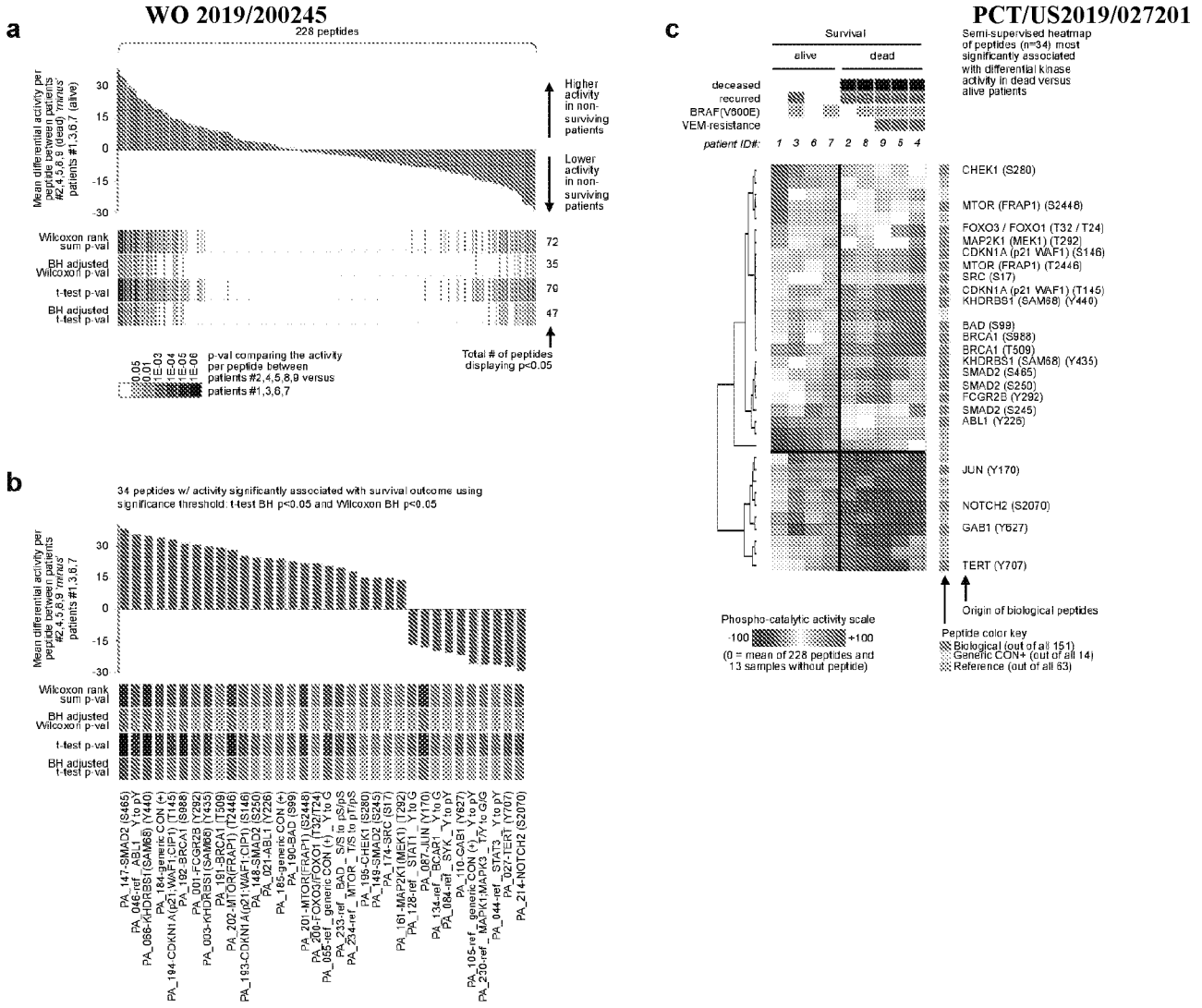
a
228 peptides
Mean differential activity per peptide between patients #2,4,5,8,9 versus patients #1,3,6,7 (alive)
Higher activity in non-surviving patients
Lower activity in non-surviving patients
Wilcoxon rank sum p-val
BH adjusted Wilcoxon p-val
t-test p-val
BH adjusted t-test p-val
72
35
70
47
p-val comparing the activity per peptide between patients #2,4,5,8,9 versus patients #1,3,6,7
Total # of peptides displaying p<0.05
b
34 peptides w/ activity significantly associated with survival outcome using significance threshold: t-test BH p<0.05 and Wilcoxon BH p<0.05
c
Survival
alive
dead
deceased
recurred
BRAF(V600E)
VEM-resistance
patient ID#:
Semi-supervised heatmap of peptides (n=34) most significantly associated with differential kinase activity in dead versus alive patients
CHEK1 (S280)
MTOR (FRAP1) (S2448)
FOXO3 / FOXO1 (T32 / T24)
MAP2K1 (MEK1) (T292)
CDKN1A (p21 WAF1) (S146)
MTOR (FRAP1) (T2446)
SRC (S17)
CDKN1A (p21 WAF1) (T145)
KHDRBS1 (SAM68) (Y440)
BAD (S99)
BRCA1 (S988)
BRCA1 (T509)
KHDRBS1 (SAM68) (Y435)
SMAD2 (S465)
SMAD2 (S250)
FCGR2B (Y292)
SMAD2 (S245)
ABL1 (Y226)
JUN (Y170)
NOTCH2 (S2070)
GAB1 (Y627)
TERT (Y707)
Origin of biological peptides
Phospho-catalytic activity scale
-100
+100
(0 = mean of 228 peptides and 13 samples without peptide)
Peptide color key
Biological (out of all 151)
Generic CON+ (out of all 14)
Reference (out of all 63)

Fig. 25 (part 1)

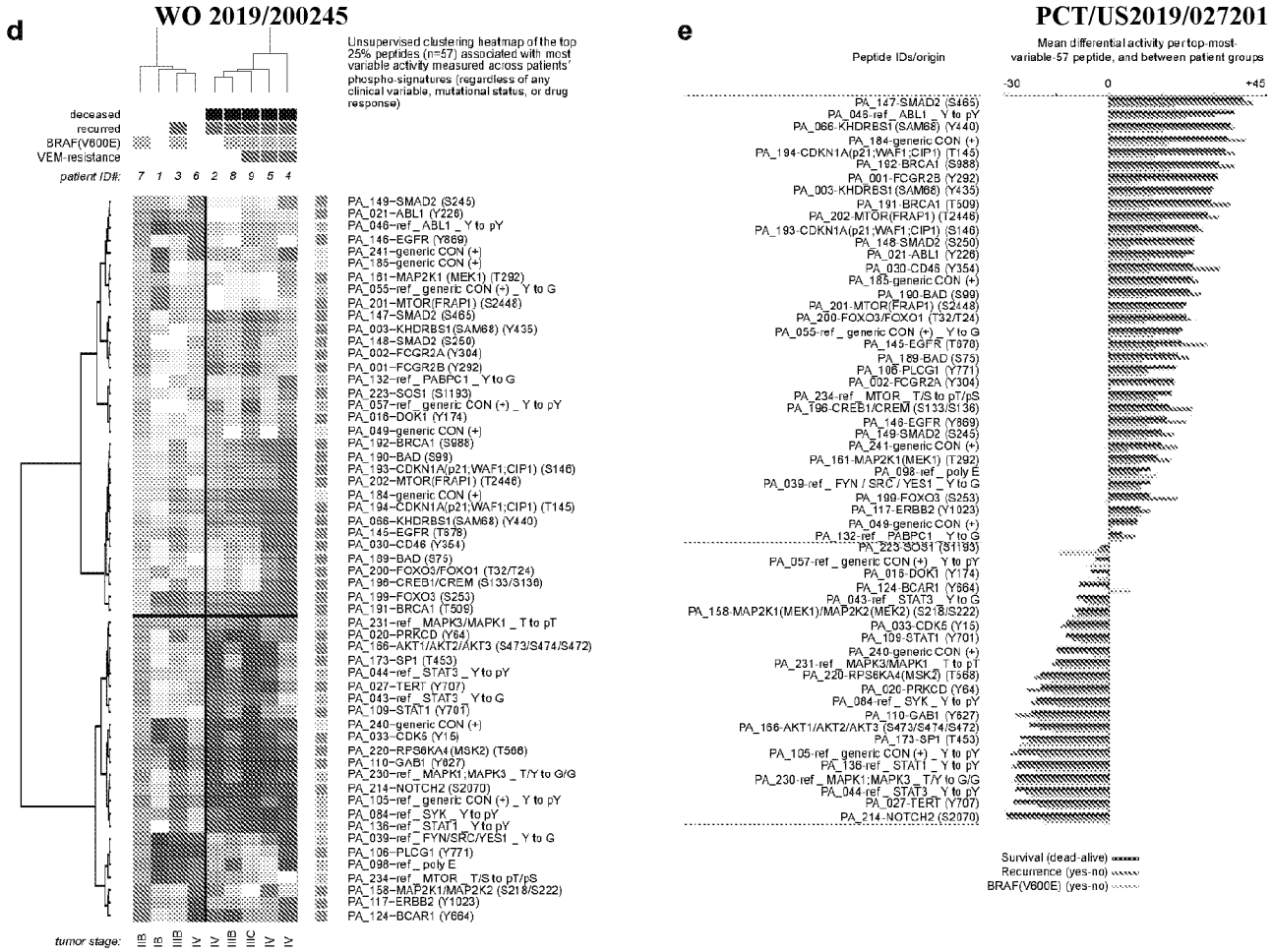
d
Unsupervised clustering heatmap of the top 25% peptides (n=57) associated with most variable activity measured across patients' phospho-signatures (regardless of any clinical variable, mutational status, or drug response)
deceased
recurred
BRAF(V600E)
VEM-resistance
patient ID#: 7 1 3 6 2 8 9 5 4
PA_149-SMAD2 (S245)
PA_021-ABL1 (Y226)
PA_046-ref _ ABL1 _ Y to pY
PA_146-EGFR (Y869)
PA_241-generic CON (+)
PA_185-generic CON (+)
PA_161-MAP2K1 (MEK1) (T292)
PA_055-ref _ generic CON (+) _ Y to G
PA_201-MTOR(FRAP1) (S2448)
PA_147-SMAD2 (S465)
PA_003-KHDRBS1(SAM68) (Y435)
PA_148-SMAD2 (S250)
PA_002-FCGR2A (Y304)
PA_001-FCGR2B (Y292)
PA_132-ref _ PABPC1 _ Y to G
PA_223-SOS1 (S1193)
PA_057-ref _ generic CON (+) _ Y to pY
PA_016-DOK1 (Y174)
PA_049-generic CON (+)
PA_192-BRCA1 (S988)
PA_190-BAD (S99)
PA_193-CDKN1A(p21;WAF1;CIP1) (S146)
PA_202-MTOR(FRAP1) (T2446)
PA_184-generic CON (+)
PA_194-CDKN1A(p21;WAF1;CIP1) (T145)
PA_066-KHDRBS1(SAM68) (Y440)
PA_145-EGFR (T878)
PA_030-CD46 (Y354)
PA_189-BAD (S75)
PA_200-FOXO3/FOXO1 (T32/T24)
PA_196-CREB1/CREM (S133/S136)
PA_199-FOXO3 (S253)
PA_191-BRCA1 (T509)
PA_231-ref _ MAPK3/MAPK1 _ T to pT
PA_020-PRKCD (Y64)
PA_166-AKT1/AKT2/AKT3 (S473/S474/S472)
PA_173-SP1 (T453)
PA_044-ref _ STAT3 _ Y to pY
PA_027-TERT (Y707)
PA_043-ref _ STAT3 _ Y to G
PA_109-STAT1 (Y701)
PA_240-generic CON (+)
PA_033-CDK5 (Y15)
PA_220-RPS6KA4(MSK2) (T568)
PA_110-GAB1 (Y627)
PA_230-ref _ MAPK1;MAPK3 _ T/Y to G/G
PA_214-NOTCH2 (S2070)
PA_105-ref _ generic CON (+) _ Y to pY
PA_084-ref _ SYK _ Y to pY
PA_136-ref _ STAT1 _ Y to pY
PA_039-ref _ FYN/SRC/YES1 _ Y to G
PA_106-PLCG1 (Y771)
PA_098-ref _ poly E
PA_234-ref _ MTOR _ T/S to pT/pS
PA_158-MAP2K1/MAP2K2 (S218/S222)
PA_117-ERBB2 (Y1023)
PA_124-BCAR1 (Y664)
tumor stage: IIB IB IIIB IV IV IIIB IIIC IV IV
e
Peptide IDs/origin
Mean differential activity per top-most-variable-57 peptide, and between patient groups
-30
0
+45
PA_147-SMAD2 (S465)
PA_046-ref _ ABL1 _ Y to pY
PA_066-KHDRBS1(SAM68) (Y440)
PA_184-generic CON (+)
PA_194-CDKN1A(p21;WAF1;CIP1) (T145)
PA_192-BRCA1 (S988)
PA_001-FCGR2B (Y292)
PA_003-KHDRBS1(SAM68) (Y435)
PA_191-BRCA1 (T509)
PA_202-MTOR(FRAP1) (T2446)
PA_193-CDKN1A(p21;WAF1;CIP1) (S146)
PA_148-SMAD2 (S250)
PA_021-ABL1 (Y226)
PA_030-CD46 (Y354)
PA_185-generic CON (+)
PA_190-BAD (S99)
PA_201-MTOR(FRAP1) (S2448)
PA_200-FOXO3/FOXO1 (T32/T24)
PA_055-ref _ generic CON (+) _ Y to G
PA_145-EGFR (T878)
PA_189-BAD (S75)
PA_106-PLCG1 (Y771)
PA_002-FCGR2A (Y304)
PA_234-ref _ MTOR _ T/S to pT/pS
PA_196-CREB1/CREM (S133/S136)
PA_146-EGFR (Y869)
PA_149-SMAD2 (S245)
PA_241-generic CON (+)
PA_161-MAP2K1(MEK1) (T292)
PA_098-ref _ poly E
PA_039-ref _ FYN / SRC / YES1 _ Y to G
PA_199-FOXO3 (S253)
PA_117-ERBB2 (Y1023)
PA_049-generic CON (+)
PA_132-ref _ PABPC1 _ Y to G
PA_223-SOS1 (S1193)
PA_057-ref _ generic CON (+) _ Y to pY
PA_016-DOK1 (Y174)
PA_124-BCAR1 (Y664)
PA_043-ref _ STAT3 _ Y to G
PA_158-MAP2K1(MEK1)/MAP2K2(MEK2) (S218/S222)
PA_033-CDK5 (Y15)
PA_109-STAT1 (Y701)
PA_240-generic CON (+)
PA_231-ref _ MAPK3/MAPK1 _ T to pT
PA_220-RPS6KA4(MSK2) (T568)
PA_020-PRKCD (Y64)
PA_084-ref _ SYK _ Y to pY
PA_110-GAB1 (Y627)
PA_166-AKT1/AKT2/AKT3 (S473/S474/S472)
PA_173-SP1 (T453)
PA_105-ref _ generic CON (+) _ Y to pY
PA_136-ref _ STAT1 _ Y to pY
PA_230-ref _ MAPK1;MAPK3 _ T/Y to G/G
PA_044-ref _ STAT3 _ Y to pY
PA_027-TERT (Y707)
PA_214-NOTCH2 (S2070)
Survival (dead-alive)
Recurrence (yes-no)
BRAF(V600E) (yes-no)

Fig. 25 (part 2)

a

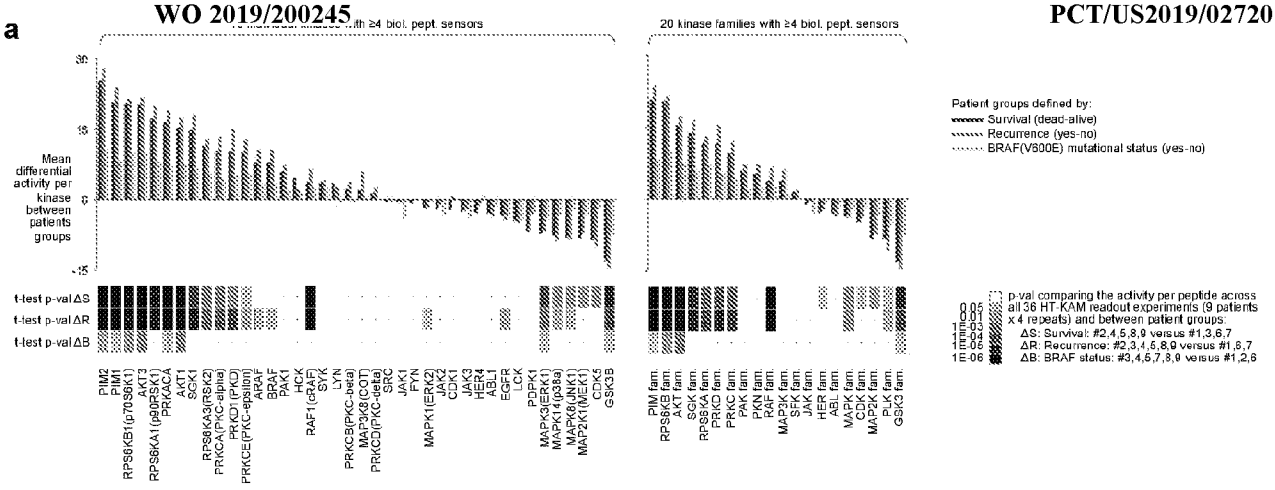

b

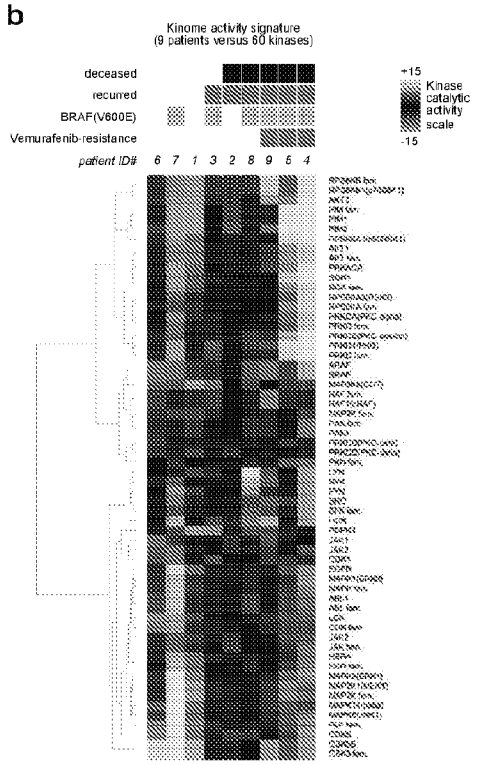

c

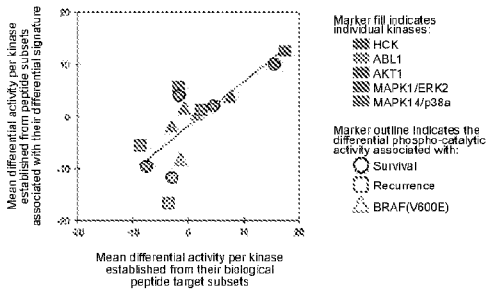

d

Significance of peptide-derived kinase activity signatures associated with survival (p-val)	Enrichments – EASE (using most significant top 34 peptides)	t-test (using all 228 peptides)
Individual kinases:		
AKT1	3.7E-03	8.0E-14
PIM1	1.1E-02	1.2E-10
PIM2	1.1E-02	2.1E-11
RPS6KB1	1.1E-02	1.4E-08
AKT3	2.5E-02	2.6E-10
Kinase families:		
AKT fam.	3.7E-03	8.0E-14
PIM fam.	1.1E-02	1.3E-10
RPS6KB fam.	1.1E-02	1.4E-08

e

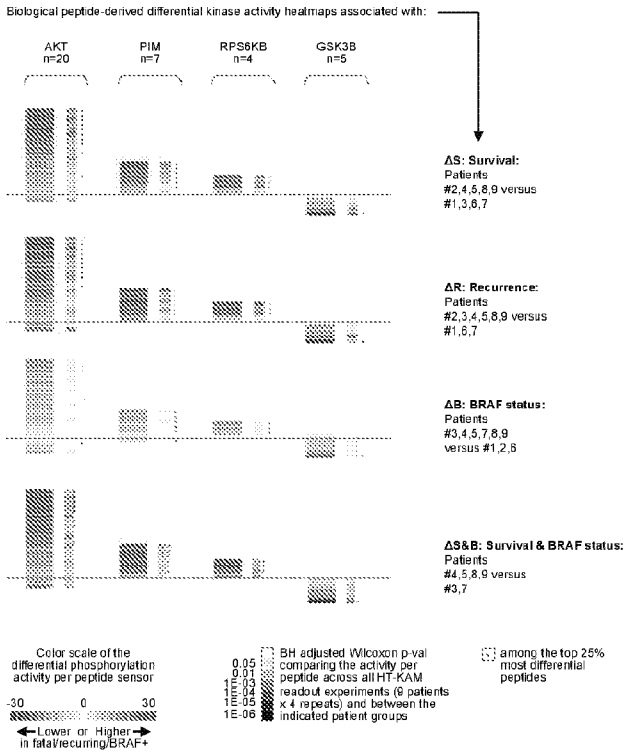

Fig. 26

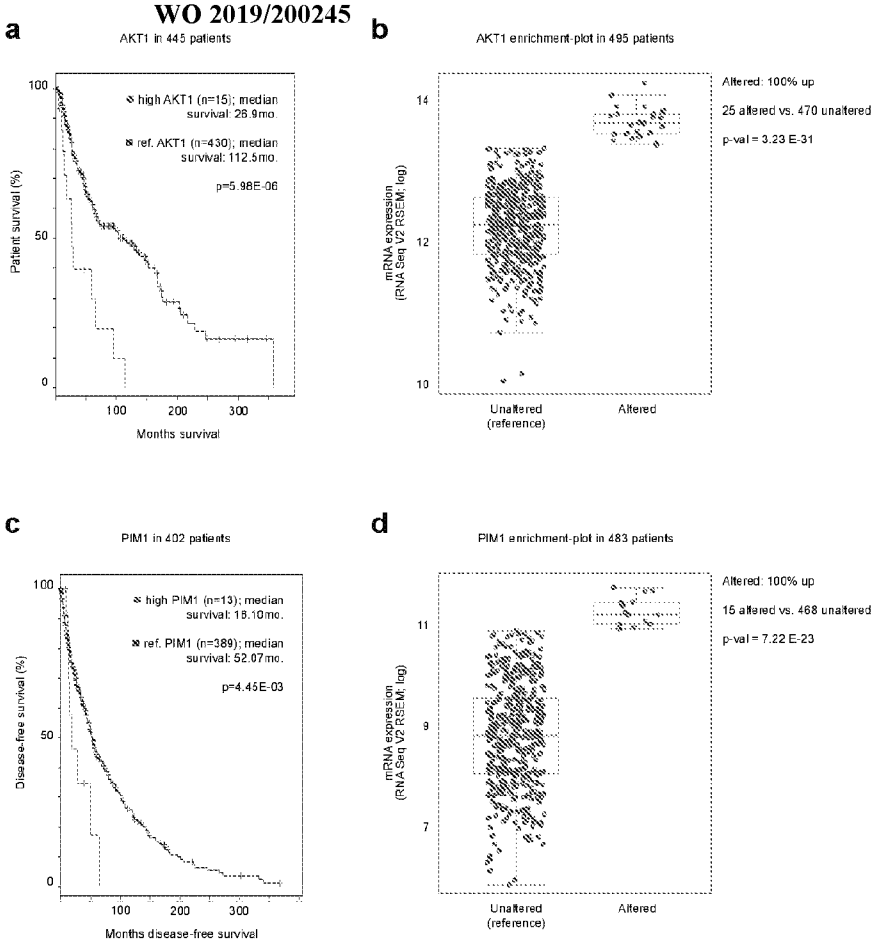
a
AKT1 in 445 patients
high AKT1 (n=15); median survival: 26.9mo.
ref. AKT1 (n=430); median survival: 112.5mo.
p=5.98E-06
Patient survival (%)
Months survival
b
AKT1 enrichment-plot in 495 patients
Altered: 100% up
25 altered vs. 470 unaltered
p-val = 3.23 E-31
mRNA expression (RNA Seq V2 RSEM, log)
Unaltered (reference)
Altered
c
PIM1 in 402 patients
high PIM1 (n=13); median survival: 18.10mo.
ref. PIM1 (n=389); median survival: 52.07mo.
p=4.45E-03
Disease-free survival (%)
Months disease-free survivel
d
PIM1 enrichment-plot in 483 patients
Altered: 100% up
15 altered vs. 468 unaltered
p-val = 7.22 E-23
mRNA expression (RNA Seq V2 RSEM, log)
Unaltered (reference)
Altered

Fig. 27

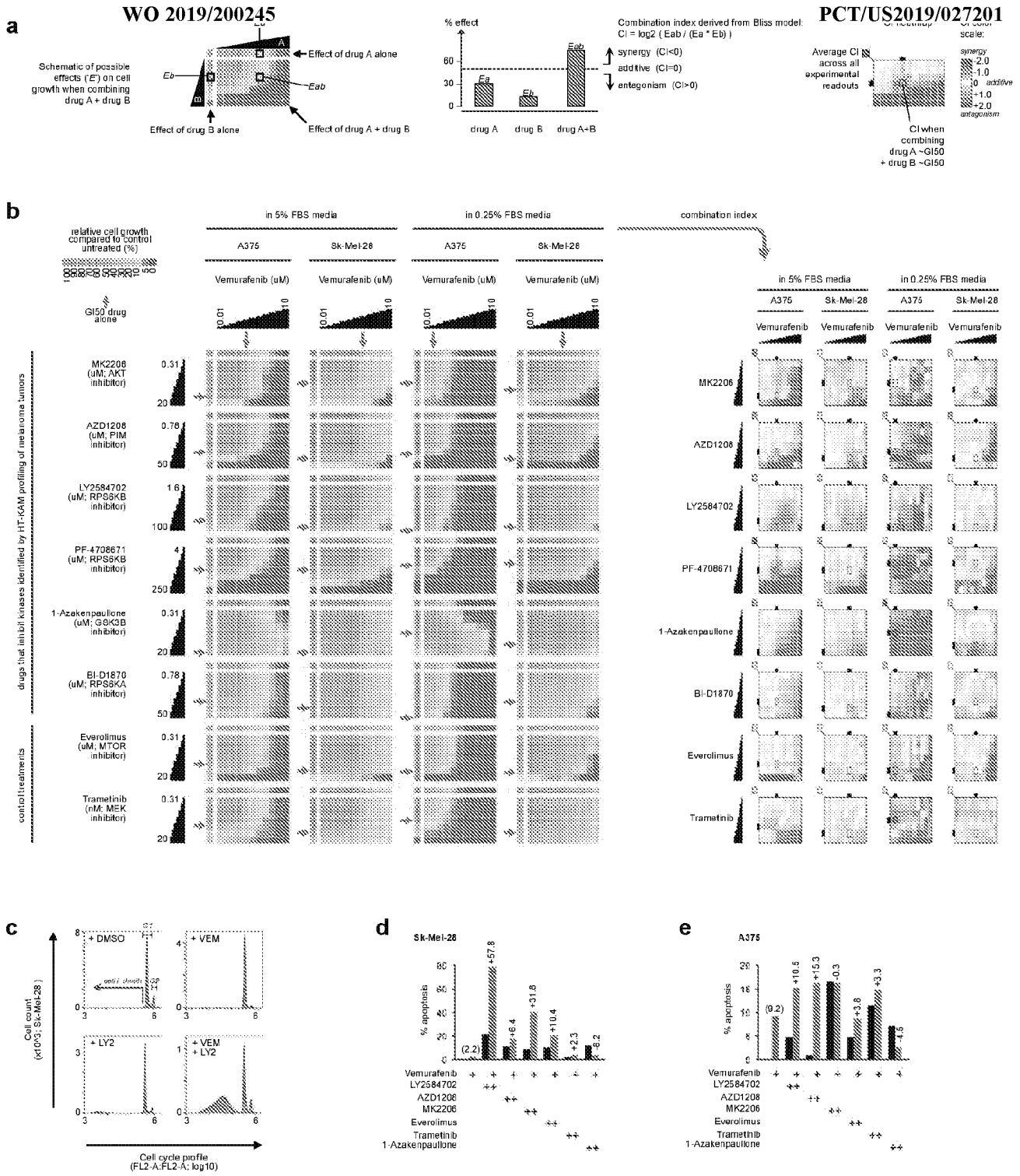
a
WO 2019/200245
PCT/US2019/027201
Schematic of possible effects ("E") on cell growth when combining drug A + drug B
Effect of drug A alone
Effect of drug B alone
Effect of drug A + drug B
% effect
Combination index derived from Bliss model:
CI = log2 (Eab / (Ea * Eb))
synergy (CI<0)
additive (CI=0)
antagonism (CI>0)
drug A
drug B
drug A+B
Average CI across all experimental readouts
CI when combining drug A ~GI50 + drug B ~GI50
b
relative cell growth compared to control untreated (%)
in 5% FBS media
in 0.25% FBS media
combination index
A375
Sk-Mel-28
Vemurafenib (uM)
GI50 drug alone
drugs that inhibit kinases identified by HT-KAM profiling of melanoma tumors
control treatments
MK2206 (uM; AKT inhibitor)
AZD1208 (uM; PIM inhibitor)
LY2584702 (uM; RPS6KB inhibitor)
PF-4708671 (uM; RPS6KB inhibitor)
1-Azakenpaullone (uM; GSK3B inhibitor)
BI-D1870 (uM; RPS6KA inhibitor)
Everolimus (uM; MTOR inhibitor)
Trametinib (nM; MEK inhibitor)
c
+ DMSO
+ VEM
+ LY2
+ VEM + LY2
Cell count (x10^3; Sk-Mel-28)
Cell cycle profile (FL2-A:FL2-A; log10)
d
Sk-Mel-28
% apoptosis
Vemurafenib
LY2584702
AZD1208
MK2206
Everolimus
Trametinib
1-Azakenpaullone
e
A375

Fig. 28

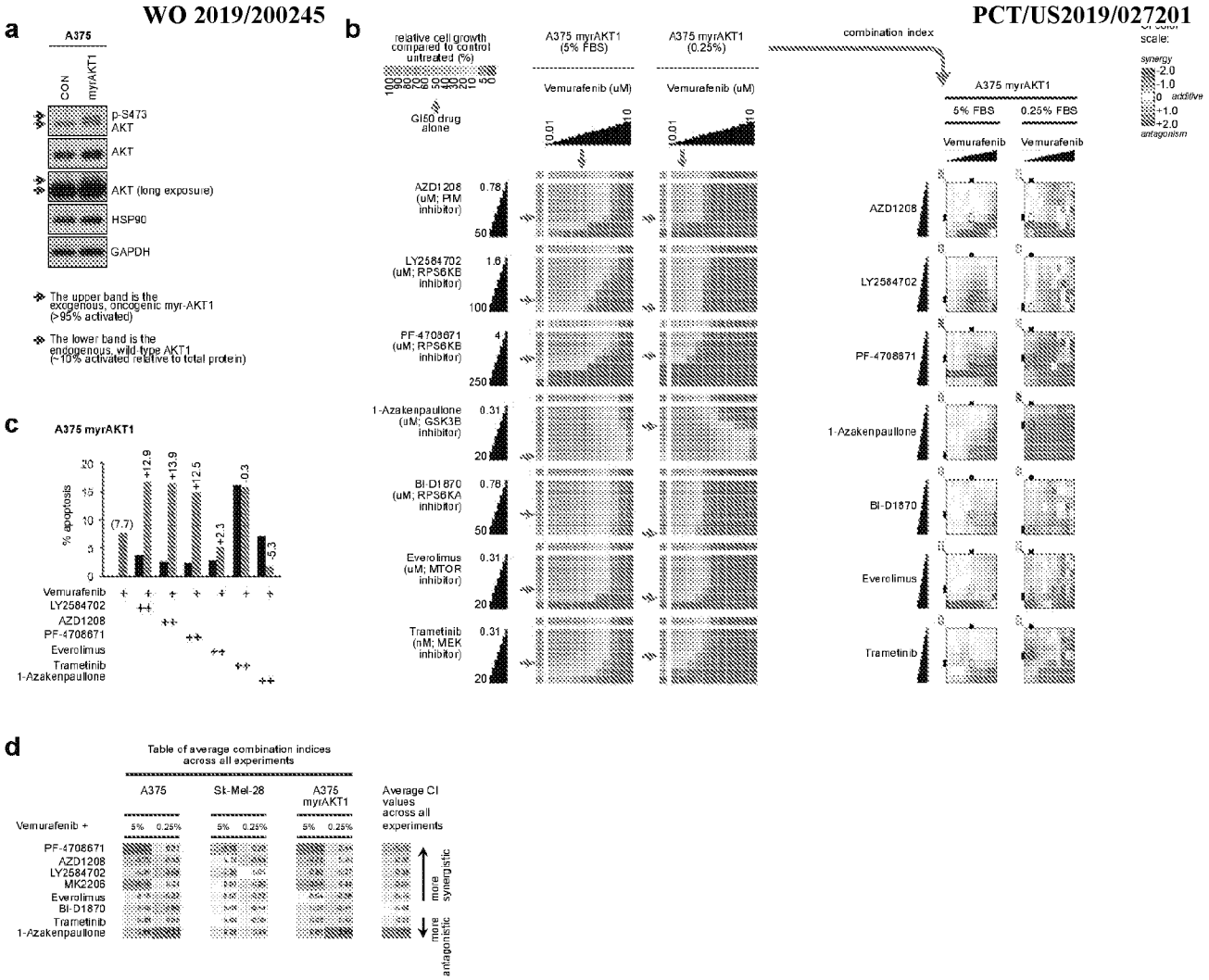
a
A375
CON
myrAKT1
p-S473 AKT
AKT
AKT (long exposure)
HSP90
GAPDH
The upper band is the exogenous, oncogenic myr-AKT1 (>95% activated)
The lower band is the endogenous, wild-type AKT1 (~10% activated relative to total protein)
b
relative cell growth compared to control untreated (%)
GI50 drug alone
A375 myrAKT1 (5% FBS)
A375 myrAKT1 (0.25%)
Vemurafenib (uM)
AZD1208 (uM; PIM inhibitor)
LY2584702 (uM; RPS6KB inhibitor)
PF-4708671 (uM; RPS6KB inhibitor)
1-Azakenpaullone (uM; GSK3B inhibitor)
BI-D1870 (uM; RPS6KA inhibitor)
Everolimus (uM; MTOR inhibitor)
Trametinib (nM; MEK inhibitor)
combination index
A375 myrAKT1
5% FBS
0.25% FBS
Vemurafenib
scale:
synergy
2.0
1.0
0 additive
+1.0
+2.0
antagonism
c
A375 myrAKT1
% apoptosis
(7.7)
+12.9
+13.9
+12.5
+2.3
0.3
-5.3
Vemurafenib
LY2584702
AZD1208
PF-4708671
Everolimus
Trametinib
1-Azakenpaullone
d
Table of average combination indices across all experiments
A375
St-Mel-28
A375 myrAKT1
Average CI values across all experiments
Vemurafenib +
5%
0.25%
PF-4708671
AZD1208
LY2584702
MK2206
Everolimus
BI-D1870
Trametinib
1-Azakenpaullone
more synergistic
more antagonistic

Fig. 29

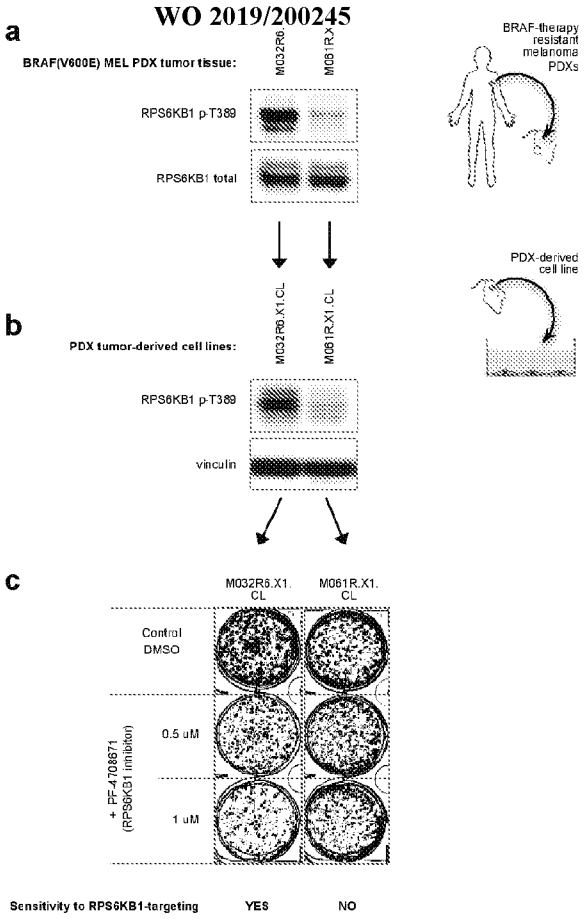
a
BRAF(V600E) MEL PDX tumor tissue:
M032R6
M061R.X1
RPS6KB1 p-T389
RPS6KB1 total
BRAF-therapy resistant melanoma PDXs
PDX-derived cell line
b
PDX tumor-derived cell lines:
M032R6.X1.CL
M061R.X1.CL
RPS6KB1 p-T389
vinculin
c
M032R6.X1. CL
M061R.X1. CL
Control DMSO
0.5 uM
1 uM
+ PF-4708671 (RPS6KB1 inhibitor)
Sensitivity to RPS6KB1-targeting
YES
NO

Fig. 30

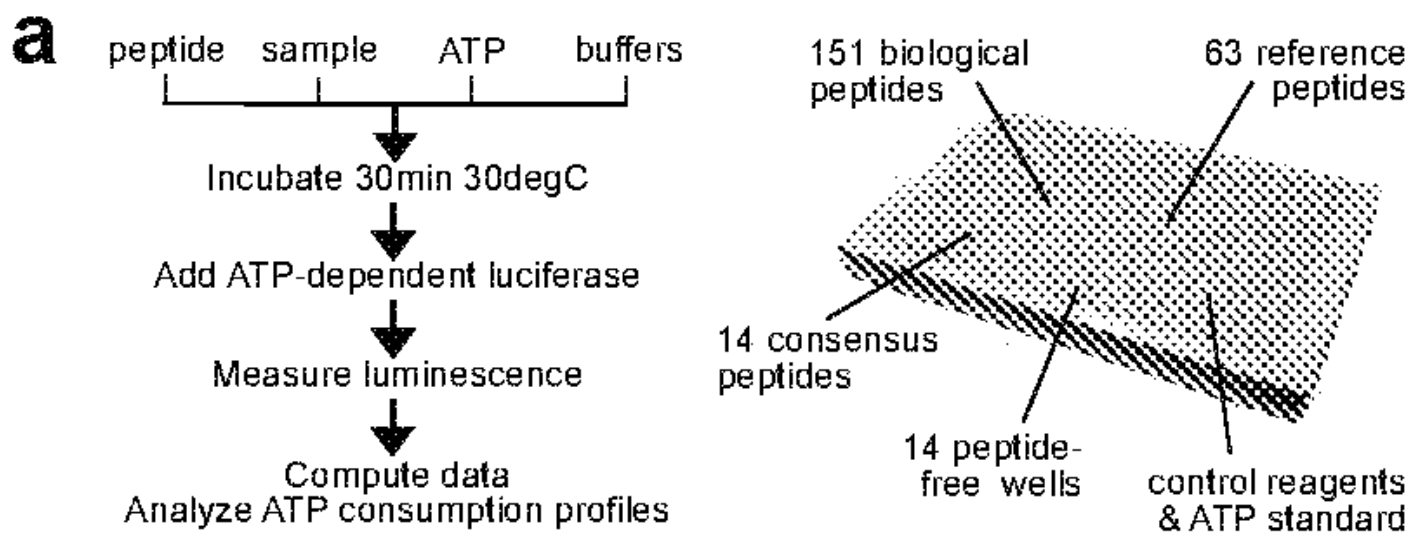
a
peptide
sample
ATP
buffers
Incubate 30min 30degC
Add ATP-dependent luciferase
Measure luminescence
Compute data
Analyze ATP consumption profiles
151 biological peptides
63 reference peptides
14 consensus peptides
14 peptide-free wells
control reagents & ATP standard

Fig. 1